WORKSHOP ON PREDICTION OF SHIP MANOEUVRABILITY

November 6th 1992
Fukuoka, Japan

The West-Japan Society of Naval Architects

WORKSHOP ON PREDICTION OF SHIP MANOEUVRABILITY

Organised by:

The West-Japan Society of Naval Architects

Organising Chairman:

Prof. M. Nakato

Department of Naval Architecture and Ocean Engineering

Hiroshima University

Organising Secretariat:

Prof. K. Kijima

Department of Naval Architecture and Marine Systems Engineering

Kyushu University

WORKSHOP ON PREDICTION OF SHIP MANOEUVRABILITY

Proceedings of Workshop on Prediction of Ship Manoeuvrability, held in Fukuoka, Japan, 6 November 1992.

Editor:
K. Kijima,
Department of Naval Architecture and
Marine Systems Engineering,
Kyushu University

OPENING ADDRESS

It is my great pleasure and privilege to celebrate this Workshop on Prediction of Ship Manoeuvrability as one of the coordinators.

The objectives of this workshop are to discuss the prediction of ship manoeuvrability in various viewpoints and to exchange the opinions of colleagues.

The prediction technology of ship manoeuvrability has been developed remarkably since the computer science was introduced in naval architecture. In the past, ship designers estimated a new ship manoeuvrability entirely by the database methods, however, nowadays they utilize the new analytical methods which include the valuable fruits of modern computational fluid dynamics.

At present time, it seems necessary to consider synthesizing the database method and the analytical method by system engineering technology.

Now, this workshop was proposed and organized by Prof. K. Kijima, taking the occasion of the ITTC Manoeuvrability Committee in Kyushu University. The plan of workshop was discussed in the Ship Performance Research Group and then the plan is supported by the West-Japan Society of Naval Architects which was established in 1924.

I would like to mention briefly of the Ship Performance Research Group. It was proposed by the late Prof. Y. Watanabe in 1959 and now it is one of the research groups in the Technical Committee of the West-Japan Society of Naval Architects. The activities of the research group have been well-known with the names of the late Prof. Y. Watanabe in stability, Prof. J. Fukuda and the late Prof. F. Tasai in seakeeping and Prof. S. Inoue and Prof. K. Nomoto in manoeuvrability.

Finally, I, as the organizing chairman of the workshop, would like to express sincere gratitude to the president of our society Dr. K. Tamura, to the organizing secretariat Prof. K. Kijima and the cooperated staffs in Kyushu University. I would like to thank all the participants in this hall who lead the workshop to the success.

Thank you very much for your kind attention.

6 November, 1992

Michio Nakato M. Nakato
Professor of Hiroshima University

CONTENTS

MEASUREMENT ERRORS AND MANOEUVRING PREDICTION

IAN W. DAND, BRITISH MARITIME TECHNOLOGY LTD., UK

1. INTRODUCTION

The process of manoeuvring prediction involves some sort of modelling process and the comparison of the results of this modelling with full scale results. It is then assumed that good agreement between the results of the model and those from full scale validates the model, which may then be used to give accurate predictions of other manoeuvres in real life.

If it is accepted that the above is a proper definition of the process of manoeuvring prediction and validation, it is wise to look in a little more detail at the meaning of key terms such as 'good agreement', 'validation', 'accurate predictions' and 'real life'. This is attempted in this paper and is necessary because all measurements are subject to error and these pervade the whole of 'prediction and validation'. Consideration of errors and accuracy is so fundamental to much of what we do in manoeuvring that it requires some rational consideration when the matter of prediction is raised.

Much of what follows is at present under active consideration by the International Towing Tank Conference (ITTC), with aspects related to manoeuvrability being considered by the ITTC Manoeuvrability Committee.

2. VALIDATION AND ERROR ANALYSIS

The dictionary tells us that something which is valid is 'founded in truth, sound and conclusive'. Validation is the test of validity of a proposition or prediction.

Many present-day manoeuvrability studies are devoted to predicting what a ship or other marine vehicle will do in a dynamic sense when some sort of control action is made.

Predictions may be based on the results of physical or mathematical models, and in all cases it is essential to know how reliable and accurate the prediction is. This demands base-line information on the way a ship or other marine vehicle behaves which is 'founded in truth, is sound and is conclusive'. We assume that if our prediction, based say, on physical or mathematical model results, agrees with the base-line data, the prediction is correct and our model is validated. We may, from this initial validation, be led to believe that all other predictions from our model are equally valid, a proposition which may not always be true.

When carrying out this validation process, it is imperative that due account is taken of the accuracy, not only of the baseline data, but also of the prediction. This involves an estimation of the errors inherent in the process under consideration and a judgement of what is an acceptable level of error for a particular purpose. As an example, simulation results

used to train mariners can be acceptable even if the predicted ship position at any instant is relatively inaccurate. However, the same level of error would be unacceptable if the simulation were to be used to predict a ship's position for the purpose of accurate navigation under a narrow bridge or determining the amount of material to be blasted out of rock to make a canal.

A knowledge of the errors inherent in a process is therefore essential if any sort of validation is to be done. 'Agreement' between prediction and measurement can only be correctly assessed if the accuracies of both the prediction and measurement are known with some certainty. We must then decide whether, for 'agreement', we need complete co-incidence of prediction and measurement or whether an overlap of the error bands (or, say, 95% confidence limits) is adequate. Furthermore, a knowledge of the accuracy of prediction and measurement allows a judgement to be made of the future direction of a particular study. For example, there is little to be gained by trying to modify a complex simulation model if the validation data against which it is being judged is inaccurate; it is better to obtain a more accurate set of validation data. This may only be obtainable by the use of physical models, but again, their accuracy must be known.

All measurements and numerical model results are subject to error. Two principal types are encountered and these are:

(a) random errors (precision)

(b) systematic errors (bias)

In this paper, an attempt is made to identify possible sources of such errors in physical and mathematical models associated with manoeuvring studies.

3. SOURCES OF ERROR

3.1 Physical Model Tests

Physical model tests under laboratory conditions provide the best means to minimise error by proper control of the experiment conditions. In what follows it is assumed that obvious sources of gross error, such as that due to faulty equipment or incorrect analysis procedures, have been eliminated by the use of proper working practices (see Section 4). What remains are the systematic and random errors which are either difficult or impossible to remove under normal conditions.

3.1.1 Random Errors

Random errors may occur in the following items where, for the moment, no measure of importance is assigned to each item:

(a) Model Manufacture

Defined by the known and measurable manufacturing tolerance.

(b) *Control Surface Positioning Accuracy*

Is a rudder angle of 20° really 20° or say, 20.1°?

(c) *Model Speed Measurement*

Are we measuring speed through the water or really speed over the ground? If the former, (as it should be) then random errors arise from limitations of the measurement equipment and the presence of random currents in the tank, etc.

Speed over the ground may also be obtained as a derived quality for free-running models. Sequential measurements of position and the time taken to move from one position to another are used, which differentiates the position measurements with time. For accurate speed assessment using this method, position measurements of high accuracy are needed and errors in derived speed can be high.

Speed through the water may also be measured directly at both model and full scale by small flush-mounted paddle wheels whose blades protrude a small distance from the hull surface. Pulses, induced by blade passage, are counted to indicate wheel revolutions and hence speed. These paddle wheels have a threshold velocity below which they cannot be relied upon, but above this velocity they can be used to measure (after suitable calibration) speed through the water during manoeuvres.

(d) *Model Attitude*

What is the accuracy of drift, heading, incidence and roll angle measurement? Random errors can arise from both the method of measurement and the equipment used. Attitude is measured using drift vanes, roll and pitch gyroscopes, angular rate gyroscopes and gyro-stabilised heading gyroscopes.

(e) *Model Position*

The accuracy of the measurement of model position in space (either relative or absolute) is of interest here. At BMT a system using pulsed ultrasound is employed for free running models which requires, among other things, a measure of the speed of sound in water. This will vary with temperature and can be measured to an accuracy limited by the equipment in use. The accurate siting and measurement of the relevant equipment both on the model and on shore is also important.

An alternative method, for free-running models or some full scale vessels, (also in regular use at BMT) is to use on-board measurements only. These consist of drift angle (using an immersed vane ahead of the bow), speed through the water (using, for example, the paddle wheel mentioned in (c) above) and heading (using, for example, a gyro-stabilised flux-gate compass). With these three measurements, vessel position and drift angle can be computed using dead reckoning for position. Drift angle measurements may need correction for heel on the turn (if this occurs), the heel angle being measured by an on-board roll gyroscope.

All of these measurements are subject to errors which will be compounded when position and attitude are computed.

Model position is more accurately measured in captive model tests on a PMM, CPMC or in an oblique tow test, but again will be subject to random error due, for example, to vibration, small, random, amounts of gear backlash and other effects.

(f) Model Ballasting and Dynamic Balancing

Random errors can occur here associated with model manufacturing accuracy, draught measurement, ballast weight calibration and dynamic balancing techniques.

(g) General Instrumentation Errors

These may arise from design limitations, calibration or other sources.

3.1.2 Systematic Errors

(a) Scale Effects

All ship model experiments are subject to scale effects to a greater or lesser degree. In this paper they are classified as systematic, rather than random, errors. The relatively few accurate full scale measurements of ship manoeuvring that have been made suggest that displacement ship models predict a manoeuvring behaviour that is slightly worse than the ship, rather than random (sometimes better, sometimes worse). Recent evidence, obtained at BMT, suggests that for high speed craft with large appendages, scale effect may give a noticeably pessimistic prediction of manoeuvrability.

(b) Steady Tank Currents

The presence of steady currents in the towing tank or manoeuvring basis will result in a systematic difference between ground speed and speed through the water. If the speed measuring system measures only speed over the ground, tank currents will be a source of systematic error. They may arise from temperature effects, causing slow speed vortex motions in the model basin, or from drift due to previous runs of the model.

(c) Wind Resistance of the Model

If the manoeuvring of high speed craft is being studied, the wind resistance of the model will inevitably be incorporated in the measurements. If this is not required in the experiments, it will be a systematic error in the tests.

(d) Instrumentation Errors

Bend on a rotating arm would cause inaccurate drift angles to be set and would enter the measurements as a systematic error. Systematic inaccuracies of absolute position measurement of free running models would arise from incorrect alignment and position of the shore-based measurement system.

(e) Tank Blockage

By this is meant all blockage and unwanted wall effects due to the finite dimensions of the tank or model basin in which the experiments are conducted. Oblique tow or PMM tests at large angles of yaw may well be subject to blockage effects which will provide a systematic error. In some cases it may be possible to allow for this, but in many it will not.

3.2 Full Scale Experiments

In full scale trials the investigators inevitably have less control over all conditions of the experiment compared to the 'laboratory' conditions of the towing tank or model basin. Proper assessment of all sources of error is therefore essential on full scale measurements because these are invariably taken as providing the ultimate validation data for physical or numerical model predictions.

Full scale manoeuvring experiments are comparatively rare (if we here make the distinction between manoeuvring *experiments*, such as those on the 'Esso Bernicia' and the 'Esso Osaka', and builder's manoeuvring *trials*) and so methods of conducting them are by no means 'standard'. If we also include System Identification techniques, we see that the proposed determination of errors is difficult and complex. However, in order to make a start, the following sources of error, which include both builder's trials and manoeuvring 'experiments' are offered as a basis for discussion.

3.2.1 Random Errors

(a) Control Surface Positioning Accuracy

If rudder angle cannot be measured directly, systematic errors could arise (see below). Even if rudder angle measurements are accurate, random errors due to limitations of the steering motor, back-lash and control system limitations, could arise.

(b) Ship Speed

As with model tests, is speed through the water or that over the ground being measured? What are the random errors when using GPS, Decca/Loran, ARPA, shore-based tracking, or even shaft rpm/speed calibrations?

(c) Heading and Ship Motions

Heading will probably be measured by a gyro compass and its random error as well as its resolution should be known. This may have to be checked, if necessary, against standard instruments. Ship motions, while not perhaps part of the measurements required for manoeuvring, should nevertheless be known and their random error (together with any cross-coupling of these into 'manoeuvring' measurements) should be assessed.

(d) Environmental Measurements

The greatest problem in full scale measurements lies in the correct determination of the environment, in particular the strength and direction of wind, waves and current. All

of these can be measured (generally at discrete points) and the random errors associated with their measurement should be assessed.

(e) Ship Position

For some trials and experiments it may be necessary to determine the absolute position of a ship at various points in time. This may be done by various means including shore-based tracking, use of an ARPA, Satnav (GPS) position fixes, radar fixes or sextant fixes. Each method is subject to random error which, in some of the methods (notably radar/ARPA and sextant fixes in poor weather/radar echo situations) may have large random errors. Repeat fixes at brief time intervals or redundancy in position fixing may be the only way to assess the magnitude of the random errors in this case.

(f) General Instrumentation Errors

As with model tests, these arise from design limitations, calibration or other sources.

3.2.2 Systematic Errors

(a) Hull Condition

The condition of the hull and its effect on the full scale measurements must remain largely unknown. This is especially true when model/simulation predictions are being made for a ship which may not have SPC hull paint or a known time out of dry dock. Voyage analysis and other studies have been carried out which may enable some sort of bands to be placed on this type of error in a given case.

(b) Rudder and Other Control Surface Positions

If direct measurement of, say, rudder angle is not possible it may be necessary to rely on measurement of 'demand' rudder angle or rudder angle repeater measurements on the bridge. In this case, the demand rudder angle will always have a 'lead' compared to the actual rudder angle (which may or may not be known) and the repeater may well have an unknown bias.

(c) Environmental Conditions

Systematic errors are bound to be present in full scale measurements from the effects of wind, waves and currents. Although 'spot' measurements may be made of the environment, their global effect will almost certainly not be known accurately and must be treated as a systematic error. This is especially true of currents which are notoriously difficult to measure and assess (in a global manner) with any degree of certainty across a manoeuvring track.

The 'Esso Osaka' trials suffered from this particular problem.

(d) Position Fixes

Position fixes from ARPA, Decca/Loran or shore based tracking will have

systematic errors arising from the absolute accuracy with which the RACON(s), Decca towers, or shore-based tracking instrumentation has been positioned. Other systematic errors inherent in radar systems will also be present.

Global Positioning Satellite (GPS) fixes are increasingly used to give accurate information on position in many parts of the world. The positional accuracy of such systems is known and may vary depending on whether 'military' or 'civilian' access to the GPS system is available.

(e) Water Depth

For shallow water tests, a knowledge of water depth is required. While height of tide at one or a number of points can be measured with some accuracy, sea bed depths cannot. In silt conditions the definition of the sea-bed is also a problem so that water depth definition becomes, at best, vague. Random and systematic errors exist in sounding measurements, when these are available, and the type of analysis used to produce them can often produce a systematic error whereby the actual bed depth is greater than that shown on a sounding chart.

(f) General Instrumentation Errors

As in all measurements, systematic error will exist in many types of instrumentation more so perhaps in full-scale measurements. In general attempts are made to reduce these to an acceptable level by the manufacturers and experiments before the trials. In most cases inherent systematic instrumentation errors will be very much smaller than those others mentioned above but they should nevertheless be acknowledged and accounted for.

3.3 Mathematical Modelling : Analysis

By mathematical modelling, manoeuvring simulation is the main consideration, but these general remarks can also apply to the analysis procedures adopted with model and full-scale experiment data.

Whereas it is comparatively straightforward to identify the sources of error in investigations involving physical measurement, it is much more difficult to do so in numerical analysis and prediction. Even if they are identified, assigning realistic values is sometimes difficult, if not impossible. To quote the ITTC Panel on Validation Procedures:

'Clearly a great deal of understanding of the numerical model's basic principles is required to make progress and also significant numerical experimentation with the model is necessary to derive the necessary quantification. To date, no comprehensive examples of such analyses have been found, but increasingly journals, such as ASME Fluids Engineering, are looking for more validation and assessment from authors. The trend will continue and ITTC committees are urged to consider the contribution that they can make in this area'.

The notes below are intended to provide a stimulus for discussion. They are by no means comprehensive, but hopefully address some of the main sources of error. Probably the best approach to error analysis in simulation models is to carry out a comprehensive sensitivity analysis by varying coefficients in the whole model in a systematic manner and judging their effect on the results. The sensitivity of the model to the accuracy of the coefficients themselves (which should be calculable, as most depend on physical measurements) can then be determined.

However, it is perhaps appropriate to consider some sources of random and systematic errors.

3.3.1 Random Errors

(a) Round-Off Noise

We assume all analysis/simulation to be performed on digital computers and therefore to be subject to round-off noise. Some numerical techniques are more sensitive to this than others, but generally an assessment can be made. Its effect can sometimes be minimised by working with double-precision mathematics.

(b) Curve Fitting

In virtually all simulation, and much analysis, least-squares curve-fitting to empirical, semi-empirical or computed data is used. Most regression programs compute the standard errors of the regression coefficients as well as measures of 'goodness-of-fit' (correlation coefficients, F values, Students' t values) so that some idea of the random errors can be obtained.

(c) Numerical Techniques

Many numerical techniques are approximate and subject to random and systematic errors. Examples are some of the approximate methods of matrix inversion and linearisation/non-linearisation. Standard numerical techniques have often been subjected to error analysis in standard tests and should be chosen with their sensitivity to error in mind.

3.3.2 Systematic Errors

Numerical models are only a manifestation of our understanding of a physical process. Gaps in our knowledge (of which there are many in manoeuvring) are often filled by means of empirical (or other) 'correction' factors, which are a way of correcting systematic errors. Those that spring to mind are:-

(a) Scale Effects

This applies both to the general problem of extrapolation of all model-based results to full scale as well as to detailed areas such as that of propeller/hull/rudder interaction. Usually some sort of assessment can be made, but these often depend on 'validation' data which itself may be subject to systematic error.

(b) Linearisation and Simplification

In many cases it is necessary to simplify a problem to make it tractable. This has certainly been the case with manoeuvring analysis and prediction since the early days. The advent of more powerful computers has reduced the need for simplification, but in some areas it remains. Linearisation is the best-known simplification with perhaps the Nomoto approach one of the most useful. This will obviously induce systematic errors into the prediction of manoeuvring abilities; these are usually recognised and allowed for by restricting the use of such models to manoeuvres (such as course-keeping) where their effect is minimal.

(c) Discretisation

Numerical models or analysis, on a digital computer, on a digital computer, of a continuous process must of necessity 'sample' that process at discrete intervals. This may induce systematic errors (such as aliasing) which can be removed to a greater or lesser degree by firstly, recognition of their existence and secondly, by choosing appropriate techniques (such as proper filtering).

4. QUALITY ASSURANCE

Although not strictly speaking part of this paper, matters of quality and accuracy are so closely allied that it is relevant to make some remarks in passing about matters of Quality Assurance (QA) in manoeuvring prediction.

Formal assurance of the quality of our predictions is becoming more and more prevalent in the world of engineering, and the specialised world of tank testing and naval architecture is no exception. Regularisation of procedures and working practices is of importance in terms of accountability, especially if something ultimately goes wrong with the performance of a vessel with which we have been associated.

Because of these overtones of accountability there is a danger that QA becomes simply an additional burden of paperwork for the already over-worked naval architect or researcher. Clearly an unnecessarily high level of paperwork should be avoided at all costs, but the goal of well-defined and understood 'good' working practices and procedures is relevant to the discussion of accuracy.

Quality springs from accuracy so that good predictions will inevitably indicate work that is of high quality. By 'good' in this sense is meant a prediction in which the level of accuracy is rationally and logically specified so that the user can gain a proper idea of its value. Part of the process whereby good and repeatable accuracy can be obtained is by the elimination (or at least minimisation) of human and systematic errors.

This is where QA is relevant to the discussion in this paper, for the adherence to properly-documented and well thought-out procedures (which can of course be modified and improved as experience builds) will lead to results which do not contain gross errors.

5. AN EXAMPLE OF ERROR ESTIMATION

An ideal source of manoeuvring error estimation would be the model, numerical and full size measurements of the 'Esso Osaka'. Once these are all complete then a valuable research exercise would be an attempt to identify and quantify the sources of error. This is especially relevant to the full scale measurements.

However, in the absence of such an analysis the following are offered as examples. The first relates to a model test carried out in shallow water where the model's tracks along a buoyed channel had to be measured. Marker buoys had been set in the basin at pre-determined positions and absolute model position, relative to the marker buoys, was of some importance in the investigation.

The purpose of the error analysis was therefore to determine the probable accuracy of the measured track of the model.

5.1 Sources of Error

The sources of error were as described in section 3.1 and will not be repeated here. However, it may be noted that track speeds were not measured directly but deduced from the first derivative, with time, of the track measurements.

5.2 Error Estimates

The standard random errors of various key measurements were first estimated. This was based on either past experience or a knowledge of the capabilities of the instrumentation involved. Systematic errors were, in this instance, assumed to be negligible.

Rudder Angle

The standard error of the measured rudder angle, δ was estimated to be $\pm 1.0°$.

Heading

The standard error of the measured heading Ψ was estimated to be $\pm 1.0°$.

Shaft rpm

The standard error of the measured shaft rpm N was estimated to be ± 1.0 rpm.

Time

Timing was derived from very accurate instrumentation. Timing errors were therefore assumed to be negligible.

Marker Buoys

The marker buoys were estimated to have a relative positional accuracy of ± 5 mm (i.e. the channel widths were accurate to this value) and an absolute positional accuracy within the basin of ± 15 mm. The buoys delineated the nominal channel boundary given on a chart which itself was presumably subject to (unknown) error. (Further errors due to scaling from the drawing probably resulted in an overall error of about ± 1.0 metre in the channel boundary definition). Therefore although the marker buoys delineated a channel, it was taken as being a 'best' representation of the particular channel in question.

Track

To illustrate the potential error of the derived (x, y) co-ordinates of the model position within the tank, we assume that position is deduced from signals obtained from two receivers at positions 1 and 2 in Figure 1. This gives two measurements of the length of the rays R_1 and R_2 from the transmitter in the model to receivers 1 and 2 (see Figure 2).

Checks on the measurement of known distances in the tank suggested that the rays would be measured to about ± 0.015 m while the base length 1 was measured to an accuracy of about ± 0.005 m.

Using these values for a position between two channel marker buoys gave values of R_1, and R_2 of 32 metres and 28 metres respectively. Using the Cosine Rule to give $\cos\alpha$ we have:

$$(R_1^2 + l^2 - R_2^2)/(2R_1 l) \qquad (1)$$

the (x, y) co-ordinates may be calculated from:

$$x = R_1 \cos\alpha \qquad (2)$$

$$y = R_1 \sin\alpha \qquad (3)$$

The error in the derived value of $\cos\alpha$ was obtained from:

$$\varepsilon^2_{\cos\alpha} = \frac{(\partial f)^2}{(\partial R_1)} \varepsilon_{R1}^2 + \frac{(\partial f)^2}{(\partial R_2)} \varepsilon_{R2}^2 + \frac{(\partial f)^2}{(\partial 1)} \varepsilon_1^2 \qquad (4)$$

where $\varepsilon\beta$ denotes the estimated error of a quantity β
f denotes the expression of the right hand side of the equation (1).

Similarly:

$$\varepsilon_x^2 = \frac{(\partial g)^2}{(\partial R_1)^2} \varepsilon_{R1}^2 + \frac{(\partial g)^2}{(\partial(\cos\alpha))} \varepsilon^2_{\cos\alpha} \qquad (5)$$

$$\varepsilon_y^2 = \frac{(\partial h)^2}{(\partial R_1)^2}\ \varepsilon_{R1}^2 + \frac{(\partial h)^2}{(\partial(\sin\alpha))}\ \varepsilon_{\sin\alpha}^2 \qquad (6)$$

where g and h are the functions on the right hand sides of equations (2) and (3).

Using values obtained for a position between the marker buoys in question gives the following percentage errors:

$$\varepsilon_{\cos\alpha} = \pm 0.00117\%$$

$$\varepsilon_x = \pm 0.051\%$$

$$\varepsilon_y = \pm 0.051\%$$

These results indicate that the x and y position co-ordinates have an absolute error of about ± 12 mm at model scale for the position chosen.

In practice, results for each position were obtained from all four receivers and a 'best fit' (in the least squares sense) result obtained for x and y. It was therefore assumed that the model (x, y) positions had an error of ± 12 mm as an upper bound. This represented a positional error of ± 0.48 metres at full scale.

Track Speed

Track speed was derived from:

$$v_t = \delta s/\delta t \qquad (7)$$

where s is the distance along track from position 1 to position 2 moved in time δt and is given by:

$$\delta s = \sqrt{(x_1 - x_2)^2 + (y_1 - y_2)^2} \qquad (8)$$

Thus we have:

$$\varepsilon v_t^2 = \frac{(\partial v_t)^2}{(\partial(\delta s))}\ \varepsilon^2{}_{\delta s} + \frac{(\delta v_t)^2}{(\partial(\delta t))}\ \varepsilon^2{}_{\delta t} \qquad (9)$$

which, because we have assumed $\varepsilon_{\delta t}$ to be zero becomes:

$$= \varepsilon_{\delta s/\delta t} \qquad (10)$$

$$\varepsilon v_t = \frac{\partial v_t}{\partial(\delta s)} \varepsilon_{\delta s}$$

Now the random error in δs is given by:

$$\varepsilon_{\delta s}^{\,2} = \frac{(\partial(\delta s))^2}{(\partial x_1)} \varepsilon_{x1}^{\,2} + \frac{(\partial(\delta s))^2}{(\partial x_2)} \varepsilon^2_{x2} + \frac{(\partial(\delta s))^2}{(\partial y_1)} \varepsilon_{y1} + \frac{(\partial(\delta s))^2}{(\partial y_2)} \varepsilon_{y2}^{\,2} \qquad (11)$$

Taking typical values of x_1, x_2, etc. at the same two marker buoys and values of ε_x, and ε_y, as given above, we obtain:

$$\varepsilon_{\delta s} = \pm\ 0.072\%$$

so that, with a 1.0 second timing interval:

$$\varepsilon v_t = \pm\ 0.072\%$$

Thus the error in speed while small, is some 40% greater than the error in position measurement.

6. CONCLUDING REMARKS

This paper has been an attempt to apply some initial thoughts on error analysis to the particular case of manoeuvring. It is presented for discussion in the firm belief that questions of accuracy and error are fundamental to much that we do in manoeuvring. We are of necessity having to compare predictions with what we take to be reality, generally without acknowledging, in a systematic manner, that *both* prediction *and* 'reality' are subject to error.

The question of what we mean by 'agreement' between prediction and measurement is by no means trivial, and, as it lies at the bottom of much that we do, deserves wider consideration than perhaps it has had in the past. It is hoped that this paper goes some way toward starting that broader discussion.

It is suggested that the idea of 'good agreement' depends very much on content. Direct coincidence between prediction and 'reality' may not always be possible - or, in some cases, necessary. However, the absence of any indication of the error inherent in the prediction almost implies that the prediction is absolute. Therefore error bands should always be provided with any prediction or measurement and it is suggested that such bands should be standardised at a total width of twice the 'standard error'. The term 'good agreement' may then be taken as overlap between the error bands of prediction and those of 'reality'.

Provision of such error bands would be valuable, not only to the end user of the information, but also to the researcher who would be able to see, at a glance, where further work should be done to improve the prediction of manoeuvring performance.

REFERENCES

A Ultrasonic Receivers
B Ultrasonic Transmitter
C Counters/Timers
D Computer Acquistion/Display
E Ultrasonic Pulse Train
F Cabling to Instrument Cabin

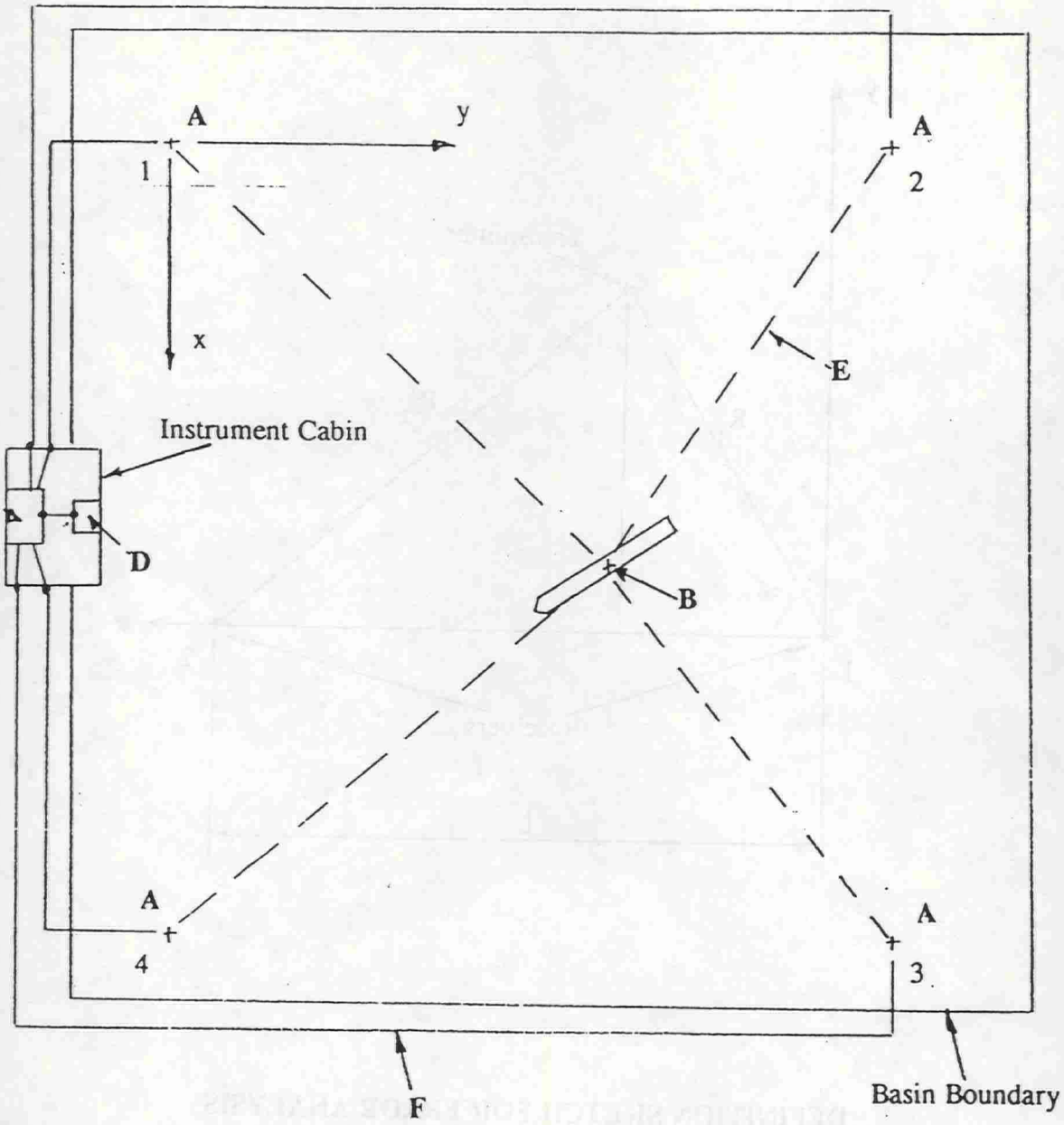

BMT ULTRASONIC TRACKING SYSTEM

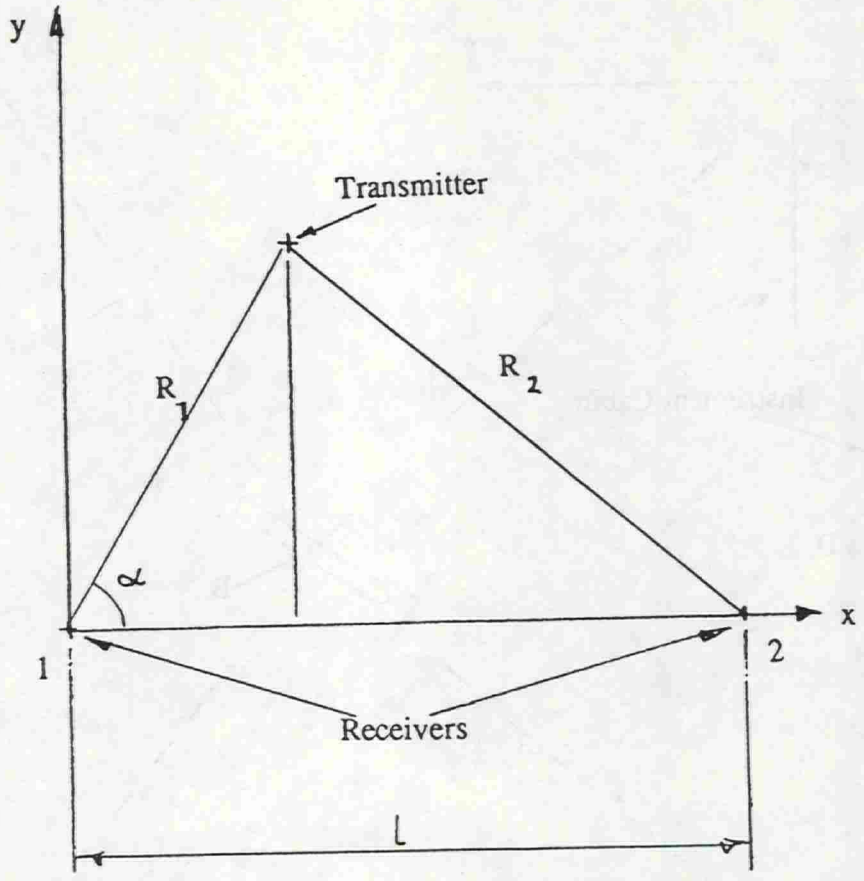

DEFINITION SKETCH FOR ERROR ANALYSIS

SOME NOTES ON PREDICTION OF SHIP MANEUVERING MOTION

MASAYOSHI HIRANO, AKISHIMA LABORATORIES (MITSUI ZOSEN) INC., JAPAN

PREFACE

This paper describes some notes on the prediction of ship maneuvering motion. Three topics are briefly discussed showing typical results obtained so far, and they are as follows.

(1) Loading Condition and Maneuverability.
(2) Hull Force Model for Low Speed Maneuvering.
(3) Maneuvering Prediction of SWATH ships.

1. LOADING CONDITION AND MANEUVERABILITY

Extensive efforts to develop the "Maneuvering Standard" are now being made at IMO, and the resolution for this "Standard" is expected to be adopted in a near future. This "Standard" is basically specified for the maneuverability in a fully loaded condition. However, for many types of ships except such a ship as an oil tanker, full scale trials can not be carried out in a fully loaded condition. As regards the turning ability for 35 degree rudder, which is one of the typical aspects of ship maneuverability, the following standard applicable for a ballast condition as well as a fully loaded condition is currently proposed and discussed at IMO.

$$\begin{aligned} &\cdot \text{Advance} && : Ad \leqq 4.5 \times L \\ &\cdot \text{Tactical diameter} && : Dt \leqq 5.0 \times L \end{aligned} \qquad (1)$$

In relation to the above, effects of loading condition on the turning ability are discussed here. Effects of loading condition on the ship maneuverability may generally be evaluated by three key factors of draft,trim and rudder area of immersed part which change according to a loading condition change [1] . These three parameters usually change from a fully loaded condition to a ballast condition in the following manner.

(a) Draft : decrease of mean draft
(b) Trim : increase of trim by stern
(c) Rudder: decrease of immersed rudder area

Viewing these parameter changes in relation to the turning ability, the above (a) may affect the turning ability in a direction of improvement. On the contrary, the above (b) and (c) may deteriorate the turning ability. Thus changes both in draft and in trim and rudder area act each other so as to cancel their effects, and this mechanism may result in the turning ability difference between a fully loaded condition and a ballast one.

One of typical examples which explain the fact mentioned above is given in Fig.1, which is obtained by maneuvering simulations for a container ship of about 200 meter long. Four typical indices which represent the ship turning ability, namely the advance: Ad/L, the transfer: Tr/L, the tactical diameter: Dt/L and the nondimensional turning rate: r'(= rL/V) are given indicating how these indices change in conjunction with a loading condition change, where rudder angle is taken in abscissa. In Fig.1, four kinds of loading conditions are supposed in a process from a fully loaded condition to a ballast one, and they are as follows.

- Full : the fully loaded condition with zero trim and a fully immersed rudder
- Ballast(1) : an imaginary ballast condition with a draft equal to a mean between fore- and aft-draft of the ballast condition where zero trim and a fully

immersed rudder are assumed

- Ballast(2) : an imaginary ballast condition with a fully immersed rudder assumed
- Ballast(3) : the ballast condition

It may be understood from the above that each change of three key factors, described in the above (a),(b) and (c), corresponds to the following loading condition change.

- Decrease of mean draft : Full → Ballast(1)
- Increase of trim by stern : Ballast(1) → Ballast(2)
- Decrease of immersed rudder area: Ballast(2) → Ballast(3)

In the example shown in Fig.1, the advance and tactical diameter (35 degree rudder) in a ballast condition are somewhat larger than those in a fully loaded one. This difference may be resulted in by a trade-off of the effects of three key factors on the turning ability mentioned above. A trim by stern of 1.0 % of ship length and a rudder area ratio of about 1/50 are assumed for the ballast condition in Fig.1. More trim by stern and less rudder area ratio in a ballast condition may easily be anticipated for such a ship with a fine hull form as the subject container ship. It should be noted that, in such a case as the above, differences in the advance and tactical diameter between a fully loaded condition and a ballast one could be much larger than the example in Fig.1.

Full scale trial results of the advance and tactical diameter in a ballast condition for various types of ships are shown, taking a block coefficient in abscissa, in Figs.2 and 3 respectively, where trial data in a vicinity of and/or above the standard line currently proposed at IMO are selected from "RR 742" data base. It may clearly be understood from these figures that, according to some circumstances, the turning ability indices (especially the tactical diameter) in a ballast condition could be considerably larger for such a fine hull form ship as that with a block coefficient less than 0.6.

2. HULL FORCE MODEL FOR LOW SPEED MANEUVERING

It may generally be accepted that the mathematical model which describes a ship maneuvering motion has well been established for the maneuvering motion with a normal advance speed. However, in a congested water area due to much traffic such as a harbor area where maneuvering safety could be seriously important, the maneuvering motion with a very low speed for which the well-established model for a normal speed range can not be applied may easily be anticipated. In relation to this fact, a mathematical model describing hull forces for a low speed maneuvering is briefly discussed in the following.

The mathematical model of hull forces for a normal speed maneuvering usually employed is derived on the assumption that the longitudinal component of ship velocity: u is sufficiently large compared with the lateral components of ship velocity. Namely, the surge velocity: u is approximately equal to the resultant ship velocity: V(= (u2+v2)1/2). In another expression, a nondimensional surge velocity: u' (= u/V) can be written as u'= 1.0 (unit). This mathematical model can not be applied to the maneuvering motion with such a low advance speed as that less than, for instance, 0.5 knots or something like that, because in such a very low speed maneuvering the magnitude of surge velocity: u is reduced to the same order of the lateral velocity (sway velocity: v and yaw angular velocity: r).

It should be noted, however, that major aspects of a ship maneuvering motion can be covered by the mathematical model for a normal speed maneuvering, because duration of such a very low speed operation as the above may be thought not to be so long even in the harbor maneuvering. From this point of view, it is desirable that the mathematical model for a low speed maneuvering is to be developed on a basis of the model for a normal speed operation by taking into consideration the speed continuity from a normal speed range to a very low speed range. In addition, it is important for the low speed mathematical model to be as simple as possible from a

practical point of view.

The following is an example of the mathematical model for a low speed maneuvering which has been developed through the basic concept mentioned above [2] .

$$
\begin{aligned}
Y_H &= - m_y v - m_x u r + (1/2)\rho L d V^2 \times [Y_v' v' + Y_r' u' r' \\
&\quad + Y_{v|v|}' v' |v'| + Y_{v|r|}' v' |r'| + Y_{r|r|}' u' r' |r'|] \\
N_H &= - J_{zz} \dot{r} + (1/2)\rho L^2 d V^2 \times [N_v' u' v' + N_r' r' \\
&\quad + N_{vvr}' v'^2 r' + N_{vrr}' u' v' r'^2 + N_{r|r|}' r' |r'|]
\end{aligned}
\tag{2}
$$

In this model, the low speed effects are reflected on four terms in which the nondimensional surge velocity: u' is added. It can easily be understood that in the case of a normal speed maneuvering, namely u'= 1.0, Eq.(2) exactly coincides with the mathematical model for a normal speed maneuvering usually employed as a practical model.

One typical example of computed motion trajectories by the use of the low speed model mentioned above is shown in Fig.4, where computations are compared with model experiments for three cases of turning motion by tugs. Computed results are given on the left side and corresponding model experiments on the right side. The top and middle figures show turning motions by a bow tug for two different approach speed, namely 0 and 4 knots, and the bottom figure shows a turning motion by a stern tug for an approach speed of 4 knots. It may be understood from this example that, even by computations based on a rather simple mathematical model like Eq.(2), satisfactory prediction can be made for such a highly nonlinear maneuvering motion as generated by tugs.

3. MANEUVERING PREDICTION OF SWATH SHIPS

Various types of advanced vessels, such as SWATH ships, SESs and so on, have been produced in consequence of the recent development in a maritime transportation. One distinct point in the performance of advanced vessels from that of conventional

displacement ships is a wide range of the advance speed. This wide range of the advance speed may generally have great influence on their maneuverability as well as other performances such as resistance and propulsion. A prediction of the maneuvering motion of SWATH (Small Water-plane Area Twin Hull) ships is briefly discussed here as a typical example of the maneuvering prediction of advanced vessels focusing on the speed effects on their maneuverability.

The SWATH ship is a novel concept of catamaran, in which each demihull consists of two distinct hull components. One is a submerged "lower hull part" with a torpedo-like hull form, which supports most of ship displacement. The other is a surface piercing "strut part" with a thin stream-lined section. In a mathematical modeling of maneuvering hydrodynamics forces acting on ship hull, these distinct features of the SWATH concept in its hull geometry should properly be taken into consideration. Three hull parameters are key factors for the mathematical modeling of hull forces of SWATH ships in a low advance speed condition with zero trim, and they are as follows.

- Ship aspect ratio : k $(= 2d/L)$
- Nondimensional lower hull diameter : ε $(= D_L/L)$ (3)
- Nondimensional space between demihulls: b' $(= 2b/L)$

In addition to the above hull parameters, two significant factors are needed for describing the mathematical model of hull forces for SWATH ships. One is advance speed effects and the other is trim effects. Fig.5 shows a typical example of model experiments concerning the speed effects on hull forces of SWATH ships [3], where the lateral force derivative with respect to sway velocity: Y_v' is given in a form of the ratio Y_v'/Y_v'(at a low speed of Fn = 0.2) taking the Froude number: Fn in abscissa. It can be seen from this figure that the hull force derivative Y_v' varies greatly depending on an advance speed, and that the amount of Y_v' variation comes up to approximately a half of Y_v' in a low speed condition. Similar discussions can be made for other linear derivatives of Y_r',

N_v' and N_r'. Through the above discussions, the linear derivatives of lateral force and yaw moment may be written in a form of

$$Y_v' = f(k,\varepsilon,b') \cdot g(Fn) \cdot h(\tau') \qquad (4)$$

where the first function $f(k,\varepsilon,b')$ denotes the hull force derivative in a low advance speed condition with zero trim, and the second and the third functions are corrections for the speed effects and trim effects respectively.

Typical computations are presented in Figs.6 and 7, where computed turning trajectories with 35 degree rudder from two different approach speed for a high speed passenger ferry "SEAGULL" are compared with full scale trial results. Fig.6 shows the turning trajectory from an approach speed of 22.5 knots (Fn = 0.66) and Fig.7 shows one from an approach speed of 13.0 knots (Fn = 0.38). Significant difference in the turning ability due to approach speed difference can be seen from these figures. The tactical diameter in the case of 22.5 knots approach speed is remarkably reduced and becomes to almost a half of that in the case of 13.0 knots approach speed. It may be understood from Figs.6 and 7 that computations agree satisfactorily with results of full scale trials and explain well the significant difference in the turning trajectories between two cases of approach speed.

REFERENCES

[1] Inoue,S., Hirano,M., Kijima,K. and Takashina,J.: A Practical Calculation Method of Ship Maneuvering Motion, International Shipbuilding Progress, Vol.28, No.325, 1981

[2] Hirano,M., Takashina,J. and Moriya,S.: A Practical Prediction Method of Ship Maneuvering Motion and Its Application, International Conference on Ship Maneuverability, RINA, London, 1987

[3] Hirano,M., Takashina,J. and Fukushima,M.: A Study on Maneuvering Motion Prediction of SWATH Ships, MARIN Jubilee Meeting, Wageningen,1992

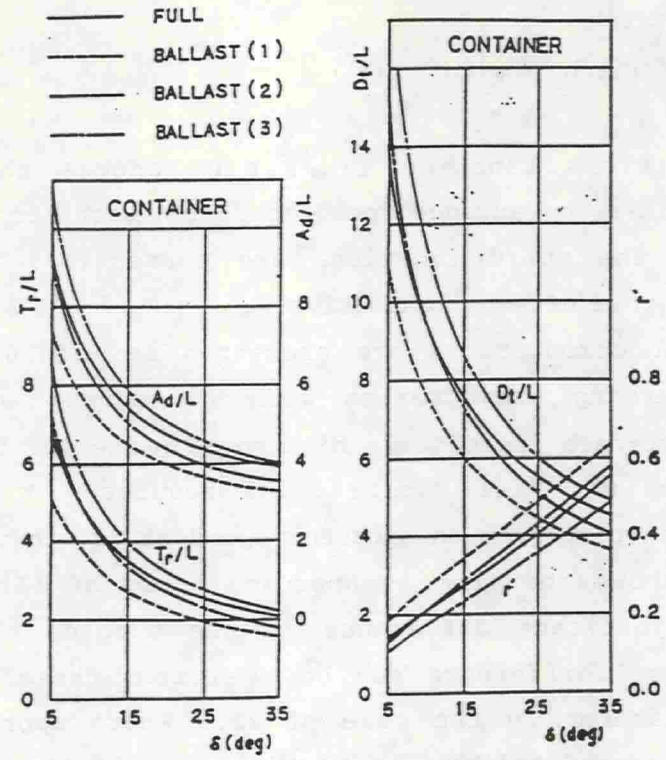

Fig.1 Turning Ability of Container Ship at Various Loading Conditions

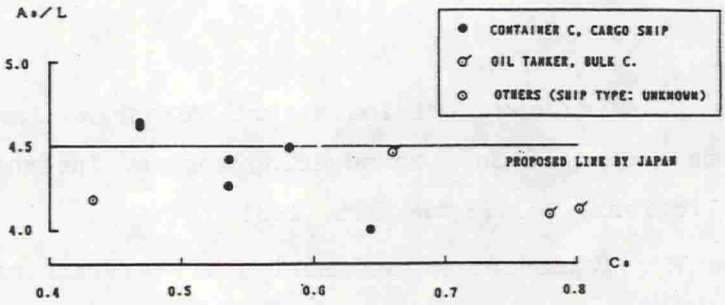

Fig.2 Trial Data of Advance

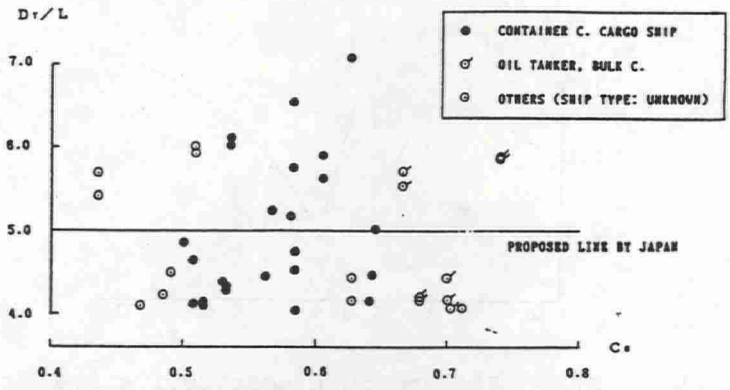

Fig.3 Trial Data of Tactical Diameter

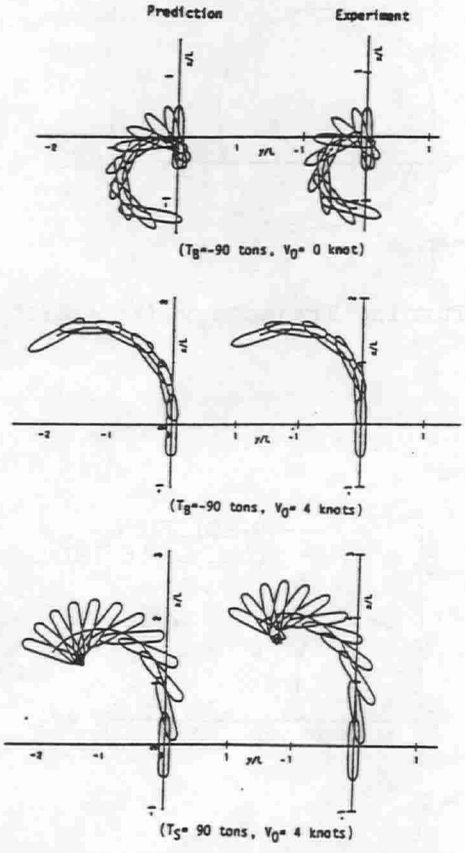

Fig.4 Turning Motion Trajectories by Tug

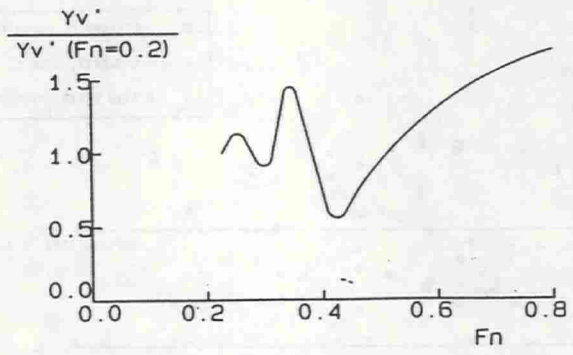

Fig.5 Speed Effects on Linear Derivative

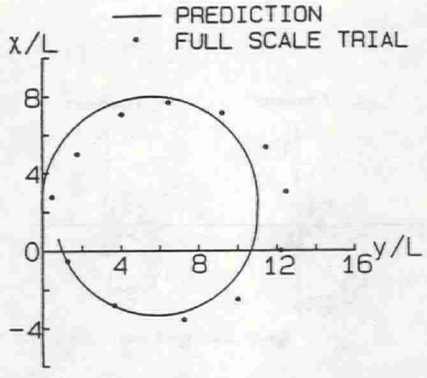

Fig.6 Turning Trajectory (V_A = 22.5 Knots)

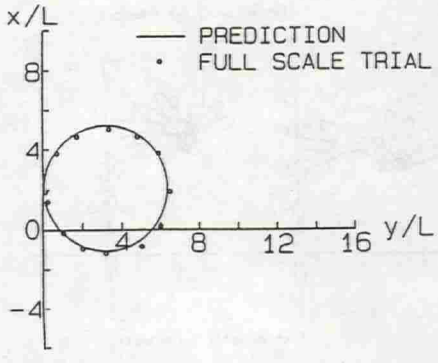

Fig.7 Turning Trajectory (V_A = 13.0 Knots)

ON KNOWLEDGE-DRIVEN SHIP MANOEUVRES / SIMULATION AND FULLSCALE

HIRONAO KASAI, NAGASAKI R & D CENTER, MHI, JAPAN
EIICHI KOBAYASHI, MHI, AMERICA, INC., N.Y., USA

Summary

Simulation of manoeuvring motions is carried out on real-time basis to verify the function of a piloting expert system, and the own ship's automatic route-tracking and collision avoidance functions are examined. The environmental conditions is varied from simpler to more complex ones. Results are shown for automatic track-keeping and avoidance including multiple meeting with targets. Results are compared with those of the corresponding full-scale ship trial tests carried out using the same knowledge-based piloting system as in the simulation. Full-scale ship piloting performance shows fairly good agreement with the simulation. Considerations are made on the results and indispensable role of simulation in developing the systems of relevant kind. Further, consideration is made on the interactive manoeuvring motion simulation by the use of the knowledge-based control system. Discussion is made on the utility of such type of simulation for an automatic qualification screening purpose. An additional discussion is made regarding the possible future use of a knowledge-based system as a manoeuvring simulation supervisory system for multi-lateral collation of manoeuvring performance and ship design evaluations in consideration of the ships' standardized manoeuvring and hazard avoiding functions.

1. INTRODUCTION

The need for an automated ship operating system has long been recognized and its study is gradually becoming popular these years especially for artificial-intelligence-based systems[1)-9)]. In the course of developing a system of this kind, manoeuvring simulation will play the key role in tuning the system up to be totally reliable for the actual use. With this sort of objectives in mind, simulation of manoeuvring motion is carried out to verify the basic function of the system for automatic route-tracking and collision avoidance manoeuvre. In the simulation, the environmental conditions are varied from simpler to more complex ones. Results show that the system has practically reasonable performance[9)]. Comparison is made with that of the corresponding full-scale ship experiment[8)] which was carried out using the same knowledge- based piloting system used in the simulation. Full-scale ship piloting performance shows fairly good agreement with the simulation. At the same time, it has been known as a practical example how much level a knowledge-based system will demand for an autonomous ship piloting system.

Reflecting the specific function of an expert system, the simulated motion contains the effect of the interaction with the knowledge. There, the manoeuvring control is made as based on frequent re-evaluation of the data states, not on any static control structure of the procedural program. In this way, evaluation and judgement enters in the simulation. Where simulation is

in need under various kinds of condition, therefore, a knowledge-based simulation control system may be helpful for performance evaluation/ assessment problems.

Present paper is a short note describing a practical experience in going through simulation and full-scale trial for knowledge-based manoeuvring.

2. Piloting System: Outline

The piloting system for the present study is a part of an integrated navigation control system originally aimed for a ship's supervisory control for steering and on-board sub-systems[9]. Its rough outline is shown in Fig.1. The function of the system depends on the quality of the knowledge-base; therefore, the knowledge has been acquired through listening to the expertise in the domain of ship handling and navigation conrol[7]. Manoeuvring by this system is realised through receiving informations and making inference and decisions, and then sumitting the resulted information signals as the orders to the steering gear and the engine control system[7].

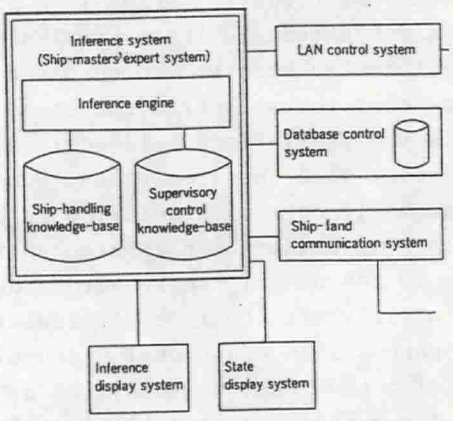

Fig.1 Outline of the system function

3. Simulation

(1) Simulation system

Simulation system used for the present study is shown in Fig.2.

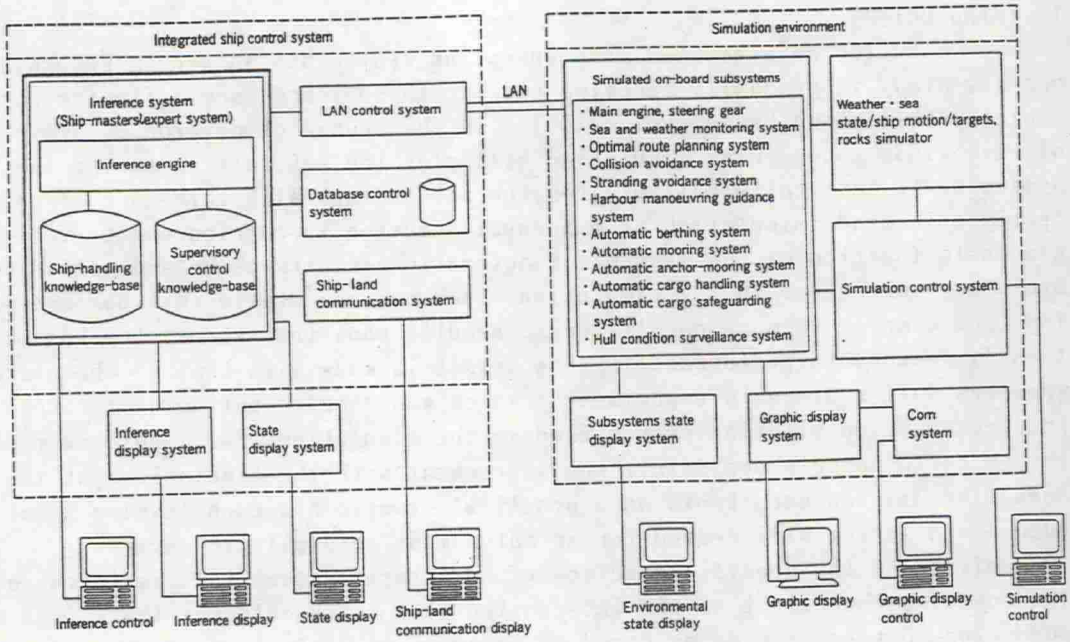

Fig.2 Simulation system for integrated ship control system

In this figure, the right-hand side block in broken-line shows the simulation control system with internal simulators for ship's navigation environment, while the left-hand side one, as referred to Fig.1, for the inference and judgement with the full use of the reference data and informations as well as the expertise knowledge of the mariners including traffic rules and regulations. In the bottom, there are the display terminals for monitoring and controls for simulation. The graphic display in the bottom right is used for displaying a bird's eye view of the navigation area with the sea-chart display in the background. The manoeuvring motion simulation model will enter the block in the top-right in the right-hand side block in broken-line to simulate the own ship's response to the rudder action and various kinds of external forces.

(2) Equations of motion

As the equations of motion for the present purpose, ordinary type in reference to the moving axes of coordinate is adopted as follows.

$$\left.\begin{aligned} m(\dot{u}-vr) &= X_H+X_P+X_R+X_S+X_A+X_W \\ m(\dot{v}+ur) &= Y_H+Y_P+Y_R+Y_S+Y_A+Y_W \\ I_{zz}\dot{r} &= N_H+N_P+N_R+N_S+N_A+N_W \end{aligned}\right\} \qquad (1)$$

where, in the usual manner, the suffix to the right-hand side terms implies: H: hull, P: propeller, R: rudder, S: side-thruster, A: wind, and W: wave (drifting) originated forces and moments, respectively. The coefficients of the components in the right side terms are mainly based on the captive model test result. The ship speed response to the main engine order is modeled with transient response by way of the propeller thrust extended at instantaneous speed of propeller revolutions, while the steering gear is approximated with a first-order response model with the corresponding time constant to the full-scale ship.

(3) Simulation control

The simulation control system function is shown in Fig.3. In the simulation of manoeuvring motion, above-mentioned model is controlled so that the ship will run

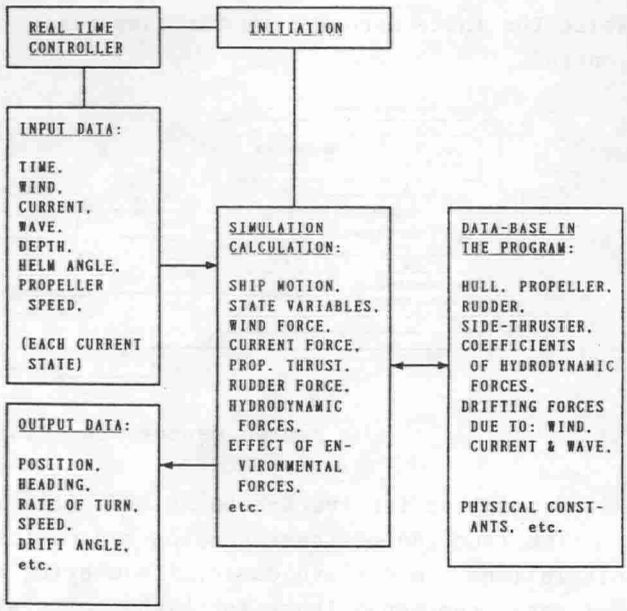

Fig.3 Simulation control function

on the real-time basis corresponding to the given full-scale ship, and the real-time history out-put data may be obtained for ship motion, speed, and rudder angle, etc.

3. Simulations and full-scale trial results

Simulations are carried out for track-keeping and collision avoidance. The track-keeping in the present case is realised as based on the information on the position and the way-points as well as the heading. Collision avoidance scheme in the present case is a sort of menu-selection by way of a tree-search in the so-called recognize-act cycles governed by the knowledge-based system in the system. The concept of tree-search for collision avoidance in the present case is illustrated in Fig.4. The mushroom-shaped menus came from the hint derived from the well-known envelope pattern of the quickest manoeuvring response to the rudder action of a ship. The number of the alternatives in each mushroom is limited within the capacity of the speed and memory of the computer. The same is true for the depth of search in the direction of the route as denoted by the number(n) in the figure.

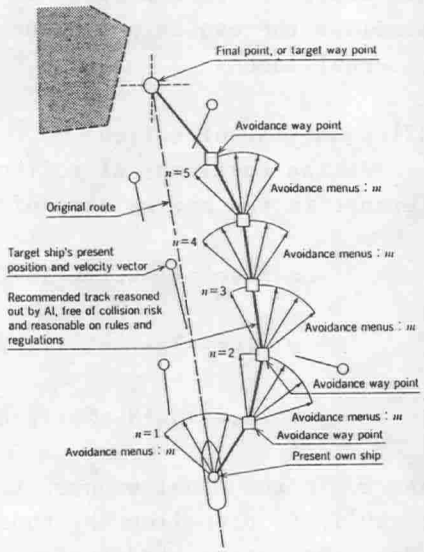

Fig.4 Concept of route-search

The block diagram of manoeuvring control inclusive of the full-scale experiment is shown in Fig.5. In this figure, the darkened arrows indicate the automatic control, while the white arrows show for comparison the traditional case of rudder control.

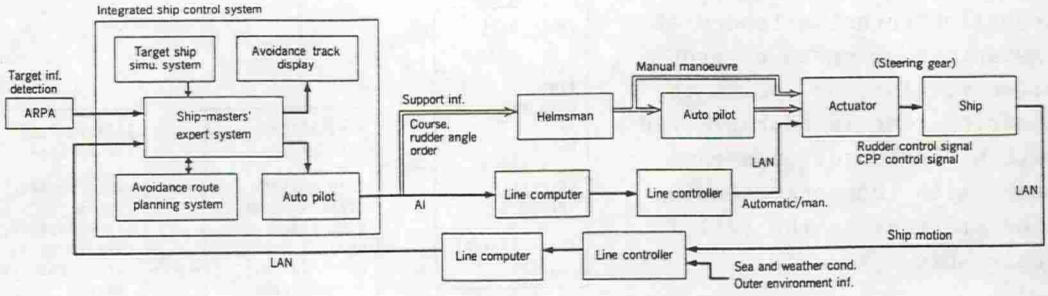

Fig.5 Manouevring control block diagram

(1) Simulation for track-keeping and collision avoidance.

The function of track-keeping and collision avoidance is first tested by simulations. As for avoidance, the meeting situation is chosen from the typical ones from among those for higher risk of collision as previously defined by Imazu[11]. The simulation is made for a training ship 'Shioji-Maru', of the

Tokyo University of Mercantile Marine; measuring 46m in length between perpendiculars, 10m in width, 425 gross-tonnes at 3.01m designed draft, diesel-powered for 14knots cruising speed with a controllable pitch propeller. An example of the results is shown in Fig.6 for the case of 1-target, while in Fig.7 for a case of 2-targets. In Fig.6, the own ship and the target-1 are in head-on situation on reciprocal courses, while the Regulation demands that

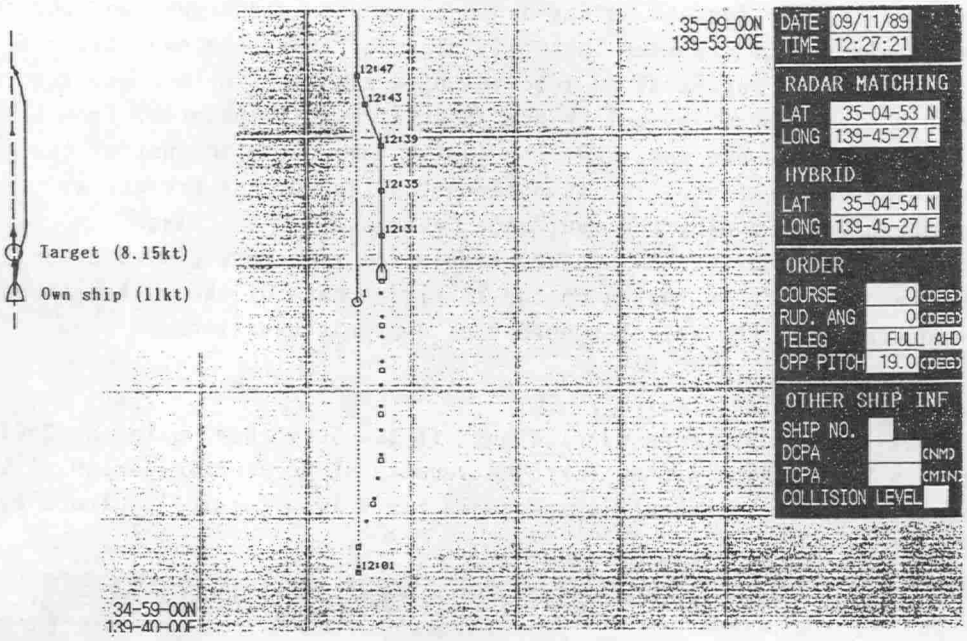

Fig.6 Simulation of route-tracking and collision avoidance

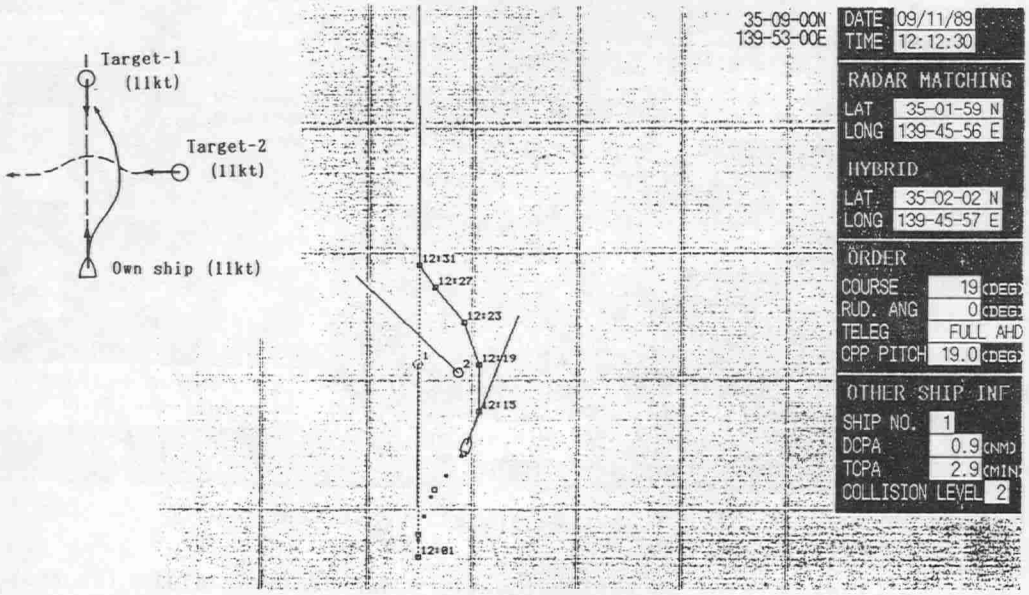

Fig.7 Simulation of route-tracking and collision avoidance

the own ship will alter her course to the starboard side to prevent collision. In Fig.7, the target-1 is head-on, while the target-2 is crossing. In this case also, the own ship is a give-way vessel. As will be mentioned later, the present system has the basic problem-solving function to plan an appropriate avoidance route and to display it graphically in a form of bridge-operation-aid. In Figs.6 and 7, it is seen that the own ship first keeps the original route; however, on recognizing the risky situation and making decision to avoid the targets, a new avoidance route is designed and the own ship immediately starts tracking the newly planned route. The own ship's trajetory in a dotted line marked at an interval of 2 minutes. In the same figures, the own ship's avoidance way-points are shown with white squares. From these, it is found that the own ship kept the course very close to that of the newly planned avoidance route. The autonomous function of the present system is thus shown for planning the avoidance route and its tracking.
For developing the present system, simulation technique played actually an indispensable role in tuning up the knowledge-base of the system through trial and error/ or the spiral sequence of design evaluations.

2) Full-scale trial results

Full-scale tests were carried out off the Tokyo Bay, using a 425GT-training-ship Shioji-Maru of the Tokyo University of Mercantile Marine. A typical example of the trial result is shown in Fig.8 in a form of a bird's-eye-view (BEV) hard-copy of the area of the test operation. Its detail is referred to elucidation in the figure. The own ship's position and speed are based mainly on the Loran-C, and electromagnetic log, while those of the targets were obtained from the processed on-line data by an ARPA(automatic radar plotting aid). The number of the way-points in the avoidance route corresponds to the depth of search

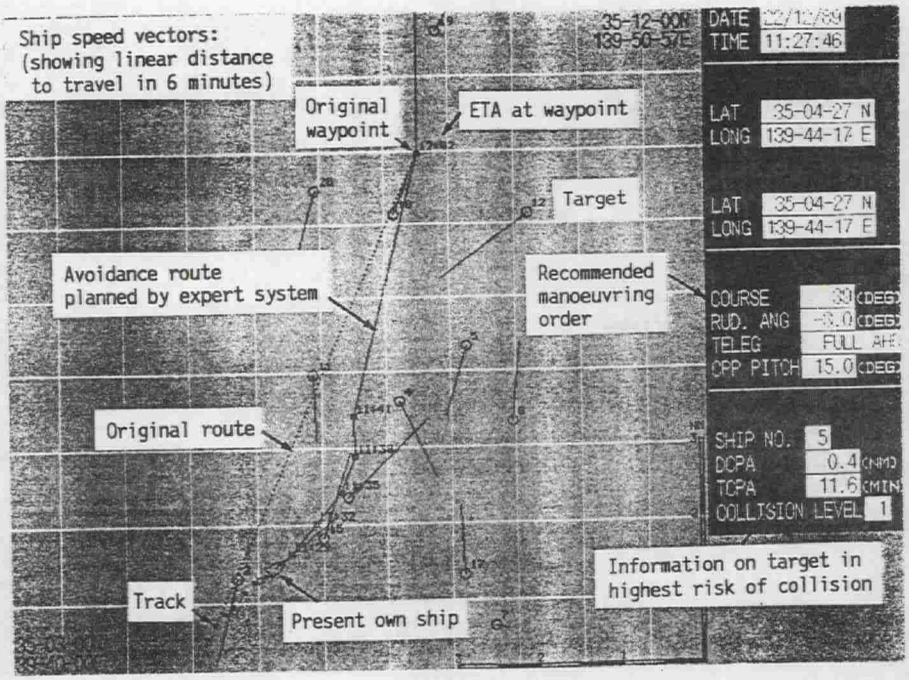

Fig.8 A typical full-scale test result

adopted for the present system. Based on the ARPA information, the maximum number of the targets displayable on the screen is 20 for the present system. An example of track-keeping test results is shown in another BEV record in Fig.9. Based on the position data by Loran-C, fairly good tracking performance is observed. Evaluation and control for tracking action are performed also by the knowledge. The target information in Fig.9 tells the fact that in the track-keeping tests, collision avoiding function of the system also was active. Prior to the full-scale collision avoidance tests, a preliminary tests were carried out. In this test, the own ship's response were examined by the use of virtual targets using the system's target-generating function. An example of such in-field simulation test result is shown in Fig.10 for the typical head-on and the crossing situations. This is almost exactly similar to the case shown in Fig.7. The own ship actually responds to the virtually-generated risk of collision; therefore, the function and effectiveness of the present system were conveniently tested without paying real risk of collision for the present.

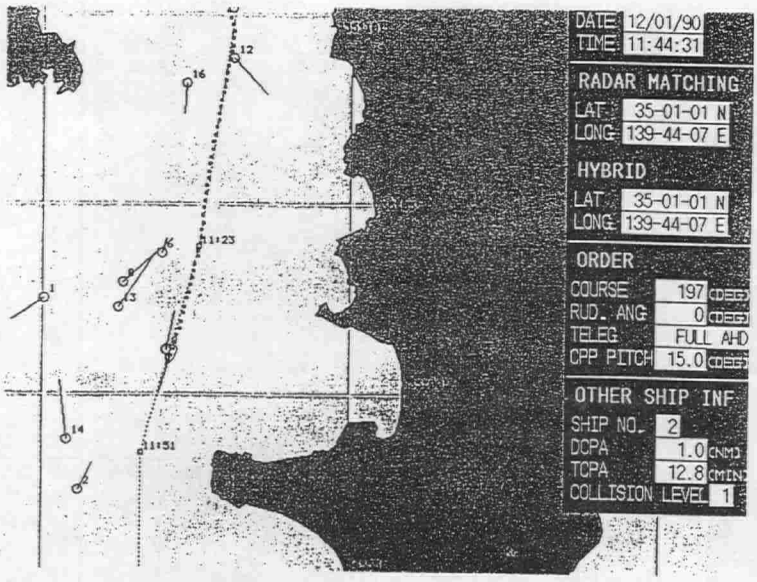

Fig.9 Automatic track-keeping test

The test for real targets were made by hunting situations in a real traffic. To make the tests effective for varied situations, the initial course was adjusted each time in accordance with changeable situation of meeting with the target(s) which appeared to be becoming available for the experiments. The tests were made persistently under natural encountering condition without using any means like a support vessel. An example of the test results for head-on/ crossing situation is shown in Fig.11 in a four continuous BEV-snapshots of the gaming situation. In the first shot, collision risk is mainly of the head-on target or targets. Four minutes later in the second shot, the first avoiding had been effective, however, there comes a crossing of the target-15. Six minutes later, collision risk had been shifted to another one, and further in the next five minutes, further shift of collision risk is observed. The corresponding pattern of meeting to the simple simulation in Figs.6 and 7 can be found; however, resulted response pattern may be understood as essentially the same as simulated. Another example of avoiding manoeuvre is shown in Fig.12 in similar kind of continuous snapshots as in the previous figure. This site is near the entrance to a highly congested

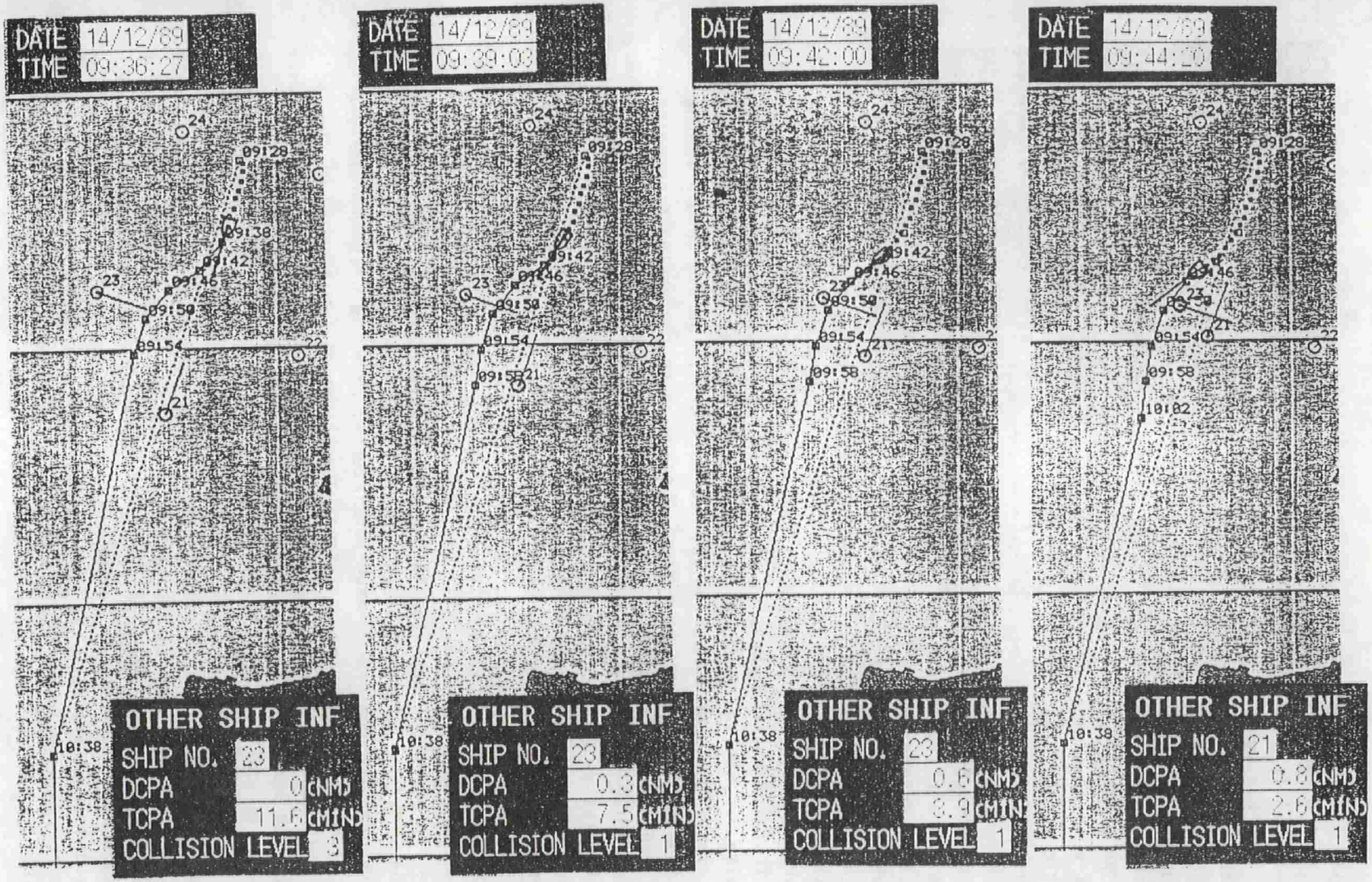

Fig.10 Full-scale trial simulation test for collision avoidance

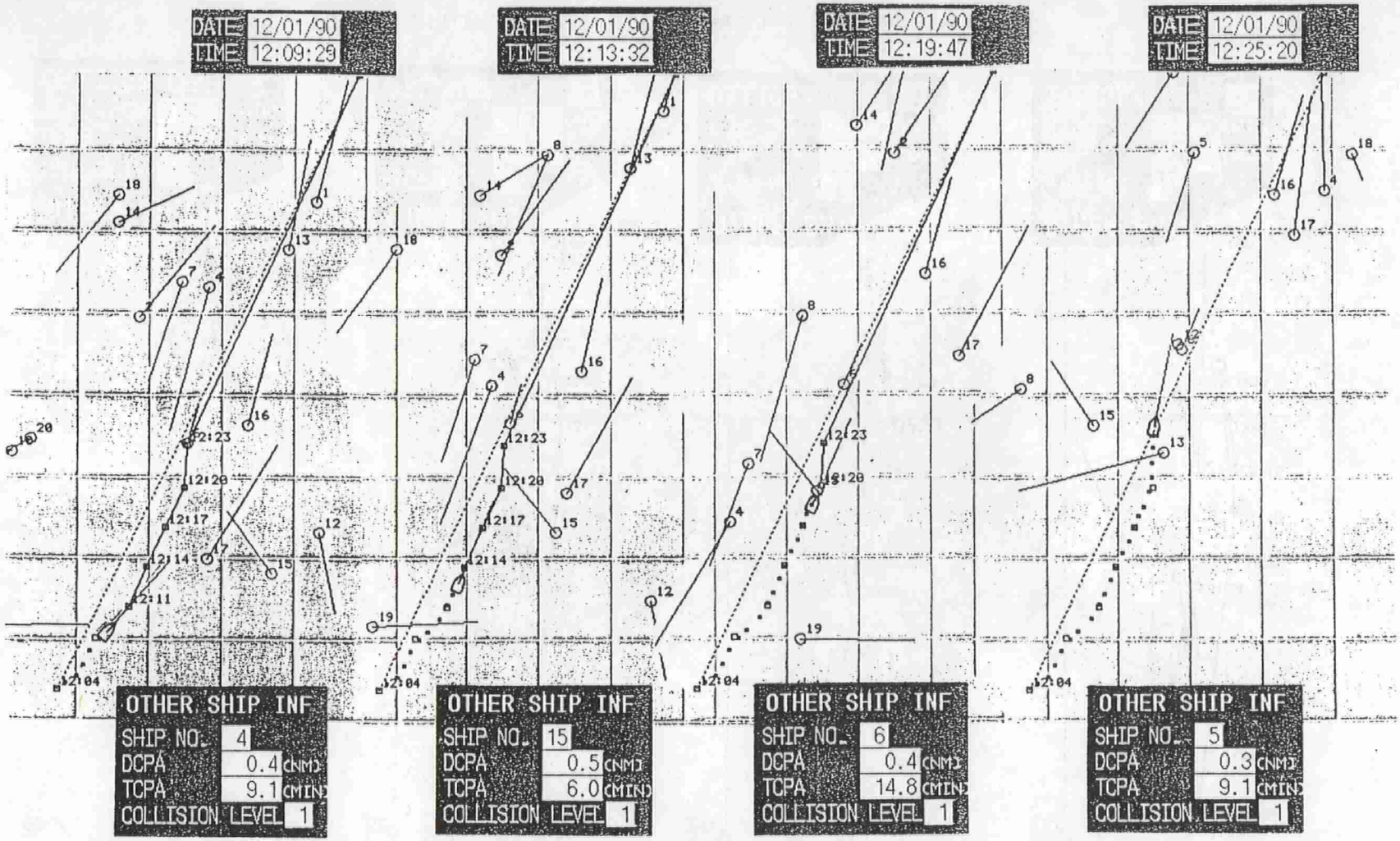

Fig.11 Full-scale test for head-on/ crossing situations

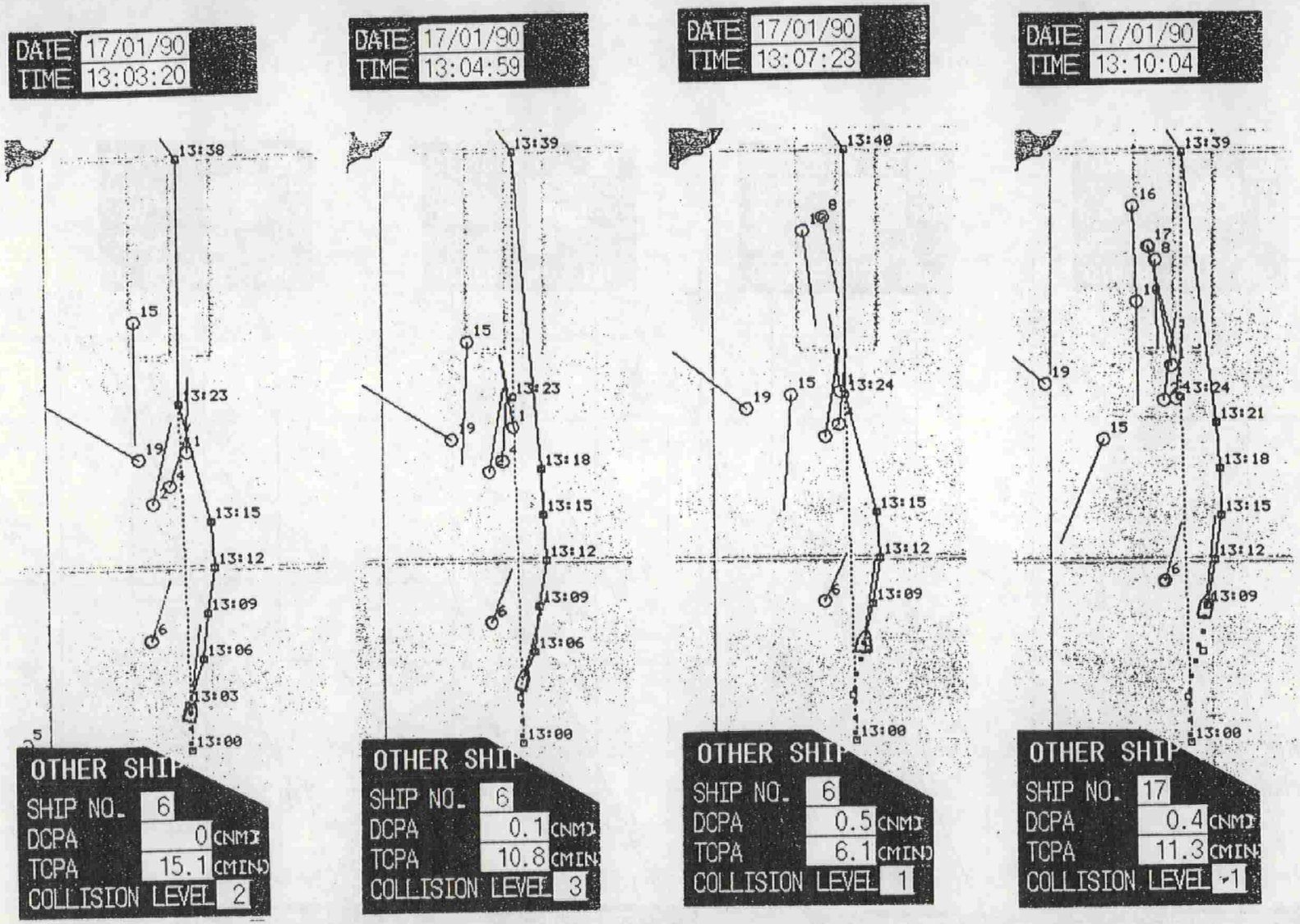

Fig.12 Full-scale test for over-taking/ head-on situations

traffic lane; therefore, there may be found a higher level of collision risk/ and higher possibility of propeller speed control in comparison with other cases. Anyway, the present system showed reasonable performance for the above cases, and still wider variety of traffic situations.

4. Steering in a knowledge-governed manoeuvre

In steering a ship with a knowledge-based navigation system like the present case, there must be an interaction of the conrol system and the knowledges. The time histories of the control variables must be reflecting its effect. In Figs.13 and 14, time-histories are shown for the own ship's speed, the heading, the rate-of-turn, and the rudder angle, corresponding each to the duration of time for each group of the snapshots shown in Figs.11 and 12. This kind of data must be full of interesting informations regarding the facts of the present system's interactions with the expertise of mariners.

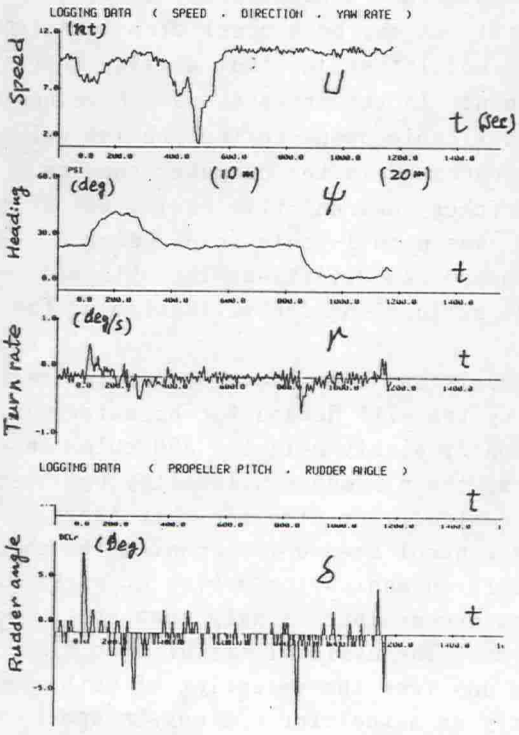

Fig.13 Time histories of collision avoidance (1); (Jan.12,'90)

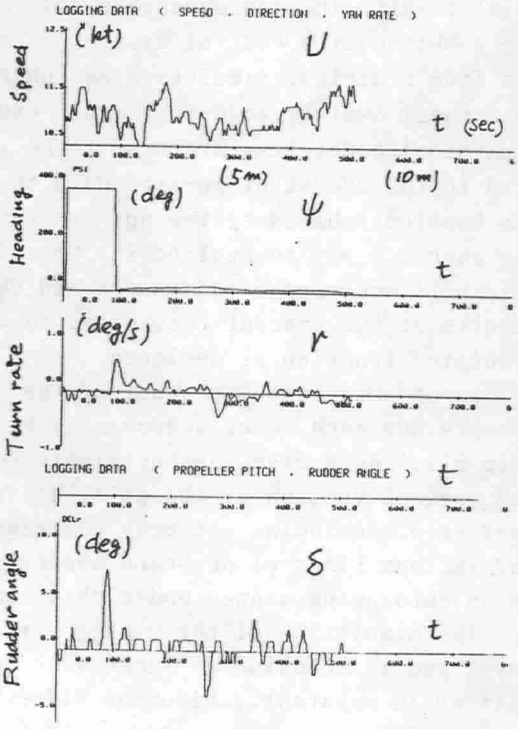

Fig.14 Time histories of collision avoidance (2); (Jan.17,'90)

Considering extremely changeable traffic conditions and related inference and the decision-making process to be eventually treated inclusively with ship speed and rudder control, there may be some kind of approach for better understanding of the intelligent control technique, and further, future gener ation manoeuvring control method.

5. On the use of knowledge-driven simulation

In the light of the increasing amount of experience in the field of knowledge-engineering applications, it appears that discussion may be needed regarding the future use of the knowledge-based-system-controlled manoeuvring simulations, and the significance of availability for their apparently normalized 'evaluation' and 'control' capabilities may be pointed out. Further, discussion is made regard-ing the utility of such type of the system used in a manoeuvring simulator as an automatic qualification screening tool either for ship's manoeuvring performance, or operational-skill. Or rather, as a simulation supervisory system for multi-lateral performance collation and ship design review/ evaluations in consideration of a ship's standardized manoeuvring and hazard avoiding functions.

6. Concluding remarks

With respect to a knowledge-based piloting system, considerations were made regarding its on-line real-time simulation and corresponding full-scale trial result. The indispensable role of simulation is emphasized. In developing a ship-motion control system, in general, it may be a ususl step to follow from a design, simulation and physical-model test (controllability test in a model basin), to a full-scale experiment. In the present case, however, a physical-model test appeared to be impracticable owing to the problem related to the amount of on-line data to be processed in the computer running the knowledge-based system and its LAN periphery on real-time basis. One of the shortest way to replace it, therefore, was a full-scale trial using a ship well-equipped with sensors and ship-board LAN utilities. The obtained results of the present case appeared to be suffuicient for validation of the simulated function as designed.

As an important byproduct of the study, it has been known as a practical example how much level a knowledge-based system will demand for an autonomous ship piloting system. Rather simple version of highly-selected 350 rules in the present version of the piloting system, the minimum availability has been confirmed, including not only the rudder control, but also for ship-speed, and various kinds of on-board supervisory control needed for running the ship in an autonomous manner under ship-land tele-communication system at work.

The simulation of the similar kind has become increasingly popular these days, and is arousing an increasing interest. The availability of such simulations is apparently becoming wider this day from the viewpoint of both hard- and soft-ware environment. Not merely as a tool for a study, a knowledge-based system-linked simulation technique appears to serve also for solving design and evaluation problems as an engineering methodology in wider sense. An additional comment was made from this viewpoint.

Acknowledgements

The present paper is an extra short note on simulation to a study on a piloting expert system. The basic part of the knowledge-based system for the present study had been developed in the Japan Shipbuilding Research Association Project for the 'Highly Automated Ship Operating System'[10] carried out

in 1983-88. The full-scale ship trial has been conducted as a Joint Tokyo University of Mercantile Marine/ Seven Japanese Shipbuilding Companies Project[8)9)] in 1989. The authors are indebted to the leaders and the members of the Committees concerned for their invaluable help and guide. Sincere thanks are also due to the members of the working-group in the subcommittee for their devoted cooperation in carrying out the present study.

References

1) Koyama,T. and Jin,Y.:On the Design of Marine Control System (1st & 2nd Report), Journ.of Naval Arch. ofJapan, Vol.162 & 164 (1987, 1988)
2) Tsuruta,S., Matsumura,N., Inaishi,M., Imazu,H., and Sugizaki,A.: Basic Research on an Expert System for Navigation at Sea, - Collision Avoidance Expert System -, Journ. Japan Inst. of Navigation, Vol.77, (Sept. 1987)
3) Grabowski,M.: The Pilot Expert System: Decision Support to Masters Pilots and Mates on Watch at Sea and Close Waters, No.MA-RD-840-88008 (Mar.1988)
4) Hasegawa,K., Kozuki,A., Muramatsu,T., Komine,H., and Watabe,Y.: Ship Auto-Navigation Fuzzy Expert System (SAFES), Journ. Soc. Naval Arch.of Japan, Vol.166, (Nov. 1989)
5) Fuwa,T., Koyama,T., Tanaka,K., and Fukuto,J.: A Knowledge-based System Applied to an Automatic Ship Navigation System, IFAC Workshop on Expert Systems and Signal Processing in Marine Automation, CAM'S 89,(1989)
6) Biancardi,C.G., Capecchi,M., Troiano,A., Trotta,A., and Vultaggio,M.: The Piloting Advisory System, Proc.MARSIM & ICSM 90, Joint Int.Conf.on Marine Simulators and Ship Manoeuvrability, Tokyo (June 1990)
7) Kose,K., Kojima,S., and Takahashi,K.: An Expert System for Collision Avoidance and Its Application to Marine Traffic Simulations Under Traffic Lane Regulations, Journ. Japan Inst. of Navigation, Vol.84, (Mar. 1991)
8) Iijima,Y., Hagiwara,H., and Kasai,H.: Results of Collision Avoidance Manoeuvre Experiments Using a Knowledge-based Autonomous Piloting System, Journ. of Navigation, Vol.44, No.2 (May 1991)
9) Kasai,H.Terada,Y., Matsuda,K., Furukawa,C., and Ishikawa,M.: Knowledge-based System Approach to Autonomous Piloting and Navigation Control of Ships, Mitsubishi Technical Review, Vol.29, No.3 (May 1991)
10) Shipbuilding Research Assoc. of Japan, Report of the Research and Development of Highly Automated Ship-operating System, (Mar. 1989))
11) Imazu,H.: On the Method of Collision Avoidance, Doctorate Dissertation, The Univesity of Tokyo, (1986)
12) Landsburg,A.C. Card,J.C., Crane Jr,J.C., Alman,P.R., Bertsche, W.R., Boylston,J.W., Eda,H., Keith,V.F., McCallum,I.R., Miller Jr,E.R., and Taplin,A.: Design and verification for Adequate Ship Maneuverability, Trans.SNAME, Vol.91, (1983)
13) Nobukawa,T., Kato,T., Motomura,K., and Yoshimura,Y.: Studies on Manoeuvrability Standards from the Viewpoint of Marine Pilot, Proc.MARSIM & ICSM 90, Tokyo, (June 1990)

ON THE MATHEMATICAL MODELLING OF SHIP MANOEUVRING UNDER ENVIRONMENTAL DISTURBANCES

STEFAN GROCHOWALSKI, INSTITUTE FOR MARINE DYNAMICS,
NATIONAL RESEARCH COUNCIL, CANADA

ABSTRACT

The methods used in predictions of ship manoeuvring under the influence of wind, current and waves are reviewed. The assumptions commonly made and the adequacy to the reality are discussed. The problem of the mathematical modelling of small ships manoeuvring in large waves is pointed out. A practical solution of the problem is suggested and the method for determination of the hydrodynamic derivatives in waves is proposed.

1. INTRODUCTION

Mathematical modelling of ship manoeuvring performance becomes increasingly important due to growing use of computer simulation techniques in the studies of ship operation in various situations, and due to dynamic development of the manoeuvring simulators technology. The simulation techniques provide an excellent tool for studies of ship manoeuvring characteristics, feasibility and safety of manoeuvres in restricted water, influence of design parameters and control devices on manoeuvring performance, design of ports and waterways, etc.

Obviously, the quality of the simulation is only as good as the mathematical model is adequate to the reality. Considerable efforts have been made in recent years by various authors to improve the mathematical models so, that they could better reflect all the factors which affect the manoeuvring characteristics. Majority of those efforts are dedicated to improvement of the mathematical representation of the hydrodynamics of the ship manoeuvring on calm water. The need for such improvements is caused by still insufficient accuracy

of predictions in many cases of ship manoeuvring on calm water, and is undisputable.

In the recent years, however, the influence of environmental conditions on ship manoeuvring performance gained lots of ship designers' and operators' attention. It is now recognized that in some cases, the influence of the environmental disturbances may severely affect ship manoeuvrability and control, creating dangerous situations or making the performance of the ship's mission impossible. Approaching an entrance to a port from the open sea during heavy storm, rescue operations in high seas, approaching an offshore platform in high waves and wind conditions, course keeping in waves, development of autopilot systems, avoidance of broaching in following and quartering seas - these are only few examples where the need for incorporation of the environmental disturbances into the mathematical models is evident.

A review and discussion of the presently used methodology in the mathematical modelling of ship manoeuvring under the influence of environmental disturbances, is the objective of this paper. Some suggestions of possible improvements are also presented. Current, wind, and waves are being considered here as the environmental influences.

2. CONVENTIONAL MODELLING OF SHIP MANOEUVRING UNDER ENVIRONMENTAL INFLUENCES

In the conventional approach which is commonly used at present, the mathematical models of ship manoeuvring under the influence of environmental conditions constitute a combination of

- a theoretical model representing manoeuvring motion on calm water, and
- the effects generated by the environmental forces, which are considered as the external forces applied to the ship performing manoeuvres on calm water.

The following fundamental assumptions are made in this approach :

- the hydrodynamic forces induced by ship manoeuvres, i.e. by ship's response to rudder action, and
- the hydrodynamic effects generated on the ship by the environmental forces,
  - are independent, and
  - do not affect each other.

With these assumptions, the manoeuvring motion in wind, waves and current can be obtained by superposition of all the responses to the individual action of each of the considered factors.

The manoeuvring motions of a ship on calm water is usually described in the form of a modular mathematical model, in which the total hydrodynamic forces and moment are split into separate parts, representing the hydrodynamic forces on the hull (subscript "h") forces generated by the propeller (subscript "p"), and forces generated by the rudder (subscript "r"). Then, the typical set of equations of motions in the horizontal plane, which is used for the simulation of manoeuvres in the environmental conditions discussed has a following form :

$$\begin{aligned} m(\dot{u}+vr-x_g r^2) &= X_h+X_p+X_r+X_{cur}+X_{wind}+X_{wave} \\ m(\dot{v}+ur+x_g \dot{r}) &= Y_h+Y_p+Y_r+Y_{cur}+Y_{wind}+Y_{wave} \\ I_z \dot{r}+mx_g(\dot{v}+ur) &= N_h+N_p+N_r+N_{cur}+N_{wind}+N_{wave} \end{aligned} \qquad (1)$$

First three components on the right hand side of each equation represent the hydrodynamic forces in manoeuvring on calm water (including interaction effects between them) and describe so-called inherent manoeuvrability, while the remaining three others represent the influence of the environmental disturbances.

In recent years, the equation of roll is usually included in the equations (1) in the recognition of the fact that the heel angle influences the other hydrodynamic forces on the hull, and thus affects the manoeuvring performance. This, however, does not change any principle of the approach, and for simplicity is not presented here.

The hydrodynamic forces acting on the hull are those acting during manoeuvres on calm water, and usually are presented in the form of a combination of linear and non-linear terms representing the hydrodynamic added masses, damping and cross coupling effects. The so-called derivative type of the hydrodynamic forces usually has the form :

$$\begin{aligned} X_h &= X_{\dot{u}}\dot{u}+(X_{vr}-Y_{\dot{v}})vr+X_{vv}v^2+X_{rr}r^2+\ldots.+X(u) \\ Y_h &= Y_{\dot{v}}\dot{v}+Y_{\dot{r}}\dot{r}+Y_v v+(Y_r+X_{\dot{u}}u)r+Y_{v|v|}v|v|+Y_{vr}v|r|+Y_{r|r|}r|r|+\ldots.. \\ N_h &= N_{\dot{r}}\dot{r}+N_{\dot{v}}\dot{v}+N_v v+N_r r+N_{r|r|}r|r|+N_{v|v|}v|v|+N_{r|v|}r|v|+\ldots.. \end{aligned} \qquad (2)$$

Various authors use various combination of the hydrodynamic derivatives depending on the methods used for their estimation and on the type of ship used in the simulations. If the hydrodynamic derivatives and the hydrodynamic forces generated by the rudder and by the propeller are estimated properly, the prediction of manoeuvring motion on calm water usually gives results good enough for practical purposes.

The assumption, which is being used in the simulations, that the hydrodynamic effects generated by ship manoeuvres and the effects caused by the external forces are independent and the principle of superposition can be applied, implies that all the hydrodynamic derivatives do not change with the action of external forces. This means that in practice, the hydrodynamic coefficients and the forces of the rudder and propeller actions are calculated (either theoretically or from the experiments) without any action of the external disturbances. The external forces are estimated separately and their effects are superimposed on the manoeuvring motion on calm water. Examples of such simulations are given in Fig.1.

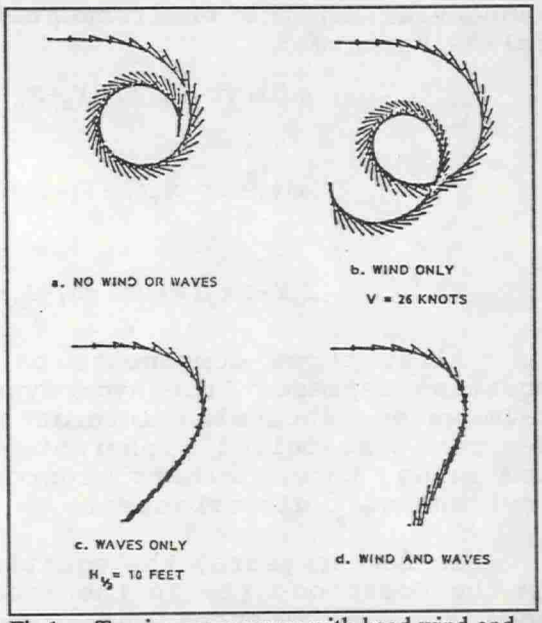

Fig.1 Turning manoeuvres with head wind and waves at ship speed 5 knots (R.A. Barr - discussion to [7])

Let us take a closer look at this methodology and examine when this approach is justified, and when it should be improved or changed.

3. WIND EFFECTS

The influence of wind on ship behaviour during manoeuvres and on course keeping is significant, in particular, in case of ships with high freeboard and large superstructure, ships carrying deck cargo and high-sided "volume carriers" like ro-ro ships, vehicles and gas carriers, container ships. Furthermore, during approaches to ports and operation in restricted areas (ports, harbours, inland waterways) where the ship speed is small, strong wind may severely affect manoeuvring performance.

Wind effects are included in the manoeuvring simulations in the form of external, aerodynamic forces and moment in the horizontal plane.

The wind speed can be considered as a composition of a steady wind with a constant mean speed, and of gusty fluctuations around the mean value. The mean speed varies with the height above the sea surface. The wind forces and turning moment are usually presented in the form :

$$X_{wind} = \frac{1}{2} C_x \varrho_a V_w^2 A_T$$

$$Y_{wind} = \frac{1}{2} C_y \varrho_a V_w^2 A_L \qquad (3)$$

$$N_{wind} = \frac{1}{2} C_n \varrho_a V_w^2 A_L X_L$$

where : A_T, A_L - transverse and longitudinal windage areas,
V_w - relative wind velocity
C_x, C_y, C_n - wind coefficients
X_L - distance between the point of application of the wind lateral force and the centre of application of the lateral hydrodynamic resistance of the submerged part of the hull.

The coefficients C_x, C_y, C_n depend on the wind direction and on the shape of the windage surface. The best way of evaluation of the wind forces and moment, is to measure the wind loading on a model of the above-water part of the ship in a wind tunnel. There are also semi-empirical methods developed by many authors on the basis of systematic wind testing of various ship superstructure forms. They provide possibility of calculation of the C_x, C_y, C_n coefficients and the total wind forces and moment. The methods yield good results if the above-water architecture of a ship is closed to those tested in the development of the semi-empirical method.

If the mathematical model of ship motion during manoeuvres is a 4-degree of freedom, or 6-degree model, the heeling moment due to lateral wind force should be included into the roll equation.

According to the assumption on wind velocity, the resultant X_{wind}, Y_{wind} forces and N_{wind} moment can be considered as a composition of a constant mean force (or moment), and the dependent on time fluctuation force (moment) around the mean value. The fluctuating forces can be calculated if the wind power spectrum is known.

In the prediction procedures of ship manoeuvres in the explicit form, the wind forces and moment are usually assumed to be constant. This allows to study the influence of wind speed and direction, and the shape of the above-water ship architecture on the manoeuvring characteristics of the ship.

However, in the studies of particular scenarios of ship navigating in restricted areas with strong wind, where the time-domain simulation is applied, the use of the fluctuating wind forces is advisable.

Wind fluctuations are not correlated with waves or with ship motion. Therefore, calculating the wind forces separately from the hydrodynamic forces and superimposing their effects on the manoeuvring motions of the ship, is justified and sound.

4. INFLUENCE OF CURRENT

In general, current affects the velocity distribution on the manoeuvring ship, changing the inflow velocities on the hull, propeller and rudder, and as a result, affects the hydrodynamic forces acting on the ship. These effects can be interpreted as the external forces generated by the current velocities, and superimposed on the hydrodynamic forces generated by the manoeuvring ship on calm water, or as a modification of the velocity field in which the ship is moving. In the later case, the hydrodynamic forces are calculated for the resultant relative velocities distribution. In practical applications this approach is usually adopted.

Two types of current are considered in the prediction of ship manoeuvrability: uniform and non-uniform (variable) current. In case of uniform current the relative velocities can be calculated as follows :

$$u_r = u - U_c \cos(\psi_c - \psi)$$

$$v_r = v - U_c \sin(\psi_c - \psi) \qquad (4)$$

where U_c and ψ_c are the current speed and direction.

The assumption of uniform current is commonly used in manoeuvring predictions. This simplifies calculations, and is particularly convenient when the hydrodynamic forces on the hull are expressed in the derivative form. Sometimes, current effects are split into the inertial and viscous effects [6], but viscous effects are usually evaluated by the relative velocity concept.

In many cases, the study of the influence of uniform current provide sufficient information from the practical point of view. Very often, however, the assumption on uniformity of current is too far from reality, and the local distribution of current velocities has to be taken into consideration.

If the mathematical model uses derivative representation of the hydrodynamic forces, the variable current has to be replaced by equivalent uniform distribution of the velocities. Various methods are used to achieve this.

Chislett and Wied (1985) proposed to use average value between the current components at the bow and stern. Assuming that current components (in the ship axis system) at the bow u_{cf}, v_{cf}, and at the stern u_{ca}, v_{ca} are known, the effective current components at the ship origin are assumed to be :

$$u_c = \frac{1}{2}(u_{cf}+u_{ca})$$

$$v_c = \frac{1}{2}(v_{cf}+v_{ca}) \qquad (5)$$

$$r_c = k(v_{cf}-v_{ca})/L_{pp}$$

where k = const $\cong$ 0.67

Wu and Li proposed (1990) the following formulas :

$$u_c = \frac{1}{L}\int_{-L/2}^{L/2} v_c' \cos\Theta_c' dx$$

$$v_c = \frac{1}{L}\int_{-L/2}^{L/2} v_c' \sin\Theta_c' dx \qquad (6)$$

$$r_c = \frac{12}{L^3}\int_{-L/2}^{L/2} v_c' \sin\Theta_c' x\, dx$$

where : $v_c'(x)$ and $\theta_c'(x)$ are the velocity and angle of current distribution along the centre plane of the ship,
u_c, v_c, r_c - equivalent uniform velocities and angular velocity of the current.

If the theoretical methods are applied for calculation of the hydrodynamic forces on the hull, then the local distribution of current velocities can be taken directly to the calculation of the local pressure distribution on the hull, and thus, there is no need for simplification in the form of equivalent uniform velocities.

The examples of the influence of current on the manoeuvring performance are presented on Fig.2 and Fig.3.

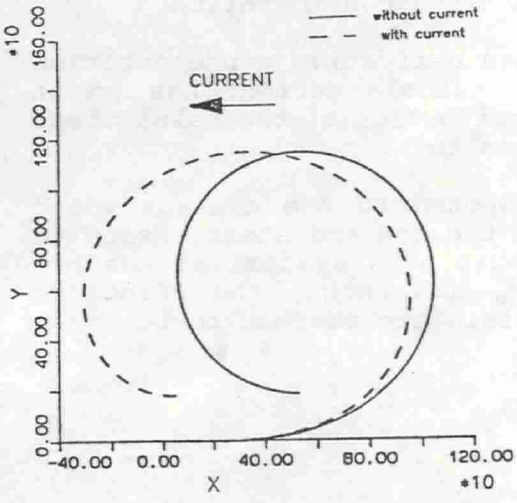

Fig.2 Turning circle test with current (from [15])

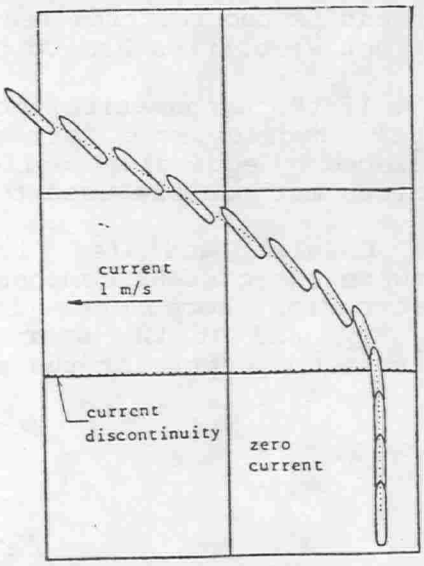

Fig.3 Change of heading induced by current gradient (ITTC'87 - Report of the Man. Committee

As the relative velocities concept is used in the calculation, the accuracy of the current effects is of the same order as the accuracy in the estimation of the hydrodynamic forces on calm water.

Although the methods for calculation of wind and current effects still require improvements, they give reasonably good results, and if cautiously used, they are satisfactory for the practical applications. Introduction of these effects in the simulation process may be considered as not a major problem.

5. SHIP MANOEUVRING IN WAVES

In the studies of the influence of waves on the manoeuvring ship, the wave exciting forces are considered as a superposition of

- first order hydrodynamic forces, proportional to wave amplitude (linear forces), oscillating with the encountered frequency, and
- second order, slowly-varying forces, proportional to square of the wave amplitude.

The time-average of the first order forces is zero, while the time-average of the non-linear hydrodynamic effects is not zero and constitutes the wave drifting force.

Ship response to the first order wave excitations is considered as high frequency oscillations in comparison with the manoeuvring motion, which is treated as a low frequency motion.

It is usually assumed that the low-frequency drifting force affects the manoeuvring motion and has to be included into the simulations as an external force and yaw moment, while the high-frequency exciting forces cause the six-degree of freedom motions around the slow manoeuvring motion, but do not affect the manoeuvring performance. Nonaka [10] proved that if the ship satisfies the slender body conditions and the viscous effects are neglected, then such an assumption is theoretically reasonable.

According to this philosophy, ship manoeuvring in waves is predicted by superposition of the manoeuvring motion on calm water under the influence of the wave drifting force and moment, and of ship oscillatory motions caused by wave exciting forces and moments. Both categories of motions are considered as independent. The oscillatory motions are predicted by use of the seakeeping methods, and the manoeuvring part by conventional equations of manoeuvring on calm water.

The wave exciting forces are calculated usually according to the potential theory, while the force induced by ship manoeuvres are still most reliably obtained from captive model tests. This is due to the problems with the theoretical calculation of hydrodynamic forces for very low frequencies and due to dominating viscous effects. However, the wave drift force and moment can be determined theoretically. There are several methods for the calculation of the mean, as well as the slowly-varying drift forces caused by waves.

The methodology discussed seems to work reasonably well in the case of very large ships, like tankers and bulkcarriers, operating in moderate seas. The gap between wave encountered frequencies and the frequency of ship response to the rudder action during manoeuvring is really large, and the assumptions on the non-interaction of the two categories of the hydrodynamic forces seems to be reasonable. Some published works confirm that in such cases, the results of simulations give sufficiently good agreement with the measured characteristics.

In the case of smaller ships, operating in high steep waves of the length not much exceeding one to two ship lengths, the presented theoretical model is not valid.

The wave action changes radically the shape and size of the immersed part of the hull. The instantaneous configuration of the hull immersed in wave is varying in time. If a small or mid size ship is operating in following or quartering seas, the wave encountered frequency is smaller. Together with the

smaller inertia and larger turning ability of small ships, this causes that the gap between the low frequency manoeuvring motion and the high frequency motions induced by waves becomes smaller or disappears. As a result, the change of the shape of the hull immersed in a wave may be slow and quite drastic (Fig.4).

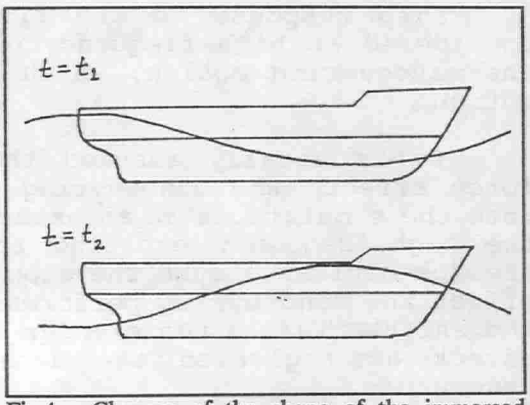

Fig.4 Changes of the shape of the immersed body in waves

Furthermore, the velocity distribution around the hull, and the inflow velocities to the propeller and rudder are modified significantly by the orbital velocities in the wave motion, and due to wave induced ship motions. This influences the fundamental hydrodynamic derivatives in the manoeuvring equations, and affects strongly the forces generated by the propeller and the rudder.

Changes of the immersed part of the hull, together with the effects of the wave induced water velocities, cause that it cannot be assumed that the hydrodynamic forces attributed to manoeuvring and determined for calm water, and the wave exciting forces do not depend upon each other and remain the same as if considered separately. They cannot be separated because there is a strong interference between the phenomena which generate them. During forced turn in a wave, the water velocities generated by forced turn interfere with velocities generated by wave itself and by the wave induced ship motions, and they cannot be separated. The ship is reacting to the resulting pressure distribution on the submerged part of the hull due to both motions simultaneously. These two categories of forces and motions cannot be treated independently, because they are interrelated and strongly affect each other.

Approach of a small or medium ship to a port from open sea in high waves can be a good illustration of such a situation. In order to keep the course to harbour entrance, the ship has to react with the rudder, then short fragments of manoeuvres are directly interfering with ship motions on the wave. The waves change the hydrodynamic derivatives in the manoeuvring equations and vice-versa: any manoeuvre influences the hydrodynamic exciting forces caused by waves.

In the recent years, some authors tried to improve the methods of prediction ship manoeuvring in waves by including:

- the influence of the circular wave velocities on the rudder forces, propeller and sometimes on the hydrodynamic derivatives,

- the influence of cross-couplings between roll, yaw and sway,
- increase of ship resistance in waves.

However, the main simplification remains: the final motion is achieved by a superposition of this modified model of ship manoeuvring motion on calm water with the motions caused by waves, determined separately.

In fact, the studies of ship manoeuvring in waves are usually dedicated rather to prediction of ship motions in waves when the ship is manoeuvring, or when the rudder is applied (like roll reduction by use of rudder), and not to the influence of waves on the manoeuvring performance. This is particularly the case, when the six-degree of freedom equations are used and the superposition principle applied in the simulations. So, this is rather analysis from the seakeeping perspective and not from manoeuvring.

The influence of waves on the hydrodynamic forces representing the effects generated by ship manoeuvres (hydrodynamic derivatives) has been recognized by researchers studying course keeping and broaching-to phenomena in following waves ([2], [3], [12]). They found that the derivatives depend on the position of the hull in the wave, and on ship heave and pitch. Also the influence of the orbital velocities was recognized [11]. Some captive model tests in following waves were performed in order to determine the dependence of the directional derivatives on the position of the wave crest with respect to the hull. The results confirm the general comments made here.

Mathematical modelling of ship performing manoeuvres in waves requires application of knowledge from two fields of ship hydrodynamics: manoeuvrability and seakeeping. Unfortunately, the methods used for the determination of the hydrodynamic forces acting on the ship are in both cases different and do not match each other.

The hydrodynamic forces induced by waves can be calculated theoretically by use of potential flow theories with addition of some semi-empirical methods for determination of the viscous damping. The categories of the calculated forces correspond to the physical nature of the forces. Currently used methods provide the results with the accuracy which can be considered as good enough for the practical predictions.

In the case of manoeuvring motion on calm water, theoretical methods of prediction of the hydrodynamic forces acting on the hull do not provide satisfactory results yet. In effect, a mathematical approximation of the total forces and moments in the form of combination of the hydrodynamic derivatives is still the best representation of these forces, and captive testing is still the best way of their

determination. This form of representation does not correspond to the physical components of the forces acting during manoeuvring, and they do not match the elements of the hydrodynamic forces calculated by potential theory methods. These two approaches are different and do not fit with each other.

What is the possible solution in this situation, if in addition to the above, the hydrodynamic forces generated by manoeuvres interfere strongly with the wave forces and should not be considered separately, as it has been pointed out earlier?

The best way to handle this problem, would be to calculate the total instantaneous pressure distribution on the hull and determine the total hydrodynamic forces by integration over the instantaneous surface of the immersed part of the ship in wave. Then, a time domain simulation, based on a mathematical model consisting of six-degree of freedom differential equation, should be applied, so that all the nonlinear effects and interactions between the motions could be included. Integration of these equations would give the total resultant manoeuvring motion of the ship in waves, without splitting it into the manoeuvring and seakeeping parts.

However, the problems with theoretical calculation of the viscous effects and hydrodynamic forces for very low frequencies do not allow to abandon the experiment methods yet, and thus maintaining the derivative form of the manoeuvring equations seems to be necessary. In order to include the wave effects into the hydrodynamic forces generated by manoeuvring, without separating them and superimposing, the mathematical model of ship manoeuvring in high waves has to be significantly modified.

The equations of the manoeuvring motion in waves in the horizontal plane should have the following form:

$$\begin{aligned} m(\dot{u}+vr-x_G r^2) &= X_H(f_w)+X_P(f_w)+X_R(f_w)+X_{CUR}+X_{WIND} \\ m(\dot{v}+ur+x_G\dot{r}) &= Y_H(f_w)+Y_P(f_w)+Y_R(f_w)+Y_{CUR}+Y_{WIND} \\ I_{zz}\dot{r}+mx_G(\dot{v}+ur) &= N_H(f_w)+N_P(f_w)+N_R(f_w)+N_{CUR}+N_{WIND} \end{aligned} \qquad (7)$$

where: f_w denotes wave parameters in general.

The hydrodynamic forces on the hull, propeller, rudder, and those generated by waves in the equations (1) have been replaced by relevant forces on the hull, propeller and rudder, but determined in waves. The forces defined this way, would be a function not only of the hull form, and accelerations and velocities induced by the manoeuvre, as it is on calm water, but also a function of wave parameters, such as:

- wave height,
- wave length (frequency),
- phase lag between the ship manoeuvring motion and the wave action,
- instantaneous ship position in the wave, etc.

As the forces on the hull during manoeuvres in waves can not be calculated theoretically yet, it seems that the practical solution would be to determine them by use of captive model testing in waves. Such tests would have to comprise standard manoeuvring Planar Motion Mechanism (PMM) tests, but carried out in waves. The presently used derivative type of the manoeuvring equations could be maintained. Appropriately measured hydrodynamic coefficients in waves should provide a good approximation of manoeuvring motion in waves.

The hydrodynamic forces on the hull could be expressed as follows:

$$X_H(f_w) = X_{\dot{u}}(f_w)\,\dot{u} + [X_{vr}(f_w) - Y_{\dot{v}}(f_w)]\,vr + X_{vv}(f_w)\,v^2 + \cdots + X(u, f_w)$$

$$Y_H(f_w) = Y_{\dot{v}}(f_w)\,\dot{v} + Y_{\dot{r}}(f_w)\,\dot{r} + Y_v(f_w)\,v + [Y_r(f_w) + X_{\dot{u}}(f_w)\,u]\,r$$

$$+ Y_{v|v|}(f_w)\,v|v| + Y_{vr}(f_w)\,v|r| + \cdots \qquad (8)$$

$$N_H(f_w) = N_{\dot{r}}(f_w)\,\dot{r} + N_{\dot{v}}(f_w)\,\dot{v} + N_v(f_w)\,v + N_r(f_w)\,r + N_{r|r|}(f_w)\,r|r|$$

$$+ N_{rv}(f_w)\,r|v| + N_{vv}(f_w)\,v|v| + \cdots$$

where the hydrodynamic derivatives are dependent on wave characteristics.

Obviously, the detailed methodology of this approach has yet to be developed. The program of captive model testing in waves would be far more complicated than the ordinary PMM or rotating arm testing on calm water. Also analysis of the measured results will be more laborious, as the hydrodynamic forces depend on the wave parameters, position of the hull in the wave, relative speed, heading angle, etc. However, by use of the multi-parameter interpolation, it should be possible to

of the multi-parameter interpolation, it should be possible to determine the hydrodynamic derivatives necessary for the mathematical model.

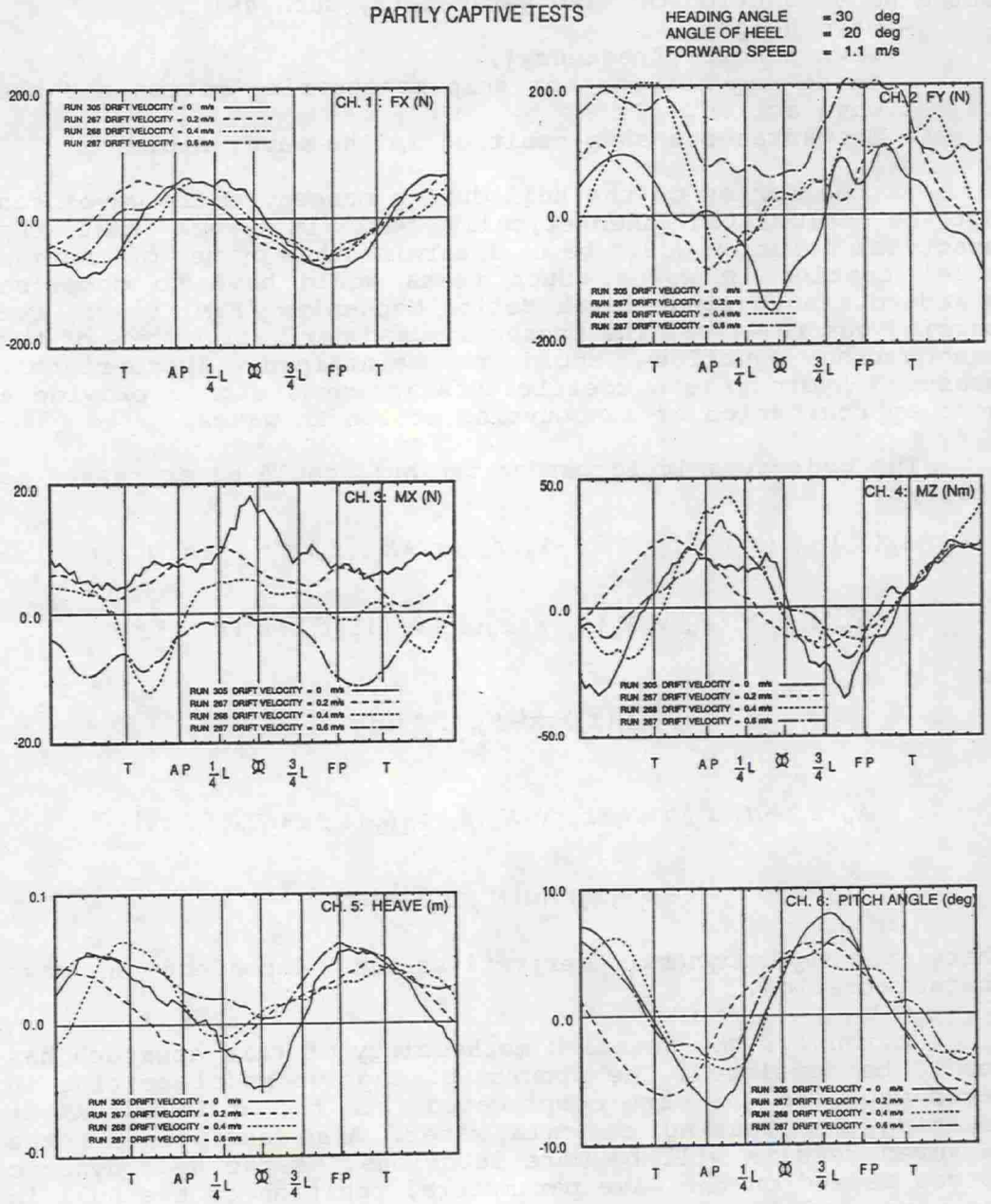

Fig.5 Influence of lateral drift on the hydrodynamic forces exerted on the hull by waves

Such a program of testing was never performed but it is feasible if appropriate facilities are available, i.e. a seakeeping basin or wide towing tank, equipped with a wavemaker, a carriage, and a PMM.

In order to illustrate the nature of such testing, an example of captive tests in steep waves is given in Fig.5. The model, fixed to the carriage at the heel angle 20 deg. and moving forward with the speed of 1.1 m/s at the heading angle 30 deg. relative to wave direction, was forced to drift with constant velocities. The measured forces and moments are presented in the form of time histories with marked positions of the wave crest with respect to the moving hull. Although the tests were carried out with the purpose of studying the extreme wave forces exerted on the ship in waves, they show the changes of the hydrodynamic forces on the hull when it was forced to drift laterally in waves.

The influence of lateral drift on the yaw moment M_z in waves of heading angle 30 deg. and 60 deg. is presented in Fig.6 and Fig.7.

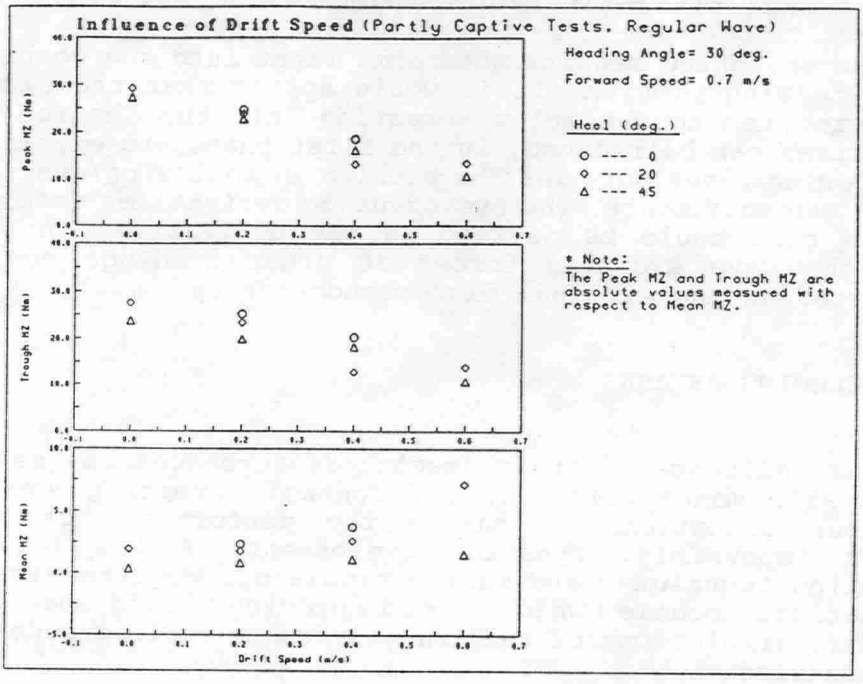

Fig.6 Influence of drift speed on yaw moment at heading angle 30 deg.

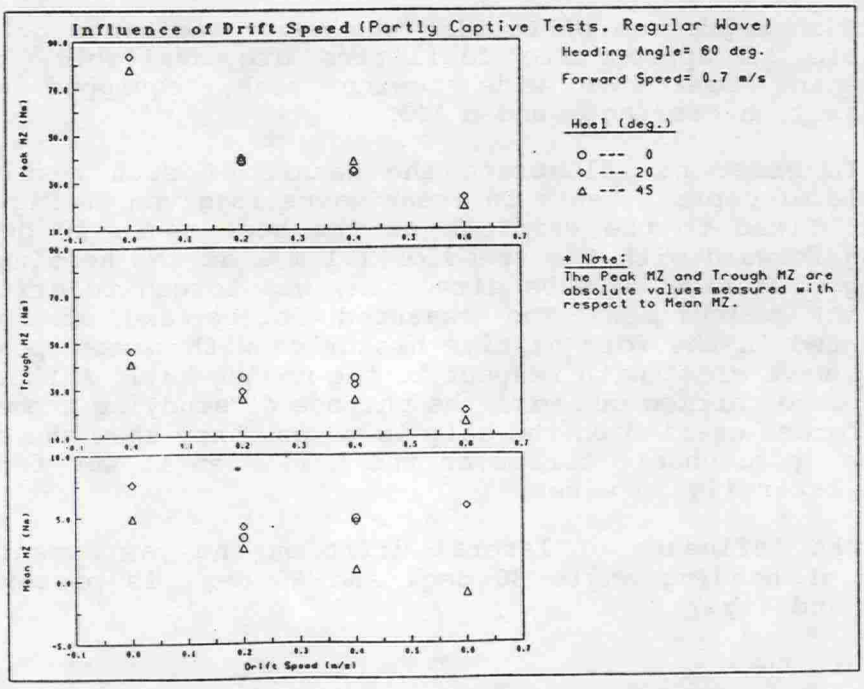

Fig.7 Influence of drift speed on yaw moment at heading angle 60 deg.

The presented results shed some light into the complexity of the testing program. If it would appear that the proposed procedure is too complex, testing of the hydrodynamic derivatives can be reduced, in the first phase, to experiments in following waves only, as the problem in following/quartering seas is the most acute. The hydrodynamic derivatives determined in this case could be defined as the derivatives in waves, while the wave exciting forces at other headings could be considered as the external disturbance forces.

6. CONCLUDING REMARKS

The influence of environmental disturbances may severely affect ship manoeuvrability and control, creating sometimes dangerous situations or making the performance of ship's mission impossible. Dynamic development of the numerical simulation techniques and marine simulators requires adequate mathematical models which could provide sound basis for realistic simulations of ship manoeuvres in various conditions and scenarios.

Present state of the art in the field of mathematical modelling of ship manoeuvring under the influence of wind, current and waves can be summarized as follows:

1. The methods used for modelling of ship manoeuvring under the influence of wind and current provide results reasonably

good for practical applications. The superposition principle used in the simulations is theoretically justifiable and sound. The accuracy of the predictions is of the same order as the predictions on calm water.

2. Simulation of ship manoeuvres in waves requires consideration of two qualitatively different cases:

   A) Manoeuvring of large ships in moderate seas. The commonly used assumption that the hydrodynamic forces caused by manoeuvres and those imposed by waves are independent and do not interact with each other, is reasonable in this instance. The prediction of ship manoeuvring characteristics by use of manoeuvring equations on calm water with addition of the second order wave drifting force and moment provides results good enough for practical purposes. Superposition of the low frequency manoeuvring motion with the higher frequency motions generated by waves simulates closely the resultant behaviour of a ship manoeuvring in waves.

   B) Smaller ships operating in high steep waves of the length between one to two ship lengths.

      Presently used theoretical model for manoeuvring in waves is not adequate, in particular, for following and quartering seas. Hydrodynamic forces generated by ship manoeuvres interact with the wave hydrodynamic forces and cannot be considered separately. The resultant ship movement during manoeuvring in waves should be predicted either by integration of the instantaneous pressure, resulting from the manoeuvre and wave action simultaneously, over the instantaneous immersed part of the hull in a wave, or the hydrodynamic forces in the conventional manoeuvring equations have to be made dependant on wave parameters and on the hull position in the wave.

The prediction of manoeuvring motion of smaller ships in large waves requires further detailed studies. As a practical solution to the problem, and idea of experimental determination of the hydrodynamic forces generated during manoeuvring in waves is proposed. The conventional equations of ship manoeuvring on calm water could be maintained, but the hydrodynamic derivatives have to represent the interaction between the manoeuvring ship and the waves. They can be determined by PMM captive model tests carried out in waves. The derivatives obtained would be dependent on wave parameters and on the position of the hull in the wave. The instantaneous values of the derivatives, necessary for time domain simulations, could be found by multiparameter interpolation.

The method has yet to be developed, but some captive model tests carried out in waves with a model forced to move with a

certain path seem to indicate that such an approach is feasible. It may provide the necessary data for practical predictions of the behaviour of a ship performing manoeuvres in large waves.

REFERENCES

1. M. Fujino - "An Introduction to the Prediction of Ship Manoeuvrability". Lectures at INSEAN, Rome, 1988.

2. M. Fujino, K. Yamasaki, Y. Ishii - "On the Stability Derivatives of a Ship Travelling in the Following Wave". Journ. Soc. Nav. Arch. Japan, vol. 152, Nov. 1982.

3. M. Hamamoto - "On the Hydrodynamic Derivatives for the Directional Stability of Ships in Following Seas" (Part 1 and 2). Journal of the Soc. Nav. Archit. Japan, vol. 130 and 133. 1971, 1973.

4. J.P. Hooft, J.B.M. Pieffers - "Manoeuvrability of Frigates in Waves". Marine Technology, vol. 25, No.4, Oct. 1988.

5. P. Kaplan, W.Y. Hwang, J.J Puglisi, C.A. Ross - "Wave Effects Included in Simulation - An Extension of Capability for Harbour and Waterway Development". STAR Symposium, Philadelphia, 1987.

6. M. Li, X.H. Wu - "Simulation Calculation and Comprehensive Assessment on Ship Manoeuvrabilities in Wind, Wave, Current and Shallow Water". MARSIM & ICSM'90, Tokyo 1990.

7. L.L. Martin - "Ship Manoeuvring and Control in Wind". SNAME Transactions, vol.88, 1980.

8. W.R. McCreight - "Ship Manoeuvring in Waves". 16th Naval Hydrodynamics Symposium, Berkely, 1986.

9. S. Motora, M. Fujino, T. Fuwa - "On the Mechanism of Broaching-to Phenomena". 2nd Intern. Conference on Stability of Ships and Ocean Vehicles, Tokyo, 1982.

10. K. Nonaka - "Manoeuvring Motion of a Ship in Waves". MARSIM & ICSM'90, Tokyo, 1990.

11. P. Ottoson, L. Bystrom - "Simulation of the Dynamics of a Ship Manoeuvring in Waves". SNAME Transactions, vol. 99, 1991.

12. M.R. Renilson, A. Driscoll - "Broaching - An Investigation

into the Loss of Directional Control in Severe Following Seas". RINA Spring Meeting, 1981.

13. Report of the Manoeuvrability Committee - 17th ITTC Conference, Göteborg, 1984.

14. Report of the Manoeuvrability Committee - 18th ITTC Conference, Kobe, 1987.

15. K.P. Rhee, C.K. Kim, C.M. Lee - "The Manoeuvring Motion of the MARAD Type Ship in Waves". MARSIM & ICSM'90, Tokyo 1990.

16. K.H. Son, K. Nomoto - "On the Coupled Motion of Steering and Rolling of a Ship in Following Seas". Journ. Soc. Nav. Arch. Japan, vol. 152, 1983.

17. D. Vassalos, C. Delvenakiotis - "The Effect of the Environment on the Stability and Turning of Ships". 2nd Intern. Conference on Manoeuvring and Control of Marine Craft, MCMC'92, Southampton, 1992.

A NEW COORDINATE SYSTEM AND THE EQUATIONS DESCRIBING MANOEUVRING MOTION OF A SHIP IN WAVES

MASAMI HAMAMOTO, OSAKA UNIVERSITY, JAPAN

Introduction

As well known, the equation of motion have been traditionally described on the basis of General body axes for manoeuvring motion of a ship in still water and on the basis of Earth fixed axes for seakeeping motion of a ship in waves. The hydrodynamic forces on a ship are usually formulated on the basis of the quasi-steady motion in time domain for manoeuvring motion and on the basis of the cyclic ship motion in frequency domain for seakeeping motion. The hydrostatic forces including Froude-Krylov force on a ship are expressed in term of the displacement and the same three Euler angles for both of manoeuvring and seakeeping motions.

The purpose of this paper is to investigate the phenomena in association with ship manoeuvring in waves by carring out numerical experiments using computer simulation. For this simulation program it is essential to find an equation of motions in a reasonable combination describing the manoeuvring motion in horizontal plane, rolling motion in lateral plane and seakeeping motion in vertical plane. The reasonable combination here is to find such a coordinate system as using the formula with respect to the hydrodynamic forces which have been developed in the field of manoeuvrability, stability and seakeeping. In general the ship motions are characterized as follows:

1) Maneuvring motions such as surge,sway and yaw in horizontal plane are responsive to external forces of zero and low-frequency range.
2) Rolling motion in the lateral plane depends on the natural frequency of roll and the change of restoring force due to the relative position of ship to wave.
3) Seakeeping motions such as heave and pitch in the vertical plane depend on oscillating frequency of a ship.

That is the main problem to be taken into account for the equations of motion.

A new coordinate system called Horizontal body axes are proposed for this problem. The equations of motion are derived on the basis of this coordinate system. Finally several examples of time domain simulation are shown for evaluating the effect of wave condition on the tactical diameter of turning test and the overshoot angles of zig-zag test. Because sea condition seems to be a important element for carring out the sea trials required by the manoeuvrability standard of IMO which is going to be finalized in 1993.

Horizontal Body Axes and Equations of Motion

Horizontal body axes $G-x',y',z'$ is shown in Fig.1 compared with the traditional coordinate systems which are called Earth fixed axes $O-\xi,\eta,\zeta$ and General body axes $G-x,y,z$. Let us consider now a ship of the mass m which is travelling with velocity $\mathbf{V}_G$ and moment of momentum $\mathbf{H}_G$ due to rotational velocity $\boldsymbol{\omega}$ of the ship. The equation of motion under the actions of certain force $\mathbf{F}$ and moment $\mathbf{G}$ are completely described by Newton's law of dynamics as follows :

$$\begin{aligned} m\frac{d\mathbf{V}_G}{dt} &= \mathbf{F} \\ \frac{d\mathbf{H}_G}{dt} &= \mathbf{G} \end{aligned} \tag{1}$$

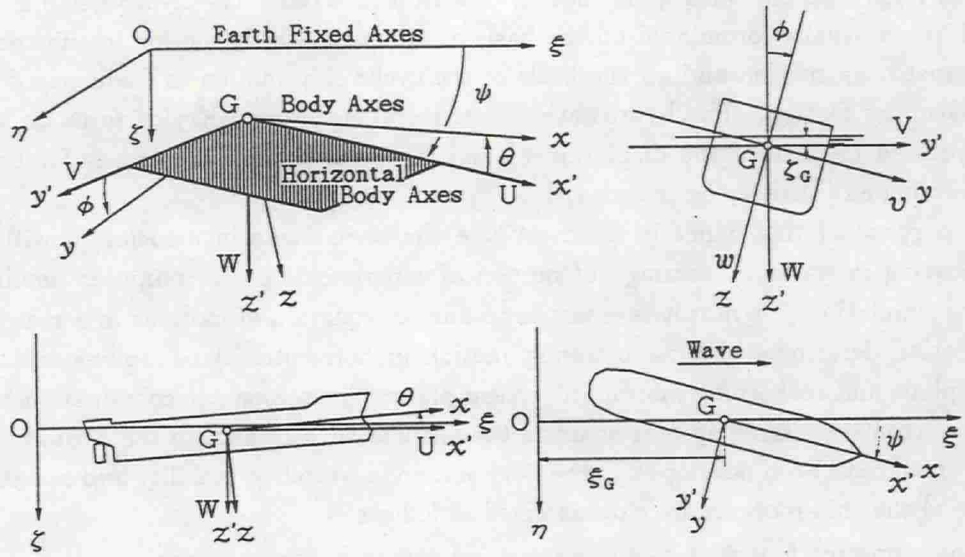

Fig.1 Coordinate Systems

Using the unit vectors $\mathbf{i},\mathbf{j},\mathbf{k}$ having the direction of Horizontal body axes $G-x',y',z'$, the translational velocity $\mathbf{V}_G$, the moment of momentum $\mathbf{H}_G$ and rotational velocity of ship $\boldsymbol{\omega}$ are decomposed as :

$$\begin{aligned} \mathbf{V}_G &= \mathbf{i}U+\mathbf{j}V+\mathbf{k}W \\ \mathbf{H}_G &= \mathbf{i}H_{x'}+\mathbf{j}H_{y'}+\mathbf{k}H_{z'} \\ \boldsymbol{\omega} &= \mathbf{i}\dot{\phi}+\mathbf{j}\dot{\theta}+\mathbf{k}\dot{\psi} \end{aligned} \tag{2}$$

where U and V are the forward and sway velocity in horizontal plane , W the heave velocity in vertical plane, $H_{x'},H_{y'}$ and $H_{z'}$ the moments of momentum about x',y' and z' axes, $\dot{\phi},\dot{\theta}$ and $\dot{\psi}$ the rotational velocity of Euler angles about x',y' and z' axes.

Then the acceleration is manipulated in the following ways

$$\begin{aligned}\frac{\mathrm{d}\mathbf{V}_G}{\mathrm{d}t} &= \mathbf{i}\dot{U} + \mathbf{j}\dot{V} + \mathbf{k}\dot{W} + U\frac{\mathrm{d}\mathbf{i}}{\mathrm{d}t} + V\frac{\mathrm{d}\mathbf{j}}{\mathrm{d}t} + W\frac{\mathrm{d}\mathbf{k}}{\mathrm{d}t} \\ &= \mathbf{i}(\dot{U} - V\dot{\psi}) + \mathbf{j}(\dot{V} + U\dot{\psi}) + \mathbf{k}\dot{W}\end{aligned} \tag{3}$$

where since Horizontal body axes have rotation about z' axis and no rotation about x' and y' axes but a ship have rotation about x' and y' axes, the time derivatives of the unit vectors are given by

$$\frac{\mathrm{d}\mathbf{i}}{\mathrm{d}t} = \mathbf{j}\dot{\psi}, \qquad \frac{\mathrm{d}\mathbf{j}}{\mathrm{d}t} = -\mathbf{i}\dot{\psi}, \qquad \frac{\mathrm{d}\mathbf{k}}{\mathrm{d}t} = 0 \tag{4}$$

So that, the rate of change of moment of momentum is

$$\frac{\mathrm{d}\mathbf{H}_G}{\mathrm{d}t} = \mathbf{i}(\dot{H}_{x'} - H_{y'}\dot{\psi}) + \mathbf{j}(\dot{H}_{y'} + H_{x'}\dot{\psi}) + \mathbf{k}\dot{H}_{z'} \tag{5}$$

Substituting Eq.(3) and Eq.(5) into Eq.(1), the equations of motion are translated into the scalar forms as :
Translational motions and Forces

$$\begin{aligned} m\,(\,\dot{U} - V\dot{\psi}\,) &= X' \\ m\,(\,\dot{V} + U\dot{\psi}\,) &= Y' \\ m\,\dot{W} &= Z' \end{aligned} \tag{6}$$

Rotational motions and Moments

$$\begin{aligned} \dot{H}_{x'} - H_{y'}\dot{\psi} &= K' \\ \dot{H}_{y'} + H_{x'}\dot{\psi} &= M' \\ \dot{H}_{z'} &= N' \end{aligned} \tag{7}$$

where X', Y' and Z' are the components of force in the direction of Horizontal body axes $G - x'y'z'$, and K', M' and N' the components of moment about x', y' and z' axes.
The components of moment of momentum may be written :

$$\begin{bmatrix} H_{x'} \\ H_{y'} \\ H_{z'} \end{bmatrix} = \begin{bmatrix} I_{x'x'} & -I_{x'y'} & -I_{x'z'} \\ -I_{y'x'} & I_{y'y'} & -I_{y'z'} \\ -I_{z'x'} & -I_{z'y'} & I_{z'z'} \end{bmatrix} \begin{bmatrix} \dot{\phi} \\ \dot{\theta} \\ \dot{\psi} \end{bmatrix} \tag{8}$$

The terms $I_{x'x'}, I_{y'y'}$ and $I_{z'z'}$ are called the moments of inertia with respect to x', y' and z' axes, and $I_{x'y'}, I_{y'z'}$ and $I_{z'x'}$ the products of inertia. They can be usually derived by integrals with respect to the mass element dm at the point x', y' and z' :

$$
\begin{aligned}
I_{x'x'} &= \int_m (y'^2 + z'^2)\, dm & I_{x'y'} &= \int_m x'y'\, dm \\
I_{y'y'} &= \int_m (z'^2 + x'^2)\, dm & I_{y'z'} &= \int_m y'z'\, dm \\
I_{z'z'} &= \int_m (x'^2 + y'^2)\, dm & I_{z'x'} &= \int_m z'x'\, dm
\end{aligned} \tag{9}
$$

Let us now determine them by using the transformation between Horizontal body axes and General body axes :

$$
\begin{bmatrix} x' \\ y' \\ z' \end{bmatrix} = \begin{bmatrix} \cos\theta & \sin\phi\sin\theta & \cos\phi\sin\theta \\ 0 & \cos\phi & -\sin\phi \\ -\sin\theta & \sin\phi\cos\theta & \cos\phi\cos\theta \end{bmatrix} \begin{bmatrix} x \\ y \\ z \end{bmatrix} \tag{10}
$$

Substituting Eq.(10) into Eq.(9), and manipulating the terms gives :
The moments of inertia

$$
\begin{aligned}
I_{x'x'} &= I_{xx}\cos^2\theta + (I_{zz}\cos^2\phi + I_{yy}\sin^2\phi)\sin^2\theta - 2I_{xz}\cos\phi\sin\theta\cos\theta \\
I_{y'y'} &= I_{yy}\cos^2\phi + I_{zz}\sin^2\phi \\
I_{z'z'} &= I_{xx}\sin^2\theta + (I_{zz}\cos^2\phi + I_{yy}\sin^2\phi)\cos^2\theta + 2I_{xz}\cos\phi\sin\theta\cos\theta
\end{aligned} \tag{11}
$$

The products of inertia

$$
\begin{aligned}
I_{x'y'} &= (I_{zz} - I_{yy})\sin\phi\cos\phi\sin\theta - I_{xz}\sin\phi\cos\theta \\
I_{y'z'} &= (I_{zz} - I_{yy})\sin\phi\cos\phi\cos\theta + I_{xz}\sin\phi\sin\theta \\
I_{z'x'} &= (I_{xx} - I_{zz}\cos^2\phi - I_{yy}\sin^2\phi)\sin\theta\cos\theta + I_{xz}\cos\phi\cos 2\theta
\end{aligned} \tag{12}
$$

The moments of inertia I_{xx}, I_{yy}, I_{zz} and product of inertia I_{xz} with respect to General body axes $G - x'y'z'$ are defined by

$$
\begin{aligned}
I_{xx} &= \int_m (y^2 + z^2)\, dm \\
I_{yy} &= \int_m (z^2 + x^2)\, dm \\
I_{zz} &= \int_m (x^2 + y^2)\, dm \\
I_{zx} &= \int_m zx\, dm
\end{aligned} \tag{13}
$$

where I_{xy} and I_{yz} are zero due to the symmetry of starboad and port side at upright condition.

For conventional ships the products of inertia are usually small and are invariably neglected. The moment of inertia I_{yy} is approximately equal to I_{zz}. The amplitude of pitching angle θ is usually smaller than 5 degree and may be assumed to be zero. So that putting $I_{xz} \cong 0, I_{yy} - I_{zz} \cong 0$ and $\theta \cong 0$ in Eq.(11), Eq.(8) reduces to :

$$\begin{bmatrix} H_{x'} \\ H_{y'} \\ H_{z'} \end{bmatrix} = \begin{bmatrix} I_{x'x'} & 0 & 0 \\ 0 & I_{y'y'} & 0 \\ 0 & 0 & I_{z'z'} \end{bmatrix} \begin{bmatrix} \dot{\phi} \\ \dot{\theta} \\ \dot{\psi} \end{bmatrix} \tag{14}$$

where

$$\begin{aligned} I_{x'x'} &\cong I_{xx} \\ I_{y'y'} &\cong I_{yy}\cos^2\phi + I_{zz}\sin^2\phi \\ I_{z'z'} &\cong I_{zz}\cos^2\phi + I_{yy}\sin^2\phi \end{aligned} \tag{15}$$

Since the moments and products of inertia with respect to Horizontal body axes are a function of pitching angle θ and rolling angle ϕ , the time derivatives for the component of moments of momentum

$$\begin{bmatrix} \dot{H}_{x'} \\ \dot{H}_{y'} \\ \dot{H}_{z'} \end{bmatrix} = \begin{bmatrix} I_{x'x'} & 0 & 0 \\ 0 & I_{y'y'} & 0 \\ 0 & 0 & I_{z'z'} \end{bmatrix} \begin{bmatrix} \ddot{\phi} \\ \ddot{\theta} \\ \ddot{\psi} \end{bmatrix} + \begin{bmatrix} 0 & 0 & -\dot{I}_{x'z'} \\ 0 & 0 & 0 \\ -\dot{I}_{z'x'} & 0 & 0 \end{bmatrix} \begin{bmatrix} \dot{\phi} \\ \dot{\theta} \\ \dot{\psi} \end{bmatrix} \tag{16}$$

where putting $I_{xz} \cong 0, I_{yy} - I_{zz} \cong 0$ and $\theta \cong 0$

$$\begin{aligned} \dot{I}_{x'x'} &= -2I_{xz}\dot{\theta}\cos\phi \cong 0 \\ \dot{I}_{y'y'} &= 2(I_{zz} - I_{yy})\dot{\phi}\sin\phi\cos\phi \cong 0 \\ \dot{I}_{z'z'} &= 2(I_{yy} - I_{zz})\dot{\phi}\sin\phi\cos\phi + 2I_{xz}\dot{\theta}\cos\phi \cong 0 \\ \dot{I}_{x'y'} &= (I_{zz} - I_{yy})\dot{\theta}\sin\phi\cos\phi - I_{xz}\dot{\phi}\cos\phi \cong 0 \\ \dot{I}_{y'z'} &= (I_{zz} - I_{yy})\dot{\phi}\cos 2\phi + I_{xz}\dot{\theta}\sin\phi \cong 0 \\ \dot{I}_{z'x'} &= I_{xx}\dot{\theta} - (I_{zz}\cos^2\phi + I_{yy}\sin^2\phi)\dot{\theta} - I_{xz}\dot{\phi}\sin\phi \\ &\cong (I_{xx} - I_{zz}\cos^2\phi - I_{yy}\sin^2\phi)\dot{\theta} \end{aligned} \tag{17}$$

Substituting Eq.(14) and Eq.(16) into Eq.(7), finally the equations of motion with respect to Horizontal body axes are obtained as :

Translational motions and forces

$$\begin{aligned} m\,(\,\dot{U}-V\dot{\psi}\,) &= X' \\ m\,(\,\dot{V}+U\dot{\psi}\,) &= Y' \\ m\,\dot{W} &= Z' \end{aligned} \tag{18}$$

Rotational motions and moments

$$\begin{aligned} I_{x'x'}\ddot{\phi}-I_{x'x'}\dot{\theta}\dot{\psi} &= K' \\ I_{y'y'}\ddot{\theta}+I_{x'x'}\dot{\psi}\dot{\phi} &= M' \\ I_{z'z'}\ddot{\psi}-(I_{x'x'}-I_{z'z'})\dot{\phi}\dot{\theta} &= N' \end{aligned} \tag{19}$$

Table 1 Traditional and New Equations of Motion

Earth Fixed Axes	General Body Axes	Horizontal Body Axes
Translational Motions and Forces $m\dot{\mathbf{V}}_G=\mathbf{F}$	Translational Motions and Forces $m(\dot{\mathbf{V}}_G+\omega\times\mathbf{V}_G)=\mathbf{F}$	Translational Motions and Forces $m(\dot{\mathbf{V}}_G+\mathrm{k}\dot{\psi}\times\mathbf{V}_G)=\mathbf{F}$
Rotational Motions and Moments $\dot{\mathbf{H}}_G=\mathbf{G}$	Rotational Motions and Moments $\dot{\mathbf{H}}_G+\omega\times\mathbf{H}_G=\mathbf{G}$	Rotational Motions and Moments $\dot{\mathbf{H}}_G+\mathrm{k}\dot{\psi}\times\mathbf{H}_G=\mathbf{G}$
where $\mathbf{V}_G = \mathrm{i}\dot{\xi}_G+\mathrm{j}\dot{\eta}_G+\mathrm{k}\dot{\zeta}_G$ $\mathbf{H}_G = \mathrm{i}H_x+\mathrm{j}H_y+\mathrm{k}H_z$ $\omega = \mathrm{i}\dot{\phi}+\mathrm{j}\dot{\theta}+\mathrm{k}\dot{\psi}$	where $\mathbf{V}_G = \mathrm{i}u+\mathrm{j}v+\mathrm{k}w$ $\mathbf{H}_G = \mathrm{i}H_x+\mathrm{j}H_y+\mathrm{k}H_z$ $\omega = \mathrm{i}p+\mathrm{j}q+\mathrm{k}r$	where $\mathbf{V}_G = \mathrm{i}U+\mathrm{j}V+\mathrm{k}W$ $\mathbf{H}_G = \mathrm{i}H_{x'}+\mathrm{j}H_{y'}+\mathrm{k}H_{z'}$ $\omega = \mathrm{i}\dot{\phi}+\mathrm{j}\dot{\theta}+\mathrm{k}\dot{\psi}$
Translational Motions and Forces $m\ddot{\xi}_G = F_\xi$ $m\ddot{\eta}_G = F_\eta$ $m\ddot{\zeta}_G = F_\zeta$	Translational Motions and Forces $m(\dot{u}+wq-vr) = X$ $m(\dot{v}+ur-wp) = Y$ $m(\dot{w}+vp-uq) = Z$	Translational Motions and Forces $m(\,\dot{U}-V\dot{\psi}\,) = X'$ $m(\,\dot{V}+U\dot{\psi}\,) = Y'$ $m\dot{W} = Z'$
Rotational Motions and Moments $I_{xx}\ddot{\phi} = G_\xi$ $I_{yy}\ddot{\theta} = G_\eta$ $I_{zz}\ddot{\psi} = G_\zeta$	Rotational Motions and Moments $I_{xx}\dot{p}-(I_{yy}-I_{zz})qr = K$ $I_{yy}\dot{q}-(I_{zz}-I_{xx})rp = M$ $I_{zz}\dot{r}-(I_{xx}-I_{yy})pq = N$	Rotational Motions and Moments $I_{x'x'}\ddot{\phi}-I_{x'x'}\dot{\theta}\dot{\psi} = K'$ $I_{y'y'}\ddot{\theta}+I_{x'x'}\dot{\psi}\dot{\phi} = M'$ $I_{z'z'}\ddot{\psi}-(I_{x'x'}-I_{z'z'})\dot{\phi}\dot{\theta} = N'$
where $I_{xx}=\int_m(y^2+z^2)\,dm$ $I_{yy}=\int_m(z^2+x^2)\,dm$ $I_{zz}=\int_m(x^2+y^2)\,dm$	where $p=\dot{\phi}-\dot{\psi}\sin\theta$ $q=\dot{\theta}\cos\phi+\dot{\psi}\sin\phi\cos\theta$ $r=\dot{\psi}\cos\phi\cos\theta-\dot{\theta}\sin\phi$	where $I_{x'x'}=I_{xx}$ $I_{y'y'}=I_{yy}\cos^2\phi+I_{zz}\sin^2\phi$ $I_{z'z'}=I_{zz}\cos^2\phi+I_{yy}\sin^2\phi$

The equations of motion with respect to Horizontal body axes are shown in table 1 compared with ones of Earth fixed and General body axes. In the translational motions of Eq.(18) the first and second equations are similar to the equation of manoeuvring motion

and the third equation is the same as the equation of seakeeping motion. In rotational motion of Eq.(19) the equations are little a bit different from one of Earth fixed axes. Based on the results mentioned above, these new equations of motion are not so much complicated in comparison with the traditional ones. So that, they would be available for practical use of experiments and computer simulation of ship motions in waves. Thus the next problem is to describe the hydrostatic force including Froude – Krylov force and the hydrodynamic force on a ship with respect to Horizontal body axes.

Hydrostatic Force including Froude – Krylov Force on a Ship

The hydrostatic pressure p including that of a sinusoidal waves ζ_w at any time t and at the position p and ζ_w are written in the following forms :

$$p = \rho g(\zeta_G - x'\theta + z') - \rho g a e^{-kd} \cos k(\xi_G + x' \cos\psi - y' \sin\psi - ct) \tag{20}$$

$$\zeta_w = -\zeta_G + x'\theta + a \cos k(\xi_G + x' \cos\psi - y' \sin\psi - ct) \tag{21}$$

where ρ is the density of water, k the wave number, a the amplitude of waves, c the phase velocity of wave and d the draft of a ship.
According to the hypothesis of Froude and Krylov, Froude–Krylov forces and moments with respect to Horizontal body axes are evaluated as follows :

Froude–Krylov forces

$$\begin{aligned}
X'_{F.K}(\zeta_G, \phi, \theta, \psi) &= -\iiint_V \frac{\partial p(F.K)}{\partial x'} \mathrm{d}V \\
&\cong \rho g\theta \int_L A(x)\mathrm{d}x - \rho g \cos\psi \int_L F(x) \sin k(\xi_G + x\cos\psi - ct)\mathrm{d}x \\
Y'_{F.K}(\zeta_G, \phi, \theta, \psi) &= -\iiint_V \frac{\partial p(F.K)}{\partial y'} \mathrm{d}V \\
&\cong \rho g \sin\psi \int_L F(x) \sin k(\xi_G + x\cos\psi - ct)\mathrm{d}x \\
Z'_{F.K}(\zeta_G, \phi, \theta, \psi) &= -\iiint_V \frac{\partial p(F.K)}{\partial z'} \mathrm{d}V \\
&\cong -\rho g \int_L A(x)\mathrm{d}x - \rho g \int_L F(x) \cos k(\xi_G + x\cos\psi - ct)\mathrm{d}x
\end{aligned} \tag{22}$$

Froude–Krylov moments

$$
\begin{aligned}
K'_{F.K}(\zeta_G,\phi,\theta,\psi) &= -\iiint_V [\, y'\frac{\partial p(F.K)}{\partial z'} - z'\frac{\partial p(F.K)}{\partial y'} \,]\mathrm{d}V \\
&\cong -\rho g \int_L y'_B A(x)\mathrm{d}x - \rho g \sin\psi \int_L F(x) z'_B \sin k(\xi_G + x\cos\psi - ct)\mathrm{d}x \\
M'_{F.K}(\zeta_G,\phi,\theta,\psi) &= -\iiint_V [\, z'\frac{\partial p(F.K)}{\partial x'} - x'\frac{\partial p(F.K)}{\partial z'} \,]\mathrm{d}V \\
&\cong \rho g \int_L x A(x)\mathrm{d}x + \rho g \int_L F(x) x \cos k(\xi_G + x\cos\psi - ct)\mathrm{d}x \\
N'_{F.K}(\zeta_G,\phi,\theta,\psi) &= -\iiint_V [\, x'\frac{\partial p(F.K)}{\partial y'} - y'\frac{\partial p(F.K)}{\partial x'} \,]\mathrm{d}V \\
&\cong \rho g \sin\psi \int_L F(x) x \sin k(\xi_G + x\cos\psi - ct)\mathrm{d}x
\end{aligned}
\tag{23}
$$

where $F(x)$ is the coefficient of pressure gradient at $A(x)$ section

$$
F(x) = ak\frac{\sin(k\frac{B(x)}{2}\sin\psi)}{k\frac{B(x)}{2}\sin\psi}e^{-kd}A(x) \tag{24}
$$

and $p(F.K)$ is the pressure over the entire immersed surface of the ship, $A(x)$ the immersed sectional area, $B(x)$ the breadth and V the immersed volume of the ship, (y'_B, z'_B) the center of buoyancy of immersed section.

Hydrodynamic Forces on a Ship

In general, the hydrodynamic forces consist of the added mass force and damping force. The hydrodynamic forces for manoeuvring motion can be treated as a quasi–steady motion and seakeeping motion will depend on the frequency of motion.

Hydrodyanamic force and moment for manoeuvring motion

According to MMG model, the added masses m_x, m_y , added moment of inertia J_{zz} and the linear derivatives Y_v, Y_r, N_v and N_r are described as follows:

$$
\begin{aligned}
X'(Manoeuvring) &= T(1-t) - R - X_{vr}V\dot{\psi} - \frac{1}{2}\rho A_R U_R^2 f_\alpha \sin\alpha_R \sin\delta \\
&\quad -m_{x'}\dot{U} + m_{y'}V\dot{\psi} + X'_{F.K}(\zeta_G,\phi,\theta,\psi)
\end{aligned}
\tag{25}
$$

$$
\begin{aligned}
Y'(Manoeuvring) &= -Y_v V + Y_r \dot{\psi} - \frac{1}{2}\rho A_R U_R^2 f_\alpha \sin\alpha_R \cos\delta \\
&\quad -m_{y'}\dot{V} - m_{x'} U\dot{\psi} + Y'_{F.K}(\zeta_G, \phi, \theta, \psi) + Y'_D(\dot{\zeta}_w, \ddot{\zeta}_w)
\end{aligned} \tag{26}
$$

$$
\begin{aligned}
N'(Manoeuvring) &= -N_v V - N_r \dot{\psi} + \frac{1}{2}\rho A_R l_R U_R^2 f_\alpha \sin\alpha_R \cos\delta \\
&\quad -J_{z'z'}\ddot{\psi} + N'_{F.K}(\zeta_G, \phi, \theta, \psi) + Y'_D(\dot{\zeta}_w, \ddot{\zeta}_w)
\end{aligned} \tag{27}
$$

where X_{vr}, Y_v, Y_r, N_v and N_r are the hydrodynamic derivatives of sway and yaw, A_R the rudder area, U_R and α_R effective inflow velocity and angle to rudder, f_α normal force coefficient of rudder force, δ rudder angle, l_R horizontal distance between rudder and C.G. of the ship, $Y_D(\dot{\zeta}_w, \ddot{\zeta}_w)$ and $N_D(\dot{\zeta}_w, \ddot{\zeta}_w)$ the differation forces and moments. Inoue's practical formulas are available for the linear derivatives Y_v, Y_r, N_v and N_r as follows :

$$
\begin{aligned}
Y_v &= \frac{\pi}{2}\left(\frac{2d}{L}\right) + 1.4 C_B \frac{B}{L} \\
N_v &= \frac{2d}{L} \\
Y_r &= \frac{\pi}{4}\left(\frac{2d}{L}\right) \\
N_r &= \frac{2d}{L}\left(0.54 - \frac{2d}{L}\right)
\end{aligned} \tag{28}
$$

and from strip method added mass m_y and added moment of inertia J_{zz} are evaluated as follows:

$$
\begin{aligned}
m_y &= \frac{\pi}{2}\rho \int_L d^2 C(x)\mathrm{d}x \\
J_{xx} &= \frac{\pi}{2}\rho \int_L x^2 d^2 C(x)\mathrm{d}x
\end{aligned} \tag{29}
$$

Hydrodyanamic moment for rolling motion

$$
\begin{aligned}
K'(Rolling) &= -J_{xx}(\ddot{\phi} - \dot{\psi}\dot{\theta}) - K_{\dot{\phi}}\dot{\phi} + m_{x'} z_G U\dot{\psi} + m_{y'} z_G \dot{V} \\
&\quad + K'_{F.K}(\zeta_G, \phi, \theta, \psi) + \frac{1}{2}\rho A_R h_R U_R^2 f_\alpha \sin\alpha_R \cos\delta
\end{aligned} \tag{30}
$$

where h_R vertical distance between rudder and C.G. of the ship, Takahashi's prctical formula is available for rolling coefficient $K_{\dot{\phi}}$

$$K_{\dot{\phi}} = 2\alpha_e(I_{xx} + J_{xx})\{1 + 0.8(1 - e^{-10F_n})\} \tag{31}$$

$$\alpha_e = \frac{2}{T_\phi} N\phi_m \tag{32}$$

Hydrodyanamic force and moment for seakeeping motion

$$\begin{aligned} Z'(Seakeeping) &= -m_z\ddot{\zeta}_G - Z'_{\dot{\zeta}_G}\dot{\zeta}_G + Z'_{\ddot{\theta}}\ddot{\theta} + Z'_{\dot{\theta}}\dot{\theta} \\ &\quad + Z'_{F.K}(\zeta_G, \phi, \theta, \psi) + Z'_D(\dot{\zeta}_w, \ddot{\zeta}_w) \\ M'(Seakeeping) &= -J_{y'y'}\ddot{\theta} - J_{x'x'}\dot{\phi}\dot{\psi} - M'_{\dot{\zeta}_G}\ddot{\zeta}_G - M'_{\dot{\zeta}_G}\dot{\zeta}_G - M'_{\dot{\theta}}\dot{\theta} \\ &\quad + M'_{F.K}(\zeta_G, \phi, \theta, \psi) + M'_D(\dot{\zeta}_w, \ddot{\zeta}_w) \end{aligned} \tag{33}$$

where the hydrodynamic coefficients of Eq.(33) are obtained from the ordinary strip method (OSM) and will depend on the frequency of ship motion. But they are approximately evaluated by the coefficient at the natural frequency of heave and pitch. m_z and $J_{z'z'}$ are added mass and added moment of inertia respectively.

Examples of Computer Simulation.

For evaluating the effect of wave condition on the tactical diameter of turning test and overshoot angles of zig–zag test, the time domain simulation for the container ship shown in Fig.2 by using Eq.(18) and Eq.(19). Fig.3 stands for the results of turning test of the ship in still water and in waves having wave height $2.3m$ and $3.45m$ of length $115m$. Fig.4 througth Fig.7 stands for the results of zig–zag test of the ship in still water and in waves having wave height $1.15m, 2.3m, 3.45m$ and $4.6m$ of length $115m$ at heading angle $\psi = 0$ degree. Fig.8 througth Fig.11 stands for the results of zig–zag test of the ship in still water and in waves having wave height $1.15m, 2.3m, 3.45m$ and $4.6m$ of length $115m$ at heading angle $\psi = 30$ degrees. Fig.12 througth Fig.15 stands for the results of zig–zag test of the ship in still water and in waves having wave height $1.15m, 2.3m, 3.45m$ and $4.6m$ of length $115m$ at heading angle $\psi = 60$ degrees.

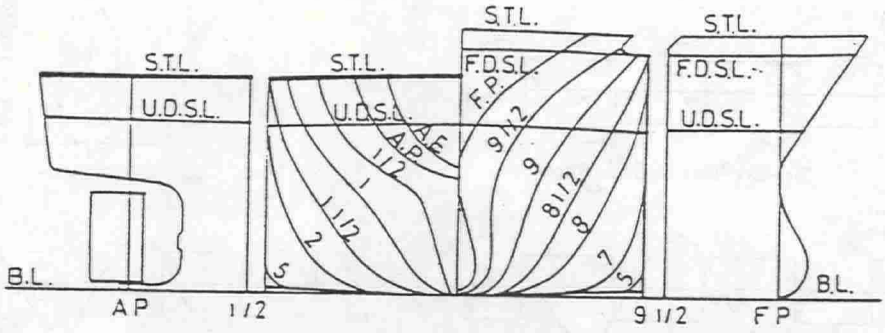

$L = 115(m)$ $B = 19(m)$ $d = 6.4(m)$ $\Delta = 10135(ton)$

Fig.2 Body Plan of 4990 GT Container Ship

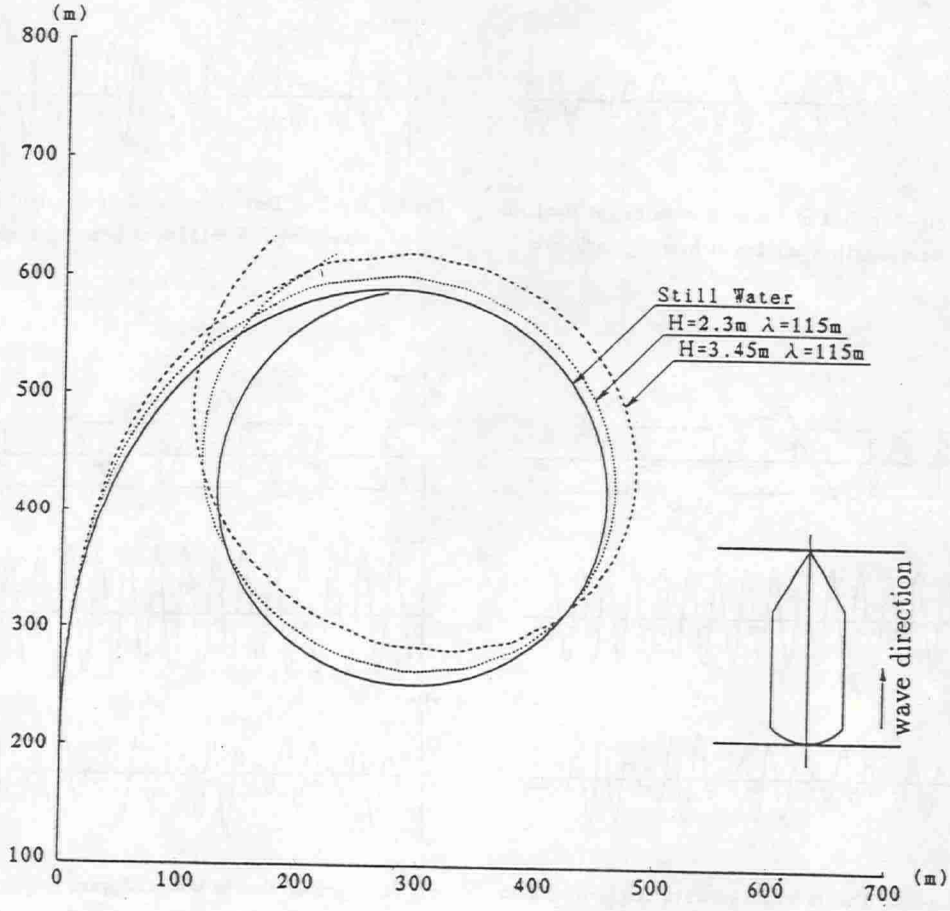

Fig.3 Turning Tests in Still Water and in Waves having Wave Height 2.3m and 3.45m

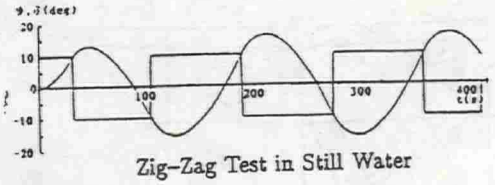

Zig–Zag Test in Still Water

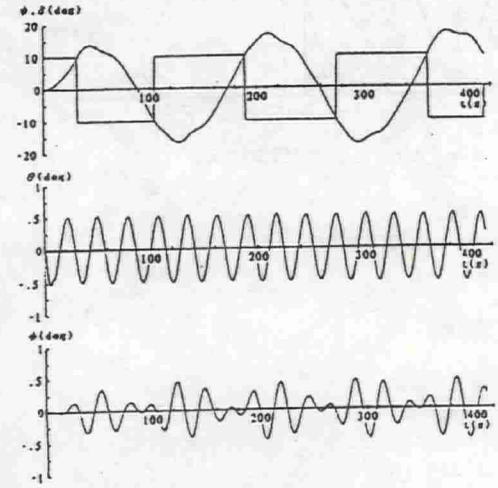

Fig.4 Zig–Zag Test in waves of wave height H=1.15m wave length λ =115m at heading angle $\psi = 0°$

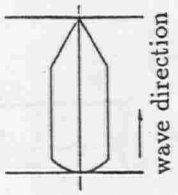

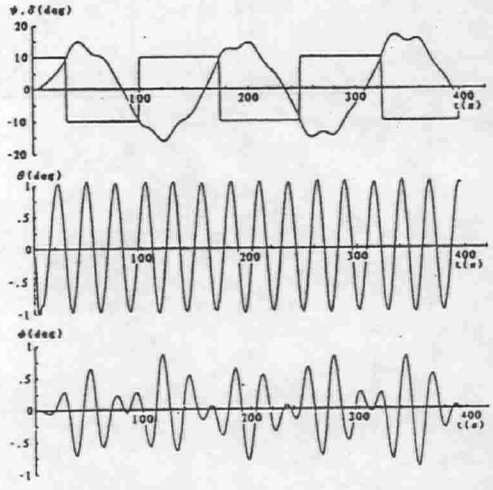

Fig.5 Zig–Zag Test in waves of wave height H=2.3m wave length λ =115m at heading angle $\psi = 0°$

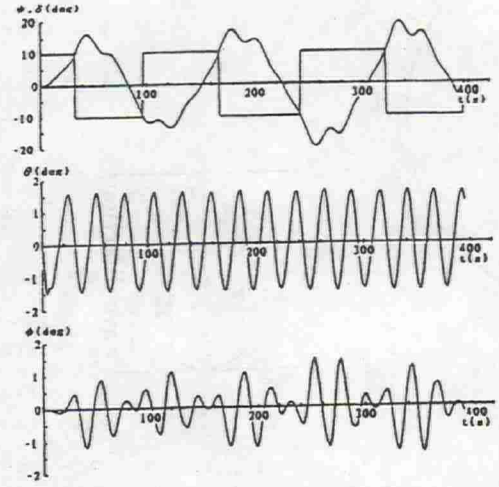

Fig.6 Zig–Zag Test in waves of wave height H=3.45m wave length λ =115m at heading angle $\psi = 0°$

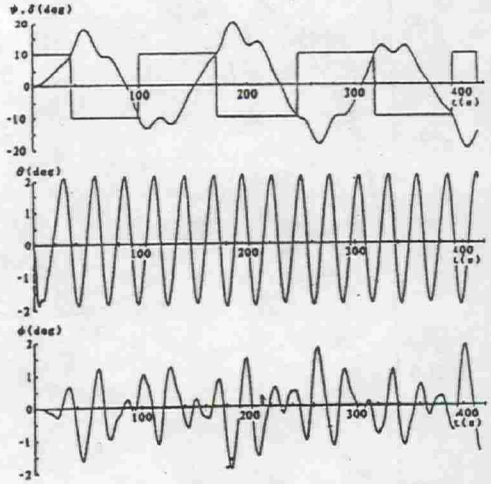

Fig.7 Zig–Zag Test in waves of wave height H=4.6m wave length λ =115m at heading angle $\psi = 0°$

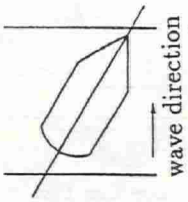

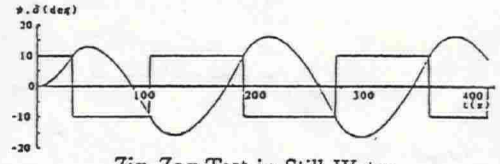

Zig–Zag Test in Still Water

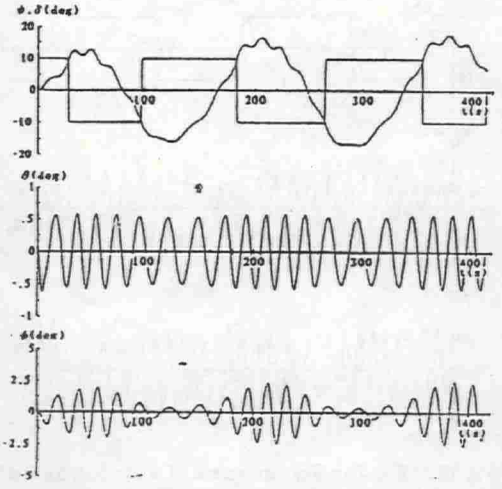

Fig.8 Zig–Zag Test in waves of wave height H=1.15m wave length λ =115m at heading angle $\psi = 30°$

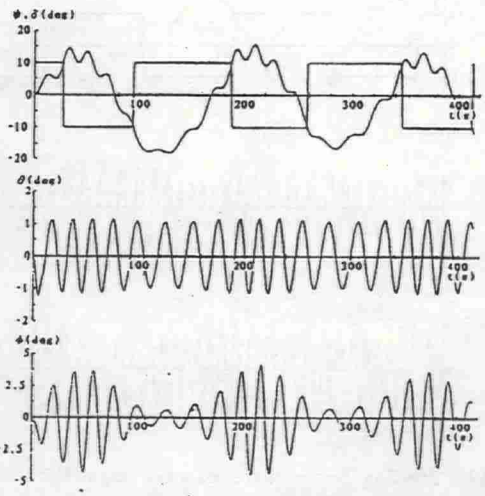

Fig.9 Zig–Zag Test in waves of wave height H=2.3m wave length λ =115m at heading angle $\psi = 30°$

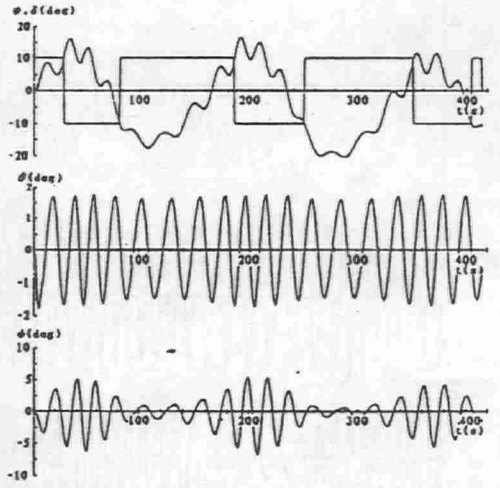

Fig.10 Zig–Zag Test in waves of wave height H=3.45m wave length λ =115m at heading angle $\psi = 30°$

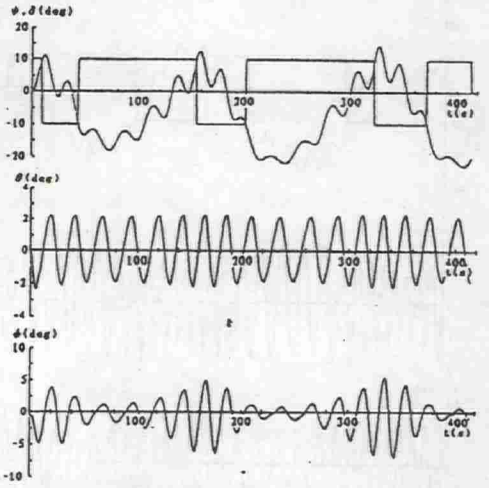

Fig.11 Zig–Zag Test in waves of wave height H=4.6m wave length λ =115m at heading angle $\psi = 30°$

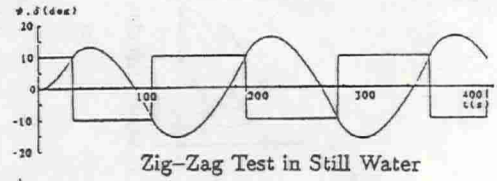

Zig–Zag Test in Still Water

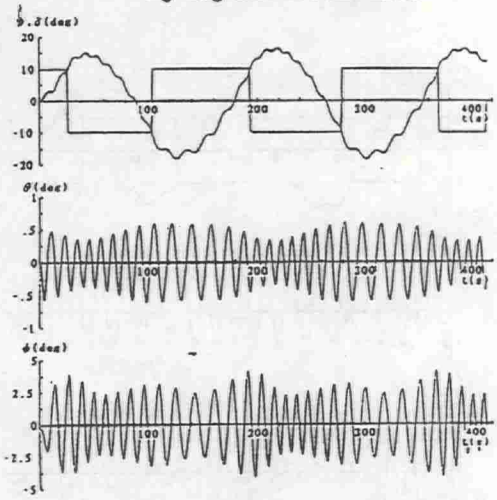

Fig.12 Zig–Zag Test in waves of wave height H=1.15m wave length λ =115m at heading angle $\psi = 60°$

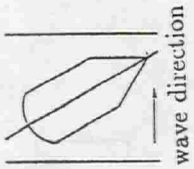

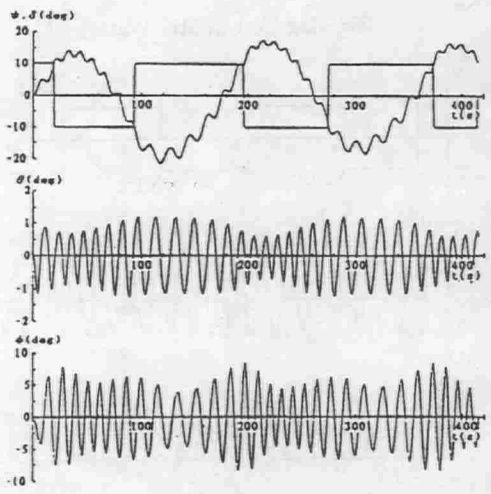

Fig.13 Zig–Zag Test in waves of wave height H=2.3m wave length λ =115m at heading angle $\psi = 60°$

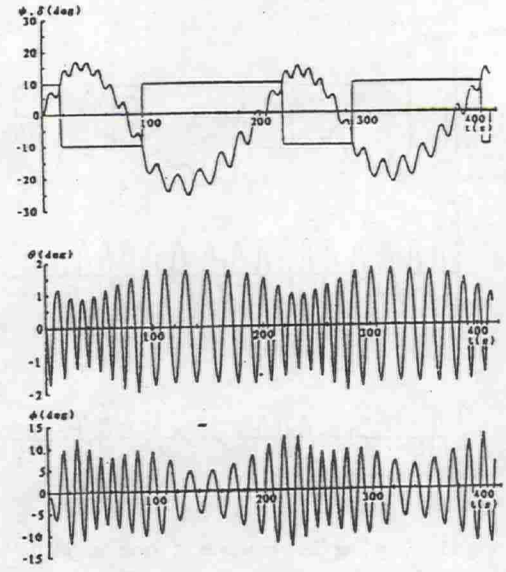

Fig.14 Zig–Zag Test in waves of wave height H=3.45m wave length λ =115m at heading angle $\psi = 60°$

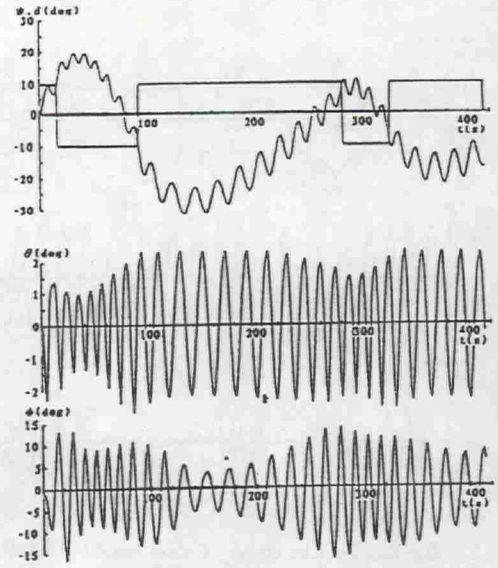

Fig.15 Zig–Zag Test in waves of wave height H=4.6m wave length λ =115m at heading angle $\psi = 60°$

Conclusions

As well known the equations of motion and the hydrodynamic model have been traditionally described with respect to the body axes coordinate system for maneouvring motion and earth axes coordinate system for seakeeping motions. However there are some problems in dealing with the hydrodynamic coefficients for time-domain simulation of ship motions having six degrees of freedom. For this program new equations of motion are derived for the manoeuvring motion of a ship in waves. Froude–Krylov forces on a ship are evaluated on the basis of Horizontal body axes. It will be an important problem for complete equations of motion to investigate the wave effect on the linear derivatives of manoeuvring motion. Finally several examples of time domain simulation are carried out for evaluating the effect of wave condition on the tactical diameter of turning test and the overshoot angles of zig–zag test.

REFERENCES

1. Tasai, F., Damping Force and Added Mass of Ships Heaving and Pitching (Continued), Trans. of the West-Japan Soc. of Naval Arch., Vol.21, 1961.

2. Du Cane, P., Goodrich, gG.J., The Following Sea, Broaching and Surging, Trans. RINA, Vol.104, April, 1962.

3. Paulling, J.R., Oakley, and Wood, P.A. "Ship Capsizing in Heavy Seas: The Correlation of theory and Experiments". International Conference on Stability of Ships and Ocean Vehicles. University of Strathclyde, 1975

4. Inoue, S., Kijima, K. and Moriyama,F., "Presumption of Hydrodynamic Derivatives on Ship Manoeuvring in Trimmed Condition" Trans. of west–japan Society of Naval Architects. No. 55, March 1978.

5. Renilson, M.R., Driscoll, A., Broaching-An Investigation into the Loss of Directional Control in Severe Following Seas, Spring Meeting RINA, 1981.

6. Motora, S., Fujino, M., Fuwa, T., On the Mechanism of Broaching-to Phenomena, STABILITY'82, 1982.

7. Ohkusu, M., Prediction of Wave Forces in a Ship Running in a Following Waves with Very Low Encounter Frequency, J. of Soc. of Naval Arch. Vol.159, 1986.

8. Hamamoto, M., Akiyoshi, T., Study on Ship Motions and Capsizing in Following Seas (1st Report), J. of Soc. of Naval Arch. Vol.163, 1988.

9. Hamamoto, M., Shirai, T., Study on Ship Motions and Capsizing in Following Seas (2nd Report), J. of Soc. of Naval Arch. Vol.165, 1989.

10. Jan O. de Kat, J. Randolph Paulling, The Simulation of Ship Motions and Capsizing in Severe Seas, The Society of Naval Architects and Marine Engineers, 1989.

11. Hamamoto, M., Kim, Y.S., Uwatoko, K., Study on Ship Motions and Capsizing in Following Seas (2nd Report), J. of Soc. of Naval Arch. Vol.165, 1989.

12. M.S,Chislet , The Addition of a Heel–Roll Servo Mechanism to the DMI Horizontal Planar Motion Mechanism, MARSIM and ICSM 90 Tokyo, Japan,1990

13. Hamamoto, M., Tsukasa, Y., An analysis of side force and yaw moment on a ship in quartering waves, J. of Soc. of Naval Arch. Vol.171, 1992

14. Hamamoto, M., Kim, Y.S., Matsuda, A., Kotani, H., An Analysis of a Ship Capsizing in Quarting Seas , J. of Soc. of Naval Arch. Vol.172, 1992

15. Hamamoto, M., Saito, K., Time-domain Analysis of Ship Motions in following Waves, 11th Austrarian Fluid Mechanis Conf. 1992

THE DATABASE SYSTEM APPROACH FOR THE MANEUVERABILITY PREDICTION AND THE DIRECTION OF THE FUTURE RESEARCH

KUNIJI KOSE, HIROSHIMA UNIVERSITY, JAPAN

WOJCIECH MISIAG, HIROSHIMA UNIVERSITY, JAPAN

ABSTRACT

A study on the database system focused on the prediction of the ship maneuverability has been carried out. The database system covering the full-scale ship performance, hydrodynamic ship model data and ship geometry is presented. The full scale ship maneuvering performance data and model hydrodynamic data are analyzed here and the derivation of the approximating models is shown. The results are explained by comparison with series ship model test data. It is pointed out that the use of the database system has limited accuracy if only ship's principal particulars are used for the database access. To remedy this situation, an idea of using a type ship concept for the improvement of the maneuverability prediction is proposed. The comparison of the hydrodynamic performance prediction using the type ship concept and the approximating formulas is given. The results of the research on the performance estimation of the special rudders are also reported.

NOTATION

L - length between perpendiculars; m, I_{ZZ} - mass, inertia moment;
B - beam; Y , N - hydrodynamic derivatives;
d - draft; U_S - ship speed;
Cb - block coefficients; K, K_V, T_1, T_2, T_3, T_4 - Nomoto equations' parameters;
Δ - displacement; v, r - sway and yaw velocities;
β - drift angle; Tr, Ad, Dt - transfer, advance, tactical diameter;
ϕ - heading angle; r_c, R_c - steady turning: yaw rate and radius;
δ - rudder angle; $k = (2d/L)$ - aspect ratio of the ship hull;
AR - rudder area; k_R - aspect ratio of the rudder;
f_α - rudder normal force coeff. derivative; γ_R - flow straigthening coeff.;
K_T - thrust coefficient; $J_S = U\cos\beta/(nD_P)$ - propeller advance coeff.;
u_p, u_r - longitudinal propeller, rudder velocity; v_R - lateral rudder inflow velocity;
χ - hull similarity parameter; PERF(), FP() - performance data and formula;

1. INTRODUCTION.

The activity of IMO in the field of ship maneuvering safety will result in establishing the required level of maneuvering performance. The adoption of maneuvering standards by IMO may happen as soon as in year 1993. This increases the importance of maneuverability prediction in early phases of the ship design.

There are many methods that may be employed for this purpose. Although the numerical approach toward the calculation of the ship's

hydrodynamic forces is the most flexible and convenient, its actual capabilities are insufficient in practical applications. Captive model tests provide accurate data for the prediction of various aspects of maneuvering behavior, so this valuable knowledge should be used conveniently. Accumulated full scale trial data also contain large amount of information and are indispensable for the verification purposes.

These lead to the investigation of a complex approach toward the problem of the maneuverability performance prediction, resulting in the integration of many information sources into one database system.
The results of so called MPR series model tests, carried out by Hiroshima University, provide an insight into the dependence of the hydrodynamic data on the hull form. The procedure to use the database is discussed and the necessity of developing of more rational approach is suggested.

2. DATABASE SYSTEM APPROACH CONCEPT FOR MANEUVERABILITY PREDICTION.

The very existence of multiple information sources leads to the investigation of a complex approach to the problem of maneuvering performance prediction. The proposed solution is an integration of that information into the form of a database system and an use of various numerical procedures for the accessing of this data.

The prediction of maneuverability using a database system involves tasks as follows:

(1) maneuvering performance <--> ship form;
(2) hydrodynamic data <--> ship model form;
(3) maneuvering performance <--> ship model performance;
(4) similarity relation among ship forms;

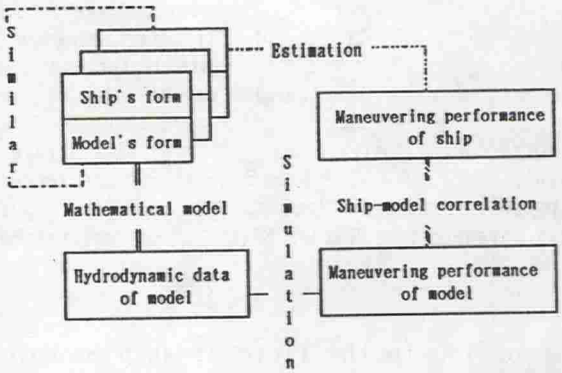

Figure 1. Relations among database system components

Figure 1 shows these relations.

Task (1) involves relations among the ship form (e.g., principal particulars, frame lines) and the maneuvering performance macro data

(e.g., turning diameter, spiral loop characteristics, zigzag test results).

Task (2) involves relations among the ship model's form and the hydrodynamic data (e.g., the parameters of the mathematical model of the ship maneuvering).

Task (3) involves the correlation between model tests and full scale trials.

Task (4) aims at the assessment of the hull forms' similarity from the viewpoints of maneuvering performance, hydrodynamic data or hull geometry.

The database system for the maneuverability investigation has been created. Figure 2 shows its outline.

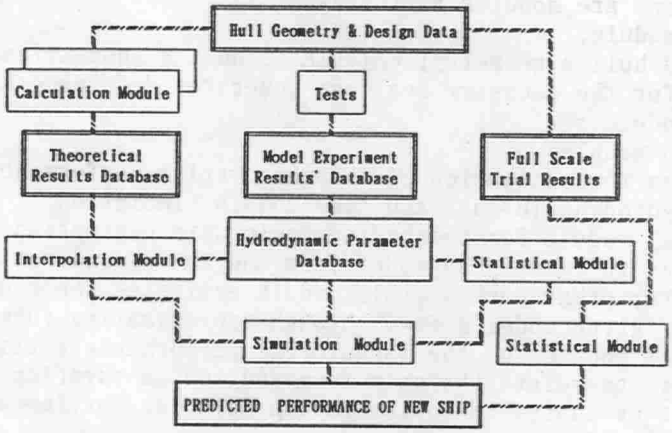

Figure 2. Database for maneuverability prediction

The system contains the following databases:

(1) ship and model hull form description database;

There are two sets of stored information:

(a) principal particulars;

It includes general data of hull, rudder and propeller; in some cases only such data are available;

(b) full form specification;

It includes general and detailed information about the hull form (e.g., frame offsets), rudder and propeller geometrical data; those data represent cases when the full information about ship model (like a body plan) is available;

(2) database of model's hydrodynamic experimental data;

There is the information constituting data for the MMG mathematical model of the ship maneuvering;

(a) derivatives of hull forces and moment;

(b) open water hydrodynamic characteristics of rudder and propeller;

(c) interaction parameters;

(3) full scale performance database;

There are information about principal particulars of hull, rudder and propeller, stern arrangement, engine, other data about the ship (e.g., nationality) and test conditions;

The performance data contain:

(a) stopping trial data;

(b) turning trial data;

(c) zigzag trial data;

A software system was built around these databases. Its purpose is to access and to process the information stored in databases.

The software is distributed into modules, which perform distinct functions. There are modules as follows:

(1) Geometry module;

It shows hull's geometry; calculates hull's geometrical data; allows for the geometry scaling; generates data necessary for other modules;

(2) Simulation module;

It serves for estimation of the maneuvering performance of a model using hydrodynamic data and time-domain simulation;

(3) Statistical module for the hydrodynamic data estimation;

It allows to relate the model form and the hydrodynamic performance data; other part of this module estimates the hydrodynamic data for given model's form through approximating formulas;

(4) Statistical module for the maneuvering performance estimation;

It allows to relate the ship form and the maneuvering performance data; it evaluates an approximation formulas for the maneuvering performance data;

(5) Hull force calculation module;

This relates hull form and hydrodynamic forces using a numerical approach; some preliminary software implementations have been made, cf. Zhu [1];

(6) The similarity assessment module;

Its purpose is to evaluate the similarity of hull forms from the hydrodynamic viewpoint;

The system allows for the systematic investigation of relations among the hull form and the maneuvering performances of ship models and full scale ships.

The full scale performance database consists of the old database published by Hydronautics [2] and recently collected data of over 170 ships built in Japan, cf.Kose [3]. The total number of ships in the database exceeds 740. The dominant type of ship is tanker.

As for now, the hydrodynamic database contains 20 detailed data sets from PMM tests performed at Hiroshima University and 22 less detailed data sets obtained from other sources. The first set provides full entries into the hull geometry database.

3. SERIES OF CAPTIVE MODEL TESTS FOR THE MANEUVERABILITY PREDICTION.

The purpose of captive series model tests is to discover the relations between systematically varied hull form and dynamic properties of ship.

In case of the ship maneuvering, one may modify the hull principal particulars (like ratios L/B, B/d, L/d, block coefficient Cb), appendages (type of rudder or propeller), stern and bow arrangements (frame line shapes in those areas). The ship dynamics is represented by a mathematical model of the ship maneuvering.

There are few data on such systematic studies, because the effort necessary to conduct the maneuvering captive model tests is excessive and the maneuverability itself has earned importance quite recently. Maneuvering series tests were done on Standard Taylor Series, on models of Series60, on Mariner series. ITTC's test maneuvering program with the "Esso Osaka" model was aimed at establishing and verification of the mathematical model of the ship maneuvering.

In the past, the maneuvering series model tests were performed several times in Japan. Their goal was to investigate the maneuverability of full form ships. Such ships had initially rather poor maneuvering performance. Propulsion and vibration factors forced designers to select stern forms that were unsuitable from the maneuvering viewpoint, in particular, the resulting course-keeping abilities were inadequate.

Those series model tests failed to discover the relations between the hull form and the hydrodynamic performance. The occurrence of so called "unusual phenomena", that were reported by Kose [4], prevented it. Those phenomena are specific for model tests only; measurements on full scale ships did not find their existence. In essence, the "unusual phenomena" are caused by large scale stern flow instabilities and separations, which result in pressure fluctuations. This in turn leads to fluctuations in the measured forces. The forces display unusual characteristics, e.g., directional hysteresis, so the results of the captive model tests cannot provide the parameters of mathematical model of the ship maneuvering that is used for the experiment analysis.

3.1 DESCRIPTION OF MPR SERIES MODEL TESTS AT HIROSHIMA UNIVERSITY.

Hiroshima University conducted the maneuvering series tests for full ship forms, called MPR series, reported by Kose [5][6]. The study of hull forms of models with "unusual phenomena" showed that the latter might be stimulated by the extensive stern fullness. Very careful design of hulls allowed to avoid the "unusual phenomena". Designers set a limit for the maximum stern fullness, which was complied with during the design process. This procedure shifted the center of buoyancy forward from the midship.

Two categories of hull forms constituted the MPR model series. The modification of the parent model's block coefficient Cb and ratio (L/B) gave the first category, named "L/B-Cb series". The block

coefficient Cb varied between 0.78 and 0.84, and (L/B) ratio spanned a range between 5.0 and 5.5. The hull form, stern and bow configurations remained unchanged in the "L/B-Cb series" category.
The stern form is important for both propulsion and maneuvering, so the alteration of the parent model's stern produced the second category, named "stern series". Two modified stern configurations - i.e., Normal stern with rectangular rudder and Mariner stern with hanging rudder - replaced the parent model's Mariner stern with hanging rudder.

The MMG modular mathematical model of the ship maneuvering was used for the analysis of the experiments.

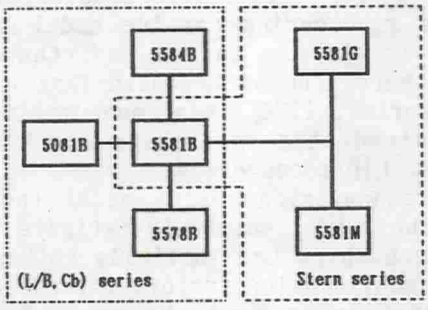

Figure 3. Dependence among models in MPR series

	5584B	5081B	5578B	5581B	5581G	5581M
Cb	0.8399	0.8101	0.7797	0.8101	0.8088	0.8085
L / B	5.5	5.0	5.5	5.5	5.5	5.5
B / d	2.8	3.08	3.08	2.8	2.8	2.8
lcb (% L)	-3.27	-3.21	-2.34	-2.80	-2.87	-2.88
Stern Type	Mar-b	Mar-b	Mar-b	Mar-b	Normal	Mar-hg
Rudder	hanged	hanged	hanged	hanged	rectng	hanged
Bow Type	U-bulb	U-bulb	U-bulb	U-bulb	U-bulb	U-bulb

Mar-b : Mariner type with a propulsion bulb
Mar-hg : Mariner type with hanged rudder
rectng : classical, rectangular, supported rudder
U-bulb : U-frames with a bulbous bow

Table 1. Principal particulars MPR series models

	5584B	5081B	5578B	5581B	5581G	5581M
$-Yv'$	0.355	0.373	0.365	0.356	0.400	0.366
Yr'	0.105	0.102	0.085	0.081	0.092	0.100
$-Nv'$	0.124	0.116	0.115	0.119	0.102	0.102
$-Nr'$	0.042	0.048	0.048	0.044	0.048	0.049

Table 2. Linear hull derivatives of MPR series models

Figure 3 shows the dependencies among members of the MPR series models family. The model marked as 5581B (code :L/B= 5.5, Cb=0.81, stern bulb) is the series' parent model. Its form is representative for the modern full form designs. Table 1 contains series' principal particulars' data, while figure 4 presents draft body lines. Table 2 lists

hulls' linear derivatives being a part of important hydrodynamic data. The other important data are lateral inflow angles to the rudder.

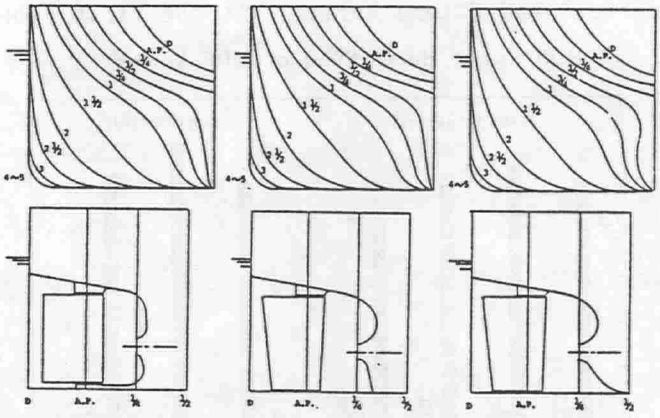

Figure 4. Body lines of MPR series

The values of the linear hull derivatives vary largely among models belonging to both series. The rudder inflow angle δ_R depends strongly on the stern type. There are also differences in the remaining hydrodynamic data, i.e., in the nonlinear hull derivatives and in the interaction coefficients.

Tests in a ballast condition were also conducted. In the ballast condition both hull form and principal particulars change with regard to the full load condition. Large differences between the hydrodynamic data in both conditions were observed; in particular, the rudder inflow angle δ_R in some cases of ballast condition was kept near zero within drift angle in range 15 degrees. In tested cases, the ballast condition with zero trim resulted in significant worsening of the directional stability, comparing to the full load and trimmed (on stern) ballast condition.

The main outcomes of the experiments are as follows:
(1) there exist large differences in both linear and nonlinear hydrodynamic hull derivatives;
(2) there are significant differences in flow patterns around models' stern, resulting in large variations of the rudder lateral inflow velocity;
(3) there are differences in interaction coefficients;
(4) experiments have not revealed the presence of the "unusual phenomena";

3.2 REANALYSIS OF THE EXPERIMENTAL RESULTS.

The success in the avoiding of the "unusual phenomena" permits for the discussion of series model tests' results.

The hydrodynamic data (derivatives and interaction coefficients) significantly depend on variations of the hull form. Figure 5 shows the distribution of the linear hull derivatives among models belonging to both "L/B-Cb series" and "stern series". At the first look, we may see

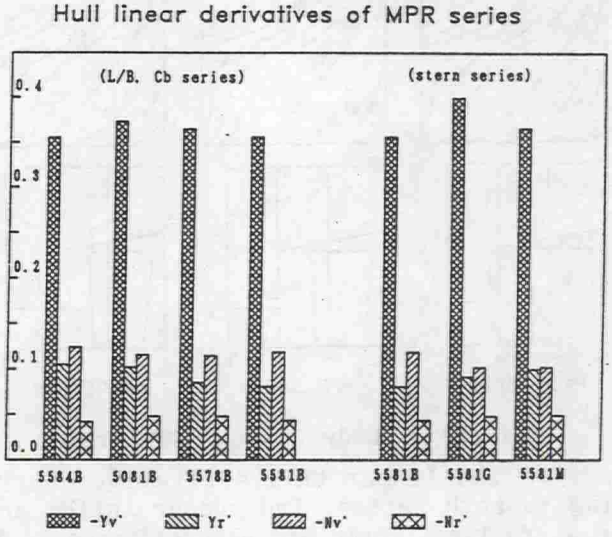

Figure 5. Linear hull derivatives in MPR series

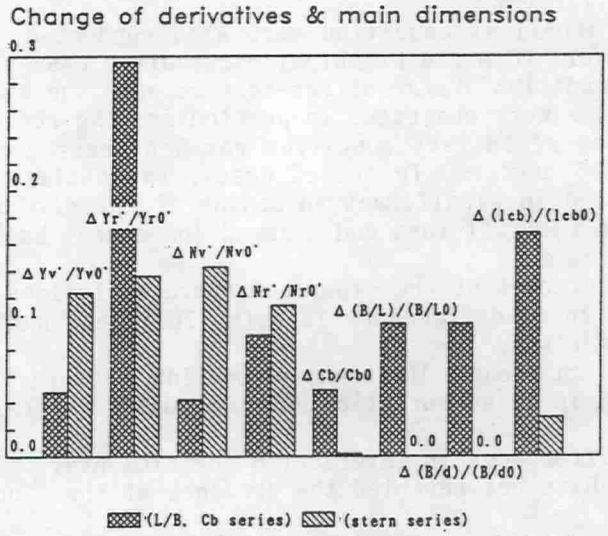

Figure 6. Changes of hull particulars and derivatives

that there are quite large differences among these data for the "stern series" models, which -on the other hand- have the same principal particulars. The differences among hydrodynamic data of geometrically

similar hulls belonging to the "L/B-Cb series" models are smaller. For making the situation more clear, the largest relative difference between every hull linear derivative and its corresponding derivative of the parent model are shown in figure 6; in the same figure, there are similar relations among models' principal particulars. It reveals that the relative variations of the hull linear derivatives are larger for "stern series" models (with the exception for the derivative Y_r). Because the principal particulars of "stern series" models are nearly identical, then the conclusion is that the stern form has strong influence on these hydrodynamic data.

As in the case of the hull linear derivatives, the flow pattern around the stern, expressed through the rudder lateral inflow angle δ_R, depends on the whole hull form (cf. ballast condition) as well as on the particular stern configuration.

Since the hull linear derivatives and the rudder inflow angle δ_R decide about the directional stability of maneuvering ship analyzed in the frame of linear theory, then the strong influence of the stern form on these hydrodynamic data is an important fact.

3.3 CONCLUSIONS REGARDING PREDICTING FORMULAS FOR THE HYDRODYNAMIC PERFORMANCE.

The "stern series" models represent ships that have the same principal particulars, but their hull forms vary. As the test results show, the linear derivatives' scatter due to differences in the form of frame lines may well exceed 10%. Other hydrodynamic data also vary. Figure 7 shows the influence of those variations on the "macro" performance of the ships in zigzag maneuvers.

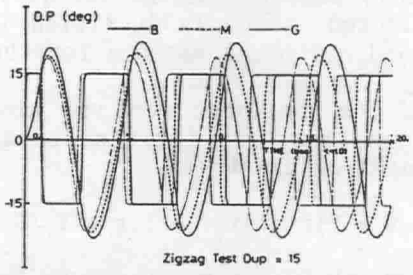

Figure 7. Hull change and maneuvering performance (Z)

The conclusion is that the frame line shape has substantial influence on the hydrodynamic performance of models. The hydrodynamic performance appears as parameters of mathematical model of the ship maneuvering. Thus the maneuvering performance of models also depends strongly on the frame line form.

There are many methods for the calculation of the ship hydrodynamic data by means of formulas that take into account ship's principal particulars exclusively. The presented experimental results suggest that

such methods cannot fully account for the variations of the hydrodynamic and maneuvering performances of ships, because those variations may be caused by fine modifications of the hull form. Thus the precision of the performance prediction, which is based on such formulas, is inherently limited.
It also suggests that for the improvement of such formulas, the information about the frame line form should be included.

4. APPLICATION OF THE FULL SCALE TRIAL DATABASE FOR THE MANEUVERING PERFORMANCE PREDICTION.

Some analysis of full-scale turning and zigzag trials follow [7].
The relations being investigated are:

(1) tactical diameter Dt - ship principal particulars;
(2) advance Ad - ship principal particulars;
(3) first overshoot angle ovs1 - ship principal particulars;

The principal particulars are the only available data describing the hull form and it is important as well to have such type formulas.

4.1 PRELIMINARY ANALYSIS.

The preliminary analysis should provide the model structure and model variables for the data fitting process.

Although the equations of ship motion are nonlinear, for the analysis this fact is neglected (first, because of analytical reasons; second, because the resulting model would have many parameters, which would put the precision of the estimation into question). The longitudinal force is also neglected, which is justified for the advance's and overshoot's analysis, and may be acceptable for the tactical diameter's one.

The conversion of the nonlinear sway and yaw equations into linearized ones leads to equations (1) (written in the coordinate system fixed to the ship's center of gravity):

$$\begin{aligned} m(\dot{v} - u_o r) &= Y_{\dot{v}}\dot{v} + Y_{\dot{r}}\dot{r} + Y_v v + Y_r r + Y_\delta \delta \\ I_{zz}\dot{r} &= N_{\dot{v}}v + N_{\dot{r}}\dot{r} + N_v v + N_r r + N_\delta \delta \end{aligned} \quad .... \quad (1)$$

These linear equations are separated into two equations for the sway velocity v(t) and yaw velocity r(t) with identical structure, being equations proposed by Nomoto.

$$\begin{aligned} T_1T_2\ddot{v} + (T_1+T_2)\dot{v} + v &= K_v(\delta + T_4\dot{\delta}) \\ T_1T_2\ddot{r} + (T_1+T_2)\dot{r} + r &= K(\delta + T_3\dot{\delta}) \end{aligned} \quad .... \quad (2)$$

The solution of these equations is well known, being a combination

of linear and exponential function. This can be seen from the Laplace transforms of equations (2):

$$r(s) = \delta(s)[K(1+T_3 s)][(1+T_1 s)(1+T_2 s)]^{-1}$$

$$v(s) = \delta(s)[K_v(1+T_4 s)][(1+T_1 s)(1+T_2 s)]^{-1} \quad \ldots\ (3)$$

The parameters of equations (2) and (3) - $K, K_v, T_{1,2,3,4}$ - depend on the coefficients of equations (1), cf. Clarke [8].

The rudder motion $\delta(t)$ is represented as a time - step function $\delta_0 H(t)$, i.e., the immediate response of rudder to the control input.

The interesting quantities - advance Ad, transfer Tr, tactical diameter Dt and overshoot angle ovs1 - are defined by integrals of the kinematic equations of the ship motion (4), given in a space-fixed coordinate system:

$$Tr = y_0(t1) = \int_0^{t1} U_s(\tau)\,\sin(\phi(\tau)+\beta(\tau))\,d\tau$$

$$Ad = x_0(t1) = \int_0^{t1} U_s(\tau)\,\cos(\phi(\tau)+\beta(\tau))\,d\tau$$

$$Dt = y_0(t2) = \int_0^{t2} U_s(\tau)\,\sin(\phi(\tau)+\beta(\tau))\,d\tau$$

$$ovs1 = \phi(t3) - \delta_0 = \int_0^{t3} r(\tau)\,d\tau - \delta_0 \quad \ldots\ (4)$$

where:

x_0, y_0	- position of ship;
U_s	- ship's speed;
r	- rate of turn;
ϕ, β, δ_0	- heading, drift angle, rudder angle;
t1	- time, when change of heading $\Delta\phi = \pi/2$;
t2	- time, when change of heading $\Delta\phi = \pi$;
t3	- time, when rate of turn in zigzag test r=0;

There is also an analytical expression for the overshoot angle ovs1, which can be easily obtained from the first of equations (3).

For performing the integration of the motion equations to obtain Ad and Tr, it is necessary to find the end time (t1) of the maneuver from the condition $\phi(t1)=\pi/2$, and to perform the integration.

The exponential functions - appearing in $\phi(t)$, $r(t)$ and $v(t)$ - are approximated by a rational function expansion. The first order approximations allow for very rough integration of the motion equations.

Assuming the step rudder motion $\delta_0 H(t)$, the solution of the yaw angle $\phi(t)$ in turning is obtained from (3), and follows:

$$\phi(t) = K\delta[t - (T_1+T_2-T_3) + (T_1-T_3)(T_1-T_2)^{-1}T_1 e^{-(t/T1)} + -(T_2-T_3)(T_1-T_2)^{-1}T_2 e^{-(t/T2)}] \quad \ldots\ (5)$$

which may be written as:

$$\phi(t) = K\delta[t - a_1 + a_2T_1e^{-(t/T1)} - a_3T_2e^{-(t/T2)}] \quad \ldots.(5')$$

$a_1 = (T_1+T_2-T_3)$; $a_2 = (T_1-T_3)/(T_1-T_2)$; $a_3 = (T_2-T_3)/(T_1-T_2)$;

Let's approximate the exponential e^{-x} through a rational function:

$e^{-x} = 1/(1+x)$, for $x > 0$

$$e^{-(t/T1)} = T_1/(T_1+t); \qquad e^{-(t/T2)} = T_2/(T_2+t) \quad \ldots. (6)$$

Using (6) in (5') we get:

$$\phi(t) = K\delta[t - a_1 + a_2T_1^2/(T_1+t) - a_3T_2^2/(T_2+t)] \quad \ldots. (7)$$

This allows for a very rough estimate of the time (t1), when the heading angle is $\phi(t_1)=\pi/2$ (the term with a_3 is rejected):

$$t1 \sim \pi / (4\delta K) - T_1 - a_1$$

$$t1 \sim \pi / (4\delta K) + (T_2-T_3)/2 + f(1/(K\delta), T_1, T_2, T_3)$$

$$t1 \sim (1/\delta)(1/K)(1/c_1) + (c_0/c_1) \quad \ldots. (8)$$

where:
c0, c1 = functions of (T_1, T_2, T_3);

The yaw rate r(t) and sway velocity v(t) are respectively:

$$r(t) = K\delta[1 - a_2e^{-(t/T1)} + a_3e^{-(t/T2)}]$$

$$v(t) = K_v\delta[1 - a_4e^{-(t/T1)} + a_5e^{-(t/T2)}] \quad \ldots. (9)$$

$a_4 = (T_1-T_4)/(T_1-T_2)$; $a_5 = (T_2-T_4)/(T_1-T_2)$;

which can be approximated through:

$$r(t) = K\delta[1- a_2T_1/(T_1+t) + a_3T_2/(T_2+t)]$$

$$v(t) = K_v\delta[1- a_4T_1/(T_1+t) + a_5T_2/(T_2+t)] \quad \ldots. (10)$$

The drift angle $\beta(t)$ is small (10-20 degrees) and approximately equals the sway velocity v(t) at normal speed:

$$\beta(t) = v(t) \quad \ldots. (11)$$

and may be expressed through the equation (10).

The same assumptions about β allows to approximate the integrand functions in equation (4), so it becomes in the first order:

$$\cos(\phi+\beta) = \cos(\phi) - \beta\sin(\phi) = 1 - \beta\phi$$

$$\sin(\phi+\beta) = \sin(\phi) + \beta\cos(\phi) = \phi + \beta \quad \ldots\ (12)$$

The advance Ad in the first order approximation, assuming no speed drop, is:

$$Ad = U_s\int_0^{t1}(1-\beta\phi)d\tau$$

$$Ad = U_s[t_1(1-a_1K_vK\delta^2) + (\text{higher order terms})] \quad \ldots\ (13)$$

The transfer Tr in the first order approximation, assuming no speed drop, is:

$$Tr = U_s\int_0^{t1}(\phi+\beta)d\tau$$

$$Tr = U_s[t_1(\delta K+\delta K_v) - K\delta a_1 + (\text{higher order terms})] \quad \ldots\ (14)$$

The approximation suggests that both the advance Ad and transfer Tr is proportional to the end time of maneuver t1.

$$Tr,\ Ad \sim U_s t1 \quad \ldots\ (15)$$

The equations (13) and (14) suggest that relations between transfer Tr, advance Ad and motion equations' parameters ($K, K_v, T_{1,2,3,4}$) may be described as follows:

$$Tr = [(1/K)(1/\delta)(1/c_1)+(c_0/c_1)](K+K_v)\delta - a_1c_2K\delta +$$

$$\{\text{higher terms in } K, K_v, T_{1,2,3,4}\}$$

$$Ad = [(1/K)(1/\delta)(1/c_1)+(c_0/c_1)](1-a_1KK_v\delta^2) +$$

$$\{\text{higher terms in } K, K_v, T_{1,2,3,4}\} \quad \ldots\ (16)$$

The analysis for the tactical diameter Dt may follow the same way, but it is better to use following simple relation:

$$Dt \sim (\text{Transfer Tr}) + (\text{Steady turning radius } R_c) \quad \ldots\ (17)$$

The steady turning radius R_c is inverse proportional to the rate of turn r_c on steady turning , so we get:

$$r_c = K\delta$$

$$R_c \sim (1/K)(1/\delta) \quad \ldots\ (18)$$

If we compare equations (16) and (18), it may be seen that the term $(1/(K\delta))$ is already present in the equation (16). The tactical diameter Dt may be expressed as:

$$Dt \sim (1/K)(1/\delta)(1/c_c)+[(1/K)(1/\delta)(1/c_1)+(c_0/c_1)](K+K_v)\delta +$$

$$-a_1c_2K\delta + \{\text{higher terms in } K,K_v,T_{1,2,3,4}\} \quad \ldots\ (19)$$

The parameters in formulas (16-19) depend on the parameters (K,K_v,T_1,T_2,T_3,T_4) of Nomoto's equations.

For relating the formulas (16-19) to the ship principal particulars, it is necessary to express the parameters (K,K_v,T_1,T_2,T_3,T_4) through the ship principal particulars. Since the parameters (K,K_v,T_1,T_2,T_3,T_4) depend on the hull and rudder derivatives, then it is necessary to express the derivatives in terms of ship principal particulars.

The parameters (K,K_v,T_1,T_2,T_3,T_4) may be expressed through the hydrodynamic derivatives as follows:

$$K = (N_vY_\delta - Y_vN_\delta)/[Y_vN_r - N_v(Y_r-m)]$$

$$K_v = [-N_rY_\delta + N_\delta(Y_r-m)]/[Y_vN_r - N_vY_r]$$

$$T_1T_2 = [(Y_{\dot v}-m)(N_{\dot r}-I_{zz}) - Y_{\dot r}N_{\dot v}]/[Y_vN_r - N_v(Y_r-m)]$$

$$T_1+T_2=[(Y_{\dot v}-m)N_r+(N_{\dot r}-I_{zz})Y_v - N_vY_{\dot r} - N_{\dot v}(Y_r-m)]/[Y_vN_r - N_v(Y_r-m)]$$

$$T_3 = [N_{\dot v}Y_\delta - (Y_v-m)N_\delta]/[N_vY_\delta - Y_vN_\delta]$$

$$T_4 = [(N_{\dot r}-I_{zz})Y_\delta - Y_{\dot r}N_\delta]/[N_rY_\delta - (Y_r-m)N_\delta] \quad \ldots\ (20)$$

Hull and rudder derivatives may be expressed in the easiest way through applying the model of small aspect ratio lifting surface (or through the corresponding slender body theory formulation).

Various formulas may be found in Clarke [8], Wolters [9], Newman [10], Inoue [11]. The following forms are cited after Clarke [5]:

$$Y_{\dot v} = k[m_1+m_2(C_bB/d)+m_3(B/L)^2] \qquad Y_v = k[m_{11}+m_{12}(C_bB/d)]$$

$$Y_{\dot r} = k[m_4(B/L)+m_5(B/d)^2] \qquad Y_r = k[m_{13}+m_{14}(B/L)+m_{15}(B/d)]$$

$$N_{\dot v} = k[m_6(B/L)+m_7(B/d)] \qquad N_v = k[m_{16}+m_{17}k]$$

$$N_{\dot r} = k[m_8+m_9(C_bB/d)+m_{10}(B/L)] \qquad N_r[m_{18}+m_{19}(B/d)+m_{20}(B/L)] \quad ..(21.a)$$

where:

$k = (2d/L)$;

m_i - constant parameters;

Rudder force and derivatives are:

$$Y_{rudder} = (1/2)\rho(AR)(U_R^2)(f_\alpha(k_R)\delta)$$

$$Y'_\delta = m_{21}(AR)/(Ld) \qquad N'_\delta = m_{22}(AR/Ld) \quad \ldots\ (21.b)$$

where:

AR - rudder area; k_R - rudder aspect ratio.

When these formulas are used, then the variables V, V1 for the models describing Ad, Tr, Dt, and ovs1 are:

V := { Cb, d/L, B/L, B/d, AR/(Ld) };
V1:= { Cb, d/L, B/L, B/d };

When expressions (21) are substituted into equations (20), then the results are rational functions of ship principal particulars. Subsequently functions (20) may be substituted into equations (16-19), which leads to complicated, rational formulas depending on ship principal particulars.

The general forms of the fitting formulas for the transfer Tr and advance Ad, following the structure of equations (16) and (19), are as follows:

$$Tr*\delta*(AR/Ld) = H1(V1) + \delta*(AR/Ld) * H2(V1)$$

$$Ad*\delta*(AR/Ld) = H1(V1) + \delta*(AR/Ld) * H2(V1) \quad .... \quad (22)$$

where:
H1 - rational function of parameters V1;
H2 - rational function of parameters V1;

The factor (AR/Ld) comes from the expressions for K and K_Y, which have in their nominators both Y_δ and N_δ; Y_δ and N_δ depend on the parameter (AR/Ld) that can be factorized out. Both sides of those equations are multiplied by $(\delta)*(AR/Ld)$, which is a normalization parameter here.

In the analysis of the tactical diameter Dt, the data Dt may be also compressed using Schoenherr's parameter, cf. Norrbin [12]:

$$(L/Dt)(\delta_0/\delta)(\Delta/(AR*L))$$

This possibility comes from the formula (19) and may be obtained in following way:

$$(Dt)(K\delta) = (1/c_3)+[(1/c_1)+(c_0/c_1)K\delta](K+K_v)\delta + \text{function}(K,K_v,T_{1,2,3,4})$$

Inverting it we may write:

$$(1/Dt)(1/K\delta) = \text{function}(K,K_v,T_{1,2,3,4},\delta)$$

From equation (20) we may get the formula for (1/K):

$$(1/K) = (1/AR)[Y_vN_r-N_v(Y_r-\Delta]/[N_vf(k_R)-Y_vf(k_R)(L/2)]$$

$$(1/K) = (1/AR)(\Delta/L)*g(Y_v, N_r, N_v, N_r)$$

Using this Schoenherr's parameter we may get a functional dependence (23) that was used for the modeling of the tactical diameter Dt data:

$$(L/Dt)(\delta_o/\delta)(\Delta/(AR*L)) = H3(V1) \quad \ldots\ (23)$$

where:

H3 - rational function of parameters V1;

Various forms of functions H1, H2 and H3 may be tried, resulting in linear and nonlinear fitting models.

The functions H1, H2 and H3 contain numerous linear and higher order terms in variables V1, so simplifications are necessary for the data fitting purposes. The problem is that the components of V1 are not quite independent; they represent the principal particulars of the same ship, so the block coefficient Cb is related to {L,B,d}, while the rudder area AR is usually picked up depending on the parameters {(Ld),Cb,L}. This often introduces the linear dependence to the fitting problem and makes more extensive data fitting models useless.

4.2 SOME RESULTS FOR PREDICTION OF FULL SCALE SHIP MANEUVERING PERFORMANCE USING SHIP PRINCIPAL PARTICULARS.

Prediction models for the full scale maneuvering performance are developed using the database of full scale maneuvering trials and the analytical functions having forms of the equations (22) and (23). The models cover the whole population of ships.

The conditions for selecting the ships from the whole population are:

(1) full load condition, i.e., trial displacement Δ_{trial} is
$0.8 * \Delta_{design} <= \Delta_{trial} <= 1.2 * \Delta_{design}$

(2) even keel, i.e., the trim is:
trim = 0.0;

In those tests the measurement errors are unknown. The errors in the parameters' estimates are calculated assuming good fit to the data.

Figure 8 presents the fitted results for the advance Ad. Figure 9 shows the fitted results for the tactical diameter Dt.

Those figures contain the formulas, values of fitted parameters, errors (standard deviations of the fitted parameters) and standard deviations of models.

The formulas for the advance Ad and tactical diameter Dt in turning maneuver have been found.

In the case of the first overshoot angle ovs1 no formula has been found that would represent the experimental data as a function of the ship principal particulars.

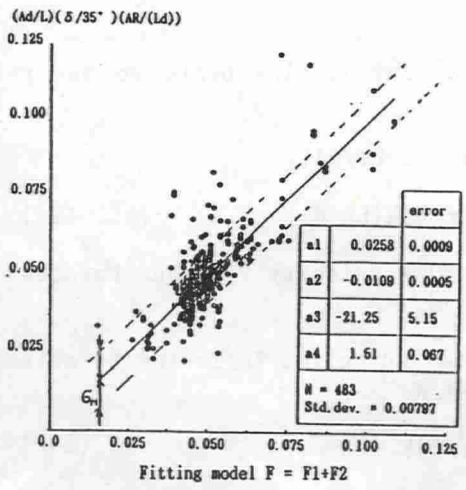

Figure 8. Advance Ad.

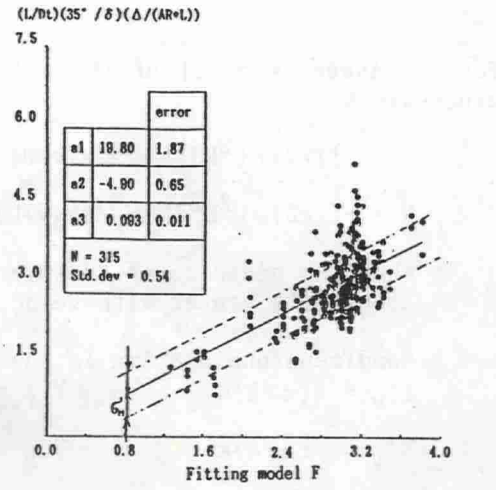

Figure 9. Tactical diameter Dt.

The results show that the performance prediction, based on formulas developed from the trial data of full scale ships, has limited accuracy. The reason it happens has been shown during the discussion of the MPR series model tests. It is pointed out there that the hydrodynamic performance depends strongly on the frame line shapes; because the full scale performance also depends on the frame line shape then the fitting formulas that use principal particulars exclusively possess a "built-in" source of errors.

5. APPLICATION OF THE MODEL HYDRODYNAMIC DATABASE FOR THE HYDRODYNAMIC PERFORMANCE PREDICTION.

Similar analysis is done on the hydrodynamic parameter database. The aim is to develop approximating formulas for linear hull derivatives using principal hull particulars and to find the limitations of such an approach. The last item arises from the series model test analysis, which disclosed that the hydrodynamic performance depended on the shape of the hull frame lines.

5.1 PRELIMINARY ANALYSIS.

The slender body theory or the theory of small aspect ratio wing gives the elementary models for hull force due to transversal and rotational motion of the hull. According to those theories we expect that the draft - length ratio k=2d/L has dominant influence on the hull

forces. Assuming model of the hull as a flat lifting plate we may get expressions:

$$Y = -(1/2)\rho U^2 Ld[(\pi/2)k(v/U) - (\pi/4)k(Lr/U)]$$

$$N = -(1/2)\rho U^2 L^2 d[(\pi/4)k(v/U) + (\pi/8)k(Lr/U)] \quad \ldots\ (24)$$

when the plate moves transversely with velocity v(t) and rotates around its center with velocity r(t).

Nondimensionalization in the system "Ld" gives following formulas:

$$Y'_v = -(\pi/2)k \qquad Y'_r = (\pi/4)k$$

$$N'_v = -(\pi/4)k \qquad N'_r = -(\pi/8)k \quad \ldots\ (24')$$

This model does not include the following effects:
(1) vortex shedding from the plate edge;
(2) vortex separation from the proximity of the leading edge;
(3) deformation of vortex layer near the plate;
(4) corrective effect for the finite body volume; this effect represents the deformation of streamlines near the body due to changes in body cross-sectional areas;

The factors (1)-(4), which are omitted in preceding derivation, are expected to be accounted for by incorporating additional terms depending on {k, Cb, B/d, B/L}. There are rather limited possibilities to derive more complex expressions. During the fitting process the combinations of those parameters is to be tried one by one and the influence of newly added terms has to be checked.

Thus the fitting models for linear hull derivatives have the following form:

$$(Y',N')_{v,r} = a*k + f(k, Cb, B/d, B/L) \quad \ldots\ (25)$$

5.2 SOME RESULTS OF HYDRODYNAMIC PARAMETER PREDICTION USING HYDRODYNAMIC DATABASE.

The tested population contains 38 ships' data being principal particulars and hull linear derivatives. The distribution of the hull linear derivatives Y'_v, Y'_r, N'_v, N'_r is shown in figure 10 as a function of the parameter k=2d/L. The original data roughly follow the trends of equations (24), but they also display some scattering.

The approximating formulas and their parameters have been found; they show moderate fit to the original data. The results of fitting with various data models are shown in figure 11 and figure 12.

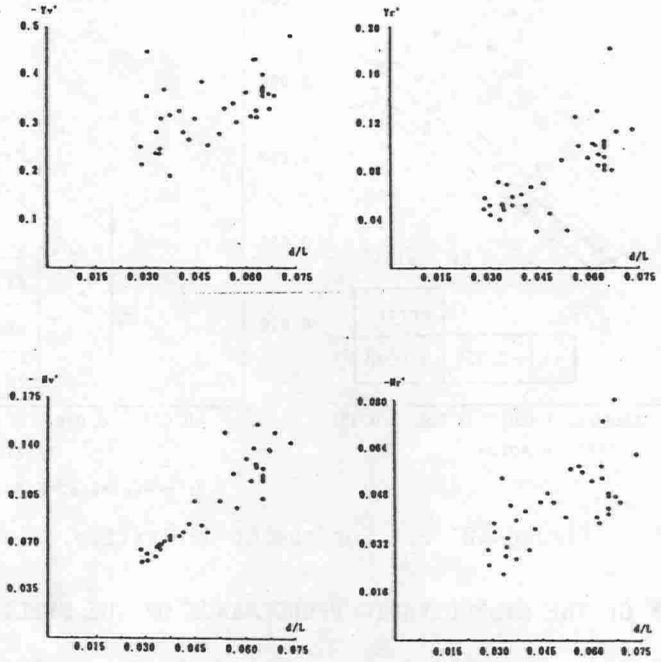

Figure 10. Hull linear derivatives in the database.

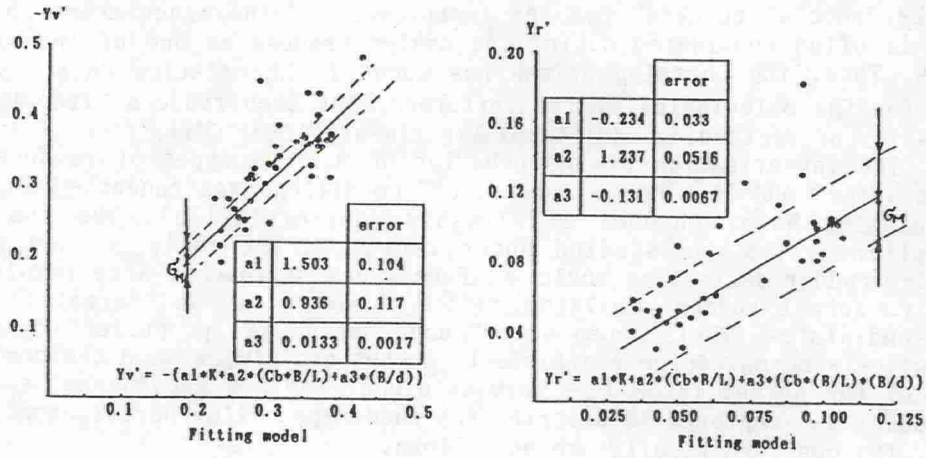

Figure 11. Fit for force derivatives.

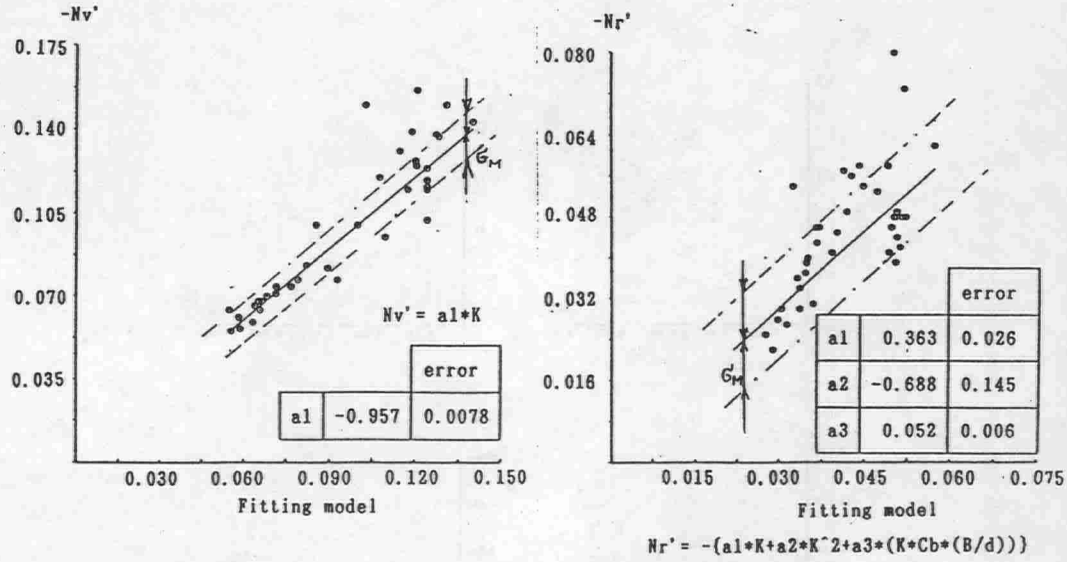

Figure 12. Fit for moment derivative.

6. PREDICTION OF THE HYDRODYNAMIC PERFORMANCE OF THE SPECIAL RUDDERS.

The prediction of the maneuvering performance of the ship using the time-domain computer simulation requires the knowledge of the hydrodynamic data of the ship hull as well as the data of the rudder-propeller system and the interaction forces. Nowadays, the installation of the "special rudders" for the improvement of the maneuvering abilities is often considered during the design process as one of the solutions. Thus, the question arises how much of the existing data may be used for the calculation of the performance of such rudders without the necessity of performing additional experiments (PMM, CMT).

The investigation of the behavior of various types of rudders in "open water" and "behind the propeller" conditions was conducted in the Circulating Water Channel of Hiroshima University[13]. The rudder-propeller system was studied under varying drift angle β and with varying rudder deflection angle δ. Four types of rudders were involved, namely: Normal rudder, Shilling rudder, Flap rudder and Normal rudder with end-plates. Their "open water" and "behind the propeller" characteristics - normal force coefficient, moment coefficient and the derivative of the normal force f_α - were obtained. The MMG modular mathematical model was employed to describe the rudder-propeller performance.

The observed results are as follows:

(1) The open water thrust coefficient $K_T(J_s)$, where the advance coefficient J_s is $J_s = U\cos\beta/(nD_p)$, almost does not depend on the propeller drift angle β. It is shown in figure 13. This fact is important for the

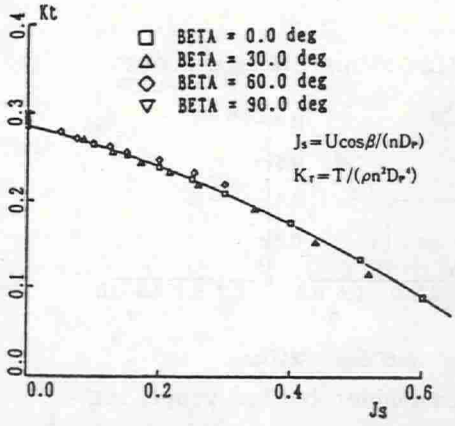

Figure 13. Open water propeller thrust coefficient K_T

	κ	ε	γ_R
Normal Rudder	0.291	1.388	1.171
Flap Rudder	0.328	1.730	0.956
Shilling Rudder	0.332	1.702	0.959
Normal Rudder With Plate	0.244	1.601	1.025

Table 3. Parameters of propeller effect on rudders

calculation of the longitudinal rudder inflow velocity u_r using the thrust equivalence method.

(2) The flow acceleration due to the propeller action, described through the interaction coefficients κ and ε, does not depend on the drift angle β; it is shown in figure 14. On the other hand, these coefficients depend on the rudder type, although the differences, comparing to the data in the case of the Normal rudder, are of the order 20% for the coefficient κ and 25% for the coefficient ε; it is shown in Table 3.

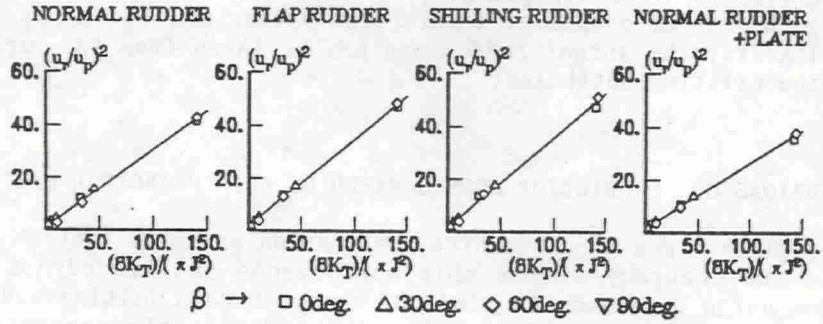

Figure 14. Flow accelerating effect of propeller

(3) The flow straightening coefficient γ_R does not depend on the drift angle β; it is shown in figure 15. Its dependence on the rudder type is very weak, which is shown in Table 3. The coefficient γ_R is almost equal 1.0 in case of "special rudders"; the differences with regard to the case of the Normal rudder do not exceed 20%.

The independence of the parameters γ_R, κ, ε on the drift angle β allows to use these data for the description of the rudder-propeller

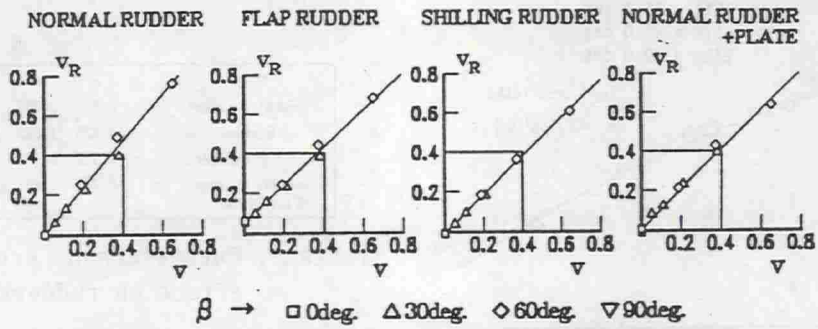

Figure 15. Lateral inflow velocity to rudder behind propeller

performance in the wide range of the maneuvering motions. The relatively weak dependence of the interaction parameters γ_R, κ, ε on the rudder type allows to use the interaction data for the Normal rudder as a rough approximation of the rudder-propeller interaction coefficients, especially in the case of γ_R coefficient.

Thus, the proposed procedure for the estimation of the rudder-propeller performance is as follows:

(1) the open water characteristics f_α can be estimated through the available formulas or from the open water experiments (e.g.,in CWC);

(2) the hull-rudder interaction parameters a_H, x_H may be assumed as for the case of the Normal rudder from the existing database formulas (cf. Kose [14]) or from experiments;

(3) the rudder-propeller interaction parameters γ_R, κ, ε may be assumed like for the Normal rudder and may be taken from the experiment or from the existing databases;

7. CONCLUSIONS ON PREDICTION MODELS BASED ON SHIP PRINCIPAL PARTICULARS

It follows from the presented application examples that:

(1) the accuracy of the ship performance and hydrodynamic data prediction using databases is limited, when the data fitting model uses the ship principal particulars only; the hydrodynamic properties are strongly influenced by the details of the hull form;

(2) data scattering in databases is large, so for better prediction one should try to restrict the search domain through the selection of a sub-population of similar ships;

(3) more rational model of data fitting and interpolation should be employed in place of models based on principal particulars when the information about hull frame shape is available;

(4) the capability to assess the hydrodynamic similarity between two hull forms would be extremely useful;

8. CONCEPT OF A TYPE SHIP FOR THE IMPROVEMENT OF MANEUVERING PERFORMANCE PREDICTION USING DATABASE.

The type ship is an initial hull form being subjected to modification process resulting in a hull form for a new design.

The designer will often face a situation, when he will possess the hydrodynamic or full scale performance data of some set of ships, including a type ship for his new design.

The question is how to use such an information for the improvement of prediction based on formulas derived through statistical analysis of some population of ship forms.

When such a problem arises, the designer has already decided about the hull form for the new design, i.e., its principal particulars, frames' form type, bow and stern configurations have been set. This allows him to estimate the hydrodynamic or performance data using some approximate formula, e.g., the ones proposed formerly. However, such an action might be of moderate accuracy. To correct his estimation he may use the TYPE SHIP concept.

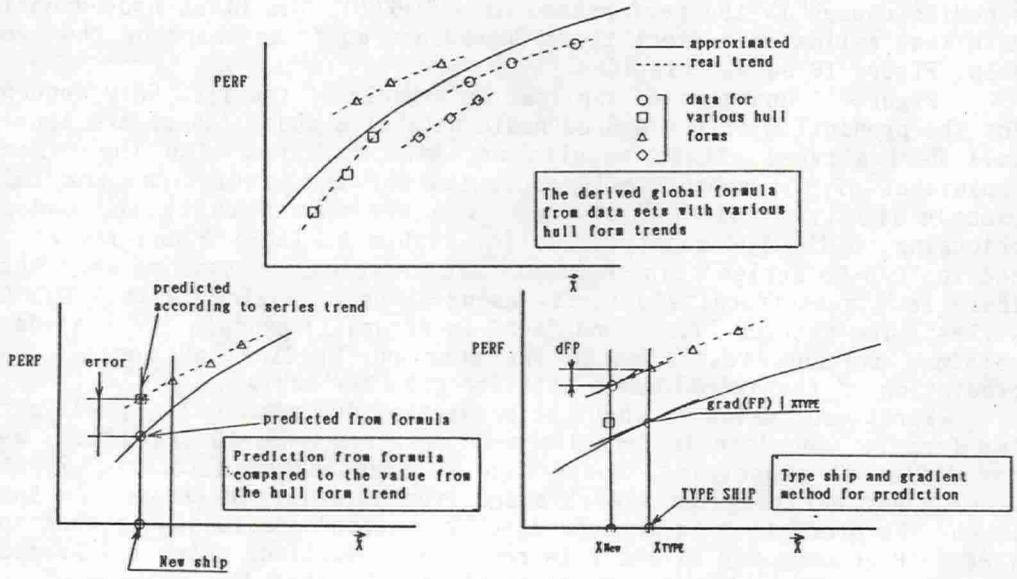

Figure 16. TYPE SHIP concept

The idea of the correction is simple and it is based on the Taylor expansion of the ship's performance PERF(X):

$$PERF(X_{New}) = PERF(X_{Type}) + d(PERF(X_{New}; X_{Type}))$$

$$d(PERF(X_{New}; X_{Type})) = grad(FP(X))_{|X=XType} * \Delta X + \ldots \quad \ldots. \quad (26)$$

where:

- $PERF(X)$ - performance data;
- $X_{New}; X_{Type}$ - vector of design parameters (principal particulars);
- $\Delta X = X_{New} - X_{Type}$;
- $FP(X)$ - formula describing performance data;
- $grad()$ - gradient taken in variables X;
- $d()$ - differential of a function;

First, the designer should select a type ship X_{Type} having the hull form - defined by the frame line type, the stern shape and configuration - closely to his new design. The selection relies on the hull form geometry, but its aim is to pick up a ship, which has the expected hydrodynamic performance close to that of the designed ship. Second, he should select a formula FP(X) relating the performance data PERF and the vector of design parameters X. Knowing the change of the design vector $\Delta X = X_{New} - X_{Type}$, he may employ the formula FP(X) to judge the corresponding change in the performance data d(PERF). The final hydrodynamic data thus estimated reflect their dependence on frame shape of the type ship. Figure 16 shows this idea.

Figure 17 contains an application example of the TYPE SHIP concept for the prediction of the hydrodynamic data of a model (there are linear hull derivatives). These results are also compared with the direct employment of the approximating formulas for the prediction. For this example the type ship and the new ship are chosen to be the models belonging to the MPR model series (cf. Table 1, Table 2 and figure 3) and to "L/B-Cb series". These models are selected, because we know that there is a geometrical similarity among ships belonging to the "L/B-Cb series". The entries "TYPE" and "New" in figure 17 contain the real data obtained in tank tests, while the entries "Prediction" contain the prediction of the hydrodynamic data for the "New" ship.

First conclusion is that the prediction depends on the approximating formula: the Inoue's formulas were obtained some 10 years ago, and for different geometrical forms than we have in the database; on the other hand, our formulas are obtained from this very database, so that is why the prediction is more precise. The second conclusion is that the TYPE SHIP concept may slightly improve the prediction, which is the case in the second example. The third conclusion is that the success of the prediction depends on the fact, how exactly the prediction formula FP(X) represents the true data trend among the type ship and the new ship geometrical forms; if the representation is poor, then the employment of the TYPE SHIP concept may give larger errors than the direct use of the approximating formulas.

When there is possible to pick up more than one type ship, all

Inoue: $Y_v = -\{(\pi/2)*k + 1.4*(Cb*B/L)\}$
$Y_r = (\pi/4)*k$
$N_v = -k$
$N_r = -\{0.54*k - k^2\}$

My form.: $Y_v = -\{1.503*k + 0.936*(Cb*B/L) + 0.0133*(B/d)\}$
$Y_r = -0.234*k + 1.237*(Cb*B/L) - 0.131*(Cb*B/L)*(B/d)$
$N_v = -0.957*k$
$N_r = -\{0.363*k - 0.688*k^2 + 0.052*(k*Cb*B/d)\}$

$k = 2d/L$

FP(X) := {Inoue form., my form.}

PERF := $\{Y_v, Y_r, N_v, N_r\}$

TYPE SHIP prediction uses equation (26)

	Name	Cb	B/L	B/d	2d/L	-Yv	Yr	-Nv	-Nr
TYPE	5581B	.81	.1818	2.80	0.130	.356	.081	.119	.044
New	5578B	.78	.1818	3.08	0.118	.365	.085	.115	.048
	Prediction using Inoue's formulas					.384	.093	.118	.050
	Prediction using my formulas					.361	.091	.113	.048
	TYPE SHIP prediction (Inoue's form.)					.330	.072	.107	.047
	TYPE SHIP prediction (my form.)					.336	.074	.108	.041

	Name	Cb	B/L	B/d	2d/L	-Yv	Yr	-Nv	-Nr
TYPE	5081B	.81	0.2	3.08	0.13	.373	.102	.116	.048
New	5584B	.84	0.1818	2.80	0.13	.355	.105	.124	.042
	Prediction using Inoue's formulas					.418	.102	.130	.053
	Prediction using my formulas					.376	.102	.124	.051
	TYPE SHIP prediction (Inoue's form.)					.372	.102	.116	.048
	TYPE SHIP prediction (my form.)					.361	.101	.116	.047

Figure 17. Example of the TYPE SHIP application

being similar to the designed ship, then the estimation of the hydrodynamic performance may be done using each of the type ships. The ultimate hydrodynamic performance is to be obtained by weighting the results $PERF(X_j)$ from the all the type ships as shown in the equation (27). During this process the weights λ_j represent the level of the hull similarity between the type ship and the new design.

$$PERF(X_{New}) = \Sigma_j\{PERF(X_{Type})_j + \lambda_j d(PERF(X_{New}; X_{Type})_j)\} \quad .... (27)$$
$$\Sigma_j\{\lambda_j\} = 1; \qquad \lambda_j >= 0$$

The formula FP(X), which describes the hydrodynamic performance and serves as a judgment of the influence of principal particulars' modifications, may be also improved. For this the concept of the hull form similarity is useful. First, the designer should pick up a ship having hull form close to the hull form of his new design. This ship will serve as a REFERENCE SHIP in the database. Second, the judgment of similarity between ships in the database and the REFERENCE SHIP should be made. Since both hull form and hydrodynamic performance for ships in the database are known, the criterion of the ships' similarity should be originated in the similarity of their hydrodynamic performances. For

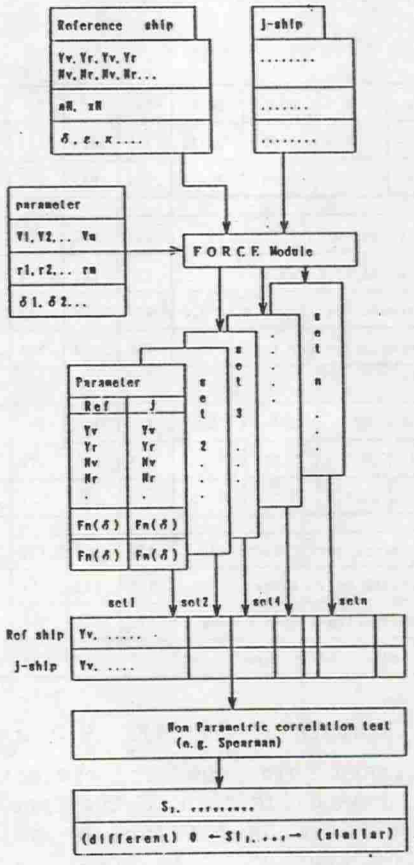

Figure 18. Hull similarity judgment

example, in the case of modular maneuvering model (e.g., MMG) there are many hydrodynamic parameters that may be used for calculation of the elementary hydrodynamic forces (like linear and nonlinear hull force components, and components of the rudder force). These elementary forces

constitute detailed ship description from the hydrodynamic viewpoint and such a description is suitable for application of nonparametric (rank) correlation tests. Figure 18 shows an arrangement for such a test. The process of the similarity judgment renders similarity numbers $s_{i,ref}$ which in turn may be used as weights for the performance data $PERF(X_j)$ during the data fitting process.

The third step is to use the formulas (26) or (27) - with the REFERENCE SHIP replacing the type ship - for the estimation of the new design's hydrodynamic performance.

Such a practical method may considerably improve the utilization of the available information. The exclusive use of formulas describing relations between hull form and hydrodynamic performance has its limits. Similarly, the hydrodynamic data of formerly tested models can not be used directly for the estimation of hydrodynamic performance of a new design. However, the combined approach uses precise data of the type ship as initial estimates that are afterward corrected through application of approximating formulas. Here it should be mentioned that the performance prediction formula FP(X) may be also given by a numerical method for the calculation of the hull hydrodynamic force.

9. CONCLUSIONS.

The integrated approach for ship's maneuverability was presented, based on the main idea of utilization of various databases. The outline of the existing system was given as well as some applications of it.

(1) The authors - using database system - proposed the procedures to estimate the maneuvering and hydrodynamic performances by means of statistical formulas based on ship principal particulars.

(2) The discussion of results of MPR series model tests suggests that hydrodynamic data depend highly on the hull's frame form; it is shown that such a dependence cannot be precisely described using model's principal particulars exclusively.

(3) This is confirmed again by the results of investigations in the ship performance database and model hydrodynamic database, where the data fitting models were assumed to depend on ship's principal particulars exclusively.

(4) A concept of type ship for practical improvement of the hydrodynamic performance prediction at the initial design stage was given. The calculation example shows that such a possibility exists, however, the success of the method depends on the proper selection of the type ship and quality of the approximating formula, describing the ship's performance.

(5) The experiments in Circulating Water Channel show that it is possible to use the interaction data for Normal rudder-propeller configuration for the estimation of the "special rudders'" hydrodynamic performance.

(6) Since the tank experimental results contain valuable information, instead of giving up the idea of the database utilization for the precise maneuverability prediction it is concluded that more rational models of the database access should be developed, namely models being capable of describing the influence of the frame form on the hydrodynamic data.

REFERENCES

[1] Zhu,J., Kose, K. (1990):"Calculation of effect of ship form on the hydrodynamic force for ships in oblique motion using slender body theory", J.China Shipbuilding, pp.20-27, 1990 (in Chinese).
[2] Barr, R. et al (1981):"Technical Basis for Maneuvering Performance Standards", Hydronautics, Inc. Report to the USCG, Washington, D.C., Dec. 1981.
[3] Kose, K. et al (1991): "Study on the Maneuvering Performance Database and the Maneuverability Standards", Trans. W-JSNA, No 82, pp.167-176, 1991 (in Japanese).
[4] Kose, K. et al (1979): "On the Unusual Phenomena in Maneuverability of Ships", Journal SNAJ, No 146, 1979 (in Japanese).
[5] Kose, K. et al (1989): "Study on Effects of Stern Forms on Maneuverability", Trans. W-JSNA, No. 78, 1989, pp.129-136 (in Japanese).
[6] Kose, K. et al (1991):"Studies on the Effect of Loading Condition on the Maneuverability of Ships", Trans. W-JSNA, No.82, Aug. 1991, pp.155-166 (in Japanese).
[7] Kose, K. et al (1992):"Database System Approach for Maneuvering Performance Prediction", in printing in J.of SNAJ, Tokyo.
[8] Clarke, D. et al (1982): "The Application of Maneuvering Criteria in Hull Design Using Linear Theory", Trans. RINA, vol.125, 1983, pp.45-68.
[9] Wolters, W. (1976): "A Linear Ship Model for Judging the Effectiveness of Steering Large Tankers", Trans. RINA, pp.177-189, 1976.
[10] Newman, J. (1977): "Marine Hydrodynamics", MIT Press, Cambridge, Mass., 1977.
[11] Inoue, S. et al (1981): "Hydrodynamic Derivatives of Ship Maneuvering", ISP, vol.28, No 321, 1981.
[12] Norrbin, N. (1987):"The Turning Circle Test - Analysis and Pre-Trial Prediction", Proc. PRADS'87, pp.507-521.
[13] Kose, K. et al (1992): "A Study on Performance Estimation of Special Rudders", Trans. W-JSNA, No 84, Aug. 1992, pp.49-58 (in Japanese).
[14] Kose, K. et al (1981): "Modern Mathematical Model of Ship Maneuvering: Expressions for Hull-Propeller-Rudder Interactions", Proc. of 3rd Symposium on Ship Maneuverability, pp.27-80, 1981, Tokyo (in Japanese).

PREDICTION OF STOPPING MANOEUVRES
-PRESENT AND FUTURE-

MASATAKA FUJINO, UNIVERSITY OF TOKYO, JAPAN

ABSTRACT

In the present paper, the prediction method of stopping manoeuvres based on the mathematical model describing surge, sway and yaw motions is briefly mentioned with comparison of predicted and observed stopping abilities. Agreement of prediction and observation seems fairly satisfactory for the practical purpose. However, there are some room for improving prediction accuracy of detailed dynamic behaviour of a ship during stopping. In particular, the mathematical expressions of hydrodynamic forces on ship's bare hull and propeller brake force should be further examined and improved.

1. MATHEMATICAL MODEL FOR STOPPING MANOEUVRES

In order to predict stopping abilities such as head reach, side reach, track reach, stopping time and stopping angle by means of numerical simulation, the mathematical modeling of hydrodynamic forces in stopping manoeuvres is primarily important. The prediction accuracy of stopping manoeuvres is significantly affected by

(i) the appropriateness of mathematical expression of hydrodynamic forces acting on a ship, and

(ii) the propriety of estimation of hydrodynamic lateral force and yaw moment induced by reverse rotation of propeller, which are called "asymmetric hydrodynamic forces" in the following.

Prior to discussing on these two items, mathematical models for stopping manoeuvres are briefly mentioned subsequently.

In the following, the stopping manoeuvres of a ship in calm water is considered exclusively. Thus, it is assumed that the ship's dynamical behaviour can be described by the equations of motions of three degrees of freedom as follows;

$$\text{surge}: \quad m(\dot{u}-vr) = X_{\dot{u}}\dot{u} + X(u,v,r) + R(u) + f(J_p)\cdot T \qquad (1)$$

$$\text{sway}: \quad m(\dot{v}+ur) = Y_{\dot{v}}\dot{v} + Y(u,v,r) + \Delta Y_o(J_p) \qquad (2)$$

$$\text{yaw}: \quad I_{zz}\dot{r} = N_{\dot{r}}\dot{r} + N(u,v,r) + \Delta N_o(J_p) \qquad (3)$$

$X(u,v,r)$, $Y(u,v,r)$ and $N(u,v,r)$ denote the hydrodynamic forces and moment acting on a bare hull, which means a hull without a propeller and a rudder. The resistance on a ship advancing without lateral motions is accounted for separately by the term $R(u)$, and thus it is not included in $X(u,v,r)$. The last terms of righthand side, $f(J_p)\cdot T$,

$\Delta Y_o(J_P)$ and $\Delta N_o(J_P)$, represent the propeller induced effective brake force, propeller induced lateral force and propeller induced yaw moment, respectively. T is the brake force of propeller, and $f(J_P)$ represents the effect of hydrodynamic interaction between propeller and ship's hull. When a ship is advancing forward with its propeller rotating in the ordinary direction, $f(J_P)$ is usually expressed as 1-t, where t denotes the thrust reduction fraction. When a propeller is rotating in the reverse direction, the interaction effect is expressed in a more general form as $f(J_P)$.

At this point, it should be noted that in the previously mentioned equations (1) to (3) the total hydrodynamic forces are assumed to be able to be expressed by linear superposition of hydrodynamic forces acting on a bare hull and those induced by a reversing propeller. The force on the rudder is not taken into consideration because it is negligibly small compared with forces on ship's hull and rudder when the propeller is reversing.

1.1 MATHEMATICAL MODELS FOR HYDRODYNAMIC FORCES ON A BARE HULL

In the early duration of stopping manoeuvres, the forward speed of a ship is dominant compared with sway velocity and yaw rate. But immediately before a ship will stop, on the other hand, sway and yaw motions prevail over the forward motion. Therefore, the mathematical model of hydrodynamic force on a bare hull should be valid for a wide range of forward speed, that is to say, valid for not only moderate forward motion but also slow forward motion. In particular, the appropriateness of mathematical model for slow forward speed is indispensable to accurate prediction of ship's lateral deviation from the initial course.

Various conceptions of mathematical modeling of hydrodynamic forces at slow forward speed have been proposed, and their validity has been fully examined [1,2,3,4,5,6,7] . Among these mathematical models for description of X(u,v,r), Y(u,v,r) and N(u,v,r), the subsequently described model which is slight modification of mathematical models proposed by Kose et al. is determined to be employed in the present analysis [8] ;

$$X^*(u,v,r) = a_1 v^* r^* + a_2 u^* v^{*2}/U^* + a_3 u^* r^{*2} \tag{4}$$

$$Y^*(u,v,r) = b_1 U^* v^* + b_2 v^* |v^*| + b_3 r^* + b_4 u^* r^* + b_5 v^{*2} r^* u^*/U^{*2} + b_6 v^* r^{*2}/U^{*4} \tag{5}$$

$$N^*(u,v,r) = c_1 u^* v^* + c_2 r^* + c_3 r^{*3} + c_4 u^* r^* + c_5 v^{*2} r^* \tag{6}$$

Here the superscripts "*" denote that the variables are nondimensionalized as follows:

$$X^*, Y^* = X, Y/(0.5\rho L^3 g) \quad , \quad N^* = N/(0.5\rho L^4 g) \tag{7}$$

$$u^*, v^*, U^* = u,v,U/\sqrt{Lg} \quad , \quad r^* = r\sqrt{L/g} \tag{8}$$

After the adequacy of conventional polynomial-type mathematical model and the model proposed by Kose et al. were examined, it was decided that the mathematical model shown in eqs. (4) to (6) is among the best ones for the prediction of stopping manoeuvres of a ship [9] .

1.2 ASYMMETRIC HYDRODYNAMIC FORCES DUE TO REVERSE ROTATION OF PROPELLER

The results of captive model tests indicate that the asymmetric hydrodynamic forces are primarily dependent on the amount of advance constant J_P even though the forward speed u and/or propeller revolution n are changed. This fact was confirmed by observation of the flow field in the vicinity and in immediate front of the propeller [10] . A number of tufts, which were free to rotate around brass needles driven normally to the hull surface of a ship model, were used to detect the flow direction and to visualize the pattern of flow disturbed by the mixing of propeller slip stream and the external main flow bound for the stern from the bow. From this observation, it was found that even when the forward speed u and/or propeller revolution n are different, the flow pattern was exactly similar to each other for different cases of u and n if the advance constant J_P is identical. However, it is important to note that the measured results of asymmetric hydrodynamic forces are likely to always scatter because of the unsteadiness or fluctuation of mixed flow.

The previously-mentioned J_P dependence of the asymmetric hydrodynamic forces differs for each individual ship [10] . In the case of a single screw ship with a propeller of righthand rotation, the asymmetric hydrodynamic lateral force generates, in general, in the direction from the starboard to the port, and thus the yaw moment resulting a righthand turning is caused when the absolute value of advance constant, $|J_P|$, is comparatively small. For a large $|J_P|$, on the contrary, the direction of application of asymmetric hydrodynamic forces differs for each individual ship.

In the case of a tank vessel, for instance, the direction of application of the asymmetric hydrodynamic forces becomes opposite, that is to say, in the starboard direction or in the port direction according to the value of advance constant of J_P. On the contrary, in cases of a coastal cargo ship and a container carrier, the direction of application does not change even for the variation of advance constant. In Fig. 1, the results of measurement of the asymmetric hydrodynamic forces are shown for these three different kinds of ships. At present, however, it is difficult to predict correctly this J_P dependence of asymmetric hydrodynamic forces only from the hull form and the particulars of propeller.

2. COMPARISON OF PREDICTED STOPPING MANOEUVRES WITH RESULTS OF FREE RUNNING MODEL TESTS

Provided that various hydrodynamic data concerning stopping manoeuvres are available, prediction of stopping abilities can be conducted without difficulty. The current schemes of predicting stopping manoeuvres are divided into two broad categories: one of

which is based on the so-called response model [11] , and the other is based on the hydrodynamic force model. In the former approach, simplified differential equations are used to describe the variation of forward speed and turning rate. In the latter approach, the stopping motion is expressed by coupling equations of surge, sway, and yaw motions as described in the previous section.

In this section, stopping manoeuvres are computed by making use of hydrodynamic force model, eqs. (1) to (3), and thus the predicted results are compared with results of free running model tests. Table 1 shows the principal particulars of a PCC model used in free running model tests. Prior to examining the prediction results as well as free running test results, some results of captive model tests which were carried out for the prediction are briefly introduced.

2.1 EFFECTIVE PROPELLER BRAKE FORCE

As previously mentioned, the last term of righthand side of eq. (1), $f(J_P) \cdot T$, expresses the effective brake force of propeller, of which the amount is greatly dependent on the advance constant of propeller J_P. As an example, nondimensionalized effective brake force measured in captive model tests is shown in Fig. 2 for two kinds of water depth, H/d=4.7 and 1.3, where H and d denote the water depth and the draft of model, respectively.

As shown there, the advance constant dependence of effective brake force is significantly similar to each other in spite of the difference in water depth. Nevertheless, the propeller thrust or brake force T itself differs definitely in different water depth. In a range of advance constant larger than about 0.8, in which the propeller blades suffer from the stall, the J_P dependence of propeller brake force is completely different in different water depth. As far as the present results of measurement are concerned, the extent of J_P dependence of propeller brake force in shallow water (H/d=1.3) is remarkably less than that in deep water.

In deep water, the propeller brake force increases as $|J_P|$ increases when $|J_P|$ is larger than about 0.8, and thus the propeller brake force in that range of $|J_P|$ becomes larger than that in $|J_P|$ less than about 0.8. In shallow water, on the contrary, the propeller brake force keeps almost the same amount independently of the value of advance constant; more precisely speaking, the propeller brake force for $|J_P|$ less than about 0.8 is slightly larger than that for $|J_P|$ larger than about 0.8.

2.2 ASYMMETRIC HYDRODYNAMIC FORCES

Hydrodynamic lateral force and yaw moment induced by reverse rotation of propeller are shown in Fig. 3 for different water depth. The positive direction of lateral force and yaw moment agrees with ITTC convention; from-port-to-starboard sway force is positive and starboard-turning yaw moment is positive. The definitions of nondimensional force and moment are as follows:

$$\Delta Y_O^* = \Delta Y_O / (\rho n^2 D^4)$$
$$\Delta N_O^* = \Delta N_O / (\rho n^2 D^4 L) \qquad (9)$$

As shown in Fig. 3, the direction of yaw moment induced by reverse rotation of propeller changes from positive to negative, that is to say, from starboard turning to port turning when $|J_P|$ becomes larger than about 1.2. This qualitative tendency is very similar to that of a tank vessel previously shown in Fig. 1.

2.3 COMPARISON OF PREDICTED AND OBSERVED STOPPING ABILITIES

Since the free running model tests of stopping manoeuvres were conducted in two kinds of water depth, H/d=4.7 and 1.3, detailed comparison will be described only for these two cases. The free running model tests were carried out, in which the propeller of a ship model advancing freely at a prescribed constant speed U_o was instantaneously made to complete stop, and then was immediately reversed to a prescribed number n of revolutions linearly with time. The experiments were conducted for the following three cases;

(i) the ship model was kept advancing straight with its rudder angle (δ) fixed at 0 deg.

(ii) The rudder angle was kept at δ =5 deg. until the propeller was reversed.

(iii) The rudder angle was kept at δ =-5 deg. until the propeller was reversed.

After the propeller reversing, the rudder was returned to its neutral position (δ =0 deg.). The experiments (ii) and (iii) were carried out to examine the effect of initial sway and yaw motions on the subsequent behaviour during stopping, in other words, stopping abilities such as stopping distance, stopping time, and stopping angle. The initial approach speed U_o is 0.797 m/sec, which corresponds to 12 kt. in full scale. The righthand side of eqs. (1) to (3), except for $f(J_P)$, were determined through various captive model tests in corresponding water depth. The interaction factor $f(J_P)$ which was obtained in H/d=4.7 was always used for different water depth in numerical simulation. This is because (1) it is known that when a ship is advancing with its propeller rotating in ordinally direction, $f(J_P)$ or 1-t varies little with the water depth [12] , and (2) the experimentally determined $f(J_P)$ in H/d=1.3 becomes very large as $|J_P|$ increases, and this should be rechecked carefully.

Fig. 4 shows ship's trajectories during stopping manoeuvres, predicted by numerical simulations and measured in free running model tests, from the instant of propeller reversing to a complete stop for H/d=4.7 and 1.3. Here, "a complete stop" is defined as the instant at which surge velocity u becomes zero. Although small discrepancies are observed between the numerical simulation results and the corresponding experimental data, especially in shallow water in which the ship tends to stop in less time in numerical simulations, the agreement is satisfactory for practical purpose.

Figs. 5 and 6 summarize and compare the experimentally measured and predicted stopping abilities in H/d=4.7 and 1.3, respectively. The stopping time means the time necessary for a ship to make a stop, u=o, from the propeller reversing. r_o is the yaw rate at the instant of the propeller reversing. The time "t_r" indicated in the figures denotes the duration of time between the instant of propeller reversing and that at which the number of propeller rotation attains the prescribed number. The definitions of head reach,

side reach, and stopping angle are schematically shown in Fig. 7.

As can be expected from the comparisons of ship trajectories shown in Fig. 4, numerical simulation results compare fairly well with experimental results except for the stopping angle in H/d=1.3. The considerable scattering of experimental data of the stopping angle in H/d=1.3 may be attributed to the unsteadiness of hydrodynamic forces acting on the ship because of the extremely restricted keel clearance under the ship bottom.

In order to further examine the shallow water effects on stopping abilities, additional numerical simulations have been carried out for two other water depth H/d=1.5 and 1.15. Fig. 8 compares the results obtained by numerical simulations in four kinds of water depth. For this purpose, needless to say, additional captive model tests were conducted in H/d=1.5 and 1.15 to measure the hydrodynamic forces on the bare hull, propeller brake force, and asymmetric hydrodynamic forces due to reverse rotation of propeller. However, from the reason previously mentioned, $f(J_P)$ obtained in H/d=4.7 was used throughout additional numerical simulations as well.

As shown in Fig. 8, the shallow water effects are not clearly recognized in the head reach and the stopping time whereas they are definitely observed in the side reach and the stopping angle.

For comparison additional numerical simulations are carried out, in which $f(J_P)$ determined from the experiments of the corresponding water depth was used [8]. Fig. 9 shows the results obtained in this way. From the figure it is found that the effects of the change of water depth is also distinct in the head reach and the stopping time. In principle, the results shown in Fig. 9 should be more accurate than those obtained by making use of the values of $f(J_P)$ at H/d=4.7, that is to say, the results shown in Fig. 8. However, from the viewpoint of the comparison with the experimental data, it is to the contrary as can be seen if we compare Fig. 6, Fig. 8 and Fig. 9. Although there can be a number of causes for this apparent contradiction, we now suspect that the pseudostationary assumption employed in the experimental determination of $f(J_P)$ is the one that explains it. That is to say, we used the values of $f(J_P)$ determined from experiments in which the model ship was towed at a constant speed U_o. On the other hand, in the stopping process of a ship, the flow field in the stern area is not steady and thus the corresponding effective propeller brake force may be different from that used in the pseudo-stationary assumption.

3. FUTURE PROBLEMS TO BE SOLVED

Although the agreement of numerical simulations and observed stopping manoeuvres is fairly well, there remains some problems to be solved in order that the prediction accuracy may be more improved.

3.1 PSEUDO-STATIONARY ASSUMPTION

As mentioned at the end of the previous section, the values of $f(J_P)$ and propeller brake force T estimated on the pseudo-stationary assumption may differ from those measured actually, especially during the early stage of stopping manoeuvres with propeller being re-

versed. In fact, the propeller brake force T measured in free running model tests of stopping does not compare well with the predicted brake force immediately after the propeller revolution is reversed and until it attains a prescribed constant revolution as shown in Figs. 10 and 11 [9] .

They show how the propeller brake force used in the numerical prediction compare to those measured in the free running model tests. Among the triangles, which indicate the propeller brake force used in the numerical prediction, white ones denote those estimated by extrapolating the results of the towing tests because the corresponding values of J_P are out of the range of the experiments. One of the most noticeable feature is that the brake force measured in the free running model tests quite oscillate in time. However, we have not fully identified the causes for these periodic oscillations yet. Further detailed investigations such as flow visualization might be necessary.

In deep water the overall variation of brake force used in the numerical prediction is in good agreement with measured one. On the other hand, in shallow water when yaw motions exist at the initial stage of stopping, the brake force around the time at which the propeller revolution reaches the prescribed number is clearly underestimated in the numerical prediction. However, at the later stage of stopping, where the propeller revolution is almost stationary, the brake force used in the numerical prediction agrees well with the measured force.

The propeller brake force during a certain short period after the propeller reversing (t=0) is clearly affected by the presence of yaw motions. This effect is especially distinct in shallow water, in which if the propeller is reversed without yaw motions the brake force gradually increased from zero whereas if yaw motions exist a certain amount of brake force is attained immediately after the reversing. The plausible cause of this fact is that when a ship has lateral velocity or yaw rate, quite an amount of flow streams along the ship's side-hull into the propeller. However, when a ship has no lateral motions, an almost dead water area is formed at the rear field of the ship.

Therefore, in order to increase the prediction accuracy of stopping abilities, it is necessary to examine the pseudo-stationary assumption of hydrodynamic forces in stopping, especially the pseudo-stationary assumption of propeller brake force.

3.2 MATHEMATICAL MODEL FOR SLOW FORWARD MOTION

In the present numerical simulations, hydrodynamic force and moment acting on the bare hull are described by eqs. (4) to (6). These expressions or mathematical models are decided to be used from the preliminary investigation into the adequacy of various kinds of mathematical models developed to describe hydrodynamic forces on the bare hull in stopping manoeuvres. However, there still remains some room for improvement of mathematical expressions, because it is likely that the mathematical models adopted here cannot explain well the change of course stability of a ship during stopping manoeuvres. The trajectory of a ship is remarkably affected by the extent of course stability; in particular, the difference in course stability

such as the difference between "stable" and "unstable" stabilities results in a drastic difference in such predicted stopping abilities as side reach and stopping angle. Hence, in order to improve the prediction accuracy of those stopping abilities, the development of mathematical model for hydrodynamic forces on the bare hull, which should be equally useful for a wide change of ship's forward speed, is very important.

REFERENCE

[1] Kose, K., Hinata, H., et al. : "On a Mathematical Model of Maneuvering Motions of Ships in Low Speeds", Jour. Soc. Nav. Archit. Japan, Vol.155 (1984).

[2] Kobayashi, E. and Asai, S. : "A Study on Mathematical Model for Manoeuvring Motions at Low Speed", Jour. Kansai Soc. Nav. Archit. Japan, No.193 (1984).

[3] Yumuro, A. : "Some Experiments on Shallow Water Effects on Maneuvering Hydrodynamic Forces Acting on a Ship Model", Ishikawajima-Harima Engineering Review, Vol.25, No.4 (1985)

[4] Takashina, J. : "Ship Maneuvering Motion due to Tugboats and its Mathematical Model", Jour. Soc. Nav. Archit. Japan, Vol.160 (1986).

[5] Yumuro, A. : "Some Experiments on Maneuvering Hydrodynamic Forces in Low Speed Condition", Jour. Kansai Soc. Nav. Archit. Japan, No.209, (1988).

[6] Karasuno, K., Yoneta, K. and Jyanuma, S.: "A New Mathematical Model of Hydrodynamic Force and Moment Acting on a Hull in Maneuvering Motion at Slow Speed and Oblique Direction", Jour. Kansai Soc. Nav. Archit. Japan, No.209, (1988)

[7] Yoshimura, Y. : "Mathematical Model for the Manoeuvring Ship Motion in Shallow Water (2nd Report)", Jour. Kansai Soc. Nav. Archit. Japan, No.210 (1988)

[8] Fujino, M., Kagemoto, H., Ishii, Y. and Kato, T. : "Prediction of Stopping Manoeuvres of a Ship in Shallow Water", Proc. Second International Conference on Manoeuvring and Control of Marine Craft, Southampton (1992)

[9] Fujino, M., Kagemoto, Kanda, A. and Koiso, K., : "Hydrodynamic Aspects Pertaining to Stopping Manoeuvres in Shallow Water", Proc. Korea-Japan Joint Workshop on Hydrodynamics in Ship Design, Seoul (1991).

[10] Fujino, M. and Kirita, A. : " On the Manoeuvrability of Ships while Stopping by Adverse Rotation of Propeller (1st Report)", Jour. Kansai Soc. Nav. Archit. Japan, No.169, (1978)

[11] Yoshimura, Y. and Nomoto, K. : "Modeling of Manoeuvring Behaviour of Ships with a Propeller Idling, Boasting and Reversing", Jour. Soc. Nav. Archit. Japan, Vol.144 (1978)

[12] Takashina, J. : "A Study on Calculation Method of Ship Maneuvering Motion in Harbors", Doctoral Dissertation, University of Tokyo (1992)

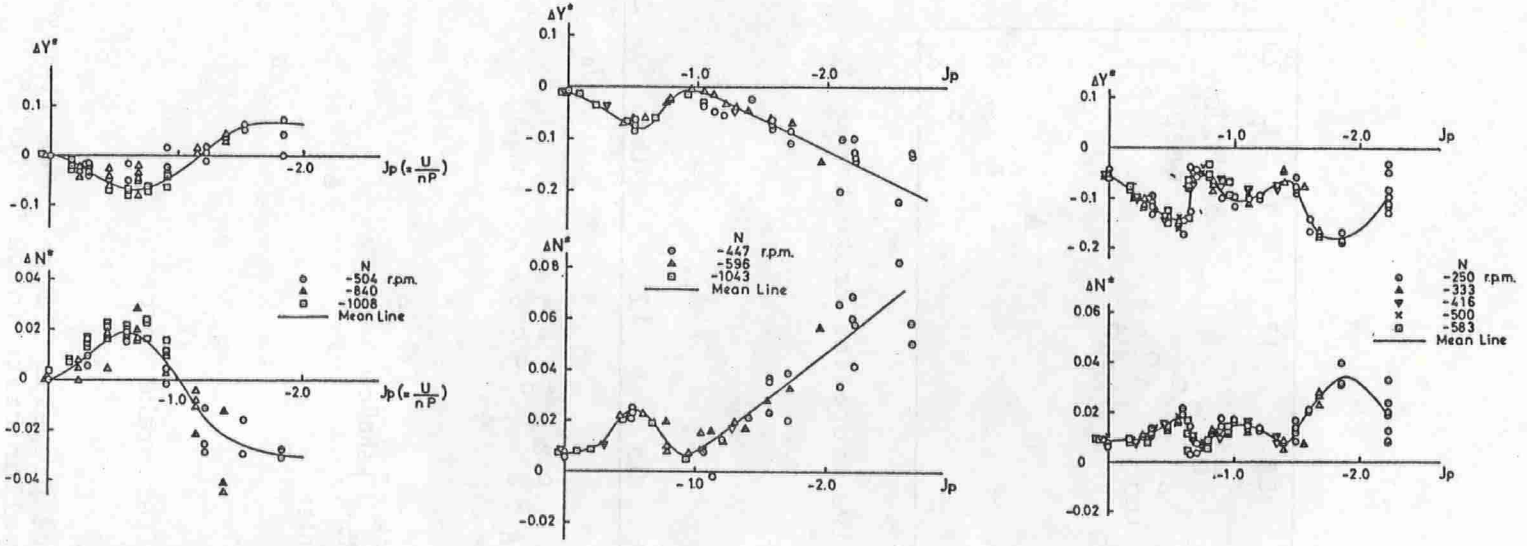

(a) Tank vessel (5.27M)

(b) Coastal cargo ship

(c) Container carrier

Fig. 1 Measured asymmetric hydrodynamic forces for three different types of ship hulls

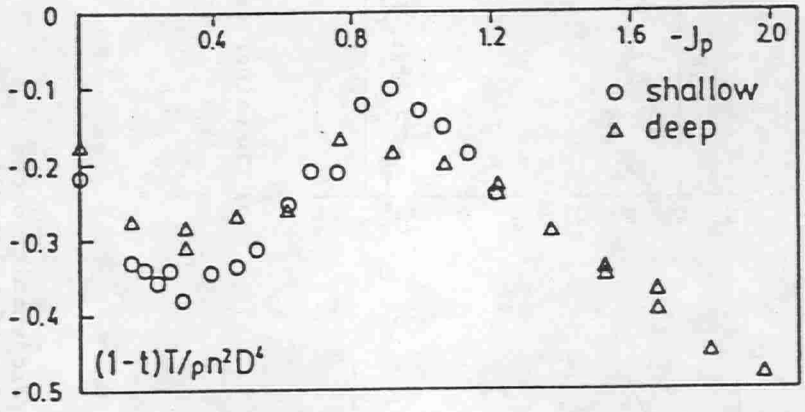

(a) Effective propeller brake force

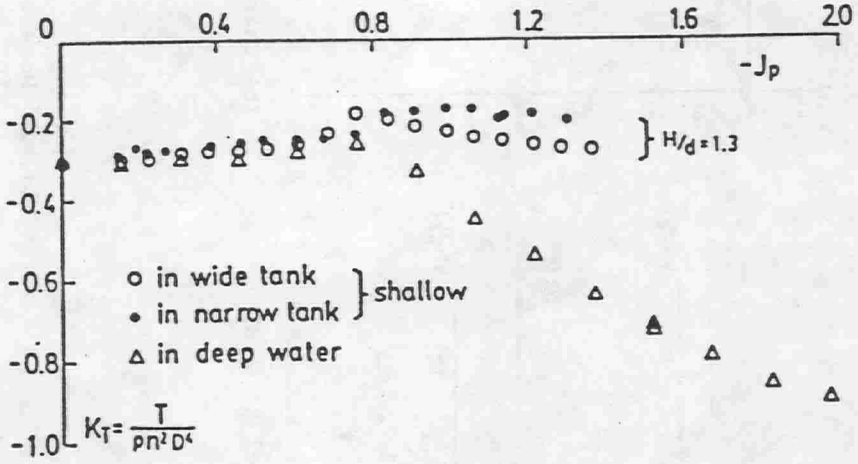

(b) Propeller brake force

Fig. 2 Effective propeller brake force (1-t)T and propeller brake force T (PCC)

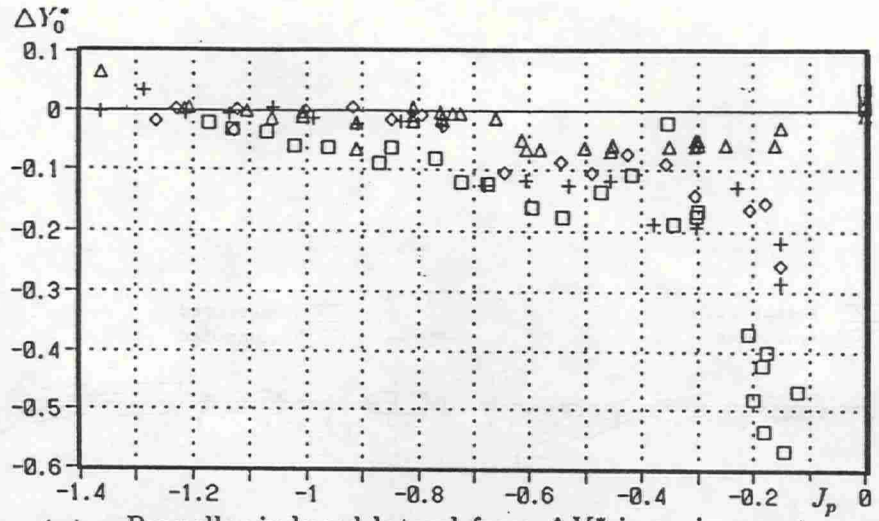

(a) Propeller induced lateral force ΔY^* in various water depth(□ H/d=1.15 + H/d=1.30 ◇ H/d=1.50 △ H/d=4.70)

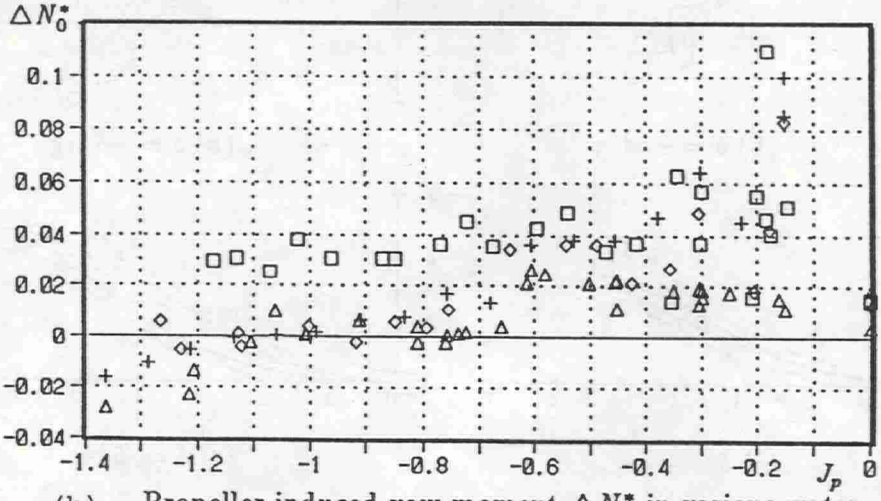

(b) Propeller induced yaw moment ΔN^* in various water depth(□ H/d=1.15 + H/d=1.30 ◇ H/d=1.50 △ H/d=4.70)

Fig. 3 Asymmetric hydrodynamic force and moment induced by reverse rotation of propeller in various water depth

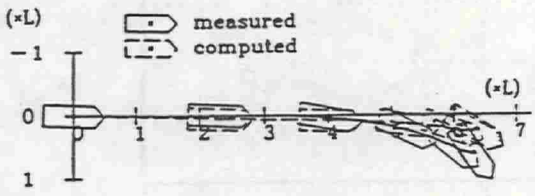

(a) δ = 0deg.

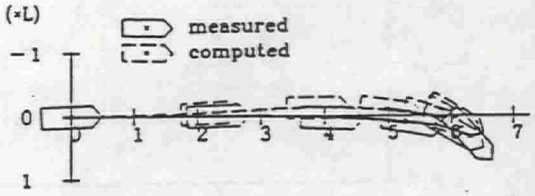

(a) δ = 0deg.

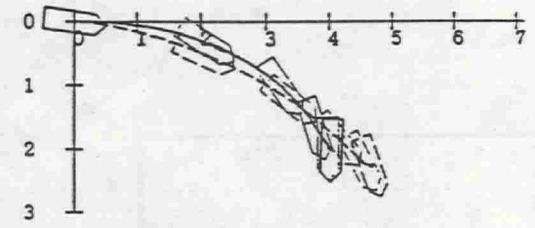

(b) δ = +5deg.

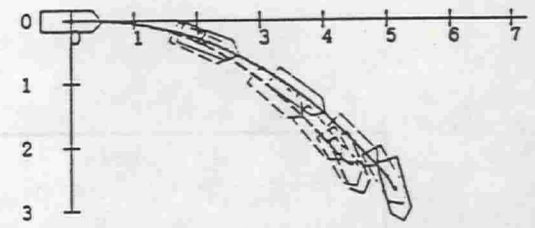

(b) δ = +5deg.

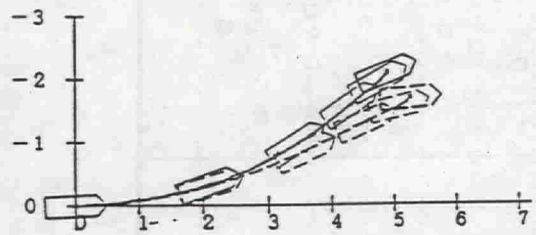

(c) δ = -5deg.

H/d = 4.7

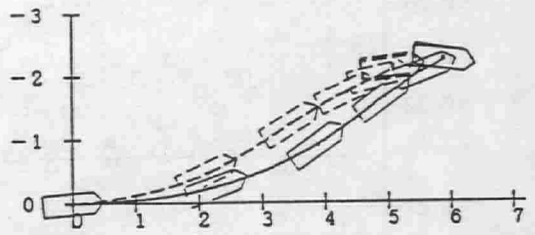

(c) δ = -5deg.

H/d = 1.3

Fig. 4 Comparisons of measured and predicted ship trajectories

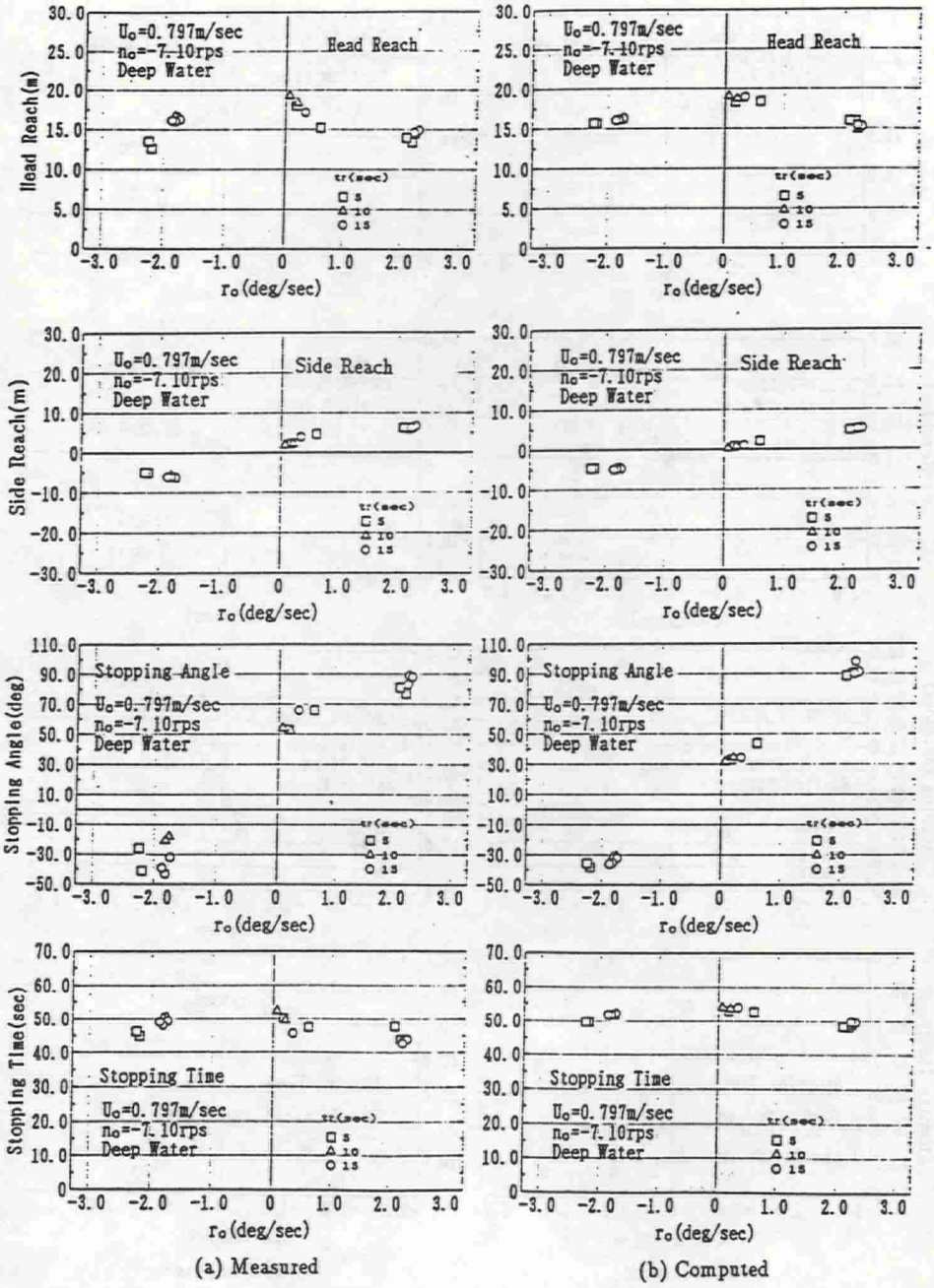

Fig. 5 Comparisons of measured and predicted stopping abilities (H/d=4.7)

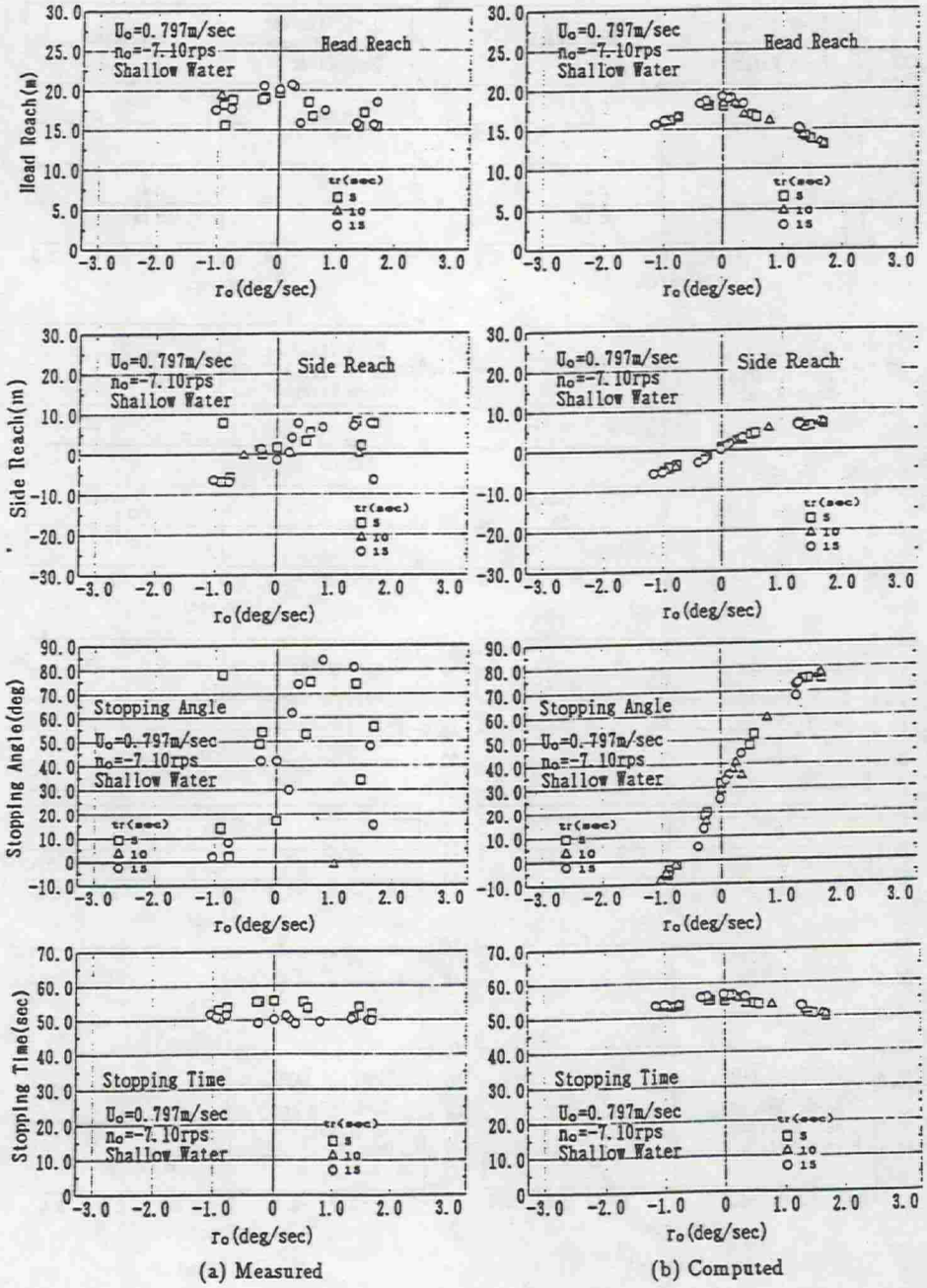

Fig. 6 Comparisons of measured and predicted stopping abilities (H/d=1.3)

Table 1 Principal particulars of the ship model used at experiments

Length between perpendiculars (L)	3.0000 m
Moulded breadth (B)	0.5367 m
Moulded draft (d)	0.1500 m
Displacement	132.94 kgf
Block coeffient (C_b)	0.550
Propeller diameter (D)	0.1067 m
Propeller pitch (P)	0.0928 m
Number of blades	5
Direction of rotation in forward motion	right
Mass moment of inertia (I_{zz})	7.625 kgf m sec^2

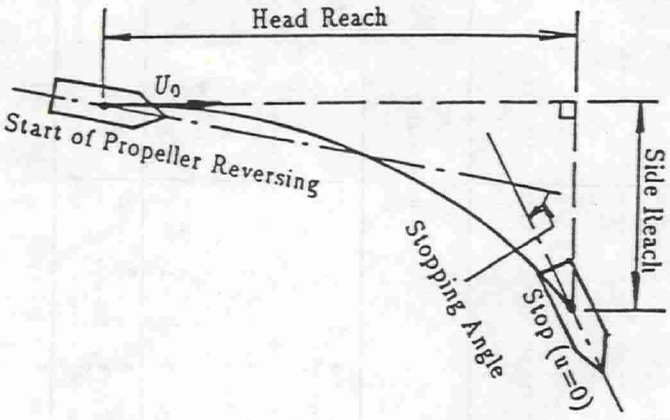

Fig. 7 Denifitions of stopping abilities

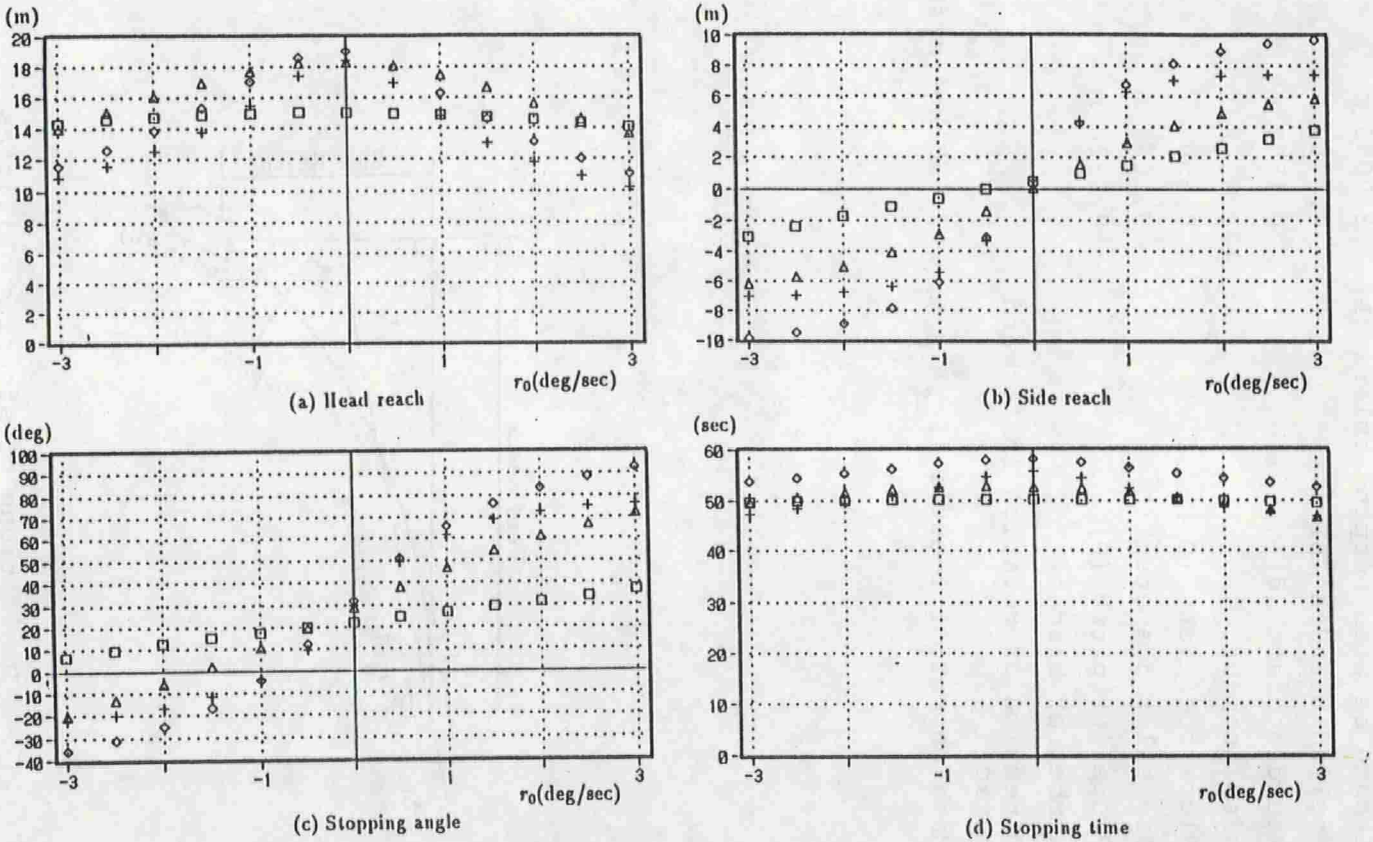

Fig. 8 Comparisons of predicted head reach, side reach, stopping angle and stopping time in various water depth ($f(J_p)$ for H/d=4.70 is used in the prediction)

(□ H/d=1.15 + H/d=1.30 ◇ H/d=1.50 △ H/d=4.70)

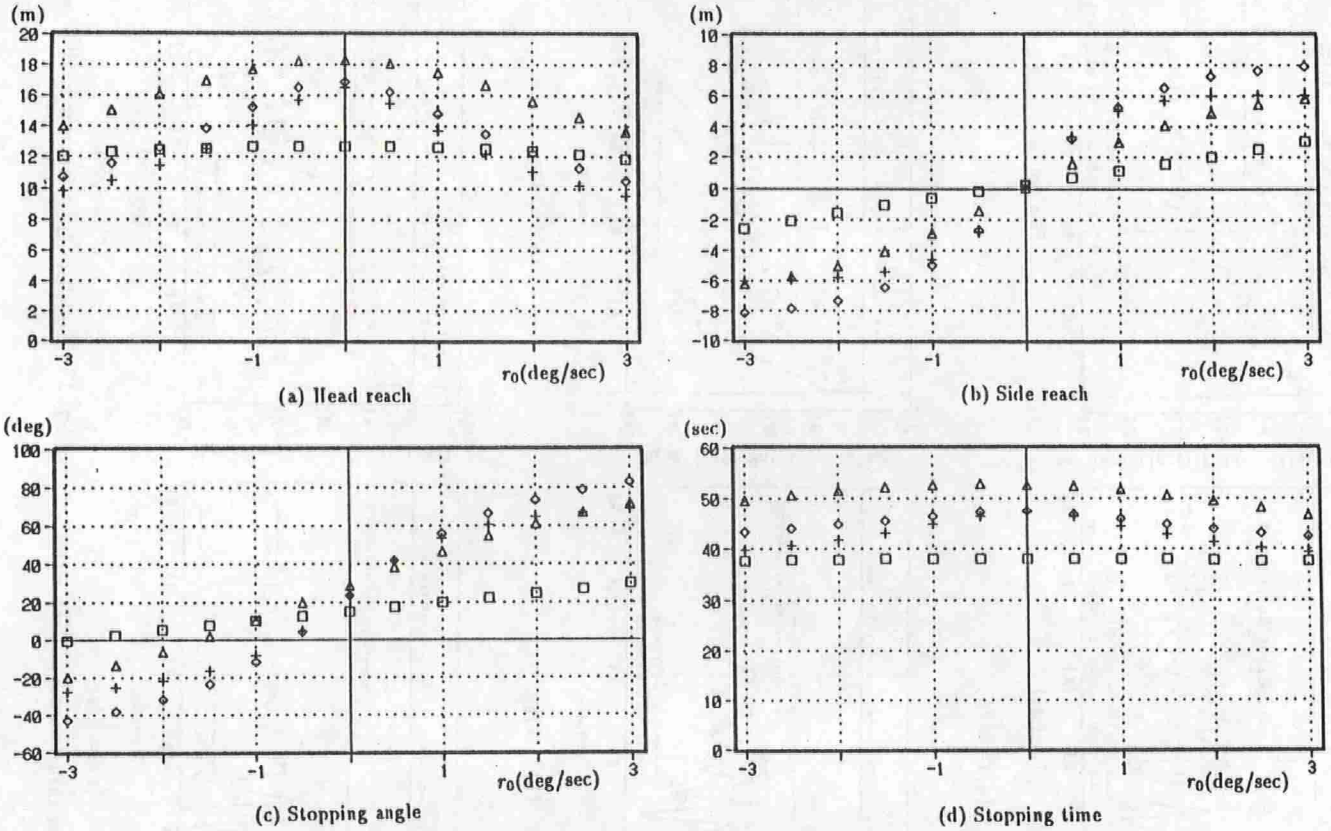

Fig. 9 | Comparisons of computed head reach, side reach, stopping angle and stopping time in various water depth (□ H/d=1.15 + H/d=1.30 ◇ H/d=1.50 △ H/d=4.70) ($f(J_p)$ for the corresponding water depth is used in the computations)

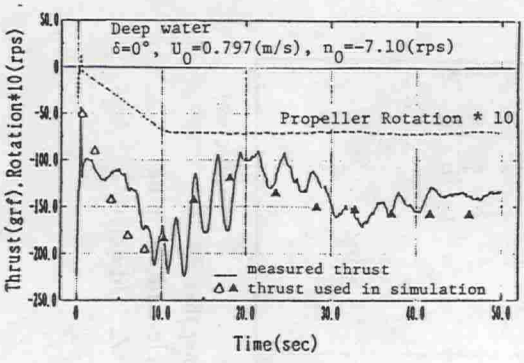

(a)δ=0deg.

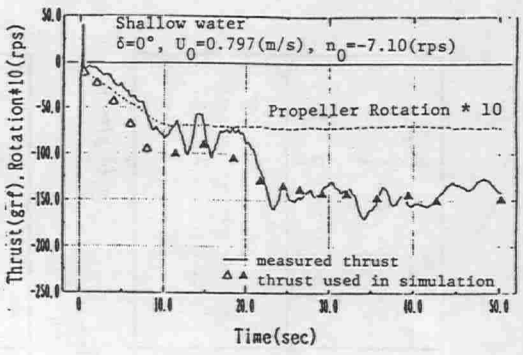

(a)δ=0deg.

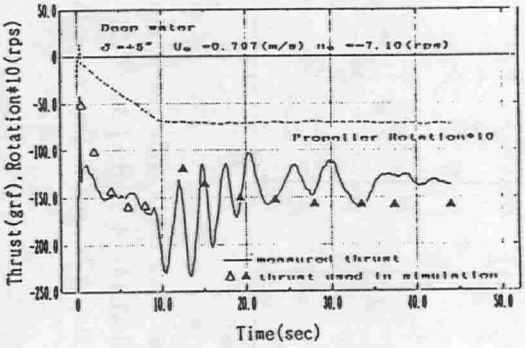

(b)δ=5deg.

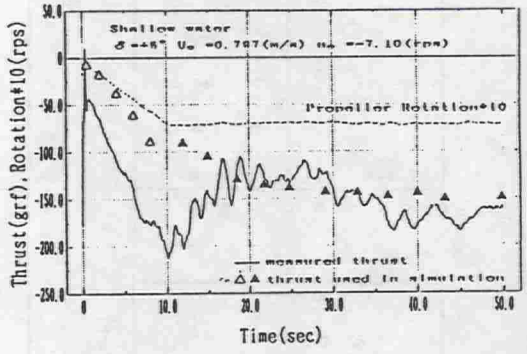

(b)δ=5deg.

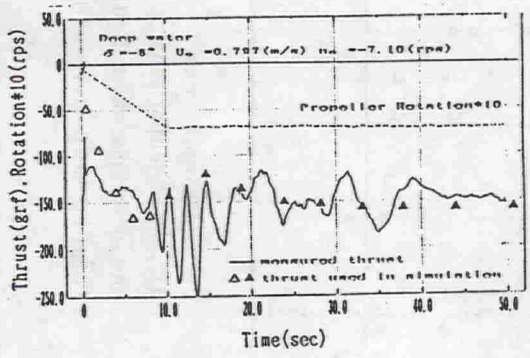

(c)δ=-5deg.

Fig.10 Propeller thrust forces in deep water

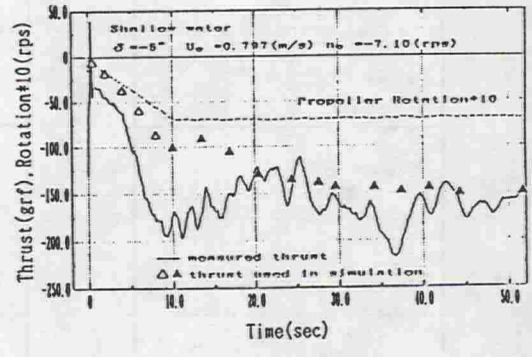

(c)δ=-5deg.

Fig.11 Propeller thrust forces in shallow water

NUMERICAL MODELLING OF HYDRODYNAMICAL ASPECTS IN SHIP MANEUVERABILITY

M. LANDRINI, I.N.S.E.A.N., ROME, ITALY
C. M. CASCIOLA, I.N.S.E.A.N., ROME, ITALY
C. COPPOLA, I.N.S.E.A.N., ROME, ITALY

Introduction

The analysis of maneuverability performance will become in the near future a basic step in the preliminary design of a ship. An efficient and reliable numerical prediction of the above performances is expected to accelerate this trend, allowing an easier approach than experimental simulation. The main difficulty is the description of the flow field around a maneuvering ship. Once this point has been assessed, the forces acting on the hull are readily available and the simulation of a full maneuver may be attempted, both at model and full scale.

In fact the flow field around a ship is highly complex and characterized by several scales, from the largest one related to the hull length to the finest related to the turbolence, which unavoidably takes place at the Reynolds numbers occuring in these applications.

Viscosity plays a basic role in determining the behaviour of the boundary layers and fixes the separation zones on the hull. From this regions highly concentrated vortex tubes are observed to penetrate in the external irrotational field [1]. Their dynamics may be described in terms of inviscid fluid mechanics, at least when the interest is pointed on the largest scales.

Secondary separations may also occur but their relevance to manoeuvrability cannot be assessed in a purely inviscid framework.

The lateral forces, namely the sway force and yaw moment, are strictly related to the strength and location of the vortices. Actually other forces occur: a resistance, to be partially ascribed to the vortex system (induced drag), generally plays a relevant role (e.g. speed drop during monoeuvring).

In the following an inviscid model for the flow around a simple ship hull is described in some details. Free surface effects are neglected and the separation region is assumed to coincide with the keel line, as it seems reasonable for the Wigley hull considered here. The main motivation for the work was to investigate the effectiveness of an inviscid model and to state the indirect effect (through fixing the separation regions) of viscosity upon manoeuvring hydrodynamics.

As it will appear, the highly nonlinear behaviour of the vortex system has a deep influence on the hydrodynamic forces. The present paper deals with the numerical modelling of these nonlinearities.

1 Mathematical Model

In the following the vortex field is described as vortex sheets imbedded in otherwise irrotational fluid which emanate from separation lines on the hull.

The velocity field may then be decomposed in the following form:

$$\vec{u}_r = \vec{u}_e + \vec{u} \,, \tag{1}$$

where $\vec{u}_r$ is the velocity field in the reference frame of the hull and $\vec{u}_e$ is the imposed external stream, which may be either a uniform stream as for the steady drifting or a complex field as for the steady turning. In general the field $\vec{u}_e$ may be rotational.

The field $\vec{u}$ is always irrotational outside the wake surfaces and represent the perturbation field in the hull frame and the total velocity field in a frame connected with the undisturbed fluid. The perturbation velocity may be then represented in the terms of vortex layers $\vec{\gamma}$ distributed on the hull and on the wake surfaces

$$\vec{u}(\vec{x}^*) = \nabla^* \times \int_{\partial\mathcal{B}} \vec{\gamma} G \, dS + \nabla^* \times \int_{\mathcal{W}} \vec{\gamma} G \, dS \,, \tag{2}$$

In the above integral representation $\partial\mathcal{B}$ is the hull and $\mathcal{W}$ is the set of wake surfaces.

From a physical point of view, the surface vorticity represents the real vorticity field in the boundary layers and in the wake, as seen from the external irrotational field.

It may be shown that when the field $\vec{u}$ is irrotational, as in the present case, the surface vorticity field is solenoidal:

$$\nabla_\Gamma \cdot \vec{\gamma} = 0 \tag{3}$$

By collocating the integral representation (2) on the hull surface and taking the normal projection, a scalar integral equation for the surface vorticity on the hull is obtatined. The system (2), (3) allows to solve for the unknown hull vorticity, once the vorticity and the geometry of the wakes were known.

Actually the geometry of the wakes is unknown, but the wake vorticity may be related, for the steady problem considered here, to the vorticity on the hull. Some analysis of the wake dynamics in now required to elucidate this relationship.

It appears that the wake is not able to sustain any pressure jump

$$[p] = 0 \tag{4}$$

([·] stands for the jump of a quantity across the surface) and that in the present steady problem, the velocity of a wake point in the direction normal to the wake surface must be zero

$$w_n = 0 \tag{5}$$

It follows from general conservation principles that the normal fluid velocity is continuos across the wake

$$[u_n] = 0 \tag{6}$$

and that for steady problems the wake surface must be a stream surface

$$u_n = 0 \,. \tag{7}$$

It is convenient to formally define the velocity of a surface wake point as

$$\vec{w} = \frac{1}{2}(\vec{u}^+ + \vec{u}^-) \,, \tag{8}$$

where direct physical meaning is attached to the only normal component. Using this definition, the pressure condition (4) may written as:

$$\vec{w} \cdot \vec{n} \times \vec{\gamma} = 0 \, . \tag{9}$$

where from the jump properties of the vortex layers, as well as from its physical meaning, we have:

$$\vec{\gamma} = [\vec{n} \times \vec{u}] \tag{10}$$

Eq. (10), togheter with eqs. (5) and (6), states that the wake vorticity $\vec{\gamma}$ is a tangent vector field always parallel to $\vec{w}$.

The surface vorticity flux across a ribbon delimitated by two lines of the flow $\vec{w}$ is constant from the solenoidality condition (3). This constant value is given by the vorticity flux across the separation lines (Kutta type condition). The value of the vortex field is then completely determined by the width of the ribbon (it is to be recalled that the direction of the vorticity vector is known from eq. (9)).

Up to this point we are able to find the whole vortex distribution, once the geometry of the wake is prescribed. To find the wake configuration a relaxation procedure is employed, which starting from an initial guess iterates the solution by updating the configuration untill the parallelism between $\vec{w}$ and $\vec{\gamma}$ is finally satisfied.

In order to solve the problem efficiently, a vortex lattice scheme has been adopted to discretize the equations, thus implicitly imposing the solenoidality of the vorticity field, which is modeled as a set of quadrangular vortex rings.

2 Numerical Results

As stated in the introduction, the hydrodynamic forces acting on the hull are expected to critically depend upon the behaviour of the vortex system. Special care is needed when using results related to the modelling of vortices. In order to gain some confidence on our results we like then to present some simple test cases. A flat plate in steady drifting conditions is considered first.

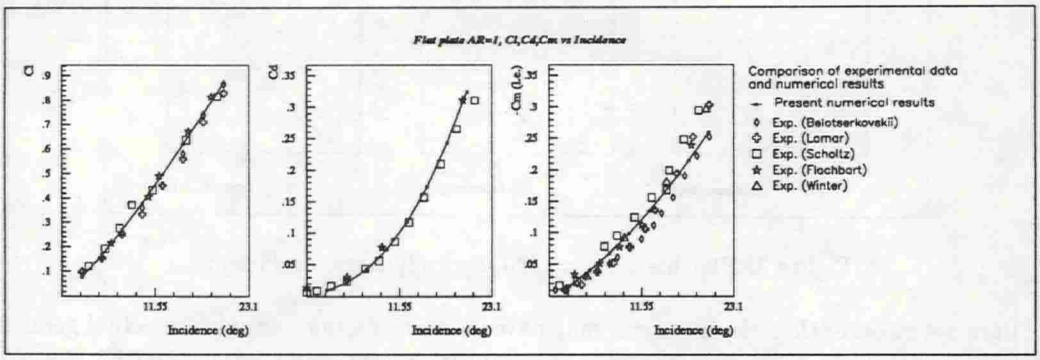

Figure 1: Flat plate AR=1, hydrodynamic coefficients.

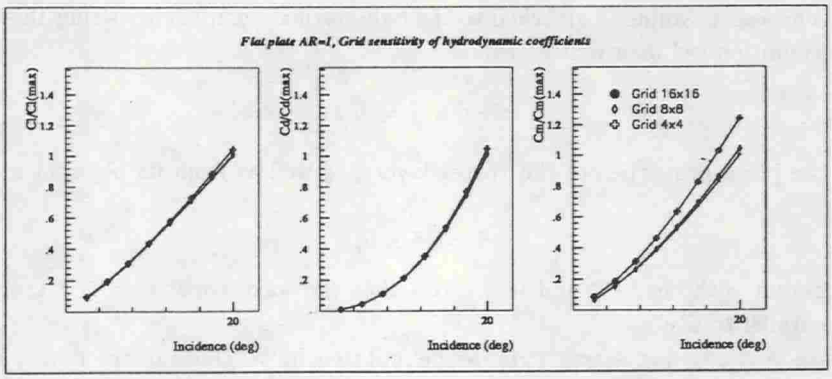

Figure 2: Grid sensitivity.

2.1 Steady drift

Vortex flows about flat plates at incidence are classical topics in aerodynamics, and great amount of results, both numerical and experimental, exist. The interest here is on very low aspect ratio plates, where the nonlinear effects due to the vortex system detaching from the tips are predominant.

In figure 1 the computed values of the relevant aerodynamic coefficients, namely C_l, C_d and C_m, for a flat plate with aspect ratio AR = 1 are shown.

A typical grid convergence analysis (see figure 2) is also included, showing plots of the hydrodynamics coefficients versus incidence for several meshes. Similar behaviours are observed for the other relevant quantities, and the numerical results are to be considered well converged with respect to the mesh size.

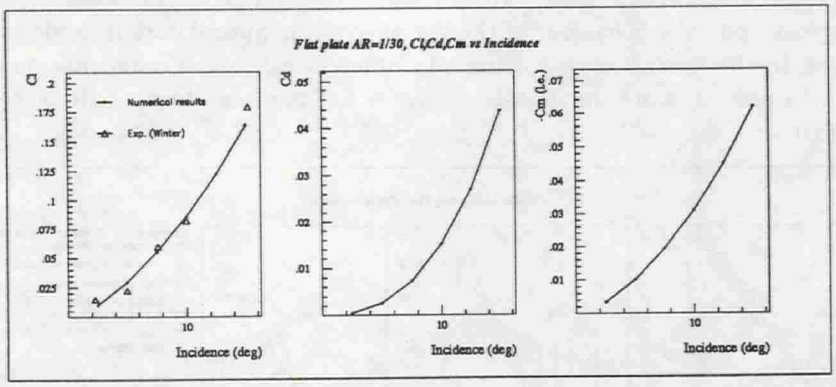

Figure 3: Flat plate AR=1/30, hydrodynamic coefficients.

Parameters other than the mesh size may have influence on the results. The actual geometry of the vortex wake is computed by means of a relaxation procedure: from an initial guess, the solution is iterated. The L^2 norm of the solution on the plate and that of the position of the vortex wake were computed at each iteration. Convergence was assumed for variations of the above norms less then 10^{-5}.

Actually the geometry of the vortex system can be computed only for a finite length downstream of the plate (the near wake). It is then prolongated using semi-infinite straigth vortex filaments (the far wake). The length of the near wake, the only portion whose nonlinear behaviour is accounted for, may affect the pressure distribution on the plate (or on the hull). Preliminary calculation were used to determine its optimal length, selected in such a way that variations less than 10^{-5} in the norm of the solution is observed when further increasing the lenght. Typically the optimum wake length critically depends upon the aspect ratio of the plate.

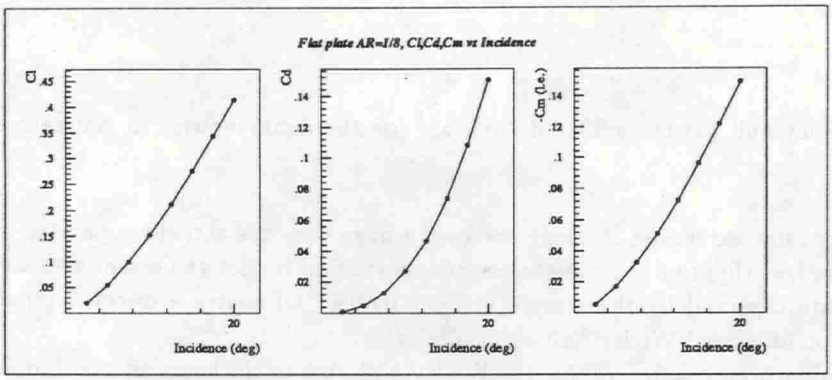

Figure 4: Flat plate AR=1/8, hydrodynamic coefficients.

The numerical results in figure 1 are compared with experiments from several authors. As it appears, they are well within the range of the experimental dispersion. It is worth noting here that not only the lift, but also the induced drag and yaw moment are well predicted by the inviscid model. Concerning the induced drag, the experimental value of the drag coefficient at zero incidence was added to the numerical results in order to account for the viscous drag. As well known, the most important contribution to the drag cames, under these conditions, from the energy loss related to the vortex system.

Although in the case above reported the tip vortices have a relevant influence on the forces, the aspect ratio is far from those encountered in ship maneuverability, when the interest is centered on the hull rather than on the control surfaces.

A more critical test is presented in the next figure, where the aspect ratio of the plate is reduced to AR $= \frac{1}{30}$. In this case we were able to find data from experiments concerning the only lift coefficient. Again the computations compare favourably with the experiments allowing some confidence with the numerical results. Assuming the longitudinal midplane as being representative of a ship hull, a reasonable value for the aspect ratio is AR $= \frac{1}{16}$. This value was selected for a preliminary calculation about a Wigley hull with beam to draft ratio $\frac{B}{T} = 1.6$. No wave effect were included in the model and the free surface were accounted for by a double model symmetry.

The separation region on the hull was assumed to coincide with the keel line. This point may be considered not completely supported by the experimantal evidence, even in the case of slender hulls, when the beam to draft ratio is not extremely small. Actually in the flow visualizations of the slender Mariner hull reported in [2], it appears that a vortex may be present at the forebody in the downstream side, but it is confined to a boundary layer cross flow. In our simulations,

Figure 5: Wigley hull (on the left) and flat plate (on the right) mowing at constant drift angle ($\beta = 10$ deg).

the detachment line extending all along the keel, a huge vortex is actually separated at the very foreend of the keel (figure 5). Nevertheless our impression is that the essential features of the vortex field are captured by this simple inviscid model. Of course a direct comparison with experiments on an actual Wigley hull seems desirable.

As appearing from the figures, for the Wigley hull, due to thickness effects, the vortices are retained to move completely over the side of the hull. This changes significantly the pressure distribution on the hull with respect to that on the flat plate.

2.2 Steady turning

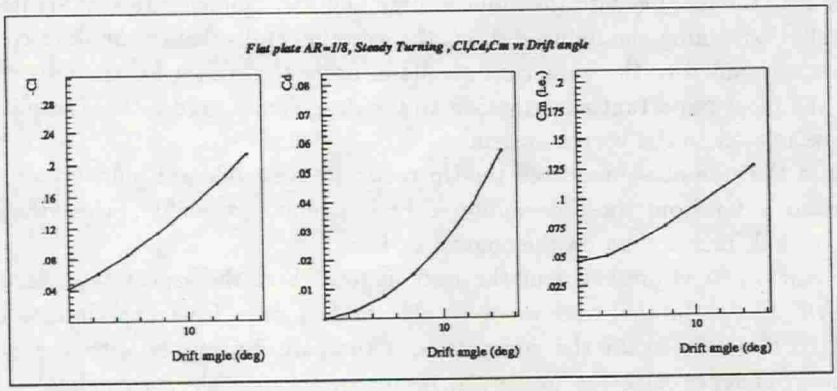

Figure 6: Steady turning

Of great relevance to ship manoeuvrability is the steady turning test. This test, for a given hull geometry, is characterized by the following parameters: the yaw rate ω, the turning radius r and the drift angle β.

Here results concerning the flat plate with $AR = 1/8$ will be briefly described, assumig $\omega = .33$ and $r = 2.5L$, where L is the length of the plate. As a reference velocity for the hydrodynamic coefficients, we used that of the midplate point (ωr). It is to be noted that in figure 6 Cl has its sign changed, thus reporting positive quantities.

Due to rotation, the incoming flow differs significantly from a uniform stream. This induces a substantial variation of the conditions at the plate surface and the local angle of attack may change its sign mowing along from the leading to the trailing edge. As a consequence, the vorticity released in the proximity of the leading edge has a sign opposite to that released in the aft, as seen from figure 7, where the vorticity flux is plotted versus the normalized distance from the leading edge.

Completely different behaviours are associated with the sign of the vorticity flux (fig. 8): the positive foreend vortices are initially convected outside the trajectory of the midplate point, while the negative ones are moved inside. Following a filament with positive vorticity, a point is reached where, essentially due to the change in the external rotating stream, the vortex is bent inwards, thus passing very close to the plate edge.

As the drift angle increases the length of the region where positive vorticity is shed decreases. For β high enough the entire side wake has a one signed (negative) vorticity. Under this conditions the whole vortex system near the plate is found inside the trajectory of the midplate point.

By comparing the figures 4 and 6, it appears that, for small drift angles the side force on the turning plate exceeds that for the steady drifting, but eventually, for increasing angles, the steady drifting plate may experience an higher lift.

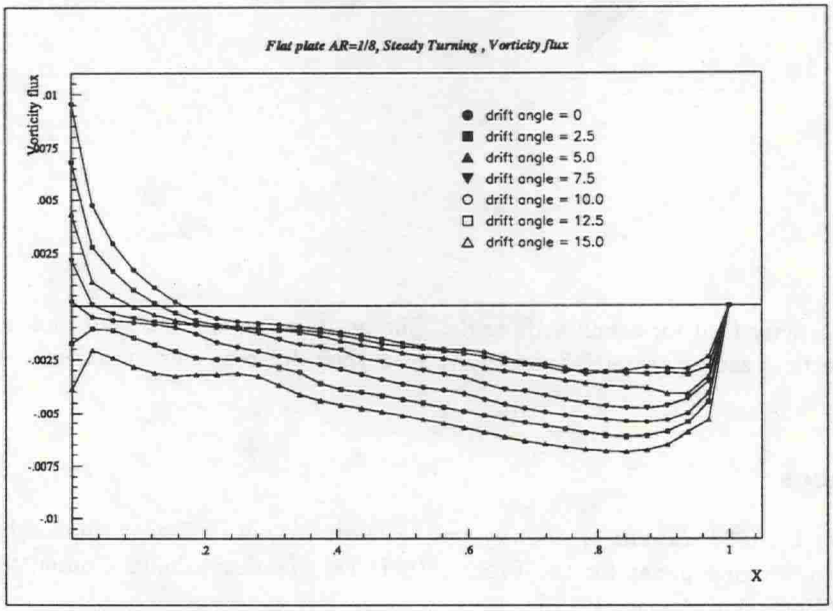

Figure 7: Vorticity flux for several drift angles.

2.3 Conclusions

Although the work is still in progress we try to draw some conclusions.

Regarding our tests with the flat plate, as may be expected, the computed results agrees well with available experimental data. In this case the dynamics of the vortices is well described

by the inviscid model and the forces are accurately predicted.

We plan to complete a parametric analysis of the steady turnig problem to elucidate the effect of changing both the yaw rate and the turning radius.

The preliminary results for the Wigley hull seems encouraging, but still needing an experimental validation. By comparing with flow visualizations on a different hull (Mariner) it appears that the foreend vortex may be actually overpredicted. Anyway, extrapolation of results from the smooth Mariner hull to a sharper one may be misleading and a comparison with experiments on the actual Wigley geometry is highly desirable.

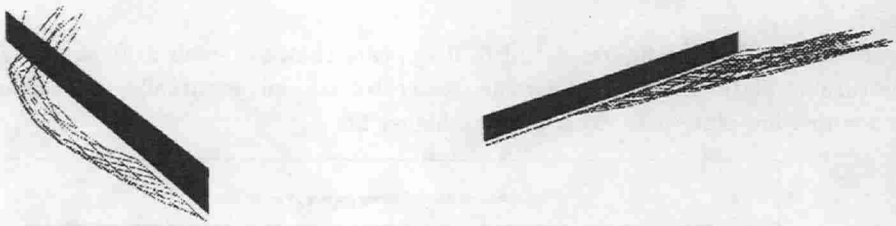

Figure 8: Vorticity field for a null drift angle. The positive (on the left side) and negative (on the right) vortices are separately shown to evidence their different configurations.

References

[1] Nikolaev E., 1988, *Results of rotating arm tests carried out in Krylov shipbuilding research institute*, working paper for the Proc. 19th ITTC Manoeuvrability Committee, Madrid, Spain (1990), Vol. 1, pag. 397. fig. 12.

[2] Newman J. N., 1966, *Some hydrodynamic aspects of ship maneuverability*, Sixth Symposium on naval hydrodynamics, Washington, D.C..

[3] Brard R., *Vortex theory for bodies moving in water*, in Ninth symposium on naval hydrodynamics, pp. 1187-1284, 1972.

[4] Yasukawa H., *Numerical Calculation of Steady Performance of a Thin Ship*, Second MCMC 1992, Southampton, UK, 1992.

[5] P. Bassanini, C.M. Casciola, M.R. Lancia, R. Piva: *A Boundary Integral Formulation for the Kinetic Field in Aerodynamics. I. Mathematical Analisys.*, Eur. J. Mech., B/Fluids, 10, n. 4, 1991.

[6] C.M. Casciola, M. Landrini, *A numerical study of hydrofoil craft hydrodynamics*, Convegno sulle Applicazioni della Matematica in Campo Navale, Livorno, Italy, 1992 (in italian).

A CONCEPT ABOUT A PHYSICAL-MATHEMATICAL MODEL OF HYDRODYNAMIC FORCES AND MOMENT ACTING ON A HULL DURING LARGE DRIFTING AND TURNING MOTION UNDER SLOW SPEED CONDITIONS

KEIICHI KARASUNO, FACULTY OF FISHERIES, HOKKAIDO UNIVERSITY, JAPAN

ABSTRACT

This paper describes the construction concept for a mathematical model incorporating physical ingredients of ship fluid-dynamic forces under conditions of turning motion and large drift. The mathematical model[2] for ship turning motion has also been derived from the physical-mathematical model[1] of ship fluid-dynamic forces in an oblique motion. The mathematical model consists of six elementary fluid-dynamic forces. They are as follows: 1) ideal force, 2) viscous lift, 3) induced drag, 4) cross-flow drag, 5) cross-flow lift due to fore and aft asymmetry of flow, and 6) frictional drag. On the model, it is assumed that the greater part of viscous lift and induced drag occurs along the leading or trailing edge of the ship's hull and these forces connect with drifting angles at each edge. Furthermore, it is assumed that the coefficient of cross-flow drag C_D is changed by drift angle at section β_x, $C_D = C_{D90} \cdot |\sin\beta_x| \cdot (1+p\cdot\cos^2\beta_x) \cdot f_2(u,v,r,x,L)$, where p value is determined from the coefficient of induced drag, which is derived from the assumption that no stall effect in the longitudinal force occurs within the range of small drift angles, and f_2 is determined from laterally turning motions (u=0).

Experimental data of fluid-dynamic forces generated in steady drifting or turning ship models, were incorporated with the mathematical model constructed above and resulted in the

following model.

$$X'=m'_y\cdot v'\cdot r'+(X'_{uvv}\cdot u'\cdot v'^2+X'_{uvr}\cdot u'\cdot v'\cdot r'+X'_{urr}\cdot u'\cdot r'^2)\cdot\frac{1}{\{u'^2+(v'+x'_t\cdot r')^2\}^{1/2}}+(X'_{uuvv}\cdot u'^3\cdot v'^2+X'_{uuvr}\cdot u'^3\cdot v'\cdot r'+X'_{uurr}\cdot u'^3\cdot r'^2)\cdot\frac{1}{\{u'^2+(v'+x'_t\cdot r')^2\}^{3/2}}+X'_{vv}\cdot v'^2+X'_{vr}\cdot v'\cdot r'+X'_{rr}\cdot r'^2+X'_{|u|u}|u'|\cdot u'$$

$$Y'=-m'_x\cdot u'\cdot r'+(Y'_{uuv}\cdot u'^2\cdot v'+Y'_{uur}\cdot u'^2\cdot r')\cdot\frac{1}{\{u'^2+(v'+x'_t\cdot r')^2\}^{1/2}}+(Y'_{uuvvv}\cdot u'^2\cdot v'^3+Y'_{uuvvr}\cdot u'^2\cdot v'^2\cdot r'+Y'_{uuvrr}\cdot u'^2\cdot v'\cdot r'^2+Y'_{uurrr}\cdot u'^2\cdot r'^3)\cdot\frac{1}{\{u'^2+(v'+x'_t\cdot r')^2\}^{3/2}}-\int C_{D90}\cdot\frac{(v'+x'\cdot r')^3}{\{u'^2+(v'+x'\cdot r')^2\}^{1/2}}\cdot\{1+p\cdot\frac{u^2}{u'^2+(v'+x'\cdot r')^2}\}\cdot f_2\cdot d'\cdot dx'$$

$$N'=(m'_x-m'_y)\cdot u'\cdot v'+(N^*{}'_{uuv}\cdot u'^2\cdot v'+N'_{uur}\cdot u'^2\cdot r')\cdot\frac{1}{\{u'^2+(v'+x'_t\cdot r')^2\}^{1/2}}+(N'_{uuvvv}\cdot u'^2\cdot v'^3+N'_{uuvrr}\cdot u'^2\cdot v'^2\cdot r+N'_{uuvrr}\cdot u'^2\cdot v'\cdot r'^2+N'_{uurrr}\cdot u'^2\cdot r'^3)\cdot\frac{1}{\{u'^2+(v'+x'_t\cdot r')^2\}^{3/2}}-\int C_{D90}\cdot\frac{(v'+x'\cdot r')^3}{\{u'^2+(v'+x'\cdot r')^2\}^{1/2}}\cdot\{1+p\cdot\frac{u'^2}{u'^2+(v'+x'\cdot r')^2}\}\cdot f_2\cdot x'\cdot d'\cdot dx'$$

where x'_l, x'_t : indicate longitudinal locations of leading and trailing edge of a ship

$$X'_{uvv}=C'_L-\Delta C'_L$$
$$X'_{uvr}=(C'_L-\Delta C'_L)\cdot 2\cdot x'_t\cdot C_{vo}$$
$$X'_{urr}=(C'_L-\Delta C'_L)\cdot x'^2_t$$
$$X'_{uuvv}=-(C'_{Di}-\Delta C'_{Di})$$
$$X'_{uuvr}=-(C'_{Di}-\Delta C'_{Di})\cdot 2\cdot x'_l\cdot C_{io}$$

$$X'_{uurr}=-(C'_{Di}-\triangle C'_{Di})\cdot x'^{2}_{l}$$

$$X'_{vv}=-C'_{LAS}$$

$$X'_{vr}=C'_{LASAF}$$

$$X'_{rr}=-C'_{LAS}/4$$

$$X'_{|u|u}=-C'_{F}$$

C_{v0}, C_{i0} : distribution factors of viscous lift and induced drag on longitudinal axis

$$Y'_{uuv}=-C'_{L}$$

$$Y'_{uur}=-C'_{L}\cdot x'_{t}\cdot C_{v0}$$

$$Y'_{uvvv}=-C'_{Di}$$

$$Y'_{uvvr}=-C'_{Di}\cdot 3\cdot x'_{l}\cdot C_{i0}$$

$$Y'_{uvrr}=-C'_{Di}\cdot 3\cdot x'^{2}_{l}$$

$$Y'_{urrr}=-C'_{Di}\cdot x'^{3}_{l}\cdot C_{i0}$$

$$N^{*}{}'_{uuv}=-x'_{t}\cdot C'_{L}\cdot C_{v0}$$

$$N'_{uur}=-x'_{t}\cdot C'_{L}\cdot x'_{t}$$

$$N'_{uvvv}=-x'_{l}\cdot C'_{Di}\cdot C_{i0}$$

$$N'_{uvvr}=-x'_{l}\cdot C'_{Di}\cdot 3\cdot x'_{l}$$

$$N'_{uvrr}=-x'_{l}\cdot C'_{Di}\cdot 3\cdot x'^{2}_{l}\cdot C_{i0}$$

$$N'_{urrr}=-x'_{l}\cdot C'_{Di}\cdot x'^{3}_{l}$$

1. INTRODUCTION

The course stability and turning characteristics of ships at cruising speed are important to ship owners and navigators with regard to fuel consumption, collision avoidance, etc. It is especially important to ease navigation and maneuverability in narrow harbors, and in the presence of other ships, under conditions of slow speed, large drifting and turning due to strong winds. Recently side thrusters and an inteligent ship handling system used to be equipped to the ship. These can control the ship in cooperation with a controllable pitch propeller, rudder, and side thrusters.

In order to estimate the ship's maneuverability mentioned above, it is useful to know not only inertia forces concerned with added masses but also other fluid-dynamic forces connected

with the ship's velocity. For this aim the mathematical model should be made to describe the fluid-dynamic forces of the ship when experiencing large drifting and turning.

Some mathematical models can describe the fluid-dynamic forces acting on a hull during large drifting and turning motion. There is, however, no mathematical model which consists of terms having the plain meanings of the physics on fluid-dynamics, especially concerning non-linear terms and the X component of the mathematical model. In the view of the physics or fluid-dynamics, this paper describes the mathematical model consisting of the elementary fluid-dynamic forces, for example the ideal fluid force, etc. Therefore ; 1) each term of the mathematical model have fluid-dynamic meanings, 2) not so many coefficients of the fluid-dynamic characteristics exist in this mathematical model, 3) many fluid-dynamic derivatives of X,Y and N components in the model arederived from fewer coefficients of the fluid-dynamic characteristicsmentioned before, and 4) the more detailed studies on the elementary fluid-dynamic forces and the scale effects will be able to estimate the fluid-dynamic forces of a full-scaled ship.

In the prospect mentioned above, the mathematical model of turning motion, which is based on the mathematcal model of the oblique motion with large drifting, is constructed with six elementary fluid-dynamic forces ; 1) ideal fluid force, 2) viscous lift, 3) induced drag, 4) cross-flow drag, 5) cross-flow lift, and 6) frictional drag. Furthermore, it is neccessary for us to consider the stole effects on the viscous lift and the induced drag, which largely affect the X force so that the stole effects may not appear in the range of small drift angles.

In addition, the viscous lift, induced drag and cross-flow lift are modeled respectively as two separate group of forces acting at the fore and aft edges of the ship, because of the assumption that those forces mentioned before are mostly generated along the fore or aft edge of the ship.

2. SIX ELEMENTS OF FLUID-DYNAMIC FORCES

The ideal fluid-dynamic force is due to hull motion generated on the hull in an ideal fluid, and is concerned with the added mass. Accordingly, the hull moving with a drift angle in the ideal fluid has no lift and drag. However, actual fluid, the viscous phenomena exists and makes some effects on the hull. The following forces are made from viscous effect, i.e. the viscous lift which is generated by bound vortices on the hull due to the Kutta-condition at the trailing edge of the hull, the induced drag which is generated by induced velocity due to the vortices shedding from the hull, the cross-flow drag which is generated laterally by the cross-flow accross the section of the hull, the cross-flow lift which is generated longitudinally by the asymmetrical cross-flow along the fore and aft edges of the hull, and the frictional drag which is generated longitudinally by the hull surface friction due to the longitudinal fluid velocity and contains the residual resistance (Figs.1,2,3).

2.1 IDEAL FLUID FORCES

If there are no viscous effects and no free surface effects, fluid-dynamic forces and moment in steady ship motion are described by following equations using added masses (Fig.4).

$$X_I = m_y \cdot v \cdot r = \frac{1}{2} \cdot \rho \cdot L_{pp} \cdot d \cdot U^2 \cdot (m'_y \cdot v' \cdot r')$$

$$Y_I = -m_x \cdot u \cdot r = \frac{1}{2} \cdot \rho \cdot L_{pp} \cdot d \cdot U^2 \cdot (-m'_x \cdot u' \cdot r')$$

$$N_I = (m_x - m_y) \cdot v \cdot r = \frac{1}{2} \cdot \rho \cdot L^2_{pp} \cdot d \cdot U^2 \cdot (m'_x - m'_y) \cdot u' \cdot v'$$

where $u' = u/U = \cos\beta$, $v' = v/U = -\sin\beta$, $r' = r \cdot L/U$

β : the drift angle at the midship section

2.2 VISCOUS LIFT

If there are any viscous effects in the fluid, we must modify the ideal forces mentioned above by adding the viscous lift due to the Kutta-condition at the trailing edge and so on. Therefore, this viscous lift is different from the conventional

lift, because the conventional lift is the sum of the ideal force and viscous lift (Fig.3).

Now, the main part of this viscous lift generates along the trailing edge of the ship and the sub-part of this lift generates along the leading edge. Then the viscous lift is modeled to generate mainly along the trailing edge and also subsidiarily along the leading edge. The viscous lift along each edge is assumed to be concerned with the geometrical inflow along each edge. The viscous lift along the leading edge $L_{v,l}$ and the lift along the trailing edge $L_{v,t}$ can be described by the following equations(Fig.5).

$$L_{v,l}=-C_{L,l}\cdot u\cdot(v+x_l\cdot r)$$
$$=-\tfrac{1}{2}\cdot\rho\cdot L_{pp}\cdot d\cdot U^2\cdot\{C'_{L,l}\cdot u'\cdot(v'+x'_l\cdot r')\}$$
$$\text{at } x=x_l \text{ : leading edge}$$

$$L_{v,t}=-C_{Lt}\cdot u\cdot(v+x_t\cdot r)$$
$$=-\tfrac{1}{2}\cdot\rho\cdot L_{pp}\cdot d\cdot U^2\cdot\{C'_{L,t}\cdot u'\cdot(v'+x'_t\cdot r')\}$$
$$\text{at } x=x_t \text{ : trailing edge}$$
$$(x_t=-x_l)$$

The direction of the viscous lift along each edge is assumed to be normal to the geometrical inflow along each edge. Therefore, X and Y components of these viscous lifts are

$$X_{L,l}=C_{L,l}\cdot u\cdot(v+x_l\cdot r)\cdot\frac{(v+x_l\cdot r)}{\{u^2+(v+x_l\cdot r)^2\}^{1/2}}$$
$$=\tfrac{1}{2}\cdot\rho\cdot L_{pp}\cdot d\cdot U^2\cdot\{C'_{L,l}\cdot u'\cdot(v'+x'_l\cdot r')\}$$
$$\cdot\frac{(v'+x'_l\cdot r')}{\{u'^2+(v'+x'_l\cdot r')^2\}^{1/2}}$$

$$Y_{L,l}=-C_{L,l}\cdot u\cdot(v+x_l\cdot r)\cdot\frac{u}{\{u^2+(v+x_l\cdot r)^2\}^{1/2}}$$
$$=-\tfrac{1}{2}\cdot\rho\cdot L_{pp}\cdot d\cdot U^2\cdot\{C'_{L,l}\cdot u'\cdot(v'+x'_l\cdot r')\}$$
$$\cdot\frac{u'}{\{u'^2+(v'+x'_l\cdot r')^2\}^{1/2}}$$

and so on. Then, the yaw-moment due to these viscous lifts are described by the followings.

$$N_{Lv}=x_l\cdot Y_{L,l}+X_t\cdot Y_{L,t}$$

$$=-x_l \cdot C_{L,l} \cdot u \cdot (v+x_l \cdot r) \cdot \frac{u}{\{u^2+(v+x_l \cdot r)^2\}^{1/2}}$$

$$-x_t \cdot C_{L,t} \cdot u \cdot (v+x_t \cdot r) \cdot \frac{u}{\{u^2+(v+x_t \cdot r)^2\}^{1/2}}$$

$$=-\frac{1}{2} \cdot \rho \cdot L_{pp} \cdot d \cdot U^2 \cdot [x'_l \cdot C'_{L,l} \cdot u' \cdot (v'+x'_l \cdot r')$$

$$\cdot \frac{u'}{\{u'^2+(v'+x'_l \cdot r')^2\}^{1/2}} + x'_t \cdot C'_{L,t} \cdot u' \cdot (v'+x'_t \cdot r')$$

$$\cdot \frac{u'}{\{u'^2+(v'+x'_t \cdot r')^2\}^{1/2}}]$$

In the case of the oblique motion (r'=0), the total visous lift L_v is the sum of both viscous lifts along the leading and trailing edges, because both of the lifts' directions are the same.

$$L_v=L_{v,l}+L_{v,t}$$

$$=-C_{L,l} \cdot u \cdot v - C_{l,t} \cdot u \cdot v$$

$$=-(C_{L,l}+C_{l,t}) \cdot u \cdot v$$

$$=-\frac{1}{2} \cdot \rho \cdot L_{pp} \cdot d \cdot U^2 \cdot (C'_{L,l}+C'_{l,t}) \cdot u' \cdot v'$$

$$=-\frac{1}{2} \cdot \rho \cdot L_{pp} \cdot d \cdot U^2 \cdot C'_L \cdot u' \cdot v'$$

where $C'_L=C'_{L.l}+C'_{L.t}$

Y component of L_v which contributes to the yaw moment, is

$$Y_{Lv}=Y_{Lv,l}+Y_{Lv,t}$$

$$=-(C_{L,l}+C_{l,t}) \cdot u \cdot v \cdot \frac{u}{\{u^2+v^2\}^{1/2}}$$

$$=-\frac{1}{2} \cdot \rho \cdot L_{pp} \cdot d \cdot U^2 \cdot (C'_{L.l}+C'_{L.t}) \cdot u' \cdot v' \cdot \cos\beta$$

$$=-\frac{1}{2} \cdot \rho \cdot L_{pp} \cdot d \cdot U^2 \cdot C'_L \cdot u' \cdot v' \cdot \cos\beta$$

and the yaw-moment is

$$N_{Lv}=-(x_l \cdot C_{L,l}+x_t \cdot C_{l,t}) \cdot u \cdot v \cdot \frac{u}{\{u^2+v^2\}^{1/2}}$$

$$=-\frac{1}{2} \cdot \rho \cdot L^2_{pp} \cdot d \cdot U^2 \cdot (x'_l \cdot C'_{L,l}+x'_t \cdot C'_{L,t}) \cdot u' \cdot v' \cdot \cos\beta$$

$$=-\frac{1}{2} \cdot \rho \cdot L^2_{pp} \cdot d \cdot U^2 \cdot x'_t \cdot (C'_{L,t}-C'_{L,l}) \cdot u' \cdot v' \cdot \cos\beta$$

$$=-\frac{1}{2} \cdot \rho \cdot L^2_{pp} \cdot d \cdot U^2 \cdot x'_t \cdot C_{vo} \cdot C'_L \cdot u' \cdot v' \cdot \cos\beta$$

where $C_{vo}=\dfrac{C'_{L.t}-C'_{L.l}}{C'_L}$ may be called as the distribution

factor of the viscous lift.
Therefore, the longitudinal location of the total viscous lift is

$$\ell'_{vo} = \frac{N_{Lv}}{Y_{Lv}} / L_{pp} = x'_t \cdot C_{vo} \simeq -\frac{1}{4} \cdot \mathrm{sgn}(u) \quad \text{due to experiments.}$$

2.3 INDUCED DRAG

The induced drag is oriented by the bound vortices of the ship under the down wash flow due to shedding vortices. Now, the main part of this induced drag generates, unlike the viscous lift, along the leading edge of the ship where the main portion of the bound vortices exists. Furthermore, the sub-part of this drag is generated along the trailing edge. Then the induced drag is modeled to generate mainly along the leading edge and also subsidiarily along the trailing edge. The induced drag along the each edge is assumed to be concerned with the geometrical inflow along each edge. The induced drag along the leading edge $D_{i,l}$ and the drag along the trailing edge $D_{i,t}$ can be described by the following equations (Fig.5).

$$D_{i,l} = C_{Di,l} \cdot u \cdot (v + x_l \cdot r) \cdot \frac{u \cdot (v + x_l \cdot r)}{u^2 + (v + x_l \cdot r)^2}$$

$$= \frac{1}{2} \cdot \rho \cdot L_{pp}^2 \cdot d \cdot U^2 \cdot C'_{Di,l} \cdot u' \cdot (v' + x'_t \cdot r') \cdot \frac{u' \cdot (v' + x'_l \cdot r')}{u'^2 + (v' + x'_l \cdot r')^2}$$

$$D_{i,t} = C_{Di,t} \cdot u \cdot (v + x_t \cdot r) \cdot \frac{u \cdot (v + x_t \cdot r)}{u^2 + (v + x_t \cdot r)^2}$$

$$= \frac{1}{2} \cdot \rho \cdot L_{pp}^2 \cdot d \cdot U^2 \cdot C'_{Di,t} \cdot u' \cdot (v' + x'_t \cdot r') \cdot \frac{u' \cdot (v' + x'_t \cdot r')}{u'^2 + (v' + x'_t \cdot r')^2}$$

The direction of the induced drag along each edge is assumed to be tangential to the geometrical inflow along each edge.
Therefore, X and Y components of these induced drags are

$$X_{Di,l} = -C_{Di,l} \cdot u \cdot (v + x_l \cdot r) \cdot \frac{u^2 \cdot (v + x_l \cdot r)}{\{u^2 + (v + x_l \cdot r)^2\}^{3/2}}$$

$$= -\frac{1}{2} \cdot \rho \cdot L_{pp}^2 \cdot d \cdot U^2 \cdot C'_{Di,l} \cdot u' \cdot (v' + x'_l \cdot r')$$

$$\cdot \frac{u'^2\cdot(v'+x'_l\cdot r')}{\{u'^2+(v'+x'_l\cdot r')^2\}^{3/2}}$$

$$Y_{Di,l}=-C_{Di,l}\cdot u\cdot(v+x_l\cdot r)\cdot\frac{u\cdot(v+x_l\cdot r)^2}{\{u^2+(v+x_l\cdot r)^2\}^{3/2}}$$

$$=-\tfrac{1}{2}\cdot\rho\cdot L_{pp}^2\cdot d\cdot U^2\cdot C'_{Di,l}\cdot u'\cdot(v'+x'\cdot r')\cdot\frac{u'\cdot(v'+x'_l\cdot r')^2}{\{u'^2+(v'+x'_l\cdot r')^2\}^{3/2}}$$

and so on. Then the yaw-moment due to these induced drag is described by the following equations.

$$N_{Di}=x_l\cdot Y_{Di,l}+x_t\cdot Y_{Di,t}$$

$$=-x_l\cdot C_{Di,l}\cdot u\cdot(v+x_l\cdot r)\cdot\frac{u\cdot(v+x_l\cdot r)^2}{\{u^2+(v+x_l\cdot r)^2\}^{3/2}}$$

$$-x_t\cdot C_{Di,t}\cdot u\cdot(v+x_t\cdot r)\cdot\frac{u\cdot(v+x_t\cdot r)^2}{\{u^2+(v+x_t\cdot r)^2\}^{3/2}}$$

$$=-\tfrac{1}{2}\cdot\rho\cdot L_{pp}^2\cdot d\cdot U^2\cdot\Big[x'_l\cdot C'_{Di,l}\cdot u'\cdot(v'+x'_l\cdot r')\cdot\frac{u'\cdot(v'+x'_l\cdot r')^2}{\{u'^2+(v'+x'_l\cdot r')^2\}^{3/2}}$$

$$+x'_t\cdot C'_{Di,t}\cdot u'\cdot(v'+x'_t\cdot r')\cdot\frac{u'\cdot(v'+x'_t\cdot r')^2}{\{u'^2+(v'+x'_t\cdot r')^2\}^{3/2}}\Big]$$

In the case of the oblique motion (r=0), the total induced drag is the sum of both induced drags along the leading and trailing edges, because the drags' directions are the same.

$$D_i=D_{i,l}+D_{i,t}$$

$$=(C_{Di,l}+C_{Di,t})\cdot u\cdot v\cdot\frac{u\cdot v}{u^2+v^2}$$

$$=\tfrac{1}{2}\cdot\rho\cdot L_{pp}^2\cdot d\cdot U^2\cdot(C'_{Di,l}+C'_{Di,t})\cdot u'^2\cdot v'^2$$

$$=\tfrac{1}{2}\cdot\rho\cdot L_{pp}^2\cdot d\cdot U^2\cdot C'_{Di}\cdot u'^2\cdot v'^2$$

where $C'_{Di}=C'_{Di.l}+C'_{Di.t}$

Y component of D_i which contributes to the yaw-moment, is

$$Y_{Di}=Y_{Di,l}+Y_{Di,t}$$

$$=-(C_{Di,l}+C_{Di,t})\cdot u\cdot v\cdot\frac{u\cdot v}{(u^2+v^2)^{3/2}}$$

$$=-\tfrac{1}{2}\cdot\rho\cdot L_{pp}^2\cdot d\cdot U^2\cdot(C'_{Di,l}+C'_{Di,t})\cdot u'\cdot v'\cdot\cos\beta\cdot\sin^2\beta$$

$$=-\tfrac{1}{2}\cdot\rho\cdot L_{pp}^2\cdot d\cdot U^2\cdot C'_{Di,l}\cdot u'\cdot v'\cdot\cos\beta\cdot\sin^2\beta$$

and the yaw-moment is

$$N_{Di}=-(x_1\cdot C_{Di,1}+x_t\cdot C_{Di,t})\cdot u\cdot v\cdot\frac{u\cdot v^2}{(u^2+v^2)^{3/2}}$$

$$=-\frac{1}{2}\cdot\rho\cdot L_{pp}^2\cdot d\cdot U^2\cdot(x'_1\cdot C'_{Di,1}+x'_t\cdot C'_{Di,t})\cdot u'\cdot v'\cdot\cos\beta\cdot\sin^2\beta$$

$$=-\frac{1}{2}\cdot\rho\cdot L_{pp}^2\cdot d\cdot U^2\cdot x'_1\cdot(C'_{Di,1}-C'_{Di,t})\cdot u'\cdot v'\cdot\cos\beta\cdot\sin^2\beta$$

$$=-\frac{1}{2}\cdot\rho\cdot L_{pp}^2\cdot d\cdot U^2\cdot x'_1\cdot C'_{io}\cdot C'_{Di}\cdot u'\cdot v'\cdot\cos\beta\cdot\sin^2\beta$$

where $C_{io}=\dfrac{(C'_{Di,1}-C'_{Di,t})}{C'_{Di}}$ may be called the distribution factor of the induced drag.

Therefore, the longitudinal location of the total induced drag is

$$\ell'_{io}=\frac{N_{Di}}{Y_{Di}}/L_{pp}=x'_1\cdot C_{io}\fallingdotseq\frac{1}{2}\cdot\mathrm{sgn}(u)\quad\text{due to experiments.}$$

2.4 CROSS-FLOW DRAG

This cross-flow drag is tangential to the cross-flow across the X axis, and is described conventionally by

$Y_c=-C_D\cdot\frac{1}{2}\cdot\rho\cdot L_{pp}\cdot d\cdot v^2$. The drag coefficient C_D should be irrelevant to the drift angle of the ship according to the principle of cross-flow theory. In this paper, however, this coefficient is assumed to be dependent to the geometrical inflow angle β_x at the ship's section and can be described by the following functions (Figs.6,7,8).

$$C_D=C_{D90}\cdot f_1(\beta_x)\cdot f_2(u,v,r,x,L_{pp})$$

C_{D90} : the coefficient of the cross flow drag on the ship's lateral motion at $\beta=90°$

β_x : the inflow angle at the section x,

$$\beta_x=-\tan^{-1}\cdot\frac{v+x\cdot r}{u}$$

$f_1(\beta_x)$: 1st modulate function due to 3-dimensional flow effect

$f_1(\beta_x)=|\sin\beta_x|\cdot(1+p\cdot\cos^2\beta_x)$: due to experiments

where p value is dependent to the ship form.

$f_2(u,v,r,x,L_{pp})$: 2nd modulate function due to the curvature of shedding vortices on turning motion

$$f_2(u,v,r,x,L_{pp}) = \frac{\{u^2+(v+x\cdot r)^2\}^{1/2}}{\{u^2+v^2+\frac{1}{3}(L_{pp}\cdot r/2)^2\}^{1/2}} = \frac{\{u'^2+(v'+x'\cdot r')^2\}^{1/2}}{\{u'^2+v'^2+\frac{1}{3}(\frac{1}{2}\cdot r')^2\}^{1/2}}$$

: due to experiments.

Then the normal forces and yaw-moment due to this drag are

$$Y_c = -\frac{1}{2}\cdot\rho\cdot\int C_D\cdot|v+x\cdot r|\cdot(v+x\cdot r)\cdot d\cdot dx$$

$$= -\frac{1}{2}\cdot\rho\cdot\int C_{D90}\cdot\frac{(v+x\cdot r)^3}{\{u^2+(v+x\cdot r)^2\}^{1/2}}\cdot\{1+p\cdot\frac{u^2}{u^2+(v+x\cdot r)^2}\}\cdot f_2\cdot d\cdot dx$$

$$= -\frac{1}{2}\cdot\rho\cdot L_{pp}\cdot d\cdot U^2\cdot\int C_{D90}\cdot\frac{(v'+x'\cdot r')^3}{\{u'^2+(v'+x'\cdot r')^2\}^{1/2}}\cdot\{1+p\cdot\frac{u'^2}{u'^2+(v'+x'\cdot r')^2}\}\cdot f_2\cdot d'\cdot dx'$$

$$N_c = -\frac{1}{2}\cdot\rho\cdot\int C_D\cdot|v+x\cdot r|\cdot(v+x\cdot r)\cdot x\cdot d\cdot dx$$

$$= -\frac{1}{2}\cdot\rho\cdot\int C_{D90}\cdot\frac{(v+x\cdot r)^3}{\{u^2+(v+x\cdot r)^2\}^{1/2}}\cdot\{1+p\cdot\frac{u^2}{u^2+(v+x\cdot r)^2}\}\cdot f_2\cdot x\cdot d\cdot dx$$

$$= -\frac{1}{2}\cdot\rho\cdot L^2_{pp}\cdot d\cdot U^2\cdot\int C_{D90}\cdot\frac{(v'+x'\cdot r')^3}{\{u'^2+(v'+x'\cdot r')^2\}^{1/2}}\cdot\{1+p\cdot\frac{u'^2}{u'^2+(v'+x'\cdot r')^2}\}\cdot f_2\cdot x'\cdot d'\cdot dx'$$

This drag is the main portion of the lateral force of the ship at the stage of the large inflow angle, but is also the residual lateral force in the range of the small inflow angle. Then we can finally determine the drag coefficient C_D after the decision of the ideal fluid force, the viscous lift, and the induced drag.

2.5 CROSS-FLOW LIFT

This cross-flow lift is normal to the cross-flow across the X axis, and is oriented by the difference of the pressure distributions between fore and aft ends of the ship due to the cross flows (Fig.6). Then

$$X_c = \frac{1}{2}\cdot\rho\cdot L_{pp}\cdot d\cdot\{C_{LASF}\cdot(v+x_F\cdot r)^2 - C_{LASA}\cdot(v+x_A\cdot r)^2\}$$
$$= \frac{1}{2}\cdot\rho\cdot L_{pp}\cdot d\cdot\{-C_{LAS}\cdot(v^2+x^2{}_F\cdot r^2)+C_{LASAF}\cdot 2\cdot x_F\cdot v\cdot r\}$$
$$= \frac{1}{2}\cdot\rho\cdot L_{pp}\cdot d\cdot U^2\cdot\{-C'_{LAS}\cdot(v'^2+x'^2{}_F\cdot r'^2)$$
$$+C'_{LASAF}\cdot v'\cdot 2\cdot x'_F\cdot r'\}$$

where x_F, x_A : longitudinal locations of F.P. and A.P.

$C'_{LAS}=C'_{LASA}-C'_{LASF}$

$C'_{LASAF}=C'_{LASA}+C'_{LASF}$

2.6 FRICTIONAL RESISTANT FORCE

The frictional effect works mainly on the longitudinal force X, and makes the longitudinal frictional resistance. Furthermore this resistance makes, what we call, the total resistance in X-direction incorporating with the eddy and wave making resistances. Under conditions of slow speed motion, the total resistance is mainly composed of the frictional resistance, so we may call it the frictional resistant force and assume that this force is concerned only with longitudinal velocity u. Then this force X_F is described as follow.

$$X_F = -\frac{1}{2}\cdot\rho\cdot S_w\cdot(1+k_e)\cdot C_{fo}\cdot|u|\cdot u$$
$$= -\frac{1}{2}\cdot\rho\cdot L_{pp}\cdot d\cdot U^2\cdot C'_F\cdot|u'|\cdot u'$$

where $$C'_F = \frac{S_w}{L_{pp}\cdot d}\cdot(1+k_e)\cdot C_{fo}$$

2.7 STOLE EFFECT ON X FORCES

As the result of the analysis about X,Y and N forces in the oblique motion, only the fluid-dynamic derivatives of X about the viscous lift and the induced drag are shown to be too small as compared with the conventional values of these derivatives (Fig.9, Table 1). This fact shows that the stole does not affect so much the Y force and N moment, but it does affect the X force. Then we assume that the stole effect works mainly to the X force

and not to the Y force and N moment, because the increase of the induced drag and the decrease of the lift cooperate with each other and likely only working in the X direction. Then the stole effect in the oblique motion is assumed to be as follows (Fig.10).

$$X_{ST}=-\Delta C_L\cdot u\cdot v\cdot\frac{v}{(u^2+v^2)^{1/2}}+\Delta C_{Di}\cdot u\cdot v\cdot\frac{u^2\cdot v}{(u^2+v^2)^{3/2}}$$

$$=-\tfrac{1}{2}\cdot\rho\cdot L_{pp}\cdot d\cdot U^2\cdot(\Delta C'_L\cdot u'\cdot v'^2-\Delta C'_{Di}\cdot u'^3\cdot v'^2)$$

$$=-\tfrac{1}{2}\cdot\rho\cdot L_{pp}\cdot d\cdot U^2\cdot\{(\Delta C'_L-\Delta C'_{Di}\cdot u'^2)\cdot v'\}\cdot u'\cdot v'$$

$$Y_{ST}=0$$

$$N_{ST}=0$$

Then, the lift decrease L_{ST} and the induced drag increase D_{ST} in the oblique motion are written as follows.

$$L_{ST}=\Delta C_L\cdot u\cdot v\cdot\frac{v^2}{u^2+v^2}-\Delta C_{Di}\cdot u\cdot v\cdot\frac{u^2\cdot v^2}{(u^2+v^2)^2}$$

$$=\tfrac{1}{2}\cdot\rho\cdot L_{pp}\cdot d\cdot U^2\cdot(\Delta C'_L\cdot u'\cdot v'^3-\Delta C'_{Di}\cdot u'^3\cdot v'^3)$$

$$=\tfrac{1}{2}\cdot\rho\cdot L_{pp}\cdot d\cdot U^2\cdot\{(\Delta C'_L-\Delta C'_{Di}\cdot u'^2)\cdot v'^2\}\cdot u'\cdot v'$$

$$D_{ST}=\Delta C_L\cdot u\cdot v\cdot\frac{u\cdot v}{u^2+v^2}-\Delta C_{Di}\cdot u\cdot v\cdot\frac{u^3\cdot v}{(u^2+v^2)^2}$$

$$=\tfrac{1}{2}\cdot\rho\cdot L_{pp}\cdot d\cdot U^2\cdot(\Delta C'_L\cdot u'^2\cdot v'^2-\Delta C'_{Di}\cdot u'^4\cdot v'^2)$$

$$=\tfrac{1}{2}\cdot\rho\cdot L_{pp}\cdot d\cdot U^2\cdot(\Delta C'_L-\Delta C'_{Di}\cdot u'^2)\cdot u'^2\cdot v'^2$$

As the stole effect hardly occurs in the range of the small drift angles, it can be assumed that the $X_{ST}-\beta$ curve is nearly equal to zero in the range of the drift angles between 0° and 30° so that $\Delta C'_{Di}$ may be equal to $\Delta C'_L$ or

$\int_{0^\circ}^{30^\circ} X_{ST}\,d\beta=\int_{0^\circ}^{30^\circ}(\Delta C'_L-\Delta C'_{Di}\cdot u'^2)\cdot u'\cdot v'^2\cdot d\beta$ may be zero.

Then we get the relation between $\Delta C'_{Di}$ and $\Delta C'_L$ that is $\Delta C'_{Di}/\Delta C'_L=1.00$ or 1.18.

Furthermore, in the case of the ship's turning motion, we may use the velocity $(v+r\cdot x)$ instead of the velocity v in the oblique motion.

3. CONSTRUCTION OF X,Y,N MATHEMATICAL MODEL DURING LARGE DRIFTING AND TURNING MOTION.

The fluid-dynamic forces acting on the hull in the large drifting and turning motion are composed of the six elementary forces mentioned before which are respectively described with the reasonable mathematical models. The total fluid-dynamic force is the sum of the six elementary forces considering the stole effects and is divided by the X,Y,N three components.
The X,Y,N components are presented precisely by the following non dimensional equations.

$$
\begin{aligned}
X' &= X'_{I} + (X'_{Lv.1} + X'_{Lv.t}) + (X'_{Di.1} + X'_{Di.t}) + X'_{C} + X'_{F} \\
&= m'_{y} \cdot v' \cdot r' + (C'_{L.1} - \Delta C'_{L.1}) \cdot u' \cdot (v' + x'_{1} \cdot r') \\
&\quad \cdot \frac{(v' + x'_{1} \cdot r')}{\{u'^{2} + (v' + x'_{1} \cdot r')^{2}\}^{1/2}} \\
&\quad + (C'_{L.t} - \Delta C'_{L.t}) \cdot u' \cdot (v' + x'_{t} \cdot r') \\
&\quad \cdot \frac{(v' + x'_{t} \cdot r')}{\{u'^{2} + (v' + x'_{t} \cdot r')^{2}\}^{1/2}} \\
&\quad - (C'_{Di.1} - \Delta C'_{Di.1}) \cdot u' \cdot (v' + x'_{1} \cdot r') \\
&\quad \cdot \frac{u'^{2} \cdot (v' + x'_{1} \cdot r')}{\{u'^{2} + (v' + x'_{1} \cdot r')^{2}\}^{3/2}} \\
&\quad - (C'_{Di.t} - \Delta C'_{Di.t}) \cdot u' \cdot (v' + x'_{t} \cdot r') \\
&\quad \cdot \frac{u'^{2} \cdot (v' + x'_{t} \cdot r')}{\{u'^{2} + (v' + x'_{t} \cdot r')^{2}\}^{3/2}} \\
&\quad - C'_{LAS} \cdot (v'^{2} + x'^{2}_{F} \cdot r'^{2}) + C'_{LASAF} \cdot v' \cdot 2 \cdot x'_{F} \cdot r' - C'_{F} \cdot |u'_{I}| \cdot u'
\end{aligned}
$$

$$
\begin{aligned}
Y' &= Y'_{I} + (Y'_{Lv.1} + Y'_{Lv.t}) + (Y'_{Di.1} + Y'_{Di.t}) + Y'_{C} \\
&= -m'_{x} \cdot u' \cdot r' - C'_{L.1} \cdot u' \cdot (v' + x'_{1} \cdot r') \\
&\quad \cdot \frac{u'}{\{u'^{2} + (v' + x'_{1} \cdot r')^{2}\}^{1/2}} \\
&\quad - C'_{L.t} \cdot u' \cdot (v' + x'_{t} \cdot r') \cdot \frac{u'}{\{u'^{2} + (v' + x'_{t} \cdot r')^{2}\}^{1/2}} \\
&\quad - C'_{Di.1} \cdot u \cdot (v' + x'_{1} \cdot r') \cdot \frac{u' \cdot (v' + x'_{1} \cdot r')^{2}}{\{u'^{2} + (v' + x'_{1} \cdot r')^{2}\}^{3/2}} \\
&\quad - C'_{Di.t} \cdot u \cdot (v' + x'_{t} \cdot r') \cdot \frac{u' \cdot (v' + x'_{t} \cdot r')^{2}}{\{u'^{2} + (v' + x'_{t} \cdot r')^{2}\}^{3/2}}
\end{aligned}
$$

$$-\int C_{D90}\cdot(v'+x'\cdot r')^2\cdot\frac{(v'+x'\cdot r')}{\{u'^2+(v'+x'\cdot r')^2\}^{1/2}}$$

$$\cdot\{1+p\cdot\frac{u'^2}{u'^2+(v'+x'\cdot r')^2}\}\cdot f_2\cdot d'\cdot dx'$$

$$N'=N'_l+(N'_{Lv.l}+N'_{Lv.t})+(N'_{Di.l}+N'_{Di.t})+N'_C$$

$$=(m'_x-m'_y)\cdot u'\cdot v'-x'_l\cdot C'_{L.l}\cdot u'\cdot(v'+x'_l\cdot r')\cdot\frac{u'}{\{u'^2+(v'+x'_t\cdot r')^2\}^{1/2}}$$

$$-x'_t\cdot C'_{L.t}\cdot u'\cdot(v'+x'_t\cdot r')\cdot\frac{u'}{\{u'^2+(v'+x'_t\cdot r')^2\}^{1/2}}$$

$$-x'_l\cdot C'_{Di.l}\cdot u'\cdot(v'+x'_l\cdot r')\cdot\frac{u'\cdot(v'+x'_l\cdot r')^2}{\{u'^2+(v'+x'_l\cdot r')^2\}^{1/2}}$$

$$-x'_t\cdot C'_{Di.t}\cdot u'\cdot(v'+x'_t\cdot r')\cdot\frac{u'+(v'+x'_t\cdot r')^2}{\{u'^2+(v'+x'_t\cdot r')^2\}^{1/2}}$$

$$-\int C_{D90}\cdot(v'+x'\cdot r')^2\cdot\frac{(v'+x'\cdot r')}{\{u'^2+(v'+x'\cdot r')^2\}^{1/2}}$$

$$\cdot\{1+p\cdot\frac{u'^2}{u'^2+(v'+x'\cdot r')^2}\}\cdot f_2\cdot x'\cdot d'\cdot dx'$$

In the case of the weak turning motion such as

$$\frac{1}{\{u'^2+(v'+x'\cdot r')^2\}}\rightarrow 1$$

where $u'^2+v'^2=1$

the viscous lift is approximated by the following,

using $x_l=-x_t$

$$X'_{Lv}=(C'_{L.l}-\Delta C'_{L.l})\cdot u'\cdot(v'-x'_t\cdot r')\cdot(v'-x'_t\cdot r')$$

$$+(C'_{L.t}-\Delta C'_{L.t})\cdot u'\cdot(v'+x'_t\cdot r')\cdot(v'+x'_t\cdot r')$$

$$=(C'_L-\Delta C'_L)\cdot u'\cdot v'^2+(\hat{C}'_L-\Delta\hat{C}'_L)\cdot 2\cdot u'\cdot x'_t\cdot r'\cdot v'$$

$$+(C_L-\Delta C_L)\cdot u'\cdot(x'_t\cdot r')^2$$

$$=(C'_L-\Delta C'_L)\cdot u'\cdot v'^2+(C'_L-\Delta C'_L)\cdot C_{vo}\cdot 2\cdot u'\cdot(x'_t\cdot r')\cdot v'$$

$$+(C_L-\Delta C_L)\cdot u'\cdot(x'_t\cdot r')^2$$

$$\fallingdotseq(C'_{L.t}-\Delta C'_{L.t})\cdot u'\cdot(v'+x'_t\cdot r')^2$$

$$Y'_{Lv}=-C'_{L.l}\cdot u'\cdot(v'-x'_t\cdot r')\cdot u'-C'_{L.t}\cdot u'\cdot(v'+x'_t\cdot r')\cdot u'$$

$$=-C'_L\cdot u'^2\cdot v'-\hat{C}'_L\cdot u'^2\cdot x'_t\cdot r'$$

$$=-C'_L\cdot u'^2\cdot(v'+C_{vo}\cdot x_t\cdot r)$$

$$N'_{Lv}=x'_t\cdot C'_{L.l}\cdot u'\cdot(v'-x'_t\cdot r')\cdot u'$$

$$
\begin{aligned}
&-x'_t \cdot C'_{L.t} \cdot u' \cdot (v' + x'_t \cdot r') \cdot u' \\
&= -x'_t \cdot \hat{C}'_L \cdot u'^2 \cdot v' - x'_t \cdot C'_L \cdot u'^2 \cdot x'_t \cdot r' \\
&= -x'_t \cdot C'_L \cdot u'^2 \cdot (C_{vo} \cdot v' + x'_t \cdot r')
\end{aligned}
$$

the induced drag is approximated by the following, using $x_t = -x_1$

$$
\begin{aligned}
X'_{Di} &= -(C'_{Di.1} - \Delta C'_{Di.1}) \cdot u' \cdot (v' + x'_1 \cdot r') \cdot u'^2 \cdot (v' + x'_1 \cdot r') \\
&\quad -(C'_{Di.t} - \Delta C'_{Di.t}) \cdot u' \cdot (v' - x'_1 \cdot r') \cdot u'^2 \cdot (v' - x'_1 \cdot r') \\
&= -(C'_{Di} - \Delta C_D{}'_i) \cdot u'^3 \cdot v'^2 - (\hat{C}'_{Di} - \Delta \hat{C}'_{Di}) \cdot 2 \cdot u'^3 \cdot x'_1 \cdot r' \cdot v' \\
&\quad -(C'_{Di} - \Delta C'_{Di}) \cdot u'^3 \cdot (x'_1 \cdot r')^2 \\
&= -(C'_{Di} - \Delta C_D{}'_i) \cdot u'^3 \cdot v'^2 - (C'_{Di} - \Delta C'_{Di}) \cdot C_{io} \cdot 2 \cdot u'^3 \\
&\quad \cdot x'_1 \cdot r' \cdot v' - (C'_{Di} - \Delta C'_{Di}) \cdot u'^3 \cdot (x'_1 \cdot r')^2 \\
&\fallingdotseq -(C'_{Di} - \Delta C_D{}'_i) \cdot u'^3 \cdot (v' + x'_1 \cdot r')^2 \\
Y'_{Di} &= -C'_{Di.1} \cdot u' \cdot (v' + x'_1 \cdot r') \cdot u' \cdot (v' + x'_1 \cdot r')^2 \\
&\quad -C'_{Di.t} \cdot u' \cdot (v' - x'_1 \cdot r') \cdot u' \cdot (v' - x'_1 \cdot r')^2 \\
&= -C'_{Di} \cdot u'^2 \cdot v'^3 - \hat{C}'_{Di} \cdot 3 \cdot u'^2 \cdot x'_1 \cdot r' \cdot v'^2 \\
&\quad -C'_{Di} \cdot 3 \cdot u'^2 \cdot (x'_1 \cdot r')^2 \cdot v' - \hat{C}'_{Di} \cdot u'^2 \cdot (x'_1 \cdot r')^3 \\
&= -C'_{Di} \cdot u'^2 \cdot v'^3 - C'_{Di} \cdot C_{io} \cdot 3 \cdot u'^2 \cdot x'_1 \cdot r' \cdot v'^2 \\
&\quad -C'_{Di} \cdot 3 \cdot u'^2 \cdot (x'_1 \cdot r')^2 \cdot v' - C'_{Di} \cdot C_{io} \cdot u'^2 \cdot (x'_1 \cdot r')^3 \\
&\fallingdotseq -C'_{Di} \cdot u'^2 \cdot (v' + C_{io}{}^{1/3} \cdot x'_1 \cdot r')^3 \\
N'_{Di} &= -x'_1 \cdot C'_{Di.1} \cdot u' \cdot (v' + x'_1 \cdot r') \cdot u' \cdot (v' + x'_1 \cdot r')^2 \\
&\quad +x'_1 \cdot C'_{Di.t} \cdot u' \cdot (v - x_1 \cdot r) \cdot u' \cdot (v' - x'_1 \cdot r')^2 \\
&= -x'_1 \cdot \hat{C}'_{Di} \cdot u'^2 \cdot v'^3 - x'_1 \cdot C'_{Di} \cdot 3 \cdot u'^2 \cdot x'_1 \cdot r' \cdot v'^2 \\
&\quad -x'_1 \cdot \hat{C}'_{Di} \cdot 3 \cdot u'^2 \cdot (x'_1 \cdot r')^2 \cdot v' - x'_1 \cdot C'_{Di} \cdot u'^2 \cdot (x'_1 \cdot r')^3 \\
&= -x'_1 \cdot C'_{Di} \cdot C_{io} \cdot u'^2 \cdot v'^3 - x'_1 \cdot C'_{Di} \cdot 3 \cdot u'^2 \cdot x'_1 \cdot r' \cdot v'^2 \\
&\quad -x'_1 \cdot C'_{Di} \cdot C_{io} \cdot 3 \cdot u'^2 \cdot (x'_1 \cdot r')^2 \cdot v' \\
&\quad -x'_1 \cdot C'_{Di} \cdot u'^2 \cdot (x'_1 \cdot r')^3 \\
&\fallingdotseq -x'_1 \cdot C'_{Di} \cdot u'^2 \cdot (C_{io}{}^{1/3} \cdot v' + x'_1 \cdot r')^3
\end{aligned}
$$

where $\hat{C}'_L = C'_{L.t} - C'_{L.1} = C'_L \cdot C_{vo}$

$\hat{C}'_{Di} = C'_{Di.1} - C'_{Di.t} = C'_{Di} \cdot C_{io}$

Then the X,Y,N components of fluid-dynamic forces are as follows in the case of the weak turning motion.

$$
\begin{aligned}
X' &= m'_y \cdot v' \cdot r' + (C'_L - \Delta C'_L) \cdot u' \cdot \{v'^2 + 2 \cdot C_{vo} \cdot v' \cdot x'_t \cdot r' + (x'_t \cdot r')^2\} \\
&\quad -(C'_{Di} - \Delta C'_{Di}) \cdot u'^3 \cdot \{v'^2 + 2 \cdot C_{io} \cdot v' \cdot x'_1 \cdot r' + (x'_1 \cdot r')^2\} \\
&\quad -C'_{LAS} \cdot (v' + x'_F{}^2 \cdot r'^2) + C'_{LASAF} \cdot v' \cdot 2 \cdot x'_F \cdot r' - C'_F \cdot |u'| \cdot u'
\end{aligned}
$$

$$\fallingdotseq m'_y \cdot v' \cdot r' + (C'_L - \Delta C'_L) \cdot u' \cdot (v' + x'_t \cdot r')^2$$
$$-(C'_{Di} - \Delta C'_{Di}) \cdot u'^3 \cdot (v' + x'_I \cdot r')^2 - C'_{LAS} \cdot (v' + x'^2_F \cdot r'^2)$$
$$+C'_{LASAF} \cdot v' \cdot 2 \cdot x'_F \cdot r' - C'_F \cdot |u'| \cdot u'$$

$$Y' = -m'_x \cdot u' \cdot r' - C'_L \cdot u'^2 \cdot (v' + C_{vo} \cdot x'_t \cdot r')$$
$$-C'_{Di} \cdot u'^2 \cdot \{v'^3 + 3 \cdot C_{io} \cdot v'^2 \cdot x'_I \cdot r'$$
$$+3 \cdot v' \cdot (x'_I \cdot r')^2 + C_{io} \cdot (x'_I \cdot r')^3\}$$
$$-\int C_{D90} \cdot (v' + x' \cdot r')^3 \cdot (1 + p \cdot u'^2) \cdot d' \cdot dx'$$
$$\fallingdotseq -m'_x \cdot u' \cdot r' - C'_L \cdot u'^2 \cdot (v' + C_{vo} \cdot x'_t \cdot r')$$
$$-C'_{Di} \cdot u'^2 \cdot \{v'^3 + C_{io}^{1/3} \cdot x'_I \cdot r')^3$$
$$-\int C_{D90} \cdot (v' + x' \cdot r')^3 \cdot (1 + p \cdot u'^2) \cdot d' \cdot dx'$$

$$N' = (m'_x - m'_y) \cdot u' \cdot v' - x'_t \cdot C'_L \cdot u'^2 \cdot (C_{vo} \cdot v' + x'_t \cdot r')$$
$$-x'_I \cdot C'_{Di} \cdot u'^2 \cdot \{C_{io} \cdot v'^3 + 3 \cdot v'^2 \cdot x'_I \cdot r' + 3 \cdot C_{io} \cdot v' \cdot (x'_I \cdot r')^2$$
$$+(x'_I \cdot r')^3\} - \int C_{D90} \cdot (v' + x' \cdot r')^3 \cdot (1 + p \cdot u'^2) \cdot x' \cdot d' \cdot dx'$$
$$\fallingdotseq (m'_x - m'_y) \cdot u' \cdot v' - x'_t \cdot C'_L \cdot u'^2 \cdot (C_{vo} \cdot v' + x'_t \cdot r')$$
$$-x'_I \cdot C'_{Di} \cdot u'^2 \cdot (C_{io}^{1/3} \cdot v' + x'_I \cdot r')^3$$
$$-\int C_{D90} \cdot (v' + x' \cdot r')^3 \cdot (1 + p \cdot u'^2) \cdot x' \cdot d' \cdot dx'$$

As the results of experiments on the oblique motion of the ship, they show that the viscous lift along the trailing edge is major and along the leading edge is minor, because of $1 > C_{vo} >> 0$. Furthermore, the experiments show that the induced drag along the leading edge is major and along the trailing edge is minor, because of $1 > C_{io} >> 0$. Then, we may be able to assume that the viscous lift and induced drag during the turning motion work along one major edge of each force instead of along the two leading and trailing edges.

Now, in order to extend the effective range of the mathematical model to the fairly sever turning motion, such as

$$\frac{1}{\{u'^2 + (v' + x' \cdot r')^2\}} \rightarrow 1 ,$$

we take the effective multiplier $\dfrac{1}{\{u'^2 + (v' + x' \cdot r')^2\}}$ into consideration.

Then

$$X' = m'_y \cdot v' \cdot r' + (C'_L - \Delta C'_L) \cdot u' \cdot \frac{\{v'^2 + 2 \cdot C_{vo} \cdot v' \cdot x'_t \cdot r' + (x'_t \cdot r')^2\}}{\{u'^2 + (v' + x'_t \cdot r')^2\}^{1/2}}$$

$$-(C'_{Di}-\Delta C'_{Di})\cdot u'^3\cdot\frac{\{v'^2+2\cdot C_{io}\cdot v'\cdot x'_1\cdot r'+(x'_1\cdot r')^2\}}{\{u'^2+(v'+x'_1\cdot r')^2\}^{3/2}}$$

$$-C'_{LAS}\cdot(v'^2+x'^2_F\cdot r'^2)+C'_{LASAF}\cdot v'\cdot 2\cdot x'_F\cdot r'-C'_F\cdot|u'|\cdot u'$$

$$\fallingdotseq m'_y\cdot v'\cdot r'+(C'_L-\Delta C'_L)\cdot u'\cdot\frac{(v'+x'_1\cdot r')^2}{\{u'^2+(v'+x'_1\cdot r')^2\}^{1/2}}$$

$$-(C'_{Di,t}-\Delta C'_{Di,t})\cdot u'^3\cdot\frac{(v'+x'_1\cdot r')^2}{\{u'^2+(v'+x'_1\cdot r')^2\}^{3/2}}$$

$$-C'_{LAS}\cdot(v'^2+x'^2_F\cdot r'^2)+C'_{LASAF}\cdot v'\cdot 2\cdot x'_F\cdot r'-C'_F\cdot|u'|\cdot u'$$

$$Y'\fallingdotseq -m_x\cdot u'\cdot r'-C'_L\cdot u'^2\cdot\frac{(v'+C_{vo}\cdot x'_t\cdot r')}{\{u'^2+(v'+x'_t\cdot r')^2\}^{1/2}}-C'_{Di}\cdot u'^2$$

$$\cdot\frac{\{v'^3+3\cdot C_{io}\cdot v'^2\cdot x'_1\cdot r'+3\cdot v'\cdot(x'_1\cdot r')^2+C_{io}(x'_1\cdot r')^3\}}{\{u'^2+(v'+x'_1\cdot r')^2\}^{3/2}}$$

$$-\int C_{D90}\cdot\frac{(v'+x'\cdot r')^3}{\{u'^2+(v'+x'\cdot r')^2\}^{1/2}}$$

$$\cdot\{1+p\cdot\frac{u'^2}{u'^2+(v'+x'\cdot r')^2}\}\cdot f_2\cdot d'\cdot dx'$$

$$\fallingdotseq -m_x\cdot u'\cdot r'-C'_L\cdot u'^2\cdot\frac{(v'+C_{vo}\cdot x'_t\cdot r')}{\{u'^2+(v'+x'_t\cdot r')^2\}^{1/2}}-C'_{Di}\cdot u'^2$$

$$-\frac{\{v'+C_{io}^{1/3}\cdot x'_1\cdot r'\}^3}{\{u'^2+(v'+x'_1\cdot r')^2\}^{3/2}}-\int C_{D90}\cdot\frac{(v'+x'\cdot r')^3}{\{u'^2+(v'+x'\cdot r')^2\}^{3/2}}$$

$$\cdot\{1+p\cdot\frac{u'^2}{u'^2+(v'+x'\cdot r')^2}\}\cdot f_2\cdot d'\cdot dx'$$

$$N'=(m'_x-m'_y)\cdot u'\cdot v'-x'_t\cdot C'_L\cdot u'^2\cdot\frac{(C_{vo}\cdot v'+x'_t\cdot r')}{\{u'^2+(v'+x'_t\cdot r')^2\}^{1/2}}$$

$$-x'_1\cdot C'_{Di}\cdot u'^2\cdot$$

$$\cdot\frac{\{C_{io}\cdot v'^3+3\cdot v'^2\cdot x'_1\cdot r'+3\cdot C_{io}\cdot v'\cdot(x'_i\cdot r')^2+(x'_1\cdot r')^3\}}{\{u'^2+(v'+x'_1\cdot r')^2\}^{3/2}}$$

$$-\int C_{D90}\cdot\frac{(v'+x'\cdot r')^3}{\{u'^2+(v'+x'\cdot r')^2\}^{1/2}}$$

$$\cdot\{1+p\cdot\frac{u'^2}{u'^2+(v'+x'\cdot r')^2}\}\cdot f_2\cdot x'\cdot d'\cdot dx'$$

$$\fallingdotseq(m'_x-m'_y)\cdot u'\cdot v'-x'_t\cdot C'_L\cdot u'^2\cdot\frac{(C_{vo}\cdot v'+x'_t\cdot r')}{\{u'^2+(v'+x'_t\cdot r')^2\}^{1/2}}$$

$$-x'_1\cdot C'_{Di}\cdot u'^2\cdot\frac{\{C_{io}^{1/3}\cdot v'+x'_1\cdot r'\}^3}{\{u'^2+(v'+x'_1\cdot r')^2\}^{3/2}}$$

$$-\int C_{D90}\cdot\frac{(v'+x'\cdot r')^3}{\{u'^2+(v'+x'\cdot r')^2\}^{1/2}}$$

$$\cdot\{1+p\cdot\frac{u'^2}{u'^2+(v'+x'\cdot r')^2}\}\cdot f_2\cdot x'\cdot d'\cdot dx'$$

Finally, we rewrite this equations in the style well known as the hydrodynamic derivatives of the ship maneuvering motion. Then we get the familiar mathematical model mentioned before in the abstract of this paper.

$$X'=m'_y\cdot v'\cdot r'+(X'_{uvv}\cdot u'\cdot v'^2+X'_{uvr}\cdot u'\cdot v'\cdot r'+X'_{urr}\cdot u'\cdot r'^2)$$

$$\cdot\frac{1}{\{u'^2+(v'+x'_t\cdot r')^2\}^{1/2}}$$

$$+(X'_{uuurr}\cdot u'^3\cdot v'^2+X'_{uuuur}\cdot u'^3\cdot v'\cdot r'+X'_{uuurr}\cdot u'^3\cdot r'^2$$

$$\cdot\frac{1}{\{u'^2+(v'+x'_l\cdot r')^2\}^{3/2}}$$

$$+X'_{vv}\cdot v'^2+X'_{vr}\cdot v'\cdot r'+X'_{rr}\cdot r'^2+X'_{|u|\,|u|}\,|u'|\cdot u'$$

$$Y'=-m'_x\cdot u'\cdot r'+(Y'_{uuv}\cdot u'^2\cdot v'+Y'_{uur}\cdot u'^2\cdot r')$$

$$\cdot\frac{1}{\{u'^2+(v'+x'_t\cdot r')^2\}^{1/2}}+(Y'_{uuvvv}\cdot u'^2\cdot v'^3$$

$$+Y'_{uuvvr}\cdot u'^2\cdot v'^2\cdot r'+Y'_{uuvrr}\cdot u'^2\cdot v'\cdot r'^2$$

$$+Y'_{uurrr}\cdot u'^2\cdot r'^3)\cdot\frac{1}{\{u'^2+(v'+x'_l\cdot r')^2\}^{3/2}}$$

$$-\int C_{D90}\cdot\frac{(v'+x'\cdot r')^3}{\{u'^2+(v'+x'\cdot r')^2\}^{1/2}}$$

$$\cdot\{1+p\cdot\frac{u'^2}{u'^2+(v'+x'\cdot r')^2}\}\cdot f_2\cdot d'\cdot dx'$$

$$N'=(m'_x-m'_y)\cdot u'\cdot v'+(N'^*_{uuv}\cdot u'+N'_{uur}\cdot u'^2\cdot r')$$

$$\cdot\frac{1}{\{u'^2+(v'+x'_t\cdot r')^2\}^{1/2}}+(N'_{uuvvv}\cdot u'^2\cdot v'^3$$

$$+N'_{uuvvr}\cdot u'^2\cdot v'^2\cdot r'+N'_{uuvrr}\cdot u'^2\cdot v'\cdot r'^2+N'_{uurrr}\cdot u'^2\cdot r'^3)$$

$$\cdot\frac{1}{\{u'^2+(v'+x'_l\cdot r')^2\}^{3/2}}$$

$$-\int C_{D90}\cdot\frac{(v'+x'\cdot r')^3}{\{u'^2+(v'+x'\cdot r')^2\}^{1/2}}$$

$$\cdot\{1+p\cdot\frac{u'^2}{u'^2+(v'+x'\cdot r')^2}\}\cdot f_2\cdot x'\cdot d'\cdot dx'$$

when

$$X'_{uvv} = C'_L - \Delta C'_L \qquad X'_{vv} = -C'_{LAS}$$

$$X'_{uvr} = (C'_L - \Delta C'_L)\cdot 2\cdot x'_t \cdot C_{vo} \qquad X'_{vr} = C'_{LASAF}$$

$$X'_{urr} = (C'_L - \Delta C'_L)\cdot x'^2_t \qquad X'_{rr} = -C'_{LAS}/4$$

$$X'_{uuvv} = -(C'_{Di} - \Delta C'_{Di}) \qquad X'_{|u|u} = -C'_F$$

$$X'_{uuvr} = -(C'_{Di} - \Delta C'_{Di})\cdot 2\cdot x'_l \cdot C_{io}$$

$$X'_{uurr} = -(C'_{Di} - \Delta C'_{Di})\cdot x'^2_l$$

$$Y'_{uuv} = -C'_L \qquad N^*{}'_{uuv} = -x'_t \cdot C'_L \cdot C_{vo}$$

$$Y'_{uur} = -C'_L \cdot x'_t \cdot C_{vo} \qquad N'_{uur} = -x'_t \cdot C'_L \cdot x'_t$$

$$Y'_{uvvv} = -C'_{Di} \qquad N'_{uvvv} = -x'_l \cdot C'_{Di} \cdot C_{io}$$

$$Y'_{uvvr} = -C'_{Di}\cdot 3\cdot x'_l \cdot C_{io} \qquad N'_{uvvr} = -x'_l \cdot C'_{Di}\cdot 3\cdot x'_l$$

$$Y'_{uvrr} = -C'_{Di}\cdot 3\cdot x'^2_l \qquad N'_{uvrr} = -x'_l \cdot C'_{Di}\cdot 3\cdot x'^2_l \cdot C_{io}$$

$$Y'_{urrr} = -C'_{Di}\cdot x'^3_l \cdot C_{io} \qquad N'_{urrr} = -x'_l \cdot C'_{Di}\cdot x'^3_l$$

4. CONCLUSIONS

This paper aims to identify a mathematical model that can describe the fluid-dynamic forces X,Y and N in large drifting and turning motion of a ship. It attempts to assign physical meaning to each term of the mathematical model, and the composition of a few fluid-dynamic characteristics in the mathematical model.

For these purposes, this paper adopts the following assumptions.

1) These are the six elementary fluid-dynamic forces.
2) The viscous lift and induced drag are generated along the leading and trailing edges of the ship, and connect with the inflow angles along both edges. The distribution factors between the leading edge and the trailing edge of the viscous lift, or the induced drag, are constant even in both oblique and turning motions.
3) The stole effect of the viscous lift and induced drag are generated only in X force.
4) The coefficient of the cross-flow drag is concerned with the inflow angle at the ship section.

As the results, the mathematical model of the fluid-dynamic forces described in this paper has the following characteristics :

1) the familiar mathematical model of X,Y and N forces,
2) having physical meaning assigned to each term of the mathematical model,
3) expressed by few fluid-dynamic characteristic coefficients, or by many fluid-dynamic derivatives concerned with the few fluid-dynamic characteristic coefficients, and
4) able to deal not only with weak turning motion, but also fairly sever turning motion.

REFERENCES

[1] Karasuno, K. Matsuno, J. Ito, T. Igarashi, K., " The mathematical model of hydrodynamic forces acting on ship moving in an oblique direction with fluid-dynamic concepts, 2nd report " , Journal of the Kansai Society of naval architects, Japan, No. 216, 1991, pp. 175-183

[2] Karasuno, K. Matsuno, J. Ito, T. Igarashi, K., " A new mathematical model of hydrodynamic forces and moment acting on a hull during maneuvering motion that occurs under conditions of slow speed and large turns, 2nd report " , Journal of the Kansai Society of naval architects, Japan, No. 217, 1992, pp. 125-135

[3] Yoshimura, Y. " Mathematical model for the manoeuvring ship motion in shallow water (2nd report) - mathematical model at slow forward speed" , Journal of the Kansai Society of naval architects, Japan, No. 210, 1988, pp. 77-84

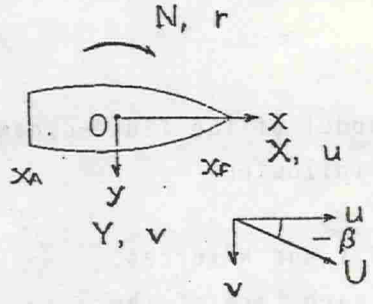

Fig. 1 Coordinate System

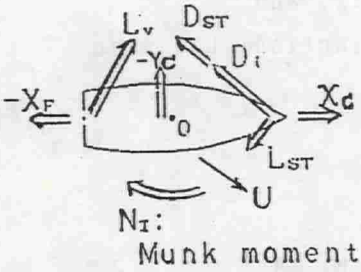

Fig. 2 Schematic model of hydrodynamic forces

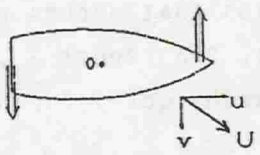

Munk moment

Fig. 4 Ideal fluid force

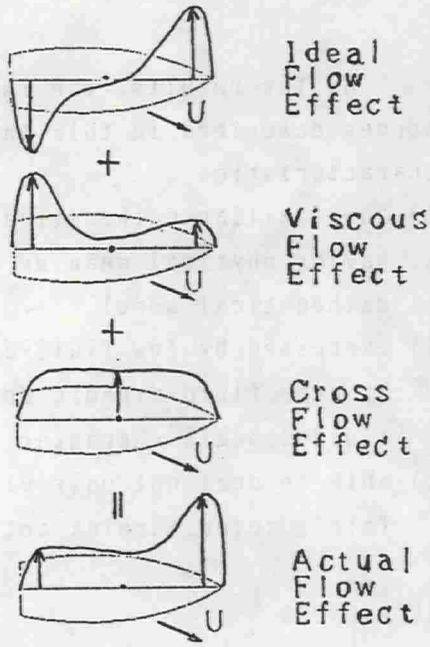

Fig. 3 Viscous lift effect in actual flow

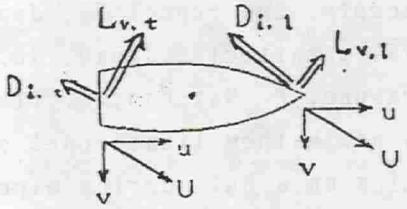

Oblique motion

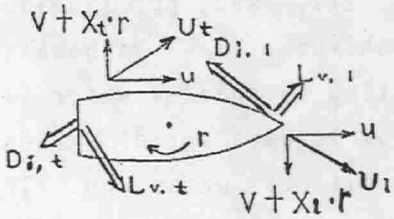

Turning motion

Fig. 5 Viscous lift and induced drag

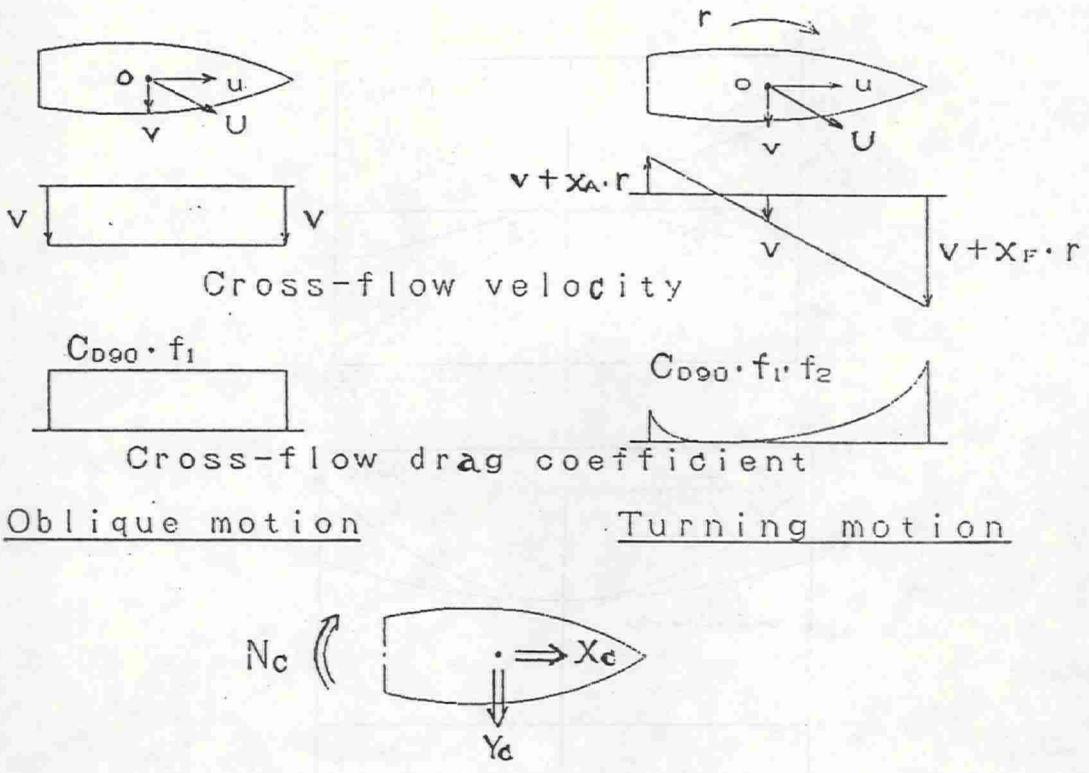

Fig. 6 Cross-flow drag and lift

Fig. 7 Cross-flow drag coefficient and its effects at r=0

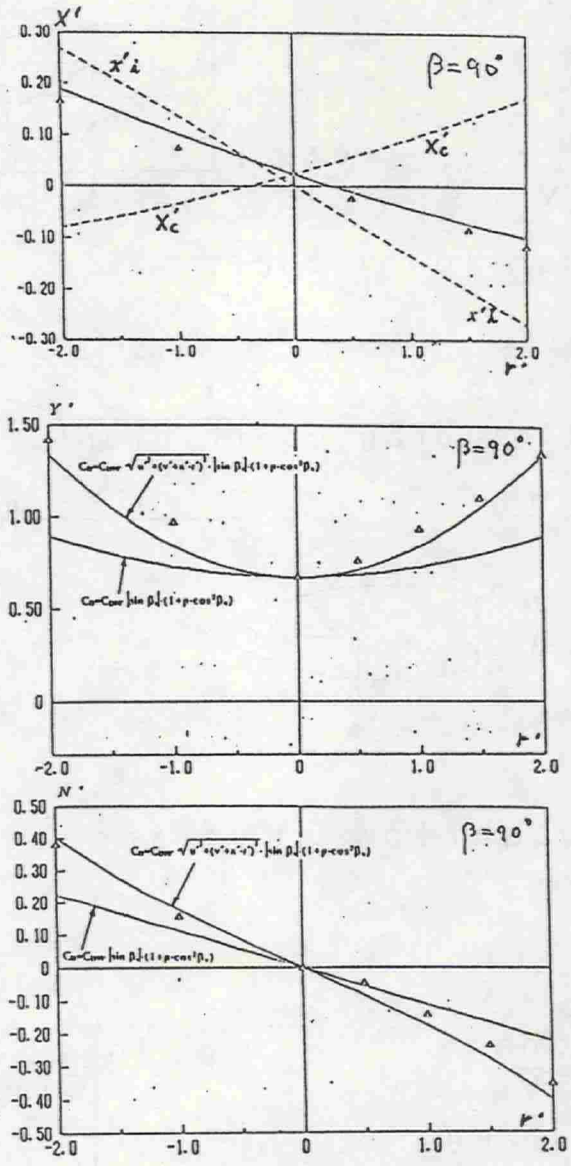

Fig.8 Cross-flow effects on X', Y' and N' in turning motion at $\beta = 90°$.

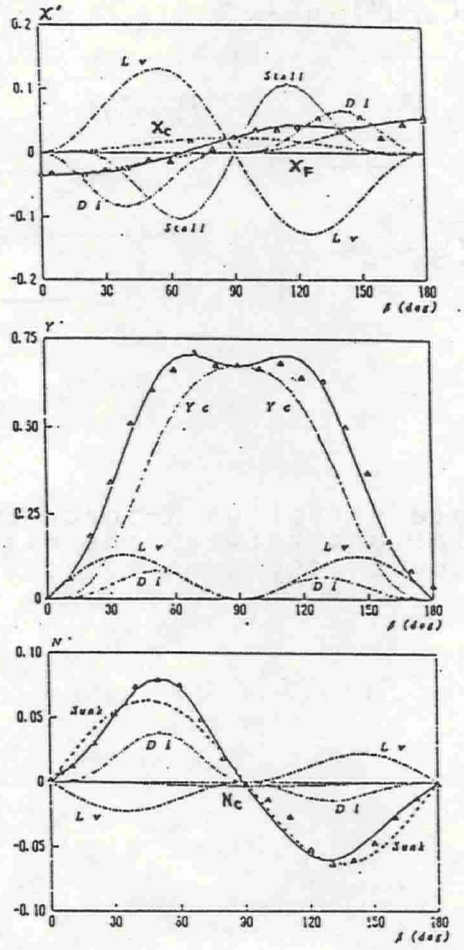

Fig.9 Analized results of hydrodynamic forces in oblique motion of PCC model ship , and experimental results [3].

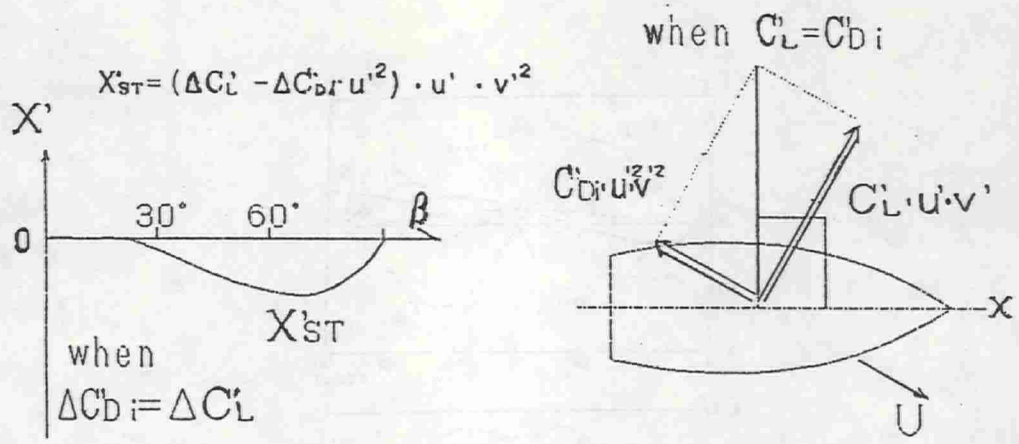

Fig. 10 Stole effect on X-force and relations between the direction of viscous resultant force and X-axis

Table 1 Coefficients of hydrodynamic forces by oblique towing test

motion	ahead	astern
$X'_{vvv} = C'_L - \Delta C'_L$	-0.037	-0.056
$X'_{vvvrr} = -C'_{Di} + \Delta C'_{Di}$	-0.009	0.108
$X'_{rrr} = -C'_F$	-0.035	-0.054
$X'_{vr} = -C'_{LAS}$	0.023	0.023
$Y'_{vvv} = -C'_L$	-0.342	-0.333
$Y'_{vvvrr} = -C'_{Di}$	-0.455	-0.351
$Y'_{vrr} = -C_{DSO} \cdot m'_0$	-0.672	-0.672
$N'_{vvr} = -C'_L \cdot \ell'_{vo}$	0.060	-0.059
$N'_{vvrrr} = -C'_{Di} \cdot \ell'_{io}$	-0.202	0.078
$N'_{vrr} = -C_{DSO} \cdot m'_1$	0.003	0.003
$m'_x - m'_y$	-0.126	-0.126
p	0.977	1.140
$\Delta C'_L$	0.379	0.391
$\Delta C'_{Di}$	0.446	0.460
C'_{Di} / C'_L	1.332	1.056
$\Delta C'_L / C'_L$	1.108	1.174
$\Delta C'_{Di} / C'_{Di}$	0.981	1.309
$\Delta C'_{Di} / \Delta C'_L$	1.177	1.176
ℓ'_{vo}	-0.174	0.177
ℓ'_{io}	0.445	-0.222

SHALLOW WATER EFFECTS ON RUDDER NORMAL FORCE AND HULL-RUDDER INTERACTION OF A THIN SHIP

HIRONORI YASUKAWA, NAGASAKI EXPERIMENTAL TANK, MHI, JAPAN

ABSTRACT

Shallow water effects are theoretically investigated on rudder normal force and hull-rudder interaction under the propelled condition by extending a method developed by the present author[12]. Calculations are made of the rudder normal force and the forces acting on the ship hull induced by the steering for various water depth. The tendency of the shallow water effects of the present calculations agrees well with that of the experiments. Through the above investigation, it is found that the present method is useful for a grasp of the tendency and a better understanding of the shallow water effects on the rudder normal force and hull-rudder interaction of the ship.

1. INTRODUCTION

For the prediction of ship maneuverability in shallow water, it is necessary to know the shallow water effects on the hydrodynamic forces acting on the ship hull, rudder and propeller. The shallow water effects are usually obtained from captive model tests in various water depth[6]. For the whole grasp of the shallow water effects, however, the model tests require much measurements of the hydrodynamic forces versus many parameters such as drifting angle, yaw rate, rudder angle, water depth and so on. In addition to that, the model tests in shallow water are often restricted by the usage of the test facilities. Then, a theoretical approach may be useful for a general grasp of the tendency and a better understanding of the shallow water effects.

Several theoretical studies on the shallow water effects have been made hitherto, for example, by Inoue[5], Newman[10], Hess[3] and Fujino[1].

In their studies, Hess and Fujino dealt with the hull-rudder interaction problems of an obliquely moving ship in shallow water. Hess evaluated the lift forces acting on the wing with a hinged flap which is regarded as the hull with a rudder under the assumption of slender ship. Fujino applied the lifting surface theory to the mutual interaction problem between the hull and rudder which are replaced by a low aspect ratio rectangular wing and its flap. The shallow water effects on the forces of the hull and rudder, and their interaction were made fairly clear by their studies. However, the propeller effects on the rudder force and hull-rudder interaction for a turning ship are not investigated in shallow water.

In this paper, a method is presented to calculate the hydrodynamic forces acting on the ship with a single rudder and a single propeller in shallow water. This method can be regarded as an extension of the method developed by the author[12] to the shallow water problems. Nonlinear lifting surface theory[8] is applied for expressing the hull and rudder, and the simple sink propeller model[9][11] is adopted under the assumption of the thin ship and thin rudder. And an attempt is made to solve the boundary value problem for a combination of hull, rudder and propeller of a turning ship in shallow water. In such a way the hydrodynamic interactions among the hull, rudder and propeller in shallow water are treated within the potential theory.

By applying the present method, shallow water effects are theoretically investigated on the rudder normal force and hull-rudder interaction. Calculations are made of the rudder normal force and the forces acting on the ship hull induced by the steering under the propelled condition for various water depth. The tendency of the shallow water effects of the present calculations agrees well with that of the experiments. As a result, it is found that the present method is useful for a grasp of the tendency and a better understanding of the shallow water effects on the rudder normal force and hull-rudder interaction of the ship.

2. A METHOD TO CALCULATE THE HYDRODYNAMIC FORCES IN SHALLOW WATER

2.1 Basic Equations

Let us consider a ship steadily turning in shallow water with propeller revolution n_P, rudder angle δ, drifting angle β and steady yaw

rate r under constant forward velocity U as shown in Fig.1. In the figure, o-xyz means the coordinate system whose origin is fixed at midship. We take $z=0$ as the plane of the undisturbed free-surface and the $z=-h(h>0)$ as the plane of the constant sea bottom. Further, we take a coordinate system o_1-$x_1y_1z_1$ whose origin is fixed at the leading edge of the rudder. The z_1-axis lies $x=x_{R0}$, $y=0$. The propeller is located at $x=x_{P0}$, $y=0$, $z=-z_{P0}(z_{P0}>0)$ and we take the propeller axis in the same direction as the x-axis.

In the present method, it is assumed that free-surface is rigid and the ship's breadth is relatively small compared to its length. Then, the hull and rudder are expressed hydrodynamically by the distribution of horse shoe vortices and line sources on their center planes. The lifting surface problems with respect to the hull and rudder are solved by using Quasi-Continuous Method (QCM)[8]. According to the QCM, loading and control points are arranged of $N_H \times M_H$ and $N_R \times M_R$ numbers on the hull and rudder surface respectively, where N_H is the number of chordwise(lengthwise) segments of the hull, M_H the number of spanwise (depthwise) segments of the hull, N_R the number of chordwise segments of the rudder and M_R the number of spanwise segments of the rudder. In order to satisfy the boundary condition of the sea bottom, the induced velocities due to mirror image of the singularities with respect to the sea bottom should be considered in the calculations. Then, the induced velocities at field point $P_{ij}(x,y,z)$ due to the vortex and source distributions are expressed as the following discretized form:

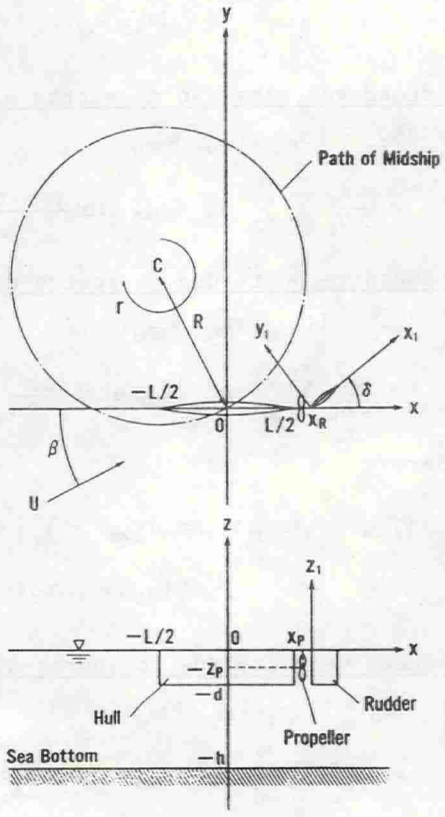

Fig. 1 Coordinate systems

Induced velocity due to vortex distribution of hull:

$$\vec{V}_{HG_{ij}} = (u_{HG_{ij}}, v_{HG_{ij}}, w_{HG_{ij}})$$

$$= \frac{\pi L}{2N_H} \sum_{k=1}^{M_H} \sum_{m=1}^{N_H} \gamma_{H_{km}} \vec{v}^{G}_{ijkm} \sin\{\frac{(2m-1)\pi}{2N_H}\}, \tag{1}$$

where

$$\vec{v}^{G}_{ijkm} = \vec{v}_G(x_{ij}, y_{ij}, z_{ij}; Q_{km}) + \sum_{n=1}^{\infty} \{ \vec{v}_G(x_{ij}, y_{ij}, z_{ij}(-1)^n + 2hn; Q_{km}) + \vec{v}_G(x_{ij}, y_{ij}, z_{ij}(-1)^n - 2hn; Q_{km}) \}, \tag{2}$$

Induced velocity due to vortex distribution of rudder:

$$\vec{V}_{RG_{ij}} = (u_{RG_{ij}}, v_{RG_{ij}}, w_{RG_{ij}})$$

$$= \frac{\pi l_R}{2N_R} \sum_{k=1}^{M_R} \sum_{m=1}^{N_R} \gamma_{R_{km}} \vec{v}^{G}_{ijkm} \sin\{\frac{(2m-1)\pi}{2N_R}\}, \tag{3}$$

Induced velocity due to source distribution of hull:

$$\vec{V}_{HS_{ij}} = (u_{HS_{ij}}, v_{HS_{ij}}, w_{HS_{ij}})$$

$$= \frac{\pi L}{2N_H} \sum_{k=1}^{M_H} \sum_{m=1}^{N_H} m_{H_{km}} \vec{v}^{S}_{ijkm} \sin\{\frac{(2m-1)\pi}{2N_H}\}, \tag{4}$$

where

$$\vec{v}^{S}_{ijkm} = \vec{v}_S(x_{ij}, y_{ij}, z_{ij}; Q_{km}) + \sum_{n=1}^{\infty} \{ \vec{v}_S(x_{ij}, y_{ij}, z_{ij}(-1)^n + 2hn; Q_{km}) + \vec{v}_S(x_{ij}, y_{ij}, z_{ij}(-1)^n - 2hn; Q_{km}) \}, \tag{5}$$

Induced velocity due to source distribution of rudder:

$$\vec{V}_{RS_{ij}} = (u_{RS_{ij}}, v_{RS_{ij}}, w_{RS_{ij}})$$

$$= \frac{\pi l_R}{2N_R} \sum_{k=1}^{M_R} \sum_{m=1}^{N_R} m_{R_{km}} \vec{v}^{S}_{ijkm} \sin\{\frac{(2m-1)\pi}{2N_R}\}, \tag{6}$$

where

L : ship length,

l_R : chord length of rudder,

γ_{Hkm}: vortex strength at the k-th loading point in the m-th strip of hull,

γ_{Rkm}: vortex strength at the k-th loading point in the m-th strip of rudder,

m_{Hkm}: source strength at the k-th loading point in the m-th strip of hull,

m_{Rkm}: source strength at the k-th loading point in the m-th strip of rudder,

$\vec{v}^{G}_{ijkm}$: induced velocity at P_{ij} due to the k-th and m-th horse shoe vortex of unit strength,

$\vec{v}^{S}_{ijkm}$: induced velocity at P_{ij} due to the k-th and m-th source strip of unit strength.

Here, m_{Hkm} and m_{Rkm} are assumed to be represented by Michell's distributions according to the thin ship theory. $\vec{v}^{S}_{ijkm}$ and $\vec{v}^{G}_{ijkm}$ can be represented by combination with the formula of induced velocity due to line source and vortex respectively[12].

Applying the simple propeller model[9][11], induced velocity due to propeller is expressed as follows:

Induced velocity at outside of slip stream due to propeller:

$$\vec{V}_{P_{ij}} = (u_{P_{ij}}, v_{P_{ij}}, w_{P_{ij}}) = -\frac{A\sigma}{4\pi}\nabla G_P(x_{ij}, y_{ij}, z_{ij}; x_{P0}, 0, -z_{P0}), \tag{7}$$

where

$$G_P(x,y,z;x_{P0},0,-z_{P0}) = G(x,y,z;x_{P0},0,-z_{P0}) + \sum_{n=1}^{\infty}\{ G(x,y,z;x_{P0},0,-z_{P0}(-1)^n+2 + G(x,y,z;x_{P0},0,-z_{P0}(-1)^n-2hn) \}, \tag{8}$$

$$G(x,y,z,;x',y',z') = \frac{1}{\sqrt{(x-x')^2+(y-y')^2+(z-z')^2}} + \frac{1}{\sqrt{(x-x')^2+(y-y')^2+(z+z')^2}}. \tag{9}$$

Here, A denotes the propeller disc area and σ the sink strength of the propeller.

Induced velocity at inside of slip stream due to propeller:

$$\vec{V}_{P_{ij}} = \vec{V}_{PS_{ij}} - \frac{A\sigma}{4\pi}\nabla G_P(P_{ij};x_{P0},0,-z_{P0}), \tag{10}$$

where

$$\vec{V}_{PS} = (\sigma, 0, 0).$$

The boundary conditions are expressed of the hull, rudder and propeller under the assumption of the thin ship as follows:

$$v_{HG} + v_{RG} + v_P + v_{HS} + v_{RS} + v_I = 0 \quad \text{on ship hull,} \tag{11}$$

$$-\{ u_{HG} + u_{RG} + u_P + u_{HS} + u_{RS} + u_I(1-w_v) \} \sin\delta + (v_{HG} + v_{RG} + v_P + v_{HS} + v_{RS} + v_I) \cos\delta = 0 \quad \text{on rudder,} \tag{12}$$

$$u_I(1-w_v) + u_{HG} + u_{RG} + u_{HS} + u_{RS} + \frac{\sigma}{2} = 2\pi n_P a \quad \text{on propeller,} \tag{13}$$

where u_I and v_I mean the inflow velocity components and a denotes the effective pitch ratio of the propeller. In the calculations of the rudder and propeller, w_v which denotes the viscous component of wake fraction is considered empirically. When n_P, δ, β, r and U are given, the vortex strength of the hull γ_H, the vortex strength of the rudder γ_R and the sink strength of the propeller σ can be obtained from eqs.(11), (12) and (13). Then, the hydrodynamic forces acting on the hull, rudder and propeller are evaluated by applying Lagally's and Kutta-Joukowski's theorems[12].

2.2 Hull-Rudder Interaction Coefficients

Referring to the simulation model presented by Kobayashi[7], hull-rudder interaction coefficients are introduced for convenience of the treatment. The lateral force and yawing moment acting on the ship(Y, N) are expressed as the sum of the forces acting on the hull(Y_H, N_H) when the rudder angle is zero, additional forces on the hull due to steering(ΔY_H, ΔN_H) and rudder forces(Y_R, N_R) as follows:

$$\begin{aligned} Y(U,\beta,r,n_p,\delta) &= Y_H(U,\beta,r,n_p,0) + \Delta Y_H(U,\beta,r,n_p,\delta) + Y_R(U,\beta,r,n_p,\delta) \\ &= Y_H(U,\beta,r,n_p,0) + (1+a_Y) Y_R(U,\beta,r,n_p,\delta), \end{aligned} \tag{14}$$

$$\begin{aligned} N(U,\beta,r,n_p,\delta) &= N_H(U,\beta,r,n_p,0) + \Delta N_H(U,\beta,r,n_p,\delta) + N_R(U,\beta,r,n_p,\delta) \\ &= N_H(U,\beta,r,n_p,0) + (1+a_N) N_R(U,\beta,r,n_p,\delta). \end{aligned} \tag{15}$$

Here, (U, β, r, n_P, δ) means the function of U, β, r, n_P and δ. a_Y and a_N which are new coefficients introduced in eqs.(14) and(15) represent the magnitude of the additional lateral force and yawing moment acting on the hull induced by the steering respectively. In this paper, we call the coefficients(a_Y, a_N) as the hull-rudder interaction coefficients.

3. SHALLOW WATER EFFECT ON RUDDER NORMAL FORCE

3.1 Rudder Normal Force of a Straightly Moving Ship

First, calculation is made of rudder normal force under the propelled condition in various water depth by use of the present method. Wigley's parabolic hull form is chosen with L/B=10.0 and L/d=16.0 where L denotes ship length, B the ship's breadth and d the ship's draft. Principal particulars of the hull, rudder and propeller are shown in Table 1. We assume that L=150(m) and U=5(knots). Further, viscous component of wake fraction(w_v) is assumed as shown in Table 2.

Table 1 Principal particulars of Wigley's parabolic hull form

Ship Length	(L)	150.00(m)
Ship Breadth	(B)	15.00(m)
Ship Draft	(d)	9.375(m)
Block Coefficient	(C_b)	0.444
Chord Length of Rudder	(l_R)	4.6875(m)
Span Length of Rudder	(d_R)	9.375(m)
Rudder Sectional Shape		NACA0008
Rudder Area Ratio	(A_R/Ld)	1/32.0
Propeller Diameter	(D_P)	4.6875(m)

Table 2 Viscous component of wake fraction for various water depth

h/d	∞	2.0	1.5	1.2
w_v	0.10	0.12	0.16	0.20

Fig.2 shows the comparison of rudder normal forces F_{NR} behind the straightly moving ship hull in β=0 and r'=0 for various water depth. Propeller revolution at self-propulsive condition is employed in the calculation. In the figure, F_{NR} is represented in the normalized form by using the rudder area and ship velocity. It can be seen that F_{NR} is almost the same for the same rudder angle in any water depths and its tendency agrees with the experimental result for Series 60(C_b=0.8). Fig.3 shows the

distributions of vortex strength of rudder and inflow velocity to rudder along the propeller axis for various water depth. It is found that both the inflow velocity to rudder and the vortex strength are almost the same for various water depth. In this connection, Fujino has already indicated that the vortex strength of rudder does not change very much for different water depth because of the interaction effect due to the ship hull[1]. In addition to Fujino's indication, here, it can be pointed out that the inflow velocity to rudder does not change also for different water depth. This can be explained as follows: the wake fraction increases with decrease of the water depth so that the inflow velocity to the propeller becomes small in shallow water. On the other hand, propeller load becomes large in shallow water because the ship resistance usually increases. This means that the rudder inflow is accelerated more remarkably in shallow water. As a result of the cancellation between the propeller inflow velocity and the acceleration due to propeller, the inflow velocity to the rudder becomes almost the same magnitude in deep and shallow waters. Consequently, F_{NR} becomes almost the same for any water depths.

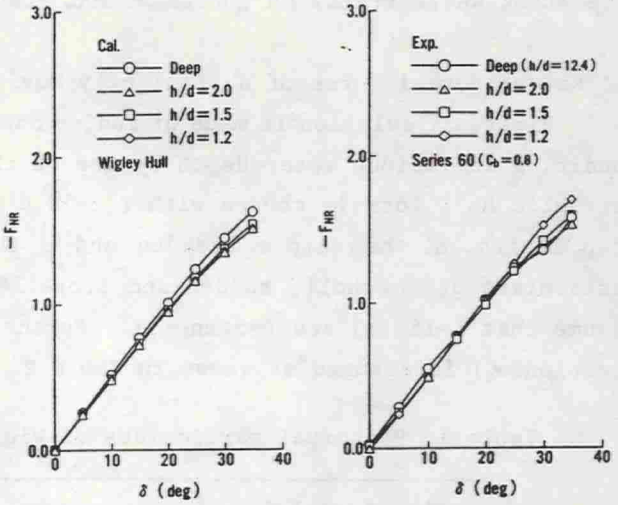

Fig. 2 Comparison of rudder normal forces for various water depth

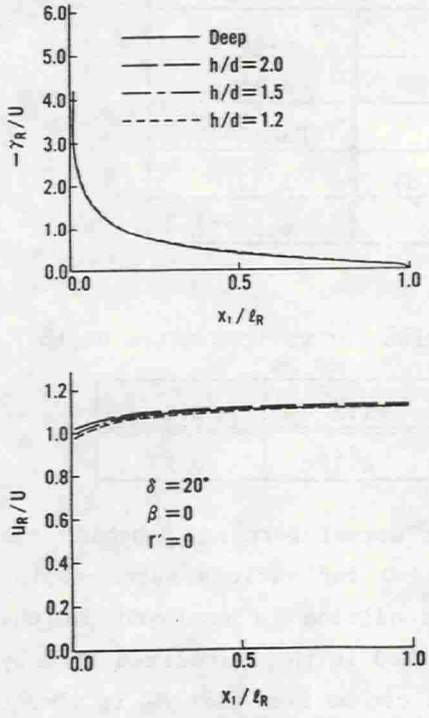

Fig. 3 Comparison of rudder vortex strength and inflow velocity to rudder

3.2 Rudder Normal Force of a Turning Ship

Fig.4 shows the comparison of rudder normal forces F_{NR} behind the turning ship hull in β=0 and δ=20(deg) for various water depth. F_{NR} becomes small with increase of r' since the geometrical inflow angle into the rudder becomes small. It can be seen that F_{NR} is almost the same for different water depth and its tendency agrees with the case of the straightly moving ship as shown in Fig.2. Thus, it can be said that shallow water effect on rudder normal force F_{NR} is not remarkable.

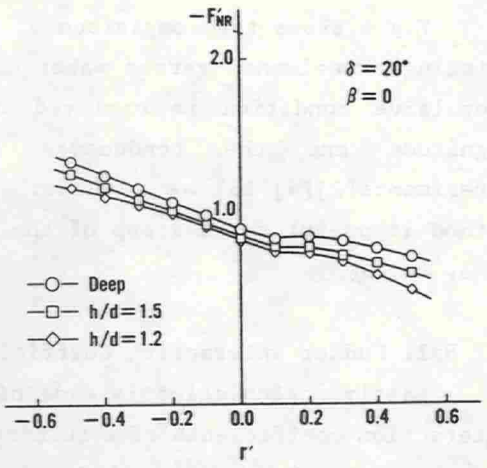

Fig. 4 Rudder normal forces of a turning ship for various water depth

4. SHALLOW WATER EFFECT ON HULL-RUDDER INTERACTION COEFFICIENTS

4.1 Hull-Rudder Interaction Coefficients of a Straightly Moving Ship

Next, calculation is made of shallow water effect on hull-rudder interaction coefficients of a straightly moving ship. Fig.5 shows the changes of hull-rudder interaction coefficients(a_Y, a_N) versus apparent advanced constant of the propeller $J_s(=U/n_PD_P$, D_P: Propeller diameter) for various water depth. We assumed that δ=20(deg), β=0 and r'=0. It can be seen that a_Y increases rapidly with the decrease of water depth since the lateral force acting on the hull induced by the steering(ΔY_H) becomes more remarkably large than the rudder force(Y_R) in shallow water. On the contrary, the shallow water effect on a_N is not so remarkable as a_Y since the acting point of the hull force induced by the steering moves forward from the stern position[1]. Further, it is found that a_Y and a_N become large with increase of J_s (decrease of propeller load) in any water depths. The reason why a_Y and a_N become large is that the hull forces induced by the steering(ΔY_H, ΔN_H) becomes more remarkably large than the rudder forces(Y_R, N_R)[12]. This means that a_Y and a_N should be treated as not constant but variation with respect to the propeller load in the simulation

model for the ship maneuverability.

Fig.6 shows the comparison of a_Y and a_N between the calculation and existing experiments versus water depth. Propeller revolution at self-propulsive condition is employed in the calculation. The orders of magnitude and the tendencies of a_Y and a_N agree with the experiments[2][4][13] as a whole. Thus, it is found that the present method is useful for a grasp of the tendency of the shallow water effect on a_Y and a_N.

4.2 Hull-Rudder Interaction Coefficients of a Turning Ship

Lastly, calculation is made of shallow water effect on hull-rudder interaction coefficients of a turning ship. Fig.7 shows the changes of a_Y and a_N versus r' for three different water depths. Although a_Y and a_N are almost the same for various r' in deep water($h/d=\infty$), they become large with increase of absolute value of r' in shallow water. Its tendency of a_Y is more remarkable than that of a_N. The reason why a_Y becomes large remarkably with increase of absolute value of r' in shallow water is due to the rapid increase of the lateral force induced by the steering(ΔY_H) as shown in Fig.8. On the contrary, the change of ΔN_H versus r' is small in any water depths.

In the simulation model of ship maneuverability, a_Y and a_N are usually dealt with as constant values with propeller load or ship maneuvering motions[7]. As mentioned above, however, it is theoretically indicated that a_Y and a_N change remarkably with the propeller load or turning motions. Therefore, it may be considered that a_Y and a_N should be treated as the function of the propeller load or turning motions for more accurate prediction of ship maneuverability.

5. CONCLUDING REMARKS

A method was presented to calculate the hydrodynamic forces acting on a thin ship in shallow water taking the interaction effects among hull, rudder and propeller into account. By applying the present method, shallow water effects were theoretically investigated on the rudder normal force and hull-rudder interaction. Calculations were made of the rudder normal force and the forces acting on the ship hull induced by the steering under

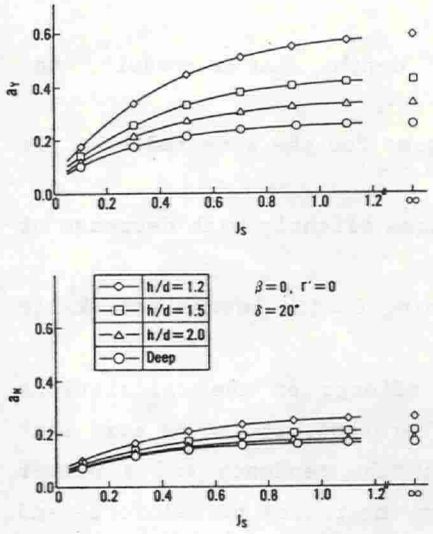

Fig.5 Hull-rudder interaction coefficients(a_Y, a_N) versus apparent advanced constant of propeller

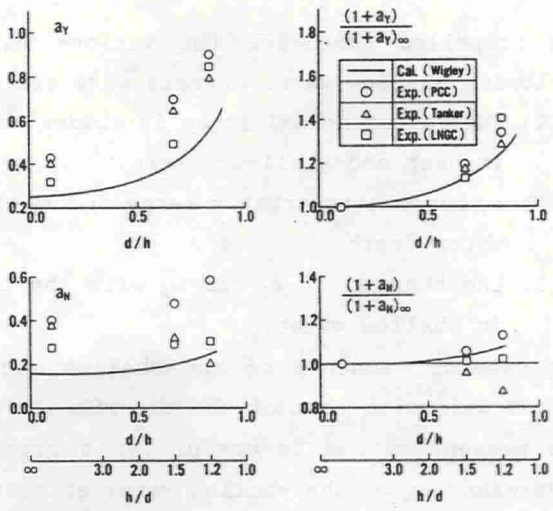

Fig.6 Comparison of hull-rudder interaction coefficients(a_Y, a_N) between calculation and experiment

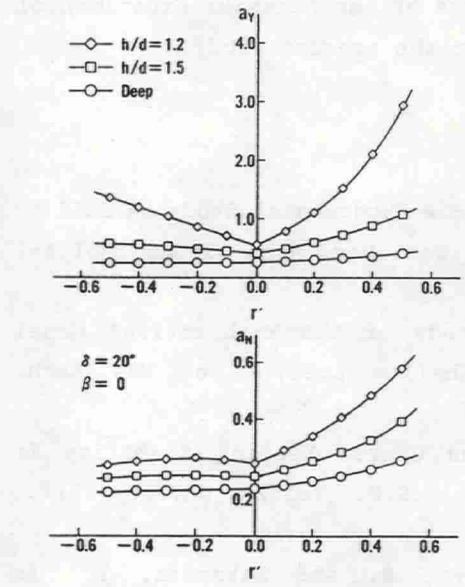

Fig.7 Changes of hull-rudder interaction coefficients(a_Y, a_N) versus r'

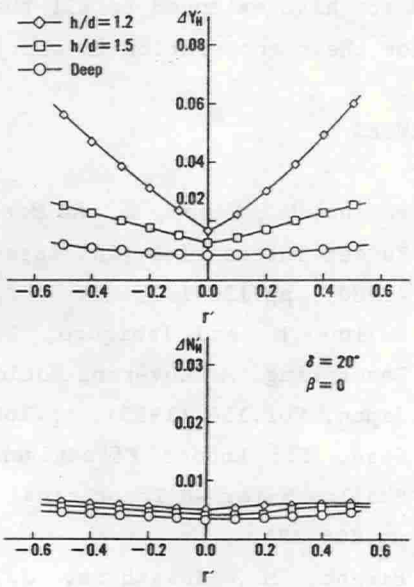

Fig.8 Lateral force and yawing moment on the hull induced by the steering(ΔY_H, ΔN_H) versus r'

the propelled condition for various water depth. As a result, the following shallow water effects were evaluated:

(1) The rudder normal force is almost the same for the same rudder angle in deep and shallow waters.

(2) a_Y becomes remarkably large and a_N changes slightly with decrease of water depth.

(3) The changes of a_Y and a_N with the turning motion become remarkable in shallow water.

The general tendency of the shallow water effects of the calculations agrees well with that of the experiments. Therefore, it can be said that the present method is useful for a grasp of the tendency and a better understanding of the shallow water effects on the rudder normal force and hull-rudder interaction of the ship.

Acknowledgements

The author would like to express his sincere gratitude to Professor K. Kijima of Kyushu University for his valuable comment and encouragement. Thanks are also extended to all the members of the Nagasaki Experimental Tank for their cooperation in carrying out the present study.

REFERENCES

[1] Fujino, M., Kanou, T. and Motora, S.: A Fundamental Study on Hull to Rudder Interaction (2nd Report), J. Soc. Nav. Arch. Japan, Vol.147 (1980), pp.136-143.

[2] Fujino, M. and Ishiguro, T.: A Study of the Mathematical Model Describing Maneuvering Motions in Shallow Water, J. Soc. Nav. Arch. Japan, Vol.156 (1985), pp.180-192.

[3] Hess, F.: Rudder Effectiveness and Course Keeping Stability in Shallow Water -A Theoretical Model-, I.S.P., Vol.24, No.276 (1977), pp.206-221.

[4] Hirano, M., Takashina, J., Moriya, S. and Nakamura, Y.: An Experimental Study on Maneuvering Hydrodynamic Forces in Shallow Water, Trans. West-Japan Soc. Nav. Arch., No.69 (1985), pp.101-110.

[5] Inoue, S. and Murayama, K.: Calculation of Turning Ship Derivatives in Shallow Water, Trans. West-Japan Soc. Nav. Arch., No.37 (1969),

pp.73-85.

[6] Kijima, K., Yoshimura, Y. and Fukazawa, T.: Maneuvering Characteristics in Shallow Water and at Slow Speed, Prediction of Ship Maneuverability and its Applications, 4th Marine Dynamics Symp., Soc. Nav. Arch. Japan (1987), 133-166.

[7] Kobayashi, E. and Asai, S.: A Simulation Study on Ship Maneuverability at Low Speeds, RINA Int. Conf. on Ship Maneuverability, Vol.1 (1987).

[8] Lan, C.E.: A Quasi-Vortex-Lattice Method in Thin Wing Theory, J. Aircraft, Vol.11, No.9 (1974), pp.518-527.

[9] Nakatake, K., Oda, K., Kataoka, K., and Nishimoto, H.: Free Surface Effect on the Propulsive Performance of a Ship(1st Report), Trans. the West-Japan Soc. Nav. Arch., No.72 (1986), pp.129-139.

[10] Newman, J.N.: Lateral Motion of a Slender Body Between Two Parallel Walls, J. Fluid Mech., Vol.39 (1969), pp.97-115.

[11] Yamazaki, R. and Nakatake, K.: Free-Surface Effect on the Hull-Propeller Interaction, Proc. 15th Symp. on Naval Hydrodynamics, Washington D.C. (1985), pp.463-479.

[12] Yasukawa, H.: Hydrodynamic Interactions among Hull, Rudder and Propeller of a Turning Thin Ship, West-Japan Soc. Nav. Arch., No.84 (1992), pp.59-83.

[13] Yoshimura, Y.: Mathematical Model for the Maneuvering Ship Motion in Shallow Water, Trans. Kansai Soc. Nav. Arch. Japan, No.200 (1986), pp.41-51.